

# **A Mesenchymal Stem Cell- Based Approach for Investigating Cardiovascular Disease-Related Genetic Variants**

**Thesis submitted for the degree of Doctor of Philosophy  
at the University of Leicester**

**Sukhvir K. Rai BSc, MSc**

**Department of Cardiovascular Sciences  
University of Leicester**

**2016**

# A Mesenchymal Stem Cell-Based Approach for Investigating Cardiovascular Disease-Related Genetic Variants

Sukhvir K. Rai

## Abstract

Genome wide-association studies (GWASs) have identified many loci that contribute to coronary artery disease (CAD). A huge challenge of the post-GWAS era is identifying the biological pathways risk variants act through to contribute to disease. I explored the use of MSCs as a model to investigate the effects of CAD-related variants *in vitro*.

To establish a MSC bank, cells were isolated from 114 umbilical cords and subsequently characterised. MSCs met the ISCT criteria; they adhered to plastic, expressed a characteristic cell surface profile and differentiated into three common lineages. As a proof of principle study, a BMI-associated variant was investigated. Speliotes *et al.*, (2010) showed rs3810291 was an eQTL for *ZC3H4* in adipose tissue. However, MSC-derived adipocytes did not recapitulate the effect of this variant. Analysis of another known eQTL (rs10840106) in adipose tissue was significantly associated with *TRIM66* gene expression in MSCs and differentiated adipocytes.

It is hypothesised CAD risk variants act in CAD-relevant cell types to exert their effects, so MSCs were differentiated towards a SMC lineage. A second proof of concept study focussed on a CAD-associated variant reported to be functional in SMCs. Pu *et al.*, (2013) showed rs3825807 affected vascular SMC migration, ADAMTS7 maturation and COMP cleavage. I did not see a genotype effect of rs3825807 on ADAMTS7 prodomain cleavage or migration of differentiated SMCs.

These findings suggest that MSCs may be robust enough to detect the association of variants on important genetic effects such as mRNA levels. However using MSCs to understand the effects of CAD-associated variants is still a difficult process. It is hindered by technical challenges such as MSC heterogeneity, variation in MSC differentiation and underpowered sample sizes. These barriers need to be overcome in order to successfully use MSCs to model disease.

## **Acknowledgements**

I would like to thank my supervisors Dr. Dave Lodwick, Dr. Thomas Webb and Prof. Nilesh Samani for all their help, support and constant guidance throughout my PhD. I am incredibly thankful to the Medical Research Council and the Leicester Cardiovascular Biomedical Research Centre for the funding for my PhD project.

I would like to acknowledge all of the members of the Department of Cardiovascular Sciences who have helped and guided me throughout my PhD, and have made the department a really nice place to be. In particular, I would like to thank Dr. Andrea Koekemoer, Jasbir Moore, David McVey, Hash Patel, Dr. Veryan Codd. Thank you to Dr. Peter Braund and Leanne Hall for all their help with the whole-genome genotyping analysis. A huge thank you to Sonja Khemiri and Barbara Horley, and the Anthony Nolan Trust nurses for all their help with the establishment of the MSC bank.

Thank you to my best friend, my husband Raman for all his constant love and support, for encouraging me and putting a smile on my face, when I needed it most. I would like to thank the Rai family for their constant support and encouragement.

I would not have been able to complete this PhD without my incredible parents. I am indebted to my mum and dad for all their love and support throughout my entire life. They have always been there for me to support me, and I would not be the person I am today without them. In addition, a huge thank you to my wonderful sister, Jaspreet and brother, Satvinder, for cheering me up when I needed it, and for their constant love and support. This thesis is dedicated to them.

# TABLE OF CONTENTS

<b>Abstract</b>	<b>i</b>
<b>Acknowledgements</b>	<b>ii</b>
<b>TABLE OF CONTENTS</b>	<b>iii</b>
<b>List of tables</b>	<b>x</b>
<b>List of figures</b>	<b>xi</b>
<b>Abbreviations list</b>	<b>xvi</b>
<b>Chapter 1- Introduction</b>	<b>1</b>
1.1. Coronary artery disease	2
1.2. Overview of CAD pathobiology	2
1.3. Risk factors of CAD	7
1.4. Genetic contribution of CAD	8
1.5. Mendelian disorders that manifest CAD	9
1.6. Genetic architecture of CAD	10
1.7. Studies to identify causative genes for CAD	11
1.7.1. Linkage analysis studies	11
1.7.2. Candidate gene studies	12
1.7.3. Genome-wide association studies	13
1.7.4. Genome-wide association studies for CAD	16
1.7.4.1. 9p21 locus	20
1.8. Disease models to investigate CAD	22
1.9. Stem cells	23
1.10. Embryonic stem cells	25
1.11. Induced pluripotent stem cells	26
1.12. Adult stem cells	27
1.13. Mesenchymal stem cells	28

1.13.1. Discovery of MSCs	28
1.13.2. Morphology of MSCs	29
1.13.3. Isolation of MSCs	30
1.13.4. Isolation of MSCs from the umbilical cord	31
1.13.5. Isolation of MSCs from Wharton's jelly	33
1.14. Aims of this thesis	35
<b>Chapter 2- Materials and Methods</b>	<b>36</b>
2.1. <u>Molecular Biology</u>	37
2.1.1. DNA extraction	37
2.1.2. Determining the concentration of DNA	37
2.1.3. Taqman <sup>®</sup> SNP Genotyping assay	37
2.1.4. Preparation of DNA samples for whole genome genotyping	38
2.1.5. Ethanol precipitation	38
2.1.6. Sample concentration	39
2.1.7. Agarose gel electrophoresis	39
2.1.8. Plating of DNA into 96 well plates	40
2.1.9. Axiom Genotyping Array	40
2.1.10. RNA extraction	40
2.1.11. Determining the concentration of RNA	42
2.1.12. cDNA synthesis	42
2.1.13. Primer design for qPCR	43
2.1.14. Optimisation of primers for qPCR	43
2.1.15. Quantitative PCR	45
2.2. <u>Cell culture</u>	47
2.2.1. Collection and transport of umbilical cords	47
2.2.2. Isolation of MSCs	48
2.2.3. Subculture and maintenance of MSCs	48

2.2.4. Cryopreservation of MSCs	49
2.2.5. Thawing and plating of MSCs	50
2.2.6. Growth curve	50
2.2.7. Population doubling time	50
2.2.8. Maintenance and culture of other cells	51
2.2.8.1. Human umbilical cord-derived MSCs	51
2.2.8.2. Human aortic smooth muscle cells	51
2.2.8.3. HepG2s	52
2.2.8.4. HEK293	52
2.2.8.5. 3T3-L1s	53
2.2.9. Adipogenic differentiation	53
2.2.9.1. Oil Red O staining	54
2.2.10. Density centrifugation of MSC-derived adipocytes	54
2.2.11. Ceiling culture separation of MSC-derived adipocytes	55
2.2.12. Chondrogenic differentiation	55
2.2.12.1. Toluidine Blue staining	56
2.2.13. Osteogenic differentiation	57
2.2.13.1. Alizarin Red S staining	57
2.2.14. Hepatogenic differentiation	58
2.2.15. Smooth muscle cell differentiation	58
2.2.16. Transformation of recombinant plasmid	59
2.2.17. Transient transfections	60
2.3. <u>Flow cytometry</u>	61
2.3.1. Preparation of MSCs	61
2.3.2. Analysis of cells on the flow cytometer	62
2.3.3. Flow cytometry for Nile red staining	63
2.3.4. Nile Red staining in 6 well plate	64

2.4. <u>Cellular assays</u>	64
2.4.1. Measurement of intracellular Ca <sup>2+</sup>	64
2.4.2. Cell Contraction Assay	65
2.4.3. Scratch assay	66
2.5 <u>Protein methods</u>	67
2.5.1. Immunofluorescence staining	67
2.5.2. Western blotting	68
2.5.2.1. Preparation of cell lysate	69
2.5.2.2. Concentration of conditioned media	70
2.5.2.3. Pierce™ BCA Protein Assay Kit	70
2.5.2.4. Western Blotting	71
2.6. <u>Statistical analysis</u>	72
<b>Chapter 3- Isolation and characterisation of mesenchymal stem cells</b>	<b>73</b>
3.1. Introduction	74
3.1.1. Mesenchymal stem cells	74
3.1.1.1. Plastic adherence	75
3.1.1.2. Cell surface markers	75
3.1.1.3. Trilineage differentiation	76
3.1.2. Aims and objectives	79
3.2. Results	80
3.2.1. Isolation, culture and morphology of MSCs	80
3.2.2. Morphological heterogeneity	82
3.2.3. Population doubling time	83
3.2.4. Growth curve	83
3.2.5. Characterisation of MSCs	84
3.2.5.1. Cell surface marker expression	84
3.2.5.2. Trilineage differentiation	87

3.2.5.2.1. Adipogenic differentiation	87
3.2.5.2.2. Chondrogenic differentiation	88
3.2.5.2.3. Osteogenic differentiation	89
3.2.6. Genotyping of MSC bank	90
3.3. Discussion	95
3.3.1. Conclusion	100
<b>Chapter 4- Analysis of a variant associated with body mass index</b>	<b>101</b>
4.1. Introduction	102
4.1.1. ZC3H4	104
4.1.2. Aims and objectives	105
4.2. Results	106
4.2.1. Heterogeneity of adipogenic differentiation	106
4.2.2. Separation of differentiated adipocytes from MSCs	110
4.2.3. Gene expression of adipogenic markers	112
4.2.4. Analysis of rs3810291 on <i>ZC3H4</i> gene expression	118
4.2.5. Analysis of rs4929949 and rs10840106 on <i>TRIM66</i> gene expression	121
4.3. Discussion	124
4.3.1. Conclusion	129
<b>Chapter 5- Hepatogenic and smooth muscle cell differentiation of MSCs</b>	<b>130</b>
5.1. Introduction	131
5.1.1. Hepatocytes	131
5.1.1.1. Markers of hepatogenic differentiation	132
5.1.1.2. Functionality of differentiated hepatocytes	133
5.1.2. Smooth muscle cells	133
5.1.2.1. Markers of SMC differentiation	135

5.1.2.2. Smooth muscle cell contraction	136
5.1.3. Aims and objectives	138
5.2. Results	139
5.2.1. Hepatogenic differentiation of MSCs	139
5.2.1.1. Morphology	139
5.2.1.2. Gene expression of hepatogenic markers	143
5.2.2. Smooth muscle cell differentiation of MSCs	146
5.2.2.1. Morphology	147
5.2.2.2. Gene expression of SMC markers	149
5.2.2.3. Protein expression of SMC markers	154
5.2.2.4. Calcium imaging	157
5.2.2.5. Cell contraction	163
5.3. Discussion	167
5.3.1. Future work	172
5.3.2. Conclusion	175
<b>Chapter 6- Functional studies on the 15q25 CAD-associated locus</b>	<b>177</b>
6.1. Introduction	176
6.1.1. ADAMTS7	177
6.1.2. Role of ADAMTS7 in the pathogenesis of CAD	181
6.1.3. Aims and objectives	184
6.2. Results	185
6.2.1. <i>ADAMTS7</i> expression in MSCs and differentiated SMCs	185
6.2.2. Analysis of rs3825807 and <i>ADAMTS7</i> expression in MSCs and differentiated SMCs	186
6.2.3. ADAMTS7 protein expression in MSCs and differentiated SMCs	189
6.2.4. Analysis of rs3825807 on ADAMTS7 protein expression and processing	192
6.2.5. Analysis of rs3825807 and cell migration	195

6.3. Discussion	199
6.3.1. Future work	204
6.3.2. Conclusion	205
<b>Chapter 7- Discussion</b>	<b>206</b>
7.1. Conclusion	217
<b>Appendix</b>	<b>219</b>
<b>References</b>	<b>236</b>

## **List of tables**

<b>Table 1.1.</b> List of 50 CAD-associated genetic variants	18
<b>Table 2.1.</b> PCR components for a 25µl qPCR reaction	44
<b>Table 2.2.</b> Details of the parameters for each gene for qPCR	46
<b>Table 2.3.</b> Antibodies added to each tube for detection of cell surface markers on MSCs	62
<b>Table 2.4.</b> Details of the antibodies, their attached fluorescent dye, lasers and specific filters present in the FACSAria II flow cytometer to detect the emitted wavelength from each dye	63
<b>Table 2.5.</b> Details of the antibody dilutions for immunofluorescence	68
<b>Table 2.6.</b> Western Blot components for a 35µl sample	71
<b>Table 2.7.</b> Details of the antibody dilutions used for Western Blotting	72
<b>Table 3.1.</b> Summary of the minimal criteria to characterise MSCs	75
<b>Table 3.2.</b> MSCs isolated from WJ analysed using flow cytometry for the expression of cell surface markers	87
<b>Table 3.3.</b> Summary of the genotypes for 50 CAD-associated SNPs in the MSC bank (114 donors)	93
<b>Table 4.1.</b> Summary of the genotype of 111 donors for rs3810291	118

## **List of figures**

<b>Figure 1.1.</b> An overview of the formation of an atherosclerotic lesion	6
<b>Figure 1.2.</b> The risk factors for cardiovascular disease	8
<b>Figure 1.3.</b> Outline of the methodology for genome-wide association studies	16
<b>Figure 1.4.</b> Schematic diagram of the hypothesised biological mechanism the 9p21 risk locus acts through	21
<b>Figure 1.5.</b> Schematic diagram of the generation of induced pluripotent stem cells (iPSCs)	27
<b>Figure 1.6.</b> Morphology of MSCs	30
<b>Figure 1.7.</b> Schematic diagram of the umbilical cord compartments containing MSCs	33
<b>Figure 3.1.</b> Schematic diagram of the trilineage differentiation of MSCs into adipocytes, chondrocytes and osteoblasts upon treatment with specialised differentiation mediums	78
<b>Figure 3.2.</b> Representative images of the migration of MSCs from Wharton's jelly (WJ) of human umbilical cord using the explant method	81
<b>Figure 3.3.</b> Morphology of MSCs isolated from Wharton's jelly (WJ) of the umbilical cord	81
<b>Figure 3.4.</b> Comparison of the morphology of MSCs isolated from Wharton's jelly (WJ) and human umbilical cord-derived MSCs purchased from ATCC	82
<b>Figure 3.5.</b> Morphological heterogeneity of MSCs	83
<b>Figure 3.6.</b> Growth curve of MSCs	84
<b>Figure 3.7.</b> Representative contour plot of the MSC population	85
<b>Figure 3.8.</b> Human umbilical cord-derived MSCs purchased from ATCC analysed using flow cytometry for the expression of cell surface markers	86
<b>Figure 3.9.</b> Representative images of adipogenic differentiation of MSCs	88
<b>Figure 3.10.</b> Representative images of the chondrogenic differentiation of MSCs	89

<b>Figure 3.11.</b> Representative images of osteogenic differentiation of MSCs	90
<b>Figure 3.12.</b> Analysis of MSC DNA, visualised by gel electrophoresis on 0.8% agarose gel	91
<b>Figure 4.1.</b> Representative images of adipogenic differentiation of MSCs from 10 different donors	107
<b>Figure 4.2.</b> Representative images of Nile red staining of MSCs and differentiated adipocytes	108
<b>Figure 4.3.</b> Flow cytometry of MSCs treated to adipogenic differentiation medium	109
<b>Figure 4.4.</b> Side scatter analysis of MSCs and differentiated adipocytes	110
<b>Figure 4.5.</b> Representative image of the differentiation of 3T3-L1 into adipocytes, upon induction with adipogenic differentiation medium	111
<b>Figure 4.6.</b> Attempt at ceiling culture separation of differentiated adipocytes	112
<b>Figure 4.7.</b> Representative agarose gel electrophoresis of qPCR products of adipocyte-specific genes in MSCs and differentiated adipocytes	113
<b>Figure 4.8.</b> Measurement of an adipogenic marker, peroxisome proliferator activated receptor (PPAR $\gamma$ ) in differentiated adipocytes	114
<b>Figure 4.9.</b> Spearman's Correlation of PPAR $\gamma$ expression between Experiment 1, 2 and 3	115
<b>Figure 4.10.</b> Measurement of the late adipogenic marker, fatty acid binding protein 4 (FABP4) in differentiated adipocytes	116
<b>Figure 4.11.</b> Evaluation of the correlation between gene expression of two adipogenesis markers	117
<b>Figure 4.12.</b> Allelic discrimination plot for rs3810291	119
<b>Figure 4.13.</b> ZC3H4 expression in homozygote majors (AA) and homozygote minors (GG) for rs3810291	120
<b>Figure 4.14.</b> Representative agarose gel electrophoresis of qPCR products for POMC and TRIM66 in MSCs and differentiated adipocytes	121
<b>Figure 4.15.</b> TRIM66 expression in homozygote (CC) and homozygote minors (TT) for rs4929949 and rs10840106	123

<b>Figure 5.1.</b> Schematic diagram of the details of contraction	137
<b>Figure 5.2.</b> Schematic diagram of the method used for the hepatogenic differentiation of MSCs	140
<b>Figure 5.3.</b> Representative images of the morphology of MSCs treated to hepatogenic differentiation medium with 0% FBS (HD+0% FBS)	141
<b>Figure 5.4.</b> Representative images of the morphology of MSCs treated to hepatogenic differentiation medium with 1% FBS (HD+1% FBS)	142
<b>Figure 5.5.</b> Gene expression of hepatogenic markers upon treatment of MSCs from Donor 6, 9 and 14 with hepatogenic differentiation medium	145
<b>Figure 5.6.</b> Preliminary experiment: Upregulation of smooth muscle cell markers upon treatment of MSCs with 10ng/ml TGF- $\beta$ 1 and 1% FBS	147
<b>Figure 5.7.</b> Morphology of MSCs differentiated into SMCs	148
<b>Figure 5.8.</b> Morphology of MSCs differentiated into SMCs after 1:2 split	149
<b>Figure 5.9.</b> Upregulation of smooth muscle cell markers upon treatment of MSCs with 10ng/ml TGF- $\beta$ 1 and 1% FBS	151
<b>Figure 5.10.</b> No upregulation of late smooth muscle cell markers upon treatment of MSCs with 10ng/ml TGF- $\beta$ 1 and 1% FBS	152
<b>Figure 5.11.</b> Downregulation of the Kruppel-like factor 4 ( <i>KLF4</i> ) transcription factor	152
<b>Figure 5.12.</b> Gene expression of vascular smooth muscle cell markers upon treatment of MSCs with SMC differentiation medium + 30 $\mu$ g/ml heparin	153
<b>Figure 5.13.</b> Representative images of immunofluorescence analysis of $\alpha$ -SMA upon treatment of MSCs with 10ng/ml TGF- $\beta$ 1 and 1% FBS	155
<b>Figure 5.14.</b> Representative images of immunofluorescence analysis of calponin upon treatment of MSCs with 10ng/ml TGF- $\beta$ 1 and 1% FBS	156
<b>Figure 5.15.</b> Aortic SMCs loaded with Ca <sup>2+</sup> indicator dye Fura-2	158
<b>Figure 5.16.</b> Representative traces of the effects of Ang II, Carbachol and KCl on aoSMCs	159
<b>Figure 5.17.</b> Representative traces of the effects of Ang II, Carbachol and KCl on MSCs and differentiated SMCs from Donor 6	160
<b>Figure 5.18.</b> Representative traces of the effects of Ang II, Carbachol and KCl on MSCs and differentiated SMCs from Donor 9	161

<b>Figure 5.19.</b> Representative traces of the effects of Ang II, Carbachol and KCl on MSCs and differentiated SMCs from Donor 14	162
<b>Figure 5.20.</b> Contractile response of aoSMCs in response to carbachol treatment	164
<b>Figure 5.21.</b> Contractile response of HeLa cells, MSCs, differentiated SMCs and aoSMCs in response to carbachol treatment	165
<b>Figure 5.22.</b> Representative images of the contractile response of aoSMCs and differentiated SMCs	166
<b>Figure 6.1.</b> Schematic diagram of ADAMTS7 protein	178
<b>Figure 6.2.</b> Proposed mechanism of rs3825807 on vascular SMCs	182
<b>Figure 6.3.</b> Upregulation of <i>ACTA2</i> , <i>ADAMTS7</i> and <i>COMP</i>	186
<b>Figure 6.4.</b> SNP cluster plot for rs3825807 in the MSC bank	187
<b>Figure 6.5.</b> Upregulation of <i>ACTA2</i> in differentiated SMCs from 10 different donors	188
<b>Figure 6.6.</b> <i>ADAMTS7</i> expression in homozygote majors (AA) and homozygote minors (GG) for rs3825807	188
<b>Figure 6.7.</b> Schematic diagram of ADAMTS7 protein and antibody specificity sites	189
<b>Figure 6.8.</b> Representative Western blot of full length ADAMTS7 and fragments in cell lysate	190
<b>Figure 6.9.</b> Western blot of HEK293 cells transfected with ADAMTS7-Ser plasmid	191
<b>Figure 6.10.</b> Western blot of ADAMTS7 and fragments in MSCs and differentiated SMC lysates	192
<b>Figure 6.11.</b> Detection and quantification of cleaved ADAMTS7 prodomain in MSCs and differentiated SMC conditioned media	194
<b>Figure 6.12.</b> Representative images of a scratch assay on MSCs analysed by Image J software	195
<b>Figure 6.13.</b> Reproducibility of the scratch assay	196
<b>Figure 6.14.</b> A scratch assay was carried out on MSCs and differentiated SMCs with the AA or GG genotype for rs3825807	198
<b>Figure S1.</b> The Anthony Nolan Cord Blood Bank Material Transfer Agreement	220

<b>Figure S2.</b> The hospital consent form completed by the baby's mother	224
<b>Figure S3.</b> SNP cluster plots for 50 CAD-associated SNPs for MSC bank	225
<b>Figure S4.</b> The linkage disequilibrium (LD) across ADAMTS7	235

## Abbreviations list

<b>αMEM</b>	Minimum Essential Medium Eagle, Alpha modification
<b>α-SMA</b>	Alpha-smooth muscle actin
<b>36B4</b>	Ribosomal protein large P0 (RPLP0)
<b>3'UTR</b>	Three prime untranslated region
<b>ADAMTS7</b>	A Disintegrin and Metalloproteinase with Thrombospondin Motifs 7
<b>AFP</b>	Alpha-fetoprotein
<b>ALB</b>	Albumin
<b>Ang II</b>	Angiotensin II
<b>ANOVA</b>	Analysis of variance
<b>ANRIL</b>	Antisense non-coding RNA in the INK4 locus
<b>aP2</b>	Adipocyte protein 2
<b>APT</b>	Affymetrix® Power Tools
<b>AoSMC</b>	Aortic smooth muscle cell
<b>APC</b>	Allophycocyanin
<b>bFGF</b>	Basic fibroblast growth factor
<b>BMI</b>	Body mass index
<b>BSA</b>	Bovine serum albumin
<b>C4D</b>	Coronary Artery Disease
<b>CAD</b>	Coronary artery disease
<b>CARDIoGRAM</b>	Coronary ARtery Disease Genome wide Replication and Meta-analysis
<b>CDKN2A</b>	Cyclin-dependent kinase Inhibitor 2A
<b>CDKN2B</b>	Cyclin-dependent kinase Inhibitor 2B
<b>cDNA</b>	Complementary DNA
<b>CEU</b>	Utah Residents (CEPH) with Northern and Western European Ancestry
<b>CFU-F</b>	Colony forming unit - fibroblast
<b>CK19</b>	Cytokeratin 19
<b>COMP</b>	Cartilage oligomeric matrix protein
<b>CVD</b>	Cardiovascular disease
<b>DAPI</b>	4',6-Diamidino-2-Phenylindole, Dilactate

<b>dbSNP</b>	Single nucleotide polymorphism database
<b>DG</b>	Diacylglycerol
<b>DMEM</b>	Dulbecco's Modified Eagle's Medium
<b>DMSO</b>	Dimethyl sulfoxide
<b>DNase</b>	Deoxyribonuclease
<b>dNTP</b>	Deoxynucleotide
<b>DQC</b>	Dish QC
<b>DTT</b>	Dithiothreitol
<b>EDTA</b>	Ethylenediaminetetraacetic acid
<b>EGF</b>	Epidermal growth factor
<b>EMEM</b>	Minimum Essential Medium Eagle
<b>eQTL</b>	Expression quantitative trait locus
<b>ESC</b>	Embryonic stem cell
<b>FABP4</b>	Fatty acid binding protein 4
<b>FBS</b>	Fetal bovine serum
<b>FDR</b>	False discovery rate
<b>FH</b>	Familial hypercholesterolaemia
<b>FITC</b>	Fluorescein isothiocyanate
<b>FS</b>	Forward scatter
<b>FTO</b>	Fat mass and obesity associated
<b>GIANT</b>	Genetic Investigation of ANthropometric Traits
<b>GPCR</b>	G-protein-coupled receptor
<b>GTC</b>	Genotyping Console™
<b>GWAS</b>	Genome wide association study
<b>HBSS</b>	Hanks' Balanced Salt Solution
<b>HDL-C</b>	High density lipoprotein-cholesterol
<b>HGF</b>	Hepatocyte growth factor
<b>HWE</b>	Hardy-Weinberg equilibrium
<b>IBMX</b>	3-isobutyl-1-methylxanthine
<b>IFN<math>\gamma</math></b>	Interferon gamma
<b>IL-1<math>\beta</math></b>	Interleukin 1 beta
<b>IMDM</b>	Iscove's Modified Dulbecco's Medium
<b>IP<math>_3</math></b>	Inositol triphosphate

<b>iPSC</b>	Induced pluripotent stem cell
<b>ISCT</b>	International Society for Cellular Therapy
<b>ITS</b>	Insulin-Transferrin-Selenium
<b>KLF4</b>	Kruppel-like factor 4
<b>LD</b>	Linkage disequilibrium
<b>LDL-C</b>	Low density lipoprotein-cholesterol
<b>LDLR</b>	Low density lipoprotein receptor
<b>LOD</b>	Log of Odds
<b>MAF</b>	Minor allele frequency
<b>MI</b>	Myocardial infarction
<b>miRNA</b>	MicroRNA
<b>MLC</b>	Myosin light-chain
<b>MSC</b>	Mesenchymal stem cell
<b>NBF</b>	Neutral-Buffered Formalin
<b>NTC</b>	No template control
<b>OR</b>	Odds ratio
<b>OSM</b>	Oncostatin M
<b>P5</b>	Passage 5
<b>PBS</b>	Phosphate Buffered Saline
<b>PCK1</b>	Phosphoenolpyruvate carboxykinase 1
<b>PCR</b>	Polymerase chain reaction
<b>PCSK9</b>	Proprotein convertase subtilisin/kexin type 9
<b>PDGF-BB</b>	Platelet derived growth factor BB
<b>PDN</b>	Population doubling number
<b>PDT</b>	Population doubling time
<b>PE</b>	Phycoerythrin
<b>PerCP-Cy5.5</b>	Peridinin chlorophyll protein with cyanine dye
<b>PFA</b>	Paraformaldehyde
<b>PKC</b>	Protein kinase C
<b>PPAR<math>\gamma</math></b>	Peroxisome proliferator activated receptor gamma
<b>QC</b>	Quality control
<b>qPCR</b>	Quantitative polymerase chain reaction
<b>RNA</b>	Ribonucleic acid

<b>RNase</b>	Ribonuclease
<b>rpm</b>	Revolutions per minute
<b>RT</b>	Reverse transcriptase
<b>SD</b>	Standard deviation
<b>SEM</b>	Standard error of the mean
<b>SM22<math>\alpha</math></b>	Smooth muscle protein 22-alpha
<b>SMC</b>	Smooth muscle cell
<b>SM-MHC</b>	Smooth muscle-myosin heavy chain
<b>SNP</b>	Single nucleotide polymorphism
<b>SS</b>	Side scatter
<b>TGF-<math>\beta</math>1</b>	Transforming growth factor-beta 1
<b>TNF-<math>\alpha</math></b>	Tumour necrosis factor-alpha
<b>TRIM66</b>	Tripartite Motif Containing 66
<b>TSP1</b>	Thrombospondin 1
<b>TSR</b>	Thrombospondin type 1 repeat
<b>WJ</b>	Wharton's jelly
<b>WTCCC</b>	Wellcome Trust Case Control Consortium
<b>YRI</b>	Yoruba in Ibadan, Nigeria
<b>ZC3H4</b>	Zinc Finger CCCH-Type Containing 4

# **Chapter 1- Introduction**

## **1.1 Coronary artery disease**

Cardiovascular disease (CVD) is a group of diseases that involve the heart and blood vessels. Common CVDs include, amongst others, coronary artery disease (CAD), peripheral arterial disease, congenital heart disease, ischaemic heart disease and cardiomyopathy.

CAD is the most common form of heart disease. It is the primary cause of morbidity and mortality in the UK and worldwide, and the occurrence of CAD is rapidly increasing in developing countries (Mackay & Mensah, 2004). Approximately 17.5 million people died from CVDs in 2012, of these 7.4 million were because of CAD (World Health Organisation, 2015). Since 1990, globally more individuals have died from CAD than any other cause, and by 2030, nearly 23.6 million people will die as a result of CAD (Lloyd-Jones *et al.*, 2009). In an individual, CAD develops gradually and is therefore seen as a disease of the elderly. CAD becomes clinically apparent at 40, but people aged 65 and above account for approximately 85% of all CAD deaths (Boudi, 2013). In addition, in 2011 the cost of CAD to the NHS was approximately £6.7 billion (British Heart Foundation, 2012). So it is vital that we continue to increase our knowledge of the underlying biological mechanisms of CAD, in order to target them for therapeutic purposes, to reduce the medical, social and economic burden caused by CAD.

## **1.2 Overview of CAD pathobiology**

CAD is a complex health condition that develops over an individuals' lifetime, normally intensified by a combination of environmental and genetic risk factors. CAD occurs when the arteries that deliver oxygen-rich blood to the heart (known as the coronary arteries) narrow due to a gradual build up of fatty material in the artery wall. This condition is called atherosclerosis; it is a chronic progressive disease that remains asymptomatic for decades, and is the single most important contributor of CAD. Atherosclerosis is the result of four main steps; 1) injury and activation of the endothelium, 2) lipid accumulation,

modification, and foam cell formation, 3) growth and fibrous cap formation and 4) plaque rupture.

A normal artery has three layers; the tunica intima (inner layer), tunica media (middle layer) and the adventitia (outer layer of the artery; **Figure 1.1A**). The tunica intima is lined by an endothelial cell monolayer which is in direct contact with flowing blood. The monolayer is underlined by a basement membrane which supports the endothelium. The intima also contains smooth muscle cells (SMCs). The tunica media, the muscular middle layer, contains more SMCs than the tunica intima, where SMCs are present in a complex extracellular matrix. The adventitia (also known as the tunica externa) is the outer layer of the arteries; it consists of connective tissue (primarily collagen) microvessels, nerve endings and mast cells (Libby *et al.*, 2011).

The understanding of the pathobiology of CAD has evolved hugely over the past century. Animal experiments and human samples postulate, the first event of atherosclerosis to occur, is a change in the endothelial cell monolayer that is in direct contact with flowing blood. The endothelium is subject to important hemodynamic forces, which are not uniform within the vasculature. The blood flow is laminar in straight parts of the vascular system, whereas at regions of arterial branching or curvature, blood flow is disturbed and the wall is subject to low shear stress. It is at these regions atherosclerotic plaques are predisposed to develop (Gimbrone, 1999).

The endothelium is an important organ system required to preserve the integrity and vascular tone of the arterial wall (Jackson *et al.*, 2012). Under normal conditions, leukocytes (white blood cells) do not attach to the endothelial cell monolayer. Upon vascular injury or when endothelial cells are exposed to irritative stimuli (e.g. high cholesterol levels or pro-inflammatory cytokines), they express adhesion molecules that stimulate rolling and adhesion of leukocytes to endothelial cells. Vascular cell adhesion molecule-1 (VCAM-1) is an example of a molecule that is expressed by endothelial cells upon cholesterol exposure, which enables leukocytes to bind to the endothelium at sites of plaque initiation (Cybulsky & Gimbrone, 1991). Interleukin-8 (IL-8), intercellular adhesion molecule (ICAM-1), E selectin and P selectin, are other chemokines and

adhesion molecules involved in this process (Businaro *et al.*, 2012). Next leukocytes are directed into the tunica intima at the junctions of endothelial cells by a process called diapedesis. Monocyte chemoattractant protein-1 (MCP-1) is a chemoattractant mediator, and is thought to mediate this process (Businaro *et al.*, 2012).

Simultaneous changes in endothelial cell and the basement membrane permeability, enables the entry of low-density lipoprotein cholesterol (LDL-C) into the arterial wall. LDL-C becomes trapped in the vessel wall and is subject to modification, including lipolysis, oxidation, proteolysis and aggregation. These modified particles can induce further leukocyte adhesion and contribute heavily to inflammation. Oxidative waste from SMCs can also result in LDL-C oxidation, where these molecules have pro-inflammatory activity. LDL-C modification is a significant step in early lesion formation (Lusis, 2000).

The main leukocytes that pass into the tunica intima, are monocytes (phagocytes), lymphocytes and to a lesser extent granulocytes. Monocytes differentiate into tissue macrophages and upregulate expression of scavenger receptors, such as CD36 and scavenger receptor A (SRA), and engulf modified LDL-C. These monocytes become lipid-laden macrophages, known as foam cells, which are a feature of an early atherosclerotic lesion (**Figure 1.1B**). Macrophages within the plaque secrete various pro-inflammatory cytokines and growth factors e.g. interleukin-1 $\beta$  (IL-1 $\beta$ ) and tumour-necrosis factor (TNF) that are implicated in plaque progression. Also, macrophages are able to undergo proliferation within the intima (Libby, 2002). Other types of leukocytes, such as lymphocytes and mast cells also build up in the plaque, but at a much lower number compared to monocytes.

Atheroma formation also involves SMCs. Resident SMCs are found in the tunica intima, however additional SMCs migrate from the tunica media to the tunica intima. SMCs undergo proliferation, upon stimulation with factors (e.g. platelet-derived growth factor) and secrete extracellular matrix components (such as collagen, elastin and proteoglycans) in the intima, which leads to the formation of a fibrous cap that covers the plaque (**Figure 1.1C**). Underneath the cap is a population of macrophage-derived foam cells. These and SMCs can

undergo apoptosis, however the dead cells are inefficiently cleared (a process called efferocytosis). This leads to a build-up of extracellular lipids and cellular debris that have been released from dead cells, forming the lipid-rich 'necrotic' core of the plaque (Tabas, 2010).

Calcification and neovascularization are common features of an 'advanced lesion', as they contribute to the stability of the lesion. Intimal calcification is a process whereby matrix scaffold is secreted by pericyte-like cells and becomes calcified. Oxysterols (oxidised derivatives of cholesterol) and cytokines regulate this process (Watson *et al.*, 1994). Neovascularization is the formation of small blood vessels, and this can occur within the tunica media, providing a channel for the entry of inflammatory cells.

Primary lesions are also known as 'fatty streaks', and are not clinically significant. Clinical manifestations are seen upon a more advanced lesion. The plaque can cause narrowing of the artery, which can lead to angina. Physical disruption of the plaque can also occur, which exposes the pro-coagulant proteins in the core of the plaque, to coagulation components in the blood, and can lead to the development of thrombosis (**Figure 1.1D**). Macrophages produce tissue factor (a pro-coagulant factor which initiates the coagulation cascade) that causes the lipid core to be thrombogenic. Oxidised LDL also causes endothelial cells to produce tissue factor (Schönbeck *et al.*, 1999). A thrombus can interrupt blood flow locally, or can come away and obstruct distal arteries, resulting in myocardial infarction (MI) or stroke (Watkins & Farrall, 2006). A plaque susceptible to rupture has a thin, collagen-poor fibrous cap, with few SMCs and numerous macrophages. Plaque disruption can be accelerated by collagenolytic enzymes that degrade collagen. In addition, inflammatory cells can produce mediators that cause SMC apoptosis, the principle source of collagen in the arterial wall (Libby, 2009).

In summary, atherosclerosis is a complex process that occurs over an individual's lifetime. It is comprised of a series of steps involving the arterial wall and blood components, where inflammation plays a key role. Atherosclerosis can ultimately lead to morbidity and mortality.

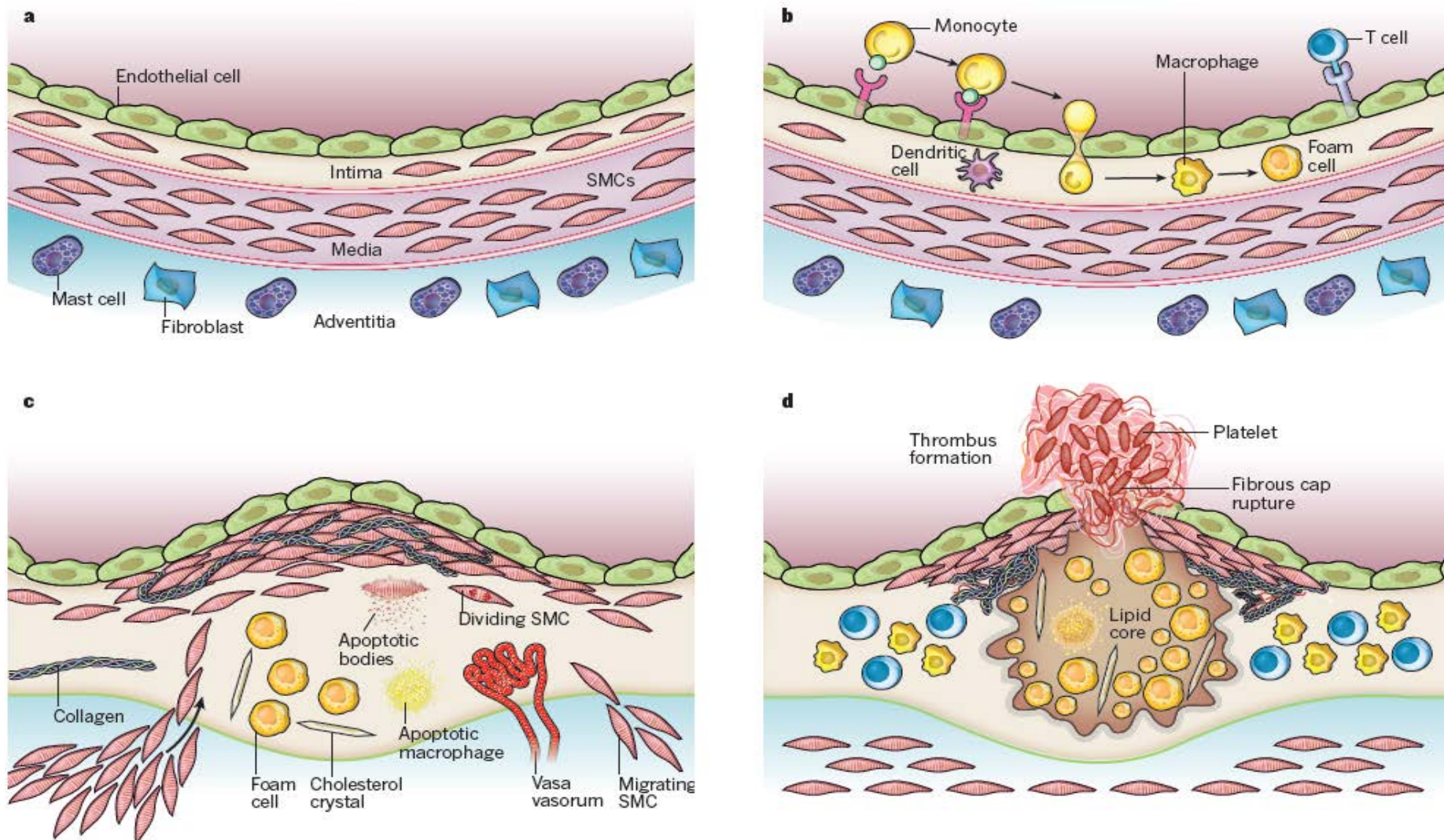


**Figure 1.1. An overview of the formation of an atherosclerotic lesion. (A)** A normal artery. **(B)** The first steps of atherosclerosis, including adhesion of monocytes to endothelial cells. **(C)** Progression of the plaque including the migration of SMCs into the intima **(D)** Physical disruption of the plaque leads to thrombus formation (Libby *et al.*, 2011).

### 1.3 Risk factors of CAD

A risk factor is a measurable variable or characteristic that associates with an increased risk of disease. The risk factors for CAD which include various environmental, lifestyle and genetic factors are well documented (**Figure 1.2**). The age of onset and severity of CAD depend on these risk factors, where an understanding is imperative in early identification, monitoring and treatment of individuals with high risk, to overall reduce the CAD burden, as small changes in lifestyle can reduce an individual's risk. For example, a CAD patient who stops smoking is associated with a 36% reduction in risk of total mortality (Critchley & Capewell, 2004).

In 1948, the USA Public Health Service set up the Framingham Heart Study to study the epidemiology and risk factors for CVD (Dawber *et al.*, 1951). The aim of the project was to investigate the development of CVD over time, in a large group of participants. After four years, researchers discovered high blood pressure and high cholesterol were risk factors for the development of CVD (Dawber *et al.*, 1957). The Framingham Heart Study has discovered many other risk factors since; changing the way CVD is managed in the clinic. It has also led to the development of the Framingham Risk Score calculator, which is a sex-specific algorithm that can be used to estimate a patient's 10-year risk of CVD (Wilson *et al.*, 1998).

The traditional risk factors for CVD are high blood pressure (hypertension), high cholesterol, age, smoking, diabetes mellitus and positive family history (Cleeman *et al.*, 2001). Diabetes mellitus, obesity, a diet high in cholesterol, smoking, hypertension and an inactive lifestyle are modifiable risk factors. The non-modifiable risk factors are sex, advanced age and family history of CAD. Additional risk factors and subclinical disease markers have also been identified (**Figure 1.2**).

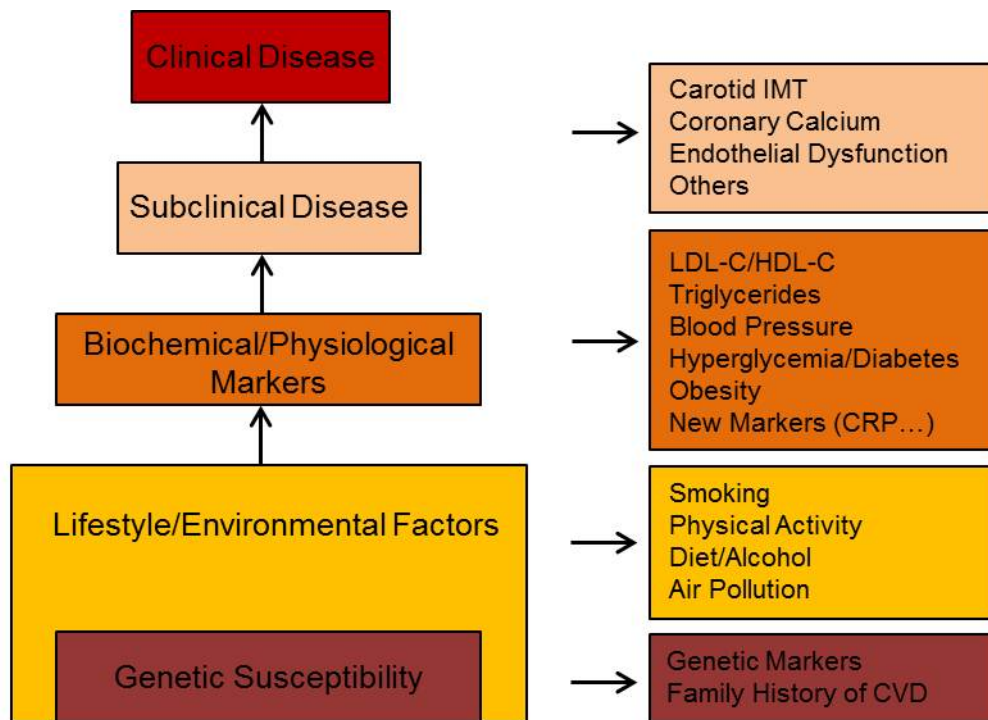


**Figure 1.2. The risk factors for cardiovascular disease.** CRP; C-reactive protein, LDL-C; low density lipoprotein cholesterol, HDL-C; high density lipoprotein cholesterol, IMT; intimal medial thickness (O'Donnell and Elosua, 2008).

#### 1.4 Genetic contribution of CAD

The contribution of the heritability of CAD has been shown to be between 40-60% (Girelli *et al.*, 2009), supported by epidemiological and family studies. Reports from the Framingham Heart Study demonstrated that men and women with a family history of CAD had a 2.4-fold and 2.2-fold increased risk of CAD, respectively (Schildkraut *et al.*, 1989). Additional studies have shown that the offspring of an affected parent are two-fold more likely to be at risk from CAD (Yusuf *et al.*, 2004; Cremer *et al.*, 1997; Murabito *et al.*, 2005; Chow *et al.*, 2011; Lloyd-Jones *et al.*, 2004). These families with a positive family history of CAD represent 72% of premature CAD cases and 48% of complete cases, but only make up 14% of the total population, illustrating the significance of the genetic predisposition for CAD (Williams *et al.*, 2001). In addition, twin studies have shown that an individual with an affected twin exhibited a 4-fold and 8-fold increased susceptibility if they were dizygotic and monozygotic twins, respectively (Marenberg *et al.*, 1994). Also, Sorensen *et al.*, (1988) study

supports the strong correlation between genetics and CAD risk. A Danish population consisting of 1000 families were investigated. The study showed that biological parents who died before the age of 50 due to vascular disease, was correlated with a 4.5-fold increase of the offspring dying from the same cause. However when the adoptive parent died from a similar cause, the risk of the offspring was not significantly increased. Furthermore, imaging-based studies have shown that the anatomy of CAD (i.e. ectasia, coronary calcifications, left main stem and proximal left anterior descending disease) is inherited, whilst carotid intima-media thickness and calcium scores, two further markers of CAD, have also shown to increase in families with a history of early CAD (Wang *et al.*, 2003b; Nasir *et al.*, 2004; Nasir *et al.*, 2007; Fischer *et al.*, 2005; Fischer *et al.*, 2007). Many of the CAD risk factors, including high cholesterol levels and diabetes mellitus also have their own strong genetic component. Consequently, these two conditions also lead to the development of CAD. However the genetic risk for CAD is a fixed factor, independent of other risk factors such as obesity, cigarette smoking, diabetes mellitus and hypertension (Roberts & Stewart, 2012). Overall there is significant evidence illustrating the strong genetic component of CAD.

### **1.5 Mendelian disorders that manifest CAD**

Mendelian disorders are single-gene traits that transmit in families through an autosomal dominant, autosomal recessive or an X-linked pattern. Mendelian disorders that clinically manifest CAD explain only a minor subset of familial CAD, but have led to fundamental insights into the biology of the disease. Over the past 50 years, gene mutations that cause Mendelian disorders manifesting premature CAD have been identified. One example of a Mendelian disorder is familial hypercholesterolemia (FH), which is an autosomal dominant disorder that occurs in 1/500 individuals. It is due to mutations (more than 700 have been identified) in the low density lipoprotein receptor (*LDLR*) gene (Heath *et al.*, 2000; Villéger *et al.*, 2002). *LDLR* encodes the LDLR protein which is a cell surface receptor that mediates the endocytosis of LDL particles from the plasma. Mutations in *LDLR* result in abnormal or non-functional LDLR,

and are classified according to their effect on the LDLR protein function (Hobbs *et al.*, 1992). In addition to *LDLR*, mutations have been identified in apolipoprotein B (*APOB*) and proprotein convertase subtilisin/kexin type 9 (*PCSK9*) which also cause FH. The analysis of individuals with homozygous FH at the molecular level, has led to the identification of the pathways involved in LDL cholesterol metabolism (Goldstein & Brown, 1973), resulting in the development of statins (Stossel, 2008).

There are other Mendelian disorders that are as a result of rare mutations in ATP-binding cassette A1 (*ABCA1*), apolipoprotein A-1 (*APOA1*) and lecithin-cholesterol acyltransferase (*LCAT*), which influence high-density lipoprotein cholesterol (HDL-C) metabolism, and are linked to Hypoalphalipoproteinemia (deficiency of low HDL-C in the blood; Frikke-Schmidt *et al.*, 2004; Cohen *et al.*, 2004).

Tangier disease and Sitosterolemia are two rare genetic lipid disorders. The study of these two diseases has enabled a deep understanding of sterol transport. Tangier disease is caused by mutations in ATP-binding cassette 1 (*ABC1*) encoding a member of the ABC transporter family. The distinct phenotype of this disease is near or complete absence of apolipoprotein A-I (a component of HDL-C), and substantial deposition of cholesterol ester in macrophages (Bodzioch *et al.*, 1999; Brooks-Wilson *et al.*, 1999; Rust *et al.*, 1999). Sitosterolemia is caused by mutations in *ABCG5* and *ABCG8* resulting in abnormalities in sterol absorption and secretion, leading to increased levels of plasma LDL-C levels (Berge *et al.*, 2000; Lee *et al.*, 2001). These are prominent examples of Mendelian disorders in the CAD field, however most CAD traits show complex inheritance.

## **1.6 Genetic architecture of CAD**

To successfully map all of the genetic components for CAD is dependent on the number of disease-associated genes, their allele frequencies and level of risk, and their interaction with environmental factors (Wright & Hastie, 2001; Reich & Lander, 2001). To complicate matters, certain CAD risk factors have

their own heritable component, for example the contribution of the heritability of Type 2 diabetes is between 40-80% (Barnett *et al.*, 1981; Gottlieb & Root, 1968; Harvald & Hauge, 1963; Newman *et al.*, 1987). In addition, premature CAD (onset before the age of 50) is rare and hence unlikely to affect reproductive success, and therefore less likely to be under selective pressure. So CAD risk or non-risk alleles may have evolved neutrally in the past, and are therefore present in the population at a range of different frequencies. This notion is the basis of the Common Disease, Common Variant hypothesis, which predicts that for common diseases such as CAD, many genetic variations with a relatively high frequency (>1%) across the genome each exert a small-to-modest effect to contribute to the disease phenotype (Reich & Lander, 2001). On the other hand, a Common Disease, Rare Variant hypothesis has been proposed. This model argues that rare variants (<1%), with relatively high penetrance and extensive allelic heterogeneity are the major contributors of common diseases (Wright & Hastie, 2001; Pritchard, 2001). Candidate gene and genome-wide association studies (GWASs) have supported both models, as they highlight the importance of common CAD alleles (Lohmueller *et al.*, 2003; the Wellcome Trust Case-Control Consortium (WTCCC), 2007) and rare allelic variants e.g. variants in *ABCA1* (Frikke-Schmidt *et al.*, 2004; Cohen *et al.*, 2004). The most probable scenario is complex diseases arise due to common and rare variants which contribute to the risk of CAD. The main point is no single locus or variant is sufficient to cause the disease.

Over the years, different methods have been utilized in an attempt to identify all the genetic components of CAD. These methods include linkage studies, candidate gene studies and GWASs.

## **1.7 Studies to identify causative genes for CAD**

### **1.7.1 Linkage analysis studies**

Initially linkage analysis studies were attempted to identify CAD genes. The method aims to identify a genetic marker (e.g. microsatellites) that co-transmits with the disease in a family pedigree. This required the selection of

many families with CAD or MI, including sib pairs. Genetic markers that evenly spanned the genome were used. The aim of the study is to discover significant linkage peaks (LOD score of greater than 3.5;  $p=1 \times 10^{-6}$ ), suggesting that a nearby gene is in linkage disequilibrium (LD) with the marker. As the position of the genetic marker is known, it is possible to map where the disease gene resides in the genome, and more specifically on which chromosome.

This approach has had several successes, including the identification of variants in the *ALOX5AP* gene (encoding 5-lipoxygenase activation protein, FLAP). The variants are implicated in the pathogenesis of MI and stroke by causing an increase in leukotriene production and subsequent increased inflammation within the wall of the arteries (Helgadottir *et al.*, 2004). Myocyte enhancer factor 2A (*MEF2A*), was also identified by linkage analysis using a pedigree, where 13 individuals had CAD. *MEF2A* is a transcription factor expressed in the endothelium of the coronary artery (Wang *et al.*, 2003a).

Excluding the several successes that have identified CAD-related genes, overall linkage analysis has been ineffective. The results are impossible to replicate for small effect, low-penetrance mutations because of low statistical power, and the approach is limited in the search to determine all the genetic components of CAD. In addition, genetic and phenotypic heterogeneity are confounding variables that reduce the power of linkage studies (Ekstrom & Dalgaard, 2003). Also, as this approach identifies the chromosomal region and not the genes directly, excluding a few cases, it is not a direct comparison method (Helgadottir *et al.*, 2004; Wang *et al.*, 2003a).

### **1.7.2 Candidate gene studies**

Candidate gene studies are based on an approach, which studies genes that encode proteins already known to be involved in pathological processes of the disease. Variation in the 'candidate gene' is hypothesised to either alter gene expression or affect protein function, resulting in disease (Kwon & Goate, 2000). For example, it was observed that inflammatory responses in atherosclerosis and chronic infection overlapped, and therefore pathogens may

prompt the formation of plaques in the arteries (Campbell & Kuo, 2004). Genes implicated in innate immunity were classified as candidate genes for CAD. One of the first candidate genes identified was *CD14*, which encodes a membrane bound glycoprotein receptor for lipopolysaccharide. A polymorphism in the promoter region (C260Thr) has been suggested to enhance transcriptional activity (Ameziane *et al.*, 2003; Arroyo-Espliguero *et al.*, 2004a; Kiechl *et al.*, 2002; LeVan *et al.*, 2001). Case-control studies have frequently investigated this variant; however consistent results have not been found (Arroyo-Espliguero *et al.*, 2004b). Leukotriene A4 hydrolase (*LTA4H*) is another gene that also associates with CAD, showing a modest association in Europeans, but a strong association in African Americans (Helgadottir *et al.*, 2006). Another study identified polymorphisms in lymphotoxin- $\alpha$  (*LTA*) gene, which encodes a member of the TNF family. 93,000 SNPs primarily based in genes were analysed in a Japanese case-control study, where they discovered *LTA* associated with MI (Ozaki *et al.*, 2002). A later study, using a larger cohort did not replicate this finding (Clarke *et al.*, 2006).

Candidate gene studies are also limited in their approach. Firstly, the function of all 20,000-25,000 genes in the human genome and their relationship with CAD remains unknown; therefore this approach is biased towards genes of known function. Secondly, this method primarily concentrates on introns, exons and adjacent regions of the gene. However, these regions only make up a small part of the genome, as the remaining genome is comprised of intergenic DNA. These intergenic regions can contain different DNA elements, such as enhancers and long non-coding RNAs. These can affect gene expression, yet these elements are not considered in candidate gene studies (Grant *et al.*, 2006). GWASs are a recent approach that has widely been used to unravel the heritable basis of complex diseases, as it overcomes many of the limitations presented by linkage and candidate gene studies.

### **1.7.3 Genome-wide association studies**

A GWAS is a 'hypothesis-free' approach to identify single nucleotide polymorphisms (SNPs) associated with complex human diseases. The feasibility of GWASs is due to the ability to measure human variation. The

human genome contains approximately 3.1 billion base pairs, of which 0.1% (~3 million base pairs) determines our inter-individuality. The majority of studies on human genetic variation have focussed on SNPs. SNPs are common genetic variants, which differ in base pair (adenine (A), guanine (G), cytosine (C) or thymidine (T)) between individuals in a population. SNPs that are linked with each other on a specific chromosome, are known as a haplotype, and are inherited together. The International HapMap Project is an international collaborative project, which aimed to produce a haplotype map of the human genome. Phase I of the HapMap Project was launched in 2002, 1.3 million SNPs were genotyped in 270 individuals, where at least one common SNP was genotyped every 5kb (International HapMap Consortium, 2005). For Phase II of the project, an additional 2.1 million SNPs were genotyped in the same 270 individuals. This has resulted in one SNP being genotyped every 1kb, covering roughly 25-35% of the 9-10 million common SNPs, with minor allele frequencies (MAFs) greater than 0.05 in the human genome (International HapMap Consortium, 2007). Phase III of the project, genotyped 1.6 million SNPs, in 914 individuals, in addition to the 270 individuals' genotyped in Phase I and II to provide further genetic variation data (International HapMap 3 Consortium, 2010).

The development and use of microarrays have also enabled the implementation of GWASs to study complex diseases. In 2005, a microarray that typed for 500,000 markers was developed. Microarrays were further improved to type up to 1 million SNPs, which were evenly spread across the genome (one every 6000 nucleotides; LaFramboise, 2009). As the HapMap project annotated SNPs to a genomic region, data from microarrays are able to be mapped to a chromosomal location. In addition, the use of powerful statistical and computational methods has enabled large-scale GWASs.

GWASs exploit the inter-individual variation that occurs between healthy individuals and individuals with the disease. The approach rapidly scans and compares the frequency of SNPs, across the genome of two large groups; healthy individuals (controls) and individuals with the disease (cases), to identify genetic variants associated with a disease (**Figure 1.3**). GWASs are unbiased, as it provides a comprehensive coverage of the genome, whilst making no prior

assumptions of the location and function of genomic regions. If a SNP is more common in cases than controls, the SNP is associated with an increased disease risk (Roberts & Stewart, 2012). The effect size of the risk allele can be measured, and is known as the odds ratio (OR).

To calculate the association of SNPs with disease requires a large number of statistical tests, where some analyses will have a p-value less than 0.05 purely due to chance. The Bonferroni correction and false discovery rate (FDR) are two approaches used to reduce the number of 'false discoveries' in GWASs. For example, analysing 1 million SNPs, a p-value of 0.05 would give approximately 25,000 false positives. Using a Bonferroni correction, where the p-value of 0.05 is divided by 1 million SNPs, provides researchers with a corrected value of  $5 \times 10^{-8}$ . The difference between the frequency of a particular SNP in both populations has to reach or exceed a 'genome-wide' significance level by at least obtaining a p-value of  $5 \times 10^{-8}$  (Petretto *et al.*, 2007). However using a Bonferroni correction also reduces the number of truly positive results that are detected. The FDR was first described by Benjamini & Hochberg, (1995) and is a recent approach being used. Like a Bonferroni correction it also determines an adjusted p-value for every test; however it assesses the proportion of false positives among all the significant results. It is a less conservative test than the Bonferroni correction, which enables it to have greater power to identify truly significant results. Upon analysis, if a SNP is significantly associated with disease in the discovery population, it has to be confirmed in an independent population (known as a replication cohort). Researchers have utilized this approach to identify loci across the genome that associate with a particular complex disease or trait e.g. LDL-C.

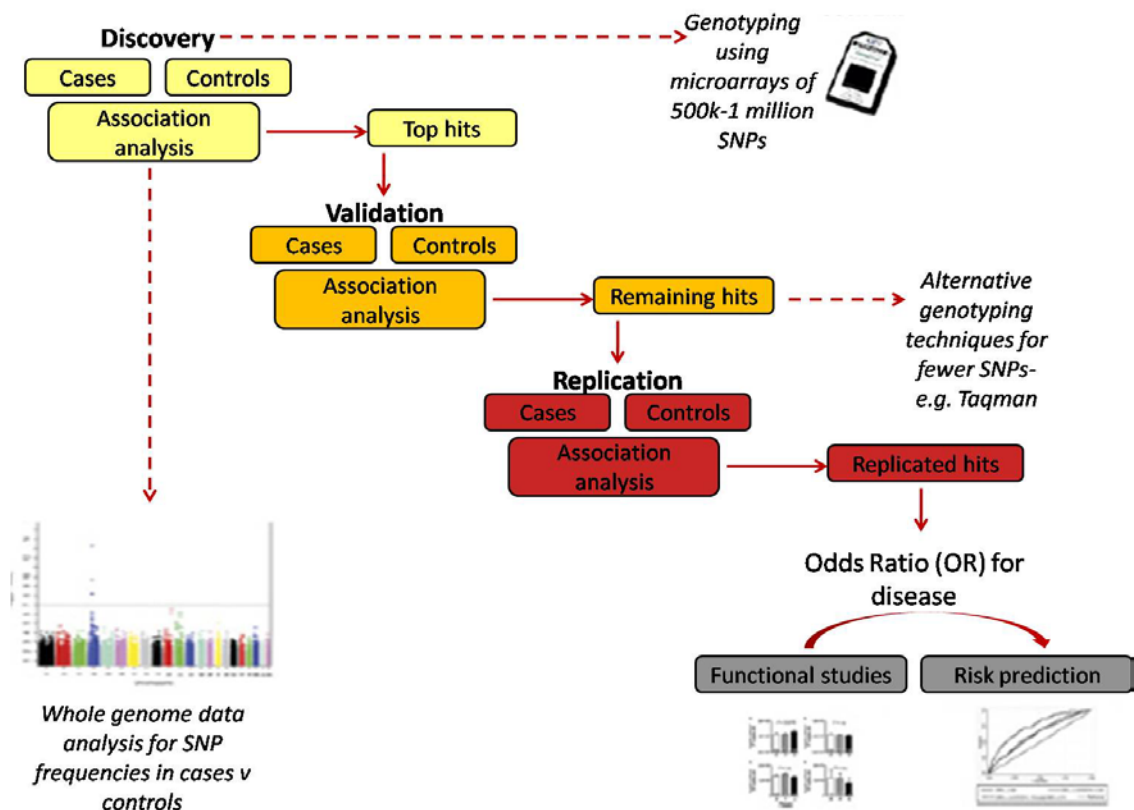


**Figure 1.3. Outline of the methodology for genome-wide association studies.** DNA from healthy individuals (controls) and individuals with the disease (cases) are genotyped using microarrays with between 500,000 to 1 million single nucleotide polymorphisms (SNPs). GWA-specific algorithms identify significant differences between the frequency of a particular SNP in both populations. 'Top hits' are further analysed in an independent replication population. If a SNP is more common in cases, than controls, the SNP is associated with an increased disease risk. Measuring the effect size of the allele is known as the odds ratio (OR). The disease loci are additionally analysed to identify casual variants and potential biological mechanisms the risk alleles may act through (Patel & Ye, 2011).

#### 1.7.4 Genome-wide association studies for CAD

GWASs have been used to identify genetic variants associated with CAD. In 2007, three research groups independently identified a region on chromosome 9p21, that associated strongly with CAD. Samani *et al.*, (2007) conducted a study using 1,926 cases and 2,938 controls from the WTCCC study. The study was replicated in the German MI family study, which consisted of 875 cases and 1,644 control subjects. The Gene Chip Human Mapping 500K Array Set was used to genotype all the samples. A 100 kb region at the 9p21.3

region was strongly associated with CAD in both cohorts. The lead SNP for this region was rs1333049 ( $p= 1.80 \times 10^{-14}$  (WTCCC) and  $p= 3.4 \times 10^{-6}$  (German MI Family Study)) which showed an OR of 1.9 for homozygote majors for the risk allele.

Helgadóttir *et al.*, (2007) led a GWAS that comprised of 4,587 cases of Icelandic patients with MI and 12,767 controls. Using the Illumina Hap300 Chip, 305,953 SNPs were genotyped for all the samples. They identified a common genetic variant on chromosome 9p21, located in a 190 kb linkage block associated with 1.64 increased risk of MI in homozygotes for the risk allele.

McPherson *et al.*, (2007) undertook a study using six independent cohorts, including more than 23,000 participants, and genotyped 100,000 SNPs. They identified a 58 kb interval on chromosome 9p21 associated with CAD.

These three independent studies, using different cohorts, identified the same region on 9p21 to be associated with CAD. 25% of Caucasians are homozygous for the risk allele, and these individuals have an increased relative risk for CAD between 30-40% (Helgadóttir *et al.*, 2007). The risk caused by this genomic region, estimated to be present in more than  $4 \times 10^9$  individuals, was independent of traditional risk factors and therefore represents a novel risk (Roberts & Stewart, 2012).

The three GWASs conducted in 2007, in addition to further studies identified other variants significantly associated with CAD detailed in **Table 1.1**. Subsequently it was hypothesised that larger case-control populations were required to detect lower frequency SNPs. Upon this basis the Coronary ARtery Disease Genome wide Replication and Meta-analysis (CARDIoGRAM) consortium was formed which included a sample size of more than 88,000 individuals where 13 new CAD-associated variants were identified (Schunkert *et al.*, 2011). Another consortium the Coronary Artery Disease (C4D) Genetics Consortium combined with CARDIoGRAM to carry out a meta-analysis on over 240,000 individuals, which lead to the discovery of another 15 novel variants (Deloukas *et al.*, 2013).

Chr.	SNP	Nearest Gene(s)	Risk Allele Freq.	Odds Ratio (95% CI)	Year Discovered
<b>Risk variants associated with LDL cholesterol</b>					
6p25.3	rs3798220	LPA	0.02 (C)	1.92 (1.48-2.49)	2009
2p24.1	rs515135	APOB	0.83 (G)	1.03	2012
1p13.3	rs599839	SORT1	0.78 (A)	1.29 (1.18-1.40)	2007
19p13.2	rs1122608	LDLR	0.77 (G)	1.14 (1.09-1.19)	2009
19q13.32	rs2075650	APOE	0.14 (G)	1.14 (1.09-1.19)	2011
2p21	rs6544713	ABCG5-ABCG8	0.29 (G)	1.07 (1.04-1.11)	2011
1p32.3	rs11206510	PCSK9	0.82 (T)	1.15 (1.10-1.21)	2009
<b>Risk variants associated with HDL cholesterol</b>					
6p21.31	rs12205331	ANKS1A	0.81 (C)	1.04	2012
<b>Risk variants associated with triglycerides</b>					
8q24.13	rs10808546	TRIB1	0.65 (A)	1.08 (1.04-1.12)	2011
11q23.3	rs964184	ZNF259-APOA5-A4-C3-A1	0.13 (G)	1.13 (1.10-1.16)	2011
<b>Risk variants associated with hypertension</b>					
12q24.12	rs3184504	SH2B3	0.44 (T)	1.13 (1.08-1.18)	2009
10q24.32	rs12413409	CYP17A1, CNM2, NT5C2	0.89 (G)	1.12 (1.08-1.16)	2011
4q31.1	rs7692387	GUCYA3	0.81 (G)	1.13	2012
15q26.1	rs17514846	FURIN-FES	0.44 (A)	1.04	2012
<b>Risk variants associated with myocardial infarction</b>					
9p34.2	rs579459	ABO	0.21 (C)	1.10 (1.07-1.13)	2011
<b>Risk variants (mechanism of unknown risk)</b>					
9p21.3	rs4977574	CDKN2A, CDKN2B	0.46 (G)	1.25 (1.18-1.31) to (1.37 (1.26-1.48)	2007
1q41	rs17465637	MIA3	0.74 (C)	1.20 (1.12-1.30)	2007
10q11.21	rs1746048	CXCL12	0.87 (C)	1.33 (1.20-1.48)	2007
2q33.1	rs6725887	WDR12	0.15 (C)	1.16 (1.10-1.22)	2009
6p24.1	rs12526453	PHACTR1	0.67 (C)	1.13 (1.09-1.17)	2009
21q22.11	rs9982601	MRPS6	0.15 (T)	1.19 (1.13-1.27)	2009
3q22.3	rs2306374	MRAS	0.18 (C)	1.15 (1.11-1.19)	2009
10p11.23	rs2505083	KIAA1462	0.42 (C)	1.07 (1.04-1.09)	2010
1p32.2	rs17114036	PPAP2B	0.91 (A)	1.17 (1.13-1.22)	2011
5q31.1	rs2706399	IL5	0.48 (A)	1.02 (1.01-1.03)	2011
6q23.2	rs12190287	TCF21	0.62 (C)	1.08 (1.06-1.10)	2011
7q22.3	rs10953541	BCAP29	0.75 (C)	1.08 (1.05-1.11)	2011
7q32.2	rs11556924	ZC3HC1	0.62 (C)	1.09 (1.07-1.12)	2011
10q23.31	rs1412444	LIPA	0.34 (T)	1.09 (1.07-1.12)	2011
11q22.3	rs974819	PDGF	0.29 (T)	1.07 (1.04-1.09)	2011
13q34	rs4773144	COL4A1, COL4A2	0.44 (G)	1.07 (1.05-1.09)	2011
14q32.2	rs2895811	HHIPL1	0.43 (C)	1.07 (1.05-1.10)	2011
15q25.1	rs3825807	ADAMTS7	0.57 (A)	1.08 (1.06-1.10)	2011
17p13.3	rs216172	SMG6, SRR	0.37 (C)	1.07 (1.05-1.09)	2011
17p11.2	rs12936587	RASD1, SMCR3, PEMT	0.56 (G)	1.07 (1.05-1.09)	2011
17q21.32	rs46522	UBE2Z, GIP, ATP5G1, SNF8	0.53 (T)	1.06 (1.04-1.08)	2011
5p13.3	rs11748327	IRX1, ADAMTS16	0.76 (T)	1.25 (1.18-1.33)	2011
6p22.1	rs6929846	BTN2A1	0.06 (T)	1.51 (1.28-1.77)	2011
6p24.1	rs6929846	C6orf105	0.07 (A)	1.65 (1.44-1.90)	2011
6p21.3	rs3869109	HCG27 AND HLA-C	0.60 (C)	1.15	2012
1q21	rs4845625	IL6R	0.47 (T)	1.09	2012

Chr 4	rs1878406	EDNRA	0.15 (T)	1.09	2012
7p21.1	rs2023938	HDAC9	0.10 (G)	1.13	2012
2p11.2	rs1561198	VAMP5-VAMP8	0.45 (A)	1.07	2012
Chr2	rs2252641	ZEB2-AC074093.1	0.45 (A)	1	2012
Chr5	rs273909	SLC22A4-SLC22A5	0.14 (C)	1.11	2012
6p21	rs10947789	KCNK5	0.76 (T)	1.01	2012
6q26	rs4252120	PLG	0.73 (T)	1.07	2012
8p22	rs264	LPL	0.86 (G)	1.06	2012
13q12	rs9319428	FLT1	0.32 (A)	1.1	2012

**Table 1.1. List of 50 CAD-associated genetic variants (Roberts, 2014).**

An additional consortium, known as the international consortium IBC 50K, discovered three additional loci associated with CAD (The IBC 50K, 2011). These studies demonstrate the tremendous efforts of the scientific community to unravel the genetic basis of CAD.

There are a number of common features for CAD-associated variants. The majority of the CAD-associated variants are very common, with an average allele frequency of 50%, ranging from 2-91% in the population. The relative increased risk for genetic variants have ORs ranging from 1.02 to 1.90, which suggests that the relative increased risk for each variant is small. The majority of variants map to non-coding DNA sequences, suggesting they exhibit a regulatory role by influencing the regulation of DNA sequences, which subsequently alter expression of protein. Once an individual has been genotyped for risk variants, this process does not need to be repeated, as the DNA sequence does not change.

#### **1.7.4.1 9p21 locus**

The role of 9p21 in CAD still remains unknown. 9p21 resides in an intergenic region, where the risk alleles and the neighbouring SNPs sit in a 58 kb region of high LD. The CAD core risk region overlaps antisense non-coding RNA in the INK4 locus (*ANRIL*), a non-coding RNA, also known as *CDKN2B-AS*. *ANRIL* is 126,000 base pairs (bps) in length (Helgadottir *et al.*, 2007) and consist of 20 exons, which undergo alternative splicing, depending on the tissue type (Folkersen *et al.*, 2009). The CAD core risk region has been proposed to influence *ANRIL* expression. Several studies have shown a significant association between 9p21 polymorphisms and *ANRIL* expression (Folkersen *et*

*al.*, 2009; Holdt *et al.*, 2010). Adjacent to *ANRIL* is cyclin-dependent kinase inhibitor 2A (*CDKN2A* coding for p16, INK4a) and cyclin-dependent kinase inhibitor 2B (*CDKN2B* coding for p15, INK4b), which are cyclin-dependent kinase inhibitors, involved in the regulation of the cell cycle to restrain irregular proliferation. It is thought, that through an unknown type of feedback, increased transcription of *ANRIL* recruits the polycomb group (PcG) protein complexes. They can remodel chromatin to induce gene silencing and regulate transcription of genes. Chromobox 7 which lies in the polycomb repressive complex 1 binds to *ANRIL*, which trimethylates histone H3 lysine 27 (H3K27), and causes the silencing of *CDKN2A* and *CDKN2B* (Yap *et al.*, 2010). Overall, it has been proposed that 9p21 risk variants exert their effects onto *ANRIL*, which depresses the actions of the cyclin-dependent kinase inhibitors, causing an increased proliferative state of vascular SMCs (Roberts & Stewart, 2012; **Figure 1.4**). Studies have shown the 9p21 risk variants are associated with reduced expression of *CDKN2A* and *CDKN2B* (Jarinova *et al.*, 2009; Liu *et al.*, 2009). However, other *in vivo* and *in vitro* studies do not support this finding, as researchers have shown a lack of correlation between the 9p21 variants and expression of *CDKN2A* and *CDKN2B* (Kim *et al.*, 2012; Folkersen *et al.*, 2009; Hamsten & Eriksson, 2012).

A 9p21 mouse model has been created where a 70 kbp genomic region was knocked out that corresponds to the human 58 kbp region on 9p21. Researchers demonstrated that SMC proliferation markedly increased, and mice went onto develop neoplasms. However mice did not go on to get atherosclerosis, most likely due to their resistance to atherosclerosis, or the low sequence homology between the two species (Visel *et al.*, 2010).

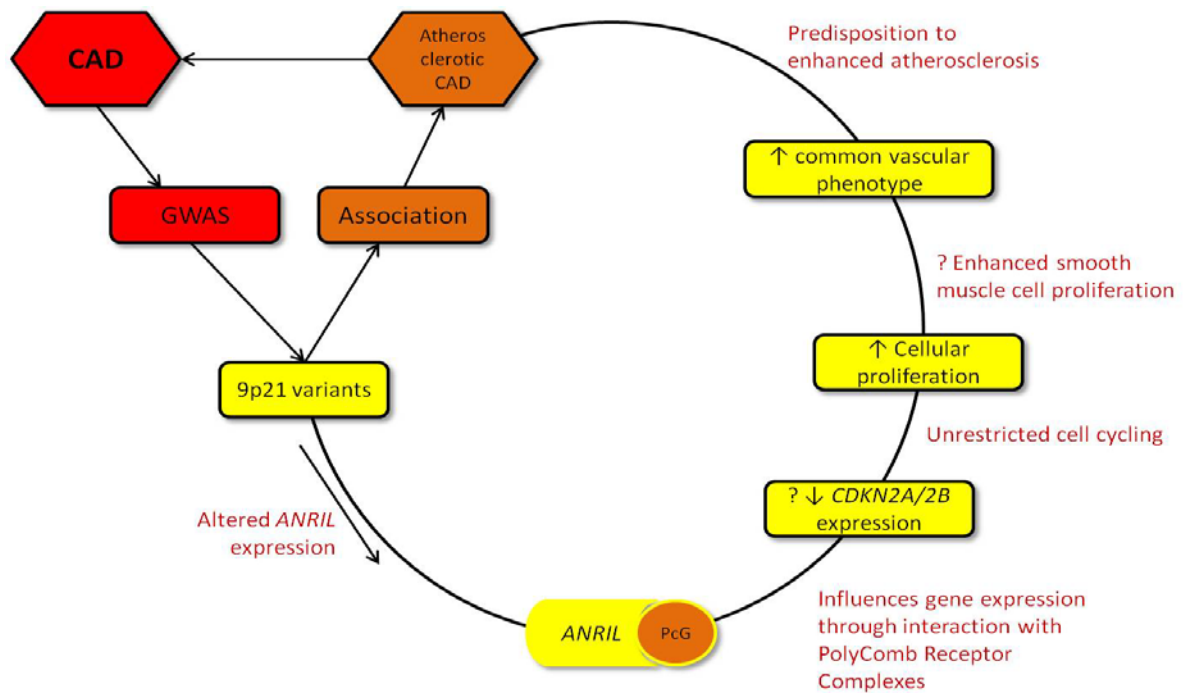


**Figure 1.4. Schematic diagram of the hypothesised biological mechanism the 9p21 risk locus acts through.** The 9p21 risk variants were discovered through genome-wide association studies (GWASs). Functional studies indicate 9p21 alters *ANRIL* expression by interaction with the PolyComb Receptor Complexes to alter *CDKN2A* and *CDKN2B* expression, leading to increased cellular proliferation of vascular SMCs. This mechanism may predispose individuals to atherosclerosis (Patel & Ye, 2012).

A different mechanism has also been proposed. It has been suggested that the CAD 9p21 region is responsive to inflammatory signalling and that 9p21 acts through interferon- $\gamma$ ; a cytokine involved in inflammation. The 9p21 risk region forms a chromatin loop which comes in close proximity to the interferon region (less than 1 million bp from 9p21). There is a STAT1 binding site at the 9p21 region, and upon interferon- $\gamma$  stimulation, STAT1 binds to this site. Harismendy *et al.*, (2011) report that induction with interferon- $\gamma$  resulted in reduced level of *CDKN2B*. However it has been demonstrated that the 9p21 risk variants, do not affect the activation of *CDKN2A* or *CDKN2B*, via interferon- $\gamma$  (Almontashiri *et al.*, 2013). Also interferon type 1 and interferon- $\alpha$ -21 are not affected by the 9p21 risk variants (Erridge *et al.*, 2013). Since its discovery in 2007, the 9p21 locus has been heavily studied; however the mechanism of how 9p21 contributes to CAD is still unknown, demonstrating how difficult it is to elucidate the mechanism of a GWAS signal.

## 1.8 Disease models to investigate CAD

Large-scale genetic studies have identified many genetic loci that contribute to CAD. However, the functional translation of these discoveries presents many challenges. The main barrier is the cellular and pathophysiologic effects of susceptibility alleles remain unknown, and alleles at unannotated loci present an even harder task to elucidate their mediated effects on CAD pathogenesis.

Firstly, functional variants that cause phenotypic changes are likely to be tissue specific, so access to healthy cells and tissue is crucial to investigate the underlying mechanisms. However, the use of patient-derived samples is not a feasible approach to study CAD risk variants. To obtain primary tissue from patients with different CVDs is limited by sample number, and it involves an invasive procedure, often uncomfortable for the patient. In addition, to obtain healthy control tissue would present a greater challenge. The opportunity to obtain CAD-relevant cell types, for example endothelial cells and vascular SMCs is limited. Tissue samples that are obtained during essential invasive procedures, such as percutaneous vascular intervention and carotid endarterectomy, exhibit the pathology of the end stages of the disease. Thus these samples are less informative to help understand the earlier pathogenic mechanisms (Shaw & Brettman, 2011). Furthermore, studying the functional effects of risk alleles using primary tissue from patients may be masked by other factors, such as environmental factors or other disease phenotypes.

Animal models do not fully recapitulate CAD pathogenesis (Heaps & Parker, 2011), and complete conservation is not observed between human and mouse. For example, the 9p21 CAD risk region in humans only shows 50% homology with the chromosome 4 region in mice (Visel *et al.*, 2010). Although animal models are useful to try and understand the function of novel or known genes that CAD risk alleles reside in. For example, two different rodent studies created whole-body knockout mice for *ADAMTS7*; a locus associated with CAD. They showed *ADAMTS7* deletion protected mice from atherosclerosis and neointima formation, concluding a pro-atherogenic role for mouse *ADAMTS7* (Bauer *et al.*, 2015; Kessler *et al.*, 2015).

To gain a greater understanding of the biological mechanisms CAD-risk variants act through requires genotype-specific disease models. These models will allow for the investigation of the effect of risk alleles in a cellular context, where the environmental influence would be controlled for in such models. Stem cells represent a prospective cell type to create genotype-specific disease models, as they can differentiate into CAD-relevant cell types, and therefore promise a new paradigm in studying the functional mechanisms of CAD-related genetic variants.

### **1.9 Stem cells**

Stem cells are a class of undifferentiated progenitor cells, and are defined by two properties. The first property is the ability to self-renew, by going through many cell cycle divisions whilst maintaining their undifferentiated state. The second property is cell potency; cells must have the capacity to differentiate into specialised cell types of the body. Stem cells can be totipotent, pluripotent, multipotent or unipotent.

Totipotency is the ability of a single cell to form all the specialised cell types in an organism, including extra-embryonic tissues (amnion, chorion, yolk sac and allantois). Upon fertilisation in humans, an ovum and a sperm cell combine to form a single cell called a zygote. The zygote is totipotent; it develops into an embryo, which forms all the different specialised cells in a human being, as well as the placenta that is required for fetal development. So a zygote is able to give rise to an entire organism. The zygote undergoes cell division and loses its totipotent ability at the 8-cell stage (known developmentally as blastomeres). It is hypothesised that this is due to early embryonic cells specialising into cells that comprise the outer layer (extra-embryonic tissue) and cells that form the inner cell mass (foetus and the trophoblast; Mitalipov & Wolf, 2009).

Pluripotency is the ability of a cell to differentiate into cells from the three different germ layers; endoderm (inner), mesoderm (middle) and ectoderm (outer). The endoderm forms when cells migrate inwards along the archenteron

(primitive gut that is formed during gastrulation) and form the inner layer of the gastrula. Cells take on a flattened morphology, but become columnar and form the lining of multiple organ systems. They can differentiate into cells including liver, lung and pancreatic cells. The mesoderm forms at the third week during the gastrulation phase in embryonic development. There are three derivatives of the mesoderm; paraxial, intermediate and lateral mesoderm. The paraxial mesoderm forms the mesenchyme of the head and gives rise to somites in occipital and caudal segments. Somites form muscle tissue, cartilage, bone and the subcutaneous tissue of the skin. The paraxial and lateral mesoderm are linked by the intermediate mesoderm. This forms the gonads, kidneys and adrenal glands (urogenital structures). Next the lateral mesoderm differentiates into the blood vessels, blood cells and heart, and into the mesodermal component of the limbs. These become muscle cells, connective tissue, in addition to other cell types. Pluripotent cells form any fetal or adult cell type, yet they are unable to give rise to a whole organism, as they lack the ability to organise into an embryo (Mitalipov & Wolf, 2009). Examples of pluripotent cells are embryonic stem cells (ESCs) and induced pluripotent stem cells (iPSCs).

Multipotency is the ability of a cell to differentiate into limited but multiple cell types. Once cells have differentiated, they are only able to produce cells of one origin, and no other cell types (Pittenger *et al.*, 1999; Dominici *et al.*, 2006). Multipotent stem cells are able to self-renew, but not indefinitely, as they do not possess high levels of telomerase. An example of multipotent cells are adult stem cells.

Unipotency is the ability of a stem cell to differentiate into only one cell type. They are also referred to as precursor cells. Unipotent stem cells can self-renew, as they are able to divide repeatedly. An example of a unipotent cell is a hepatoblast that differentiates into hepatocytes.

### **1.10 Embryonic stem cells**

Embryonic stem cells (ESCs) are pluripotent cells; they are able to differentiate into every germ layer and somatic cell type of the body. They self-

renew and maintain expression of certain factors required for their pluripotent properties. ESCs are located in the inner cell mass of the embryo, from where they can be isolated and grown in culture. ESCs are seen as the 'gold standard' for pluripotent stem cells.

Evans & Kaufman (1981) and Martin (1981) were the first to isolate ESCs from mouse embryos. Subsequently in 1998, ESCs were isolated from human embryos (Thomson *et al.*, 1998). These findings led to a surge of interest, resulting in the production of over a thousand hESC lines (Löser *et al.*, 2010). ESCs can be derived from fresh or frozen blastocysts. There are three main techniques to isolate ESCs; laser dissection, mechanical dissection and immunosurgery. Laser dissection involves creating a small opening in the zona pellucida (structure that covers the blastocyst) and isolating the cells using a laser. Mechanical micro dissection uses fine needles to isolate ESCs from the inner cell mass. Immunosurgery involves lysing the trophectoderm (outer layer of the blastocyst) using an anti-human whole serum antibody with a guinea pig complement. All the cells with the antibody attachment are lysed, leaving the inner cell mass. If the ESCs are required for clinical purposes, then immunosurgery is the least suitable technique, as it uses non-human proteins and antibodies. Upon isolation of ESCs, to maintain them in culture, cells are grown on feeder layers, which help ESCs attach and provides them with nutrients. If ESCs are required for clinical applications, alternative systems to maintain them in culture are being used. Extracellular matrices, such as fibronectin and matrigel have been utilized.

When ESCs are removed from the inner cell mass, the blastocyst is destroyed. Destroying a potential human life raises ethical concerns. The key debated ethical issue is whether the embryo has the same moral status as a more developed human being, and if yes, then a potential human is being destroyed (Baldwin, 2009). The moral status of an embryo is a controversial and complicated ethical issue.

### 1.11 Induced pluripotent stem cells

Due to the ethical concerns raised with the use of ESCs, the breakthrough technology of iPSCs has been paramount within the stem cell field. Shinya Yamanaka's lab carried out an elegant screen of 24 genes associated with ESC pluripotency. They showed that the insertion of four transcription factors turned murine adult and embryonic fibroblasts into iPSCs. The four genes were *OCT4*, *SOX2*, *KLF4* and *c-MYC* (Takahashi & Yamanaka, 2006). A year later they demonstrated the same principle but using human adult dermal fibroblasts (Takahashi *et al.*, 2007). iPSCs have a pluripotent nature, since 2007 they have been shown to differentiate into cells of all three germ layers including mature B cells (Hanna *et al.*, 2008), adipose cells (Ahfeldt *et al.*, 2012) and keratinocytes (Maherali *et al.*, 2008). These findings demonstrate iPSCs have great potential in becoming many different cell types, and their use in disease modelling holds great potential. Since 2007, many research groups have replicated the method to produce iPSCs, with the aim of improving the efficiency. In general there are three main steps to produce iPSCs (**Figure 1.5**). Firstly, the starting cell e.g. adult fibroblasts are sourced and cultured *in vitro*. Secondly, the cells are made into iPSCs, by introducing factors into the cells. Initial reports used retroviruses to introduce reprogramming factors to the cell; however there is a risk of tumorigenesis and transgene reactivation. The emphasis has shifted to using transgene free methods; these include viral transduction, plasmid, minicircle and transposon transduction, recombinant proteins, and using small molecule and miRNA methods. Next transfected cells are placed onto feeder layers (like ESCs), and left to become iPSCs. The cells then undergo morphological and phenotypical characterisation (Singh, 2015).

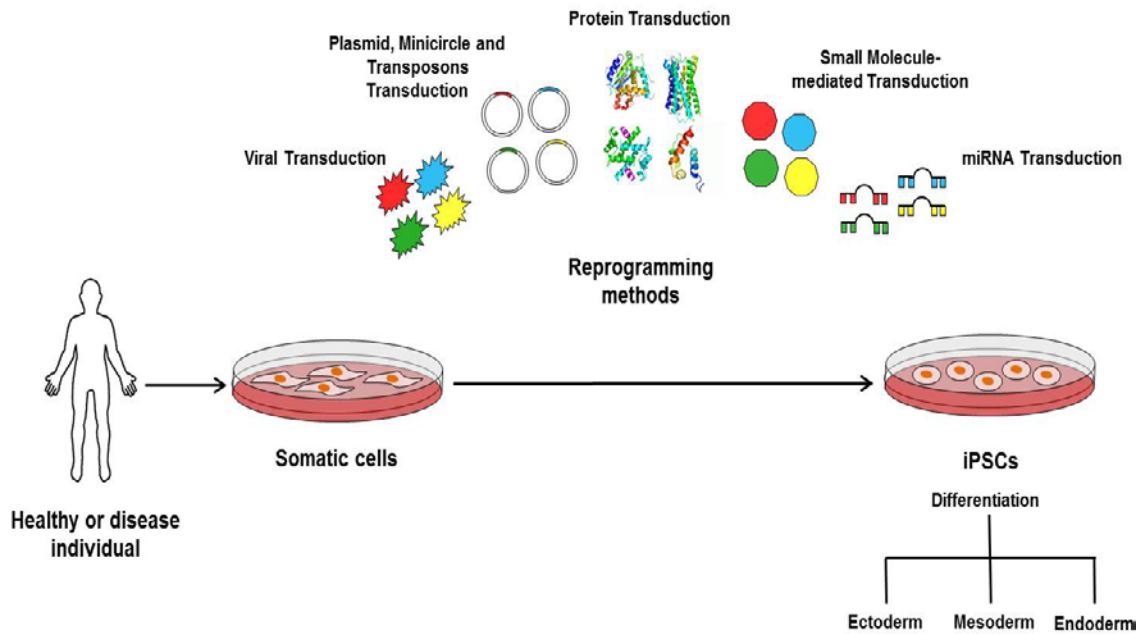


**Figure 1.5. Schematic diagram of the generation of induced pluripotent stem cells (iPSCs).** Somatic cells are taken from a healthy or diseased individual. Reprogramming factors are introduced into the cells to generate iPSCs, which have the potential to differentiate into cells from all three germ layers (adapted from Dash *et al.*, 2015).

### 1.12 Adult stem cells

Adult stem cells are an undifferentiated cell type, located in tissues and organs among differentiated cells. They are found in tissues that rapidly turnover e.g. liver, pancreas, bone marrow, skin and skeletal muscle. Adult stem cells are also known as somatic stem cells, which are defined as cells of the body, and not sperm, egg or germ cells. Adult stem cells can self-renew, but are limited due to low telomerase levels. They can also differentiate into restricted cell lineages. Their main role is to maintain and repair damaged tissue in which they are located. In each type of tissue, they commit to differentiate into mature functional cells, to perform a specific function (Wagers & Weissman, 2004). ESCs are clouded by ethical issues; however adult stem cells are mainly exempt as they are derived from adult tissues as opposed to embryos.

There are three main types of adult cells; hematopoietic stem cells, neural stem cells and mesenchymal stem cells (MSCs). Hematopoietic stem

cells are located in the bone marrow, and differentiate into all the different types of blood cells (Gunsilius *et al.*, 2001). Neural stem cells give rise to cells of the nervous system, mainly neurons, astrocytes and oligodendrocytes (Kennea & Mehmet, 2002). In this thesis I focussed on MSCs.

### **1.13 Mesenchymal stem cells**

MSCs are defined as a heterogeneous population of progenitor cells, which are also referred to as mesenchymal progenitor cells or marrow stromal cells. MSCs have a fibroblast-like morphology, proliferate, self-renew and form colonies *in vitro*. MSCs are multipotent, so can differentiate into a limited number of lineages including adipocytes, chondrocytes and osteoblasts (Horwitz *et al.*, 2005).

#### **1.13.1 Discovery of MSCs**

A German pathologist named Julius Cohnheim was the first to propose the presence of non-haematopoietic stem cells in the bone marrow 130 years ago. His observations were suggestive of the idea that fibroblasts, which deposited collagen fibres involved in wound repair, were located in the bone marrow (Prockop, 1997). Following on from Cohnheims work, Friedenstein and co-workers investigated these cells further (Friedenstein *et al.*, 1966; Friedenstein *et al.*, 1968; Friedenstein *et al.*, 1974). Bone marrow samples were taken from the iliac crest and placed onto plastic culture dishes. Non-adherent cells were removed after 4 hours, and adherent cells remained on the plate. In culture, they observed a heterogeneous population of which most were spindle-shaped. Passaging the cells several times, altered their morphology to exhibit a homogenous fibroblast-like appearance. Cells were also clonogenic, which Friedenstein described as colony-forming unit fibroblasts (CFU-F). In addition, they discovered that cells differentiated into colonies that looked like small deposits of cartilage or bone. Throughout the 1980s, other groups investigating these cells confirmed Friedenstein's observations (Ashton *et al.*, 1980; Bab *et al.*, 1986; Castro-Malaspina *et al.*, 1980). Friedenstein's isolation method

yielded cells that were able to differentiate into adipocytes, chondrocytes, osteoblasts and myoblasts. In reference to Friedenstein *et al.*, work Caplan (1991) popularized the term MSCs, as they are able to differentiate into mesenchymal-type cells.

### 1.13.2 Morphology of MSCs

MSCs are fibroblast-like in appearance, have a small cell body and long, thin cell processes (**Figure 1.6**). They possess large, irregular shaped nuclei and prominent round nucleoli found near the perinuclear cisternae. Chromatin is present throughout the nucleus excluding the thin dense layer found inside the perinuclear cisternae. The cytoplasm contains round, elongated mitochondria, Golgi apparatus and rich, granular endoplasmic reticulum. Ribosomes are also present in the cytoplasm, mainly around the endoplasmic reticulum (Raimondo *et al.*, 2006; Momin *et al.*, 2010).

MSCs display morphological heterogeneity, as many different terms have been used to describe their appearance, including fibroblast-like cells, small round cells, giant fat cells, blanket cells, spindle shaped and flattened cells (Pevsner-Fischer *et al.*, 2011). In culture, the morphology of MSCs can be greatly affected by the seeding density at which cells are plated, especially when cells become confluent. Overall the relationship between the morphological characteristics and cell function of MSCs is still unclear (Wong, 2011).

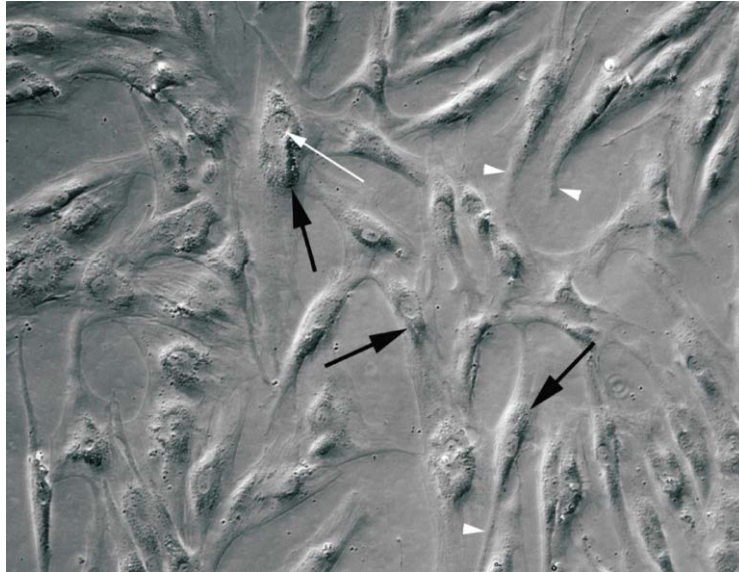


**Figure 1.6. Morphology of MSCs.** MSCs display long thin processes (white arrowheads), large nuclei (black arrows) and prominent round nucleoli (white arrows; Momin *et al.*, 2010).

### 1.13.3 Isolation of MSCs

MSCs were first isolated from humans, and since then they have been harvested from various species including dog, porcupine, mouse and rat (Baddoo *et al.*, 2003; Moscoso *et al.*, 2005; Santa Maria *et al.*, 2004; Silva *et al.*, 2005).

Human MSCs are normally isolated from the mononuclear layer of the bone marrow after density gradient centrifugation (Colter *et al.*, 2000). Cells are typically cultured in medium containing 10% fetal bovine serum (FBS). Replacement of culture medium removes non-adherent cells such as hematopoietic cells, and allows adherent, fibroblast-like cells to remain. Cells go through an initial lag phase, followed by a rapid division of cells. Bone marrow derived-MSCs are seen as the 'gold standard' for MSCs. However, to extract MSCs from the bone marrow entails a medical procedure, often painful for the donor. So the focus has shifted to isolating MSCs from other tissues. Since their initial isolation from the bone marrow, they have been harvested from many other tissues including dental pulp, tendons, adipose tissue, skeletal muscle, amniotic fluid and the umbilical cord (da Silva Meirelles *et al.*, 2006).

#### 1.13.4 Isolation of MSCs from the umbilical cord

The umbilical cord is derived from the extraembryonic mesoderm, at day 13 of embryonic development. It is located in the womb, and connects the developing foetus to the placenta. The umbilical cord is covered by the umbilical epithelium, which is a single or multiple layer of squamous-cubic epithelial cells (Mizoguchi *et al.*, 2004). It consists of a vein that provides oxygenated, nutrient-rich blood to the fetus and two arteries which carry deoxygenated, nutrient-depleted blood away from the fetus. These vessels are surrounded by a connective tissue known as Wharton's jelly (WJ). The umbilical cord varies in length between 20 and 120cm, with an average length of 50cm. It weighs approximately 40 grams, with a mean diameter of 1.5cm (Raio *et al.*, 1999; Di Naro *et al.*, 2001).

MSCs can be isolated from the umbilical cord. Umbilical cord-derived MSCs are also referred to as perinatal stem cells as the umbilical cord is classed as a perinatal tissue. 'Perinatal' describes the period around the time of birth, however in principle refers to the time from the 20<sup>th</sup> week of gestation to the first 28 days after birth. Perinatal stem cells biologically lie between ESCs and adult MSCs (Pappa & Anagnou, 2009; De-Miguel *et al.*, 2009). MSCs have been shown to be positive for ESC cell surface markers Tra-1-60, Tra-1-81, Oct-4, SSEA-1, SSEA-4 and alkaline phosphatase. In addition, they have been shown to form embryoid bodies (Fong *et al.*, 2007). Umbilical cord-derived MSCs also express the pluripotency markers; *NANOG*, *SOX2* and *OCT4* at decreased levels compared to ESCs (La Rocca *et al.*, 2009; Fong *et al.*, 2011). This evidence supports the primitive nature of umbilical cord-derived MSCs, thought to be the most primitive cells found in the body (Bongso *et al.*, 2008). In addition, MSCs from tissue that support prenatal development, may have a higher capacity for pluripotency than somatic stem cells, substantiated by findings that umbilical cord-derived MSCs express markers from all three germ layers (Fong *et al.*, 2011), and can give rise to cells from all three germ layers (Can & Karahuseyinoglu, 2007).

There are many advantages of MSCs harvested from the umbilical cord, in addition to their higher pluripotent capacity. Umbilical cord-derived MSCs

exhibit higher self-renewal capacity and proliferation rates than MSCs derived from adult tissues (Troyer & Weiss, 2008). The umbilical cord is an abundant source of tissue as it can be up to 120cm long. In addition, the umbilical cord is discarded as a waste product of parturition, therefore using this tissue to isolate stem cells is a safe, non-invasive approach with little or no legal or ethical constraints (Lee *et al.*, 2004), whereas collection of bone marrow or adipose tissue from a donor, is an invasive surgical procedure. MSCs derived from fetal sources have a shorter population doubling time, and longer time to senescence than MSCs from adult sources. This latter difference is thought to be due to fetal MSCs having longer telomeres (Campagnoli *et al.*, 2001; Guillot *et al.*, 2007). Also MSCs from the umbilical cord have a relatively higher CFU-F, and do not lose their potency (Troyer & Weiss, 2008). Overall umbilical cord-derived MSCs have a more primitive nature and represent a younger MSC in comparison to MSCs from adult tissues (Troyer & Weiss, 2008; Carlin *et al.*, 2006; Friedman *et al.*, 2007). The young chronological age of umbilical cord-derived MSCs minimises environmental factors and somatic mutations. This is particularly important when studying the effects of a single SNP or subset of SNPs with modest effects. Therefore, umbilical cord-derived MSCs are advantageous to study CAD-related genetic variants.

So far five compartments within the umbilical cord have shown to contain MSCs; (1) umbilical cord blood (2) umbilical vein subendothelium (3) subamnion (4) perivascular region and (5) intervascular region (**Figure 1.7**; Troyer & Weiss, 2008). MSCs from these regions are plastic adherent, multipotent and express characteristic cell surface markers (Karahuseyinoglu *et al.*, 2007).

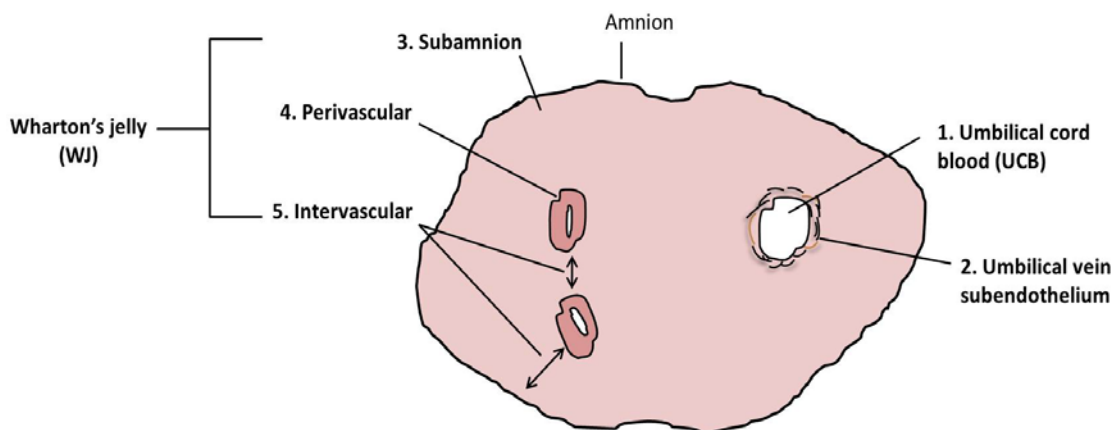


**Figure 1.7. Schematic diagram of the umbilical cord compartments containing MSCs.** Wharton's jelly (WJ) is a unique, connective tissue in between the vessels and the amniotic epithelium, which includes the subamnion (zone 3), perivascular (zone 4) and intervascular (zone 5) regions (adapted from Troyer & Weiss, 2008).

### 1.13.5 Isolation of MSCs from Wharton's jelly

WJ was first isolated and described by Thomas Wharton in 1656. WJ is a gelatinous, connective tissue between the vessels and the amniotic epithelium, and its primary role is to protect the umbilical cord vessels from any bending, torsion or compression. The tissue consists of different isoforms of mucopolysaccharides and proteoglycans (Sobolewski *et al.*, 1997). McElreavey *et al.*, (1991) was the first to report the culture of cells from WJ. MSCs most likely have become fixed in WJ during embryogenesis. During the third week of embryogenesis, haematopoiesis occurs in the yolk sac and subsequently in the aorta-gonad-mesonephros region. During embryonic day 4 and 12, a group of primitive haematopoietic cells and MSCs, move through the umbilical cord to the placenta (Wang *et al.*, 2008). A second wave of migration means they further migrate back to the primitive umbilical cord to the fetal liver, and ultimately to the fetal bone marrow. In the bone marrow, MSCs and haematopoietic stem cells remain here throughout life and are the precursors of both stem cells. It has been hypothesised that when MSCs are travelling through the umbilical cord, to the placenta during embryogenesis, the cells become fixed in the WJ and reside in this tissue during gestation (Wang *et al.*, 2008).

MSCs derived from WJ include cells from the subamniotic, intervacular and the perivascular region (Karahuseyinoglu *et al.*, 2007). MSCs found close to the amniotic surface possess enhanced proliferative ability, whereas MSCs located near the umbilical vessels are more differentiated (Karahuseyinoglu *et al.*, 2007; Nanaev *et al.*, 1997). In conclusion, the rich source, as it is possible to isolate up to  $1.6 \times 10^6$  cells/cm<sup>2</sup> of umbilical cord (Tsagias *et al.*, 2011), and primitive nature of MSCs from WJ, make them an ideal source of MSCs in which to study CAD-related genetic variants.

To isolate MSCs from WJ, investigators use either an explant method, whereby MSCs migrate out of the WJ tissue blocks (Mitchell *et al.*, 2003; Conconi *et al.*, 2006) or use collagenase containing solutions to digest WJ to isolate MSCs. MSCs can be cultured to expand proficiently in culture, yet this expansion is very variable, and has even been observed between two samples from the same individual (DiGirolamo *et al.*, 1999). The initial tissue used to isolate MSCs is very important, as tissue with an initial abundance of MSCs, means the cells do not have to undergo extensive multiplication, and possible epigenetic damage (Boquest *et al.*, 2006; Noer *et al.*, 2007). MSCs can be cultured *in vitro*, for more than 80 population doublings, showing no alterations in morphology or signs of senescence (Mitchell *et al.*, 2003). However MSCs at a higher passage have a significantly longer population doubling time (Karahuseyinoglu *et al.*, 2007; Conconi *et al.*, 2006; Weiss *et al.*, 2006; Lu *et al.*, 2006). In addition, for MSCs at a very high passage, there is a chance that karyotype abnormality may occur, so it may be applicable to verify a normal karyotype. If this occurs novel cell lines may be formed, which would not be considered as MSCs (Dominici *et al.*, 2006). This wide variation observed amongst laboratories, is suggestive of MSCs from the umbilical cord containing subsets of primitive stem cells, yet this remains to be proved. Overall there are many factors including tissue culture factors i.e. number of passages, frequency of medium change, oxygen levels, and cell confluency that can alter the behaviour of MSCs (Barrilleaux *et al.*, 2006).

### 1.14 Aims of this thesis

A huge challenge of the post-GWAS era is identifying the biological mechanisms and pathways that CAD-related genetic variants act through to contribute to disease. I sought to explore the use of MSCs as an investigative model for CAD risk variants. MSCs can be isolated from a number of sources including the umbilical cord. So my first aim is to, using published methods, isolate, culture and characterise MSCs from WJ from the umbilical cord.

To investigate the use of MSCs as a model, a proof of concept study will be carried out. Speliotes *et al.*, (2010) functionally annotated 18 novel BMI-associated loci and reported rs3810291 was associated with *ZC3H4* gene expression in adipose tissue. Recapitulating this association in MSC-derived adipocytes will confirm the potential of MSC-derived cells.

Next, using published methods, I will aim to differentiate MSCs into CAD-relevant cell types, as it is hypothesised that phenotypic changes influenced by CAD-related genetic variants are likely to act in specific cell types. Using published methods, MSCs will be differentiated into hepatocytes and SMCs, and resultant cells characterised to ensure they are phenotypically authentic.

Upon successful differentiation into SMCs, another proof of concept study will be performed. Donors that are homozygous major and homozygous minor for the CAD-associated variant rs3825807 (15q25) will be differentiated into SMCs. Recapitulation of the effect of rs3825807 on ADAMTS7 prodomain processing, COMP cleavage and SMC migration demonstrated by Pu *et al.*, (2013) will confirm the possible use of MSCs in CAD disease modelling at the phenotypic level.

# **Chapter 2- Materials and Methods**

All experimental steps were carried out at room temperature unless stated otherwise. Materials are listed before each method.

## **2.1 Molecular Biology**

### **2.1.1 DNA extraction**

- Mammalian Genomic DNA Miniprep Kit (Sigma-Aldrich)

DNA was extracted from passage 5 (P5) MSCs using the Mammalian Genomic DNA Miniprep Kit following the manufacturer's protocol. DNA was extracted from up to  $5 \times 10^6$  cells. Briefly, cell pellets were resuspended in Resuspension Solution, followed by cell lysis by incubation with Proteinase K (20mg/ml), and passed through the GenElute Miniprep Binding Column to allow the DNA to bind. The column was washed twice, and the DNA eluted in 200 $\mu$ l Elution Solution. The 200 $\mu$ l eluted sample was added again to the same binding column and centrifuged at 8,000 rpm for 1 minute. The samples were stored at -20°C.

### **2.1.2 Determining the concentration of DNA**

The purity and concentration of each DNA sample was analysed using the NanoDrop 1000 Spectrophotometer (Thermo Scientific). 1 $\mu$ l of sample was loaded onto the platform, and the Nucleic Acids method on the ND-1000 V2.0.0 software was used to analyse each sample. The DNA concentration was recorded and the purity of the sample was determined by the 260/280 and 260/230 ratio. DNA samples were stored at -20°C until further use.

### **2.1.3 Taqman<sup>®</sup> SNP Genotyping assay**

- Taqman<sup>®</sup> SNP Genotyping assay mix; rs3810291 (Life Technologies)
- AccuStart Genotyping ToughMix<sup>®</sup> (Quanta Biosciences)
- Optical Disposable Adhesive Seals for PCR Plates (Gene Flow)

The Taqman<sup>®</sup> Genotyping assay was used to genotype DNA from donors for rs3810291. To each well on a 384 well plate 1µl of DNA (10ng/µl) was added. 5µl of master mix (600µl Genotyping ToughMix<sup>®</sup>, 395µl MilliQ water and 5µl SNP mix) was added to each well. Two no template controls (NTCs) were added to each plate. A disposable adhesive seal was used to seal the plate, and centrifuged at 1500 g for 1 minute. The sample underwent a 45 cycle PCR reaction on the ViiA<sup>™</sup> 7 Real-Time PCR System (Life Technologies) using the ViiA<sup>™</sup> 7 software v1.1 (Life Technologies). An initial 10 minute denaturation step at 95°C was carried out. The details of the 45 cycle reaction were; 92°C for 15 seconds, 54°C for 1 minute and 60°C for 1 minute. A final extension step was run at 72°C for 10 minutes. The genotype of each donor was determined.

#### **2.1.4 Preparation of DNA samples for whole genome genotyping**

DNA samples were sent to Affymetrix for whole genome genotyping. DNA samples had to meet certain requirements for successful genotyping; **1)** a 260/280 ratio between 1.8 and 2.0, **2)** a 260/230 ratio greater than 1.5 and **3)** a concentration of 50ng/µl. If DNA did not meet the 260/280 or 260/230 ratio requirements samples were ethanol precipitated to purify the DNA. If DNA had a concentration below 50ng/µl, samples were concentrated.

#### **2.1.5 Ethanol precipitation**

- Sodium acetate (Sigma-Aldrich; made to 2M at pH 5.2).
- Ethanol (Genta Medical)
- Elution solution (Sigma-Aldrich)

1/10<sup>th</sup> of 2M sodium acetate was added to each sample and mixed. 2-3 volumes of 100% ethanol was added to each sample, vortexed and stored at -20°C overnight. Samples were centrifuged at maximum speed (13,200 rpm) for 10 minutes, and the supernatant was carefully discarded. The pellets were air dried for 15 minutes before resuspending in 50µl of Elution Solution.

### 2.1.6 Sample concentration

The Jouan RC1010 Centrifugal evaporator vacuum concentrator centrifuge (Thermo Electron Corporation) was used to concentrate DNA samples. The caps were removed from each 2ml microtube and placed carefully onto the rotor, so the rotor was balanced. The samples were vacuumed for 30-45 minutes, the concentration of each DNA sample was analysed using the NanoDrop 1000 Spectrophotometer, described in **Section 2.1.2**. The samples were placed back onto the rotor if further concentration was required.

### 2.1.7 Agarose gel electrophoresis

- Agarose, Electrophoresis Grade (Melford Laboratories)
- 50x TAE (484g Tris in 1 litre of dH<sub>2</sub>O, 114.2ml acetic acid, 37.2g EDTA, pH to 7.6 with concentrated HCl, and made up to 2 litres with dH<sub>2</sub>O)
- Ethidium Bromide (0.625 mg/ml; Severn Biotech Ltd)
- 5x DNA loading buffer, Blue (Bioline)
- HyperLadder™ I (Bioline)

To verify the quality of DNA, samples were run on a 0.8% agarose gel. 0.8g of agarose was added to 100ml of 1x TAE (50x TAE diluted in dH<sub>2</sub>O). Upon cooling ethidium bromide was added at a final concentration of 420ng/ml. The solution was poured into a gel tray with a gel comb and allowed to set. The comb was removed, and the tray was placed into a gel tank with 1x TAE. 1µl of DNA, 9µl of dH<sub>2</sub>O and 2µl of 5x loading dye was added into a 0.2ml PCR tube and mixed. 10µl of Hyperladder I was added to the first well on the agarose gel. DNA from every tenth donor was loaded onto the gel. A positive and negative electrode was attached to either side of the tank and run at 125v until the DNA ladder had run halfway down the agarose gel. The gel was visualised using Gene Genius Bio-Imaging Systems (Syngene), and the Genesnap v6.03 (Syngene) software was used to capture images of the agarose gel.

### **2.1.8 Plating of DNA into 96 well plates**

DNA was diluted to 60ng/μl, and 40μl was loaded into each well on a 96-well plate. Onto each plate, two NTCs were added; 40μl of dH<sub>2</sub>O. One well contained a positive control, which was a DNA sample diluted to 100ng/μl and added to every plate. The 96 well plate was sealed, a barcoded was added to the side of the plate, and kept at -20°C until shipping.

### **2.1.9 Axiom Genotyping Array**

The Axiom™ Genome-Wide UKB WCSG Genotyping Array (Affymetrix) is a powerful array to analyse genome-wide variants. It also includes markers of specific interest, for example markers involved in cardiometabolic traits. Its comprehensive coverage includes copy number regions, pharmacogenomics markers, expression quantitative trait loci (eQTLs) variants and rare coding variants. There were a total of 845,487 probesets on the array, covering 825,928 SNPs.

In brief, genomic DNA was amplified across the whole genome. DNA was subsequently fragmented, precipitated and resuspended in a hybridisation cocktail. The samples were transferred to the Affymetrix GeneTitan® Multi-Channel Instrument, where automated hybridisation, staining, washing and imaging occurred.

The analysis was performed by a Statistician and Research Associate within the Department of Cardiovascular Sciences. They used the Affymetrix® Genotyping Console™ (GTC) version 4.2 and the Affymetrix® Power Tools (APT) version 1.16.1 for calling, scoring and clustering genotypes for the genotyping analysis.

### **2.1.10 RNA extraction**

- TRIzol® Reagent (Invitrogen)
- RNeasy Mini Kit (Qiagen)
- Chloroform (Sigma-Aldrich)
- 70% ethanol

- RNase-free DNase set (Qiagen)
- DNase I Amplification Grade (Sigma-Aldrich)

RNA was extracted via an adapted method using TRIzol<sup>®</sup> Reagent and the RNeasy Mini Kit, to obtain maximum yield of RNA from a small cell number. RNA was extracted from up to  $5 \times 10^6$  cells. 0.5ml TRIzol<sup>®</sup> Reagent was added directly onto cells in each well on a 6-well plate. For cells that had been grown in a T25 or T75 flask, 1ml of TRIzol<sup>®</sup> Reagent was added. The cells were lysed with repeated pipetting. The homogenised sample was incubated for 5 minutes at room temperature. 200 $\mu$ l of chloroform was added; the sample was shaken vigorously and incubated at room temperature for 3 minutes. Samples were centrifuged at 14,000 rpm for 10 minutes at room temperature. The aqueous phase was removed and placed into a new tube, whilst avoiding removal of any of the interphase or organic layer. An equal volume of 70% ethanol was added and mixed well. 700 $\mu$ l of sample was added to a RNeasy column (from RNeasy Mini Kit) and centrifuged at 10,000 rpm for 20 seconds. The flow-through was discarded and the remaining ethanol-sample was added to the RNeasy column. The flow-through was discarded. 350 $\mu$ l of RWI buffer was added to the column and centrifuged for 20 seconds, and flow-through discarded. An additional step was incorporated using the RNase-free DNase Set to digest DNA. 10 $\mu$ l of DNase I was added to 70 $\mu$ l of Buffer RDD, and mixed gently by inverting the tube. The DNase I 80 $\mu$ l incubation mix was added to the centre of the RNeasy spin column and incubated at room temperature for 20 minutes. 350 $\mu$ l of RWI buffer was added and spun at 10,000 rpm for 20 seconds, after the flow through was discarded. 500 $\mu$ l of RPE buffer was added left at room temperature for 5 minutes and centrifuged at 10,000 rpm for 2 minutes. This step was repeated. The collection tube was replaced and an additional 'dry spin' step was carried out at maximum speed. The column was transferred to an eppendorf; 25 $\mu$ l of RNase free water was added and spun at 10,000 rpm for 2 minutes. The sample was passed through the column again at 10,000 rpm for 2 minutes. A further DNase I step was carried out to further eliminate DNA from the RNA preparation. To a RNase free PCR tube 20 $\mu$ l of RNA, 2 $\mu$ l of 10x Reaction Buffer and 2 $\mu$ l of DNase I, Amplification Grade (1 unit/ $\mu$ L) was added, mixed gently and incubated for 15 minutes at room temperature. 2 $\mu$ l of Stop Solution was

added and incubated at 70°C for 10 minutes. The samples were chilled on ice before determining the concentration of RNA.

### **2.1.11 Determining the concentration of RNA**

The purity and concentration of each RNA sample was analysed using the NanoDrop 1000 Spectrophotometer (Thermo Scientific). 1µl of sample was loaded onto the platform, and the Nucleic Acids method on the ND-1000 V2.0.0 software was used to analyse each sample. The RNA concentration was recorded and the purity of the sample was determined by the 260/280 and 260/230 ratio. For long-term storage, samples were stored at -80°C.

### **2.1.12 cDNA synthesis**

- SuperScript<sup>®</sup> III First-Strand Synthesis System (Invitrogen) including; 50µM Oligo (dT)<sub>20</sub>, 10x RT buffer, 25mM MgCl<sub>2</sub>, 0.1M DTT, 10nM dNTP, 200U/µl SuperScript<sup>®</sup> III RT

Complementary DNA (cDNA) was synthesised from RNA via a reverse transcription reaction using the SuperScript<sup>®</sup> III First-Strand Synthesis System. To optimise primers for qPCR 5µg of RNA was transcribed to cDNA in one reaction, to provide enough template for the reactions. For all other experiments 1µg of RNA was synthesised. RNA was added to 1µl of 10mM dNTP mix, 1µl of 50µM Oligo(dT)<sub>20</sub> and made up to a volume of 10µl with UV-treated H<sub>2</sub>O. Samples were incubated at 65°C for 5 minutes, and placed on ice for at least one minute. A cDNA Synthesis Mix was prepared; 2µl 10x RT buffer, 4µl 25mM MgCl<sub>2</sub>, 2µl 0.1M DTT, 1µl SuperScript<sup>™</sup> III RT (200U/µl) and 1µl dH<sub>2</sub>O. For the minus reverse transcriptase (-RT) control, 1µl dH<sub>2</sub>O replaced the SuperScript<sup>™</sup> III RT. 10µl of the cDNA Synthesis Mix was added to each sample, mixed gently and collected by brief centrifugation. The sample was loaded onto the G-Storm GS4 thermal cycler (G-Storm Ltd) and run on the following programme; 50°C for 50 minutes and 85°C for 5 minutes. The samples were chilled on ice and briefly centrifuged. 1µl of RNase H was added to each tube and incubated at 37°C for 20 minutes. Samples were diluted with dH<sub>2</sub>O to the required concentration, and stored at -20°C.

### 2.1.13 Primer design for qPCR

The UCSC Genome Browser software was used to obtain the exon sequence of the gene of interest. The Primer3 online tool was used to design PCR primers. Primers were designed using the following guidelines;

- Primer length- 18-22 base pairs
- Melting temperature- 52-60°C
- GC content - 40-60%
- Amplicon length- 80-150bp
- Span an intron-exon boundary

Once Primer3 (<http://primer3.ut.ee/>) had generated potential forward and reverse primers, they were verified using two online tools called OligoCalc (<http://www.basic.northwestern.edu/biotools/oligocalc.html>) and OligoAnalyzer (<https://eu.idtdna.com/calc/analyzer>). The general primer properties were determined such as melting temperature, potential dimers, hairpins and mismatches. The BLAT function on the UCSC Genome Browser software was used to confirm the correct genomic region the forward and reverse primers were expected to bind. The In Silico PCR function on the UCSC Genome Browser software was also used. It searched a sequence database using a pair of PCR primers, to determine the size of the PCR product and the genomic region the primers will amplify. The primer sequences were sent to Thermo Fisher for synthesis.

### 2.1.14 Optimisation of primers for qPCR

- SensiMix™ SYBR No-ROX (2x; Biorline)
- Designed primer pairs (Thermo Fisher). Prepared to 10µM stock with dH<sub>2</sub>O.
- Quantitech Primer Assays (Qiagen)
- HyperLadder™ 100bp (Biorline)
- GelRed™ Nucleic Acid Gel Stain, 10,000X in Water (Biotium)

Quantitative PCR (qPCR) is a technique that quantifies the amount of target DNA in a sample. A fluorescence reporter e.g. SYBR Green, binds to double stranded DNA, and therefore DNA can be measured in real-time. This detection is recorded at each cycle of the PCR process, which results in a quantitative relationship between the quantity of PCR product accumulated and the quantity of starting target sequence. It is during the exponential phase that the increase in PCR product correlates directly with the starting amount of target template. This stage is log linear, assuming the amplification is doubling at 100% efficiency. When this parameter is measured it is known as the ‘take-off’.

Firstly, primers were optimised for each gene. A qPCR reaction was performed for each primer set using a starting primer concentration of 0.3 $\mu$ M and 0.5 $\mu$ M, as detailed in **Table 2.1**. The samples were run on either a 2 step or 3 step qPCR programme, both of which had an initial step of 95°C for 10 minutes. The two step programme consisted of 35 cycles; denaturation (95°C 15 seconds) and a combined annealing and extension step (58°C 45 seconds). The three step programme consisted of 35 cycles; denaturation (95°C 15 seconds), annealing (58°C 15 seconds) and extension step (72°C 30 seconds).

Reagent	Vol. for 0.3 $\mu$ M primer concentration	Vol. for 0.5 $\mu$ M primer concentration
SensiMix™ SYBR No-ROX (2x)	12.5 $\mu$ l	12.5 $\mu$ l
Forward primer (10 $\mu$ M)	0.75 $\mu$ l	1.25 $\mu$ l
Reverse primer (10 $\mu$ M)	0.75 $\mu$ l	1.25 $\mu$ l
dH <sub>2</sub> O	9 $\mu$ l	8 $\mu$ l

**Table 2.1.** PCR components for a 25 $\mu$ l qPCR reaction.

Samples were run on an agarose gel to ensure primers produced a single product of the correct size. 15 $\mu$ l of PCR sample was added to 3 $\mu$ l of 5x loading dye and run on a 1.5% agarose gel (described in **Section 2.1.7**). However instead of ethidium bromide, GelRed was added at a dilution of 1:10,000 to the agarose. 10 $\mu$ l of Hyperladder™ 100bp was loaded into the first well. A melt curve analysis was also included to verify the amplification of a

single product. Primer sets were taken forward for standard curve analysis, if a single product was observed on the agarose gel. If non-specific bands were seen, further optimisation was carried out, such as primer titration or alteration of PCR programme conditions.

For standard curve analysis, a 3-fold dilution series was used to obtain 6 different concentrations. The results were used to plot the log of the input concentrations against the take-off value. The line of regression was calculated to determine the linearity of the data (known as  $R^2$ ), an  $R^2$  value greater than 0.98 indicated good linearity. The slope of the standard curve enabled the efficiency of the reaction to be calculated, by using the formula:  $E=10^{(-1/\text{slope})}$ . A slope of -3.32 equates to 100% doubling at each cycle. For each primer pair an acceptable slope parameter was between -3.6 to -3.1 (equivalent to 90-110% efficiency).

#### **2.1.15 Quantitative PCR**

For each experiment, two controls were included; a NTC and no-reverse transcriptase control (-RT control). NTC accounted for contamination of PCR reagents and primer dimers. The -RT control accounted for contamination of genomic DNA or non-specific products. For experiments, each sample was run in triplicate for accuracy. **Table 2.2** details the parameters for each gene. The QIAgility (Qiagen) is a bench-top robot and was used to set up qPCR experiments. The QIAgility software (Qiagen) was used to set up the automated reaction. The samples were run on the Rotor-Gene (Qiagen), which ensures thermal uniformity as samples are placed on a circular rotor. The samples are spun at 400 rpm during the run, safeguarding against condensation issues. Data was analysed using the Rotor-Gene Q software (Qiagen), using 'comparative quantification'. Technical replicate samples were removed if they were not within 0.2 (if the reaction was set up using the QIAgility) or 0.5 (if the reaction was set up manually) cycles of each other. The data was then normalised to the housekeeping gene;  $\beta$ -actin or *36B4* (for adipocyte experiments), and the fold change against the control sample was calculated.

Primer	Sequence	Amplicon length	Primer [ ]	PCR profile
<b>AFP</b>	F-GTAGCGCTGCAAACAATGAA-R F-CCCTCTTCAGCAAAGCAGAC-R	161bp	0.3µM	2 step; 35 cycles; 95°C 15s, 58°C 45s
<b>CK19</b>	F-TTTGAGACGGAACAGGCTCT-R F-AATCCACCTCCACACTGACC-R	211bp	0.3µM	2 step; 30 cycles; 95°C 15s, 58°C 35s
<b>ALB</b>	F-GCAAGGCTGACGATAAGGAG-R F-CCTAAGGCAGCTTGACTTGC-R	76bp	0.5µM	3 step; 35 cycles; 95°C 15s, 58°C 15s, 72°C 30s
<b>PCK1</b>	F-ATCTTTGGAGGCCGTAGACC-R CCCCACAAAGACTCCATGTT-R	78bp	0.5µM	3 step; 35 cycles; 95°C 15s, 58°C 15s, 72°C 30s
<b>ACTA2</b>	F-CTGTTCCAGCCATCCTTCAT-R F-CCGTGATCTCCTTCTGCATT-R	175bp	0.3µM	3 step; 35 cycles; 95°C 15s, 58°C 15s, 72°C 20s
<b>CNN1</b>	F-ACATTTTTGAGGCCAACGAC-R F-ACTTCACTCCCACGTTCCACC-R	120bp	0.5µM	3 step; 35 cycles; 95°C 15s, 58°C 15s, 72°C 30s
<b>TAGLN</b>	Quantitech Primer Assay	-	-	2 step; 35 cycles; 95°C 10s, 60°C 30s
<b>MYH11</b>	F-AGATGGTTCTGAGGAGGAAACG-R F- AAAACGTAGAAAGTTGCTTATTCAC T-R	85bp	0.5µM	3 step; 40 cycles; 95°C 15s, 58°C 15s, 72°C 20s
<b>SMTN</b>	F-CGAGTGAACAAAGCACCAGA-R F-ATGAGCTTCCGCTCTTCAA-R	125bp	F (0.3µM) R (0.4µM)	2 step; 40 cycles; 95°C 15s, 58°C 35s
<b>KLF4</b>	Quantitech Primer Assay	-	-	2 step; 35 cycles; 95°C 10s, 60°C 30s
<b>ADAMT S7</b>	F-TGGAGACCCTGGTAGTAGCT-R F-ATGGTGATGTGGATGGGGTT-R	142bp	0.5µM	3 step; 35 cycles; 95°C 15s, 58°C 15s, 72°C 20s
<b>COMP</b>	F-AAGGGAGATCGTGCAGACAA-R F-GTAGCCAAAGATGAAGCCCG-R	139bp	0.5µM	2 step; 35 cycles; 95°C 15s, 58°C 45s
<b>PPARy</b>	F-ACAGATCCAGTGGTTGCAGA-R F-GATGCAGGCTCCACTTTGAT-R	80bp	0.5µM	3 step; 35 cycles; 95°C 15s, 58°C 15s, 72°C 30s
<b>FABP4</b>	Quantitech Primer Assay	-	-	2 step; 35 cycles; 95°C 10s, 60°C 30s

<b>ZC3H4</b>	F-GATTTTCAGCCCCAGTGAGAA-R F-TCTTGCTGTCCATCTTGGAG-R	136bp	0.2 µM	2 step; 35 cycles; 95°C 15s, 58°C 35s
<b>TRIM66</b>	Quantitech Primer Assay	-	-	2 step; 35 cycles; 95°C 10s, 60°C 30s
<b>36B4</b>	F-TCGACAATGGCAGCATCTAC-R F-GCCTTGACCTTTTCAGCAAG-R	221bp	0.3µM	3 step; 35 cycles; 95°C 15s, 58°C 15s, 72°C 20s
<b>BACTIN</b>	F-GGACTTCGAGCAAGAGATGG-R F-AGCACTGTGTTGGCGTACAG-R	234bp	0.5µM	2 step; 30 cycles; 95°C 15s, 58°C 45s

**Table 2.2. Details of the parameters for each gene for qPCR.** Shown are the sequence for each primer pair, the length of the amplicon, the optimised primer concentration, and the qPCR programme for each gene.

## 2.2 Cell culture

### 2.2.1 Collection and transport of umbilical cords

- Hanks' Balanced Salt Solution (HBSS; Invitrogen)
- 100x Antibiotic-Antimycotic Solution (Invitrogen)

Non-identifiable tissue was collected by Anthony Nolan Trust midwives and provided under the cord blood sample transfer protocol and material transfer agreement (**Figure S1**). Ethical approval for the work was covered by the generic approval granted to Anthony Nolan Trust. Signed informed consent was obtained from the mother, for every umbilical cord collected. The mother was asked to complete a form regarding the medical history of the baby's biological family (**Figure S2**). Umbilical cords were obtained from natural or caesarean deliveries. Ten-to-twenty centimetres was cut from the fetal end of the umbilical cord, and immersed in sterile HBSS supplemented with 1% antibiotic-antimycotic solution, and transferred to the tissue culture room. The samples were processed within two hours from the time of birth. For each umbilical cord sample processed; date, time of birth, time of collection and the length of the umbilical cord processed was recorded.

### 2.2.2 Isolation of MSCs

- Phosphate Buffered Saline (PBS; Oxoid)
- Cell culture plasticware (Greiner Bio One)
- Serological pipettes (Corning® Costar®)
- Swann Morton Sterile Scalpels (Fisher Scientific)
- Complete medium; 45% Minimum Essential Medium Eagle, Alpha modification ( $\alpha$ MEM; Sigma-Aldrich), 45% Ham's F-12 (PAA), 10% Fetal Bovine Serum (FBS; PAA), 1% Antibiotic-Antimycotic Solution and 5ng/ml Basic Fibroblast Growth Factor (bFGF; Peprotech)

The explant method was used to isolate MSCs from WJ of the umbilical cord. The umbilical cord was washed several times with PBS to remove residual blood, and cut into 1.5-2cm<sup>2</sup> pieces. Each piece was dissected longitudinally, and the umbilical vessels were removed. WJ was excised from the amniotic epithelium and diced into 4-5mm<sup>2</sup> pieces with a sterile scalpel. 4-5 tissue fragments were placed into each well of a 6-well plate. The 6-well plates were incubated at 37°C in a 5% CO<sub>2</sub> atmosphere for 30-60 minutes, to facilitate tissue attachment to the plastic. Pre-warmed complete medium was added to each well until the tissue fragments were immersed. Samples were incubated at 37°C in a 5% CO<sub>2</sub> atmosphere for 5-7 days to allow cell migration from the explants. After 7 days the medium was replaced twice a week. Cell migration was monitored using a Nikon Diaphot Inverted Microscope (Nikon). When cells reached 80-90% confluency around the tissue blocks MSCs were subcultured. I isolated MSCs from Donors 1-20; subsequent preparations were undertaken by two Technicians within the Department of Cardiovascular Sciences.

### 2.2.3 Subculture and maintenance of MSCs

- 10x Trypsin-EDTA (0.05% Trypsin, 0.02% EDTA; PAA)
- 0.4% Trypan Blue Solution (Fisher Scientific)

Upon confluency, the waste medium was discarded and the tissue fragments and cell monolayer were washed with PBS. The adherent cells were

detached with 1x Trypsin/EDTA (1:10 dilution of 10x Trypsin/EDTA in PBS). 1ml of Trypsin/EDTA was added for every 25cm<sup>2</sup> for 2-5 minutes at 37°C, until cells detached from the plastic surface. An equal volume of complete medium was added to inactivate the trypsin. The cell suspension was transferred to a sterile centrifuge tube. The trypsinized surface was washed with PBS, and also placed into the centrifuge tube. Using the Nikon Diaphot Inverted Microscope an estimate of the number of cells in each well was determined. If cells' migrating from only one tissue fragment was observed, the cell population was split at a 1:3 ratio. If several wells were confluent, the cells were pooled and centrifuged at 1,500 rpm for 5 minutes. After centrifugation, the supernatant was discarded, and the cell pellet was re-suspended in 1ml of pre-warmed medium. 10µl of cell suspension was mixed with 10µl of 0.4% Trypan Blue solution, and pipetted onto a haemocytometer to perform a cell count and determine cell viability. Next cells were plated at a cell density of 5x10<sup>3</sup> cells/cm<sup>2</sup> in the appropriate culture flask. A Nikon Diaphot Inverted Microscope was used to monitor the phenotype and growth of the cells, and upon 80-90% confluency, the cells were passaged. For all further passages primary MSCs were split at a 1:3 ratio.

#### **2.2.4 Cryopreservation of MSCs**

- Dimethyl Sulfoxide (DMSO; Sigma-Aldrich)
- Cryovial tubes (Sarstedt)

MSCs were trypsinized as described in **Section 2.2.3**. After centrifugation the supernatant was discarded. The cell pellet was resuspended at a density between 8-40 x 10<sup>5</sup> cells in cryoprotectant solution (50% complete medium, 40% FBS and 10% DMSO) and transferred to cryovials. The cells were stored overnight at -80°C, and subsequently transferred to a liquid nitrogen tank for long term storage.

### **2.2.5 Thawing and plating of MSCs**

Cryovials were removed from liquid nitrogen and placed in a 37°C water bath with constant, moderate agitation for 1-2 minutes. The contents of the cryovial were transferred to a sterile centrifuge tube to which 10ml of pre-warmed complete medium was slowly added. MSCs were left for 5 minutes to acclimatize. The cells were centrifuged at 1,500 rpm for 5 minutes. The medium was removed and cells were resuspended in 1ml complete medium. The cell suspension was transferred to a culture flask and cultured at 37°C, 5% CO<sub>2</sub>. Cells were subcultured when confluency was observed, as described in **Section 2.2.3**.

### **2.2.6 Growth curve**

Third passage (P3) cells were seeded, in duplicate, at a density of  $6 \times 10^3$  cells/cm<sup>2</sup> in 12-well plates. Every two days the cells were trypsinized and the cell number was determined as described in **Section 2.2.3**. The mean number of cells for each day was recorded. The data for MSCs from three different donors was used to plot growth curves.

### **2.2.7 Population doubling time**

The population doubling time (PDT) for MSCs isolated from WJ was determined, using the following formula  $PDT = \text{culture time (CT)} / \text{population doubling number (PDN)}$ . PDN was determined by using the equation  $PDN = \log(N_1/N_0) \times 3.31$ , where  $N_0$  = number of cells at the start of culture time,  $N_1$  = number of cells at the end of culture time. To deduce the parameter values, P3 cells were seeded at  $1 \times 10^4$  cells/cm<sup>2</sup> in T25 flasks. The cells were cultured and checked daily until MSCs reached confluency. The cells were trypsinized and counted as described in **Section 2.2.3** to determine  $N_1$ . PDT was calculated using data obtained from MSCs from three different donors.

## **2.2.8 Maintenance and culture of other cells**

### **2.2.8.1 Human umbilical cord-derived MSCs**

- Human Umbilical Cord-Derived Mesenchymal Stem Cells (minimum of  $5 \times 10^5$  viable cells; ATCC)
- Complete growth medium; Mesenchymal Stem Cell Basal Medium (ATCC), 3% Mesenchymal Stem Cell Growth Kit (ATCC), 0.5% Gentamicin-Amphotericin B Solution (ATCC) and 0.5% Penicillin-Streptomycin-Amphotericin B Solution (ATCC)
- Trypsin-EDTA for primary cells (0.05% Trypsin, 0.02% EDTA; ATCC)

Cryovials of human umbilical cord-derived MSCs were removed from liquid nitrogen and thawed rapidly in a 37°C waterbath for 1-2 minutes. 1ml of cell solution was transferred to a sterile centrifuge tube. 3ml of complete growth medium was added. 1ml of cell solution was transferred to a T25 flask already containing pre-warmed complete medium, to obtain a seeding density of  $5 \times 10^3$  cells/per  $\text{cm}^2$ . The seeded culture flasks were placed in an incubator at 37°C, 5%  $\text{CO}_2$  atmosphere. Cells were grown until 70-80% confluency was observed. The cells were trypsinized and counted as described in **Section 2.2.3**, and seeded at a cell density of  $5 \times 10^3$  cells/ $\text{cm}^2$ .

### **2.2.8.2 Human aortic smooth muscle cells**

- Human Aortic Smooth Muscle Cells (HAoSMC; Invitrogen; provided by a Research Associate within the Department of Cardiovascular Sciences)
- Medium 231 (Invitrogen)
- Smooth Muscle Growth Supplement (SMGS; Invitrogen)
- 100x Penicillin/Streptomycin (PAA)

Cryovials of human aortic smooth muscle cells (HAoSMCs; P6-8) were taken out of liquid nitrogen and thawed in a water bath at 37°C for 1-2 minutes. 9ml of supplemented Medium 231 with Smooth Muscle Growth Supplement (Medium 231, 5% SMGS and 1x Penicillin/Streptomycin) was added to a T75 flask to which 1ml of cell suspension was added. The flask was swirled gently to

ensure even coverage and placed in an incubator at 37°C, 5% CO<sub>2</sub> atmosphere. After 24 hours, the media was replaced with fresh media. HAoSMCs were grown until they were 70-80% confluent. Cells were trypsinized with 1x Trypsin-EDTA and split at a 1:3 ratio.

#### **2.2.8.3 HepG2s**

- HepG2s (ATCC; provided by a PhD student within the Department of Cardiovascular Sciences)
- Minimum Essential Medium Eagle (EMEM; Sigma-Aldrich)
- Foetal Bovine Serum (PAA)
- 100x Penicillin/Streptomycin (PAA)

A cryovial of HepG2s (P13) were removed from liquid nitrogen and thawed in a water bath at 37°C for 1-2 minutes. 10ml of pre-warmed supplemented EMEM (with 10% FBS and 1x Penicillin/Streptomycin) was added to a T75 flask. 1ml of cell suspension was added to the flask and gently swirled. Cells were incubated at 37°C, 5% CO<sub>2</sub> atmosphere. After 24 hours, fresh media was added to remove any remaining DMSO. When cells were confluent, they were split at a 1:10 ratio using 2x Trypsin-EDTA.

#### **2.2.8.4 HEK293**

- HEK293 (Cell Lines Service; provided by a PhD student within the Department of Cardiovascular Sciences)
- Dulbecco's Modified Eagle's Medium (DMEM; Sigma-Aldrich)

HEK293 cryovials were stored in liquid nitrogen. A vial was removed and thawed at 37°C for 1-2 minutes. 10ml of pre-warmed supplemented DMEM (with 10% FBS and 1x Penicillin/Streptomycin) was added to a T75 flask. The contents of the cryovial was slowly added to the flask, and gently swirled to ensure a homogenous suspension. HEK293s were incubated at 37°C, 5% CO<sub>2</sub> atmosphere. After 24 hours, the culture medium was replaced with fresh supplemented DMEM. When cells approached confluency, 2x Trypsin-EDTA was used to split cells at a 1:10 ratio.

### **2.2.8.5 3T3-L1s**

- 3T3-L1 cells (provided by a Research Fellow within the Department of Cardiovascular Sciences)
- 3-isobutyl-1-methylxanthine (IBMX; Sigma-Aldrich). Made a 10mg/ml stock using ethanol.
- Dexamethasone (Sigma-Aldrich). Made a 1mg/ml stock in ethanol, and then added 49ml of DMEM
- Insulin from bovine pancreas (Sigma-Aldrich). Made a 10mg/ml stock using 1M acetic acid.

A cryovial of 3T3-L1 cells were removed from liquid nitrogen and thawed at 37°C for 1-2 minutes. The cells were transferred to a 15ml centrifuge tube, to which 15ml of DMEM (with 10% FBS and 1x Penicillin/Streptomycin) was added. The cells were left for 5 minutes, before transferring into a T75 flask. After 24 hours, the culture medium was replaced with fresh supplemented DMEM. Upon confluency cells were split at a 1:5 ratio. The media was replaced every two days.

For adipogenic differentiation of 3T3-L1s, cells were plated at  $5 \times 10^4$  cells per well in a 6 well plate, in 2ml of growth medium. The medium was changed after 1, 3 and 5 days. At 7 days, cells were very confluent. 2ml of adipogenic differentiation medium (DMEM with 0.5mM 3-isobutyl-1-methylxanthine, 2µg/ml bovine insulin and 0.25µmol/L dexamethasone) was added to each well, and left for 3 days. The adipogenic differentiation medium was removed carefully, and replaced with 2ml of DMEM (with 10% FBS and 1x Penicillin/Streptomycin). Media was replaced every two days until day 6, where there was significant differentiation of 3T3-L1 cells into adipocytes.

### **2.2.9 Adipogenic differentiation**

- STEMPRO<sup>®</sup> Adipogenesis Differentiation Kit (Invitrogen)
- 0.5% Oil Red O; 0.5g Oil Red O (Sigma-Aldrich) in 100ml propan-2-ol (Fisher Scientific).
- Formaldehyde Solution (Fisher Scientific)

- Mayer's hematoxylin (Sigma-Aldrich)

*In vitro* adipogenic differentiation of MSCs was induced by using the STEMPRO<sup>®</sup> Adipogenesis Differentiation Kit (Invitrogen) following the manufacturer's protocol. P5 MSCs were seeded at  $1 \times 10^4$  cells/cm<sup>2</sup> in 12-well plates, with complete medium at 37°C in a 5% CO<sub>2</sub> atmosphere for up to four days, until cells reached near or complete confluency. The medium was replaced with 1ml of pre-warmed Adipogenesis Medium (1x STEMPRO<sup>®</sup> Adipocyte Differentiation Basal Medium, 1x STEMPRO<sup>®</sup> Adipogenesis Supplement and 1% Antibiotic-Antimycotic Solution). The medium was replaced every three days. Negative control samples were also established; MSCs were cultured in complete medium. After 14 days cells subjected to adipogenic medium, were assessed for adipogenic differentiation by Oil Red O staining.

#### **2.2.9.1 Oil Red O staining**

Adipogenesis Medium and complete medium was removed from wells, and 400µl of 4% formaldehyde was added for 30 minutes. After fixation, the cells were washed twice with PBS. 3 parts of 0.5% Oil Red O stock was added to 2 parts of dH<sub>2</sub>O, left for ten minutes, and filtered through a 0.22µm filter. 200µl of Oil Red O solution was added to each well and incubated for 30 minutes in the dark. Cells were washed three times with DPBS. 400µl of Mayer's haematoxylin was incubated with the cells for 1 minute and rinsed with PBS until clear. 1ml of DPBS was added and the cells were visualised and photographed using the EVOS xl core Microscope (Advanced Microscopy Group).

#### **2.2.10 Density centrifugation of MSC-derived adipocytes**

MSCs were differentiated into adipocytes as described in **Section 2.2.9**. Cells were washed with PBS, and trypsinized with 1x Trypsin/EDTA, until all cells were in suspension. 10ml of pre-warmed medium was added to the cells and transferred to a 15ml centrifuge tube. Cells were centrifuged at 150 g for 5 minutes. The supernatant was discarded and the cell pellet was resuspended in

5ml PBS. The cells were centrifuged again. 100µl of supernatant was taken from the top of the meniscus, 1cm below, 2cm below and just above the pellet. Samples were transferred to a new well and 2ml of adipogenic differentiation medium added. Cells were visualised after 24 hours to determine the presence of mature adipocytes.

### **2.2.11 Ceiling culture separation of MSC-derived adipocytes**

MSCs were differentiated into adipocytes for 14 days as described in **Section 2.2.9**. Cells were washed with PBS, and trypsinized with 1x Trypsin/EDTA, until all cells had been removed from the surface. A flask completely filled with medium, which had a solid screw top has been equilibrated in the incubator for 4 hours. The cell suspension was carefully added to this flask, ensured the flask was completely full and placed back into the incubator at 37°C, 5% CO<sub>2</sub>. Cells were left for 4 hours and 72 hours, and visualised to determine if mature adipocytes had separated and adhered to the top of the flask.

### **2.2.12 Chondrogenic differentiation**

- STEMPRO<sup>®</sup> Chondrogenesis Differentiation Kit (Invitrogen)
- 10% Neutral-Buffered Formalin (0.65g disodium hydrogen phosphate, anhydrous, 0.4g sodium dihydrogen phosphate, monohydrate. 90ml dH<sub>2</sub>O was added and adjusted to pH 7.4. 10ml of 40% formaldehyde was added and stored at 4°C)
- Agarose, Electrophoresis Grade (Melford Laboratories)
- Tissue-Tek<sup>®</sup> Mega-Cassette (Sakura)
- Ethanol (Genta medical)
- 1% Toluidine Blue; 1g Toluidine Blue (Sigma-Aldrich) in 100ml dH<sub>2</sub>O. Filtered before use.
- DPX mountant (VWR International Ltd)
- 22mm circle coverslips (Fisher Scientific)

P5 MSCs were assessed for their ability to differentiate into chondrocytes via a pellet cultural system.  $5 \times 10^5$  cells were pelleted by centrifugation at 1,500 rpm for 5 minutes. The supernatant was removed from the pellet and 0.5ml of pre-warmed Chondrogenesis Medium (1x STEMPRO<sup>®</sup> Osteocyte/Chondrocyte Differentiation Basal Medium, 1x STEMPRO<sup>®</sup> Chondrogenesis Supplement and 1% Antibiotic-Antimycotic Solution) was added and incubated at 37°C in a humidified atmosphere of 5% CO<sub>2</sub>. Medium was replaced every three days, carefully without disturbing the pellet. As a negative control, pellets were cultured in 0.5ml of complete medium. Cell pellets were harvested after 28 days for assessment of chondrogenic differentiation by Toluidine Blue staining.

### **2.2.12.1 Toluidine Blue staining**

Chondrogenesis medium and complete medium was removed, and the cell pellets were washed with PBS. 1ml of 10% Neutral-Buffered Formalin (NBF) was added to the pellets, for fixation and left overnight. The cell pellet was gently loosened and 1-2 ml of 2% agarose was added to each centrifuge tube and left to set. The agarose plug was slowly removed from the centrifuge tube; the excess agarose was removed, and the plug was placed into a Tissue-Tek<sup>®</sup> Mega-Cassette. The cassette was placed into 100% ethanol and processed by the Core Biotechnology Services (CBS) at The University of Leicester. The pellet underwent a series of processes; 70% IMS- 1 hour, 99% IMS- 1 hour, xylene-1½ hours, xylene-1½ hours, wax - 1 hour, wax - 1½ hours, wax - 1½ hours. 4µM sections were created using the Leica rm2125RT Microtome (Leica Microsystems). A hematoxylin and eosin (H&E) stain was performed using an automated Leica ST 4040 Linear stainer (Leica Microsystems) to determine the cellular morphology.

Next the slides were subjected to Toluidine Blue staining. The slides were placed in xylene for 10 minutes and further rinsed in xylene for 10 minutes. Slides were put into 100% ethanol for 10 minutes (twice), 90% ethanol (10 minutes) and 70% ethanol (10 minutes) and finally in dH<sub>2</sub>O. 1% Toluidine Blue was pipetted onto each slide, and left for 2 minutes. After 2 minutes the slides

were rinsed in dH<sub>2</sub>O. The samples were dehydrated through a graded ethanol series (70% (30 seconds), 100% (5 minutes; twice) and finally xylene (10 minutes; twice). DPX mountant was pipetted onto coverslips, and lowered onto the slide and left to dry for 30 minutes. Samples were visualised and photographed using the Leica DM2500 microscope (Leica Microsystems) and the Leica Application Suite V4.0 (Leica Microsystems).

### **2.2.13 Osteogenic differentiation**

- STEMPRO<sup>®</sup> Osteogenesis Differentiation Kit (Invitrogen)
- 2% Alizarin Red S; 2g Alizarin Red S (Sigma-Aldrich) in 100ml dH<sub>2</sub>O. Adjusted to pH 3 with 10% Ammonium Hydroxide. Filtered before use.
- Formaldehyde Solution (Fisher Scientific)

STEMPRO<sup>®</sup> Osteogenesis Differentiation Kit (Invitrogen) was used to differentiate MSCs into osteoblasts following the manufacturer's protocol. P5 cells were seeded at cell density of  $5 \times 10^3$  cells/cm<sup>2</sup> in 12-well plates and incubated with complete medium at 37°C in a humidified atmosphere of 5% CO<sub>2</sub> until the cells were confluent. The medium was replaced with 1ml of pre-warmed Osteogenesis Medium (1x STEMPRO<sup>®</sup> Osteocyte/Chondrocyte Differentiation Basal Medium, 1x STEMPRO<sup>®</sup> Osteogenesis Supplement and 1% Antibiotic-Antimycotic Solution). The Osteogenesis Medium was replaced every three days. Corresponding negative control wells were also seeded with MSCs grown in complete medium. After 28 days, MSCs that were subjected to osteogenic medium were assessed for differentiation by Alizarin Red S staining.

#### **2.2.13.1 Alizarin Red S staining**

Osteogenesis medium and complete medium was removed from wells, and 400µl of 4% formaldehyde was added for 30 minutes. After fixation, cells were rinsed twice with dH<sub>2</sub>O, and 200µl of 2% Alizarin Red S (pH 3) was added to the wells for 2-3 minutes. The wells were rinsed three times with dH<sub>2</sub>O. DH<sub>2</sub>O

was left in the wells, samples were visualised and photographed using the EVOS xl Core Microscope (Advanced Microscopy Group).

#### **2.2.14 Hepatogenic differentiation**

- Collagen I Rat Protein, Tail (Invitrogen)
- Iscove's Modified Dulbecco's Medium (IMDM; PAA)
- Recombinant Human Fibroblast Growth Factor, Basic (bFGF; Peprotech)
- Recombinant Human Epidermal Growth Factor (EGF; Peprotech)
- ITS+ Universal Culture Supplement Premix (BD Biosciences)
- Recombinant Human Hepatocyte Growth Factor (HGF; Peprotech)
- Nicotinamide (Sigma-Aldrich)
- Dexamethasone (Sigma-Aldrich)
- Recombinant Human Oncostatin M (Invitrogen)

6-well plates were coated with  $5\mu\text{g}/\text{cm}^2$  of collagen I solution, according to the manufacturer's protocol. MSCs (P5) were seeded in 6-well plates at a density of  $1.5 \times 10^4$  cells/ $\text{cm}^2$ . For control wells, MSCs were seeded at a density of  $4 \times 10^3$  cells/ $\text{cm}^2$  and grown in complete medium. After 24 hours, MSCs underwent a pretreatment step. MSCs were grown in IMDM containing 10ng/ml bFGF, 20ng/ml EGF and 1% antibiotic-antimycotic solution for two days. The media was changed, so MSCs were cultured in IMDM supplemented with 10ng/ml bFGF, 20ng/ml HGF, 0.61g/l nicotinamide, 1% ITS, 1% FBS and 1% antibiotic-antimycotic solution for 7 days. For the next 14 days, cells were treated with IMDM containing  $1\mu\text{mol}/\text{l}$  dexamethasone, 20ng/ml oncostatin M, 1% ITS, 1% FBS and 1% antibiotic-antimycotic solution. For each differentiation step, medium was replaced every three days. A Nikon Diaphot Inverted Microscope was used to monitor the phenotype and growth of the cells during the differentiation process.

#### **2.2.15 Smooth muscle cell differentiation**

- Collagen I, Coated Plate 6 Well (Invitrogen)

- Recombinant Human Transforming Growth Factor- $\beta$ 1 (TGF- $\beta$ 1; Peprotech)
- Smooth Muscle Cell Differentiation Medium ; 48%  $\alpha$ MEM (Sigma-Aldrich), 48% Ham's F-12 (PAA), 1% FBS (PAA), 1% Antibiotic-Antimycotic Solution (Invitrogen) and 10ng/ml TGF- $\beta$ 1

The literature suggests TGF- $\beta$ 1 is the main driver for SMC differentiation. The literature has reported use of TGF- $\beta$ 1 concentrations of 1-10ng/ml (Kinner *et al.*, 2002; Jeon *et al.*, 2006; Narita *et al.*, 2008). 10ng/ml TGF- $\beta$ 1 was used to induce the highest response of differentiation. Cells were seeded into pre-coated Collagen I, 6 well plates. MSCs (P5) were seeded into each well at  $4 \times 10^3$  cells/cm<sup>2</sup> for controls and grown in complete MSC medium. For smooth muscle cell differentiation, MSCs were seeded at a density of  $8 \times 10^3$  cells/cm<sup>2</sup>. MSCs were grown to 70% confluency, which took approximately 1-2 days. The complete MSC medium was removed, and the cells were washed once with 1x PBS. 2ml of Smooth Muscle cell Differentiation Medium was added to each well on a 6 well plate. The medium was replaced every 3 days. MSCs were visualised and photographed every three days using the EVOS XL Core Microscope (Advanced Microscopy Group).

### **2.2.16 Transformation of recombinant plasmid**

- DH5 $\alpha$  competent E.coli cells (Bioline)
- Difco™ Agar, granulated (BD Biosciences; 1.5g into 100ml dH<sub>2</sub>O, and autoclaved)
- Ampicillin Sodium Salt (Sigma-Aldrich). Prepared 100mg/ml stock in dH<sub>2</sub>O.
- Luria broth (Sigma-Aldrich; 2.5g into 100ml dH<sub>2</sub>O, and autoclaved)
- PeqGOLD Plasmid MiniPrep Kit II (Peqlab)

The ADAMTS7-Ser plasmid was available within the research group. It had previously been cloned into the pLEICS-49 vector using the Protein Expression Laboratory (PROTEX) cloning service at the University of Leicester.

The ADAMTS7-Ser plasmid was transformed into subcloning efficiency DH5 $\alpha$  competent E.coli cells. Firstly cells were thawed on ice; 40 $\mu$ l was transferred to a new tube, to which 2 $\mu$ l of plasmid was added and the tube flicked gently. The tube was incubated on ice for 30 minutes. The cells were then heat shocked for 45 seconds at 42°C, followed by 2 minute incubation on ice. 250 $\mu$ l of Luria broth (LB) was added, and incubated in a shaking incubator at 37°C at 200 rpm for 1 hour. 75 $\mu$ l of sample was spread onto a LB-agar plate (containing 100 $\mu$ g/ml ampicillin) using aseptic techniques, to allow for the growth of transformed cells. Plates were inverted and incubated overnight at 37°C. The next day, successful transformation was indicated by the growth of white colonies. The plates were stored at 4°C. A pipette tip was used to pick single colonies and placed in a universal with pre-warmed LB (containing 100 $\mu$ g/ml ampicillin). Universals were placed in a shaking incubator at 37°C at 200 rpm overnight. To extract plasmid DNA, the PeqGOLD Plasmid MiniPrep Kit II was used following the manufacturer's instructions. The concentration of plasmid DNA was measured using the ND-8000 Nanodrop spectrophotometer (described in **Section 2.1.2**) and stored at -20°C. To create glycerol stocks for future use, 400 $\mu$ l of overnight culture was mixed with 600 $\mu$ l of glycerol and stored at -80°C.

### **2.2.17 Transient transfections**

- Lipofectamine<sup>®</sup> LTX Reagent with PLUS<sup>™</sup> Reagent (Life Technologies)
- Opti-MEM<sup>®</sup> I Reduced Serum Media (Life Technologies)
- pEGFP-C2 plasmid (Clontech)

The ADAMTS7-Ser plasmid was transfected into HEK293 cells. 1.5x10<sup>5</sup> cells were seeded into each well of a 6 well plate, which enabled 80% confluency after 24 hours. Lipofectamine LTX plus reagent was used according to the manufacturer's protocol. Briefly 1.25 $\mu$ g of ADAMTS7-Ser plasmid and 1.25 $\mu$ g of GFP plasmid (pEGFP-C2) was added to 125 $\mu$ l of Opti-MEM<sup>®</sup> I Reduced Serum Media. The GFP plasmid was available within the research group, and used to determine approximate transfection efficiency. As a control sample, ADAMTS7-Ser plasmid was not added. 5 $\mu$ l of Plus<sup>™</sup> Reagent was

added, mixed and incubated for 7 minutes. 15µl of Lipofectamine™ LTX was added to 125µl of Opti-MEM® I Reduced Serum Media. The diluted plasmid DNA and diluted Lipofectamine™ LTX was combined gently and incubated for 15 minutes. 750µl of Opti-MEM® I Reduced Serum Media was added and mixed gently. 1ml of DMEM (+10% FBS) was added to each well, followed by 1ml of the diluted complex. After 6 hours, the media was replaced with serum-free DMEM and incubated at 37°C, 5% CO<sub>2</sub> for 48 hours.

## **2.3 Flow cytometry**

### **2.3.1 Preparation of MSCs**

- Sodium Azide (Sigma-Aldrich)
- Human MSC Analysis Kit (BD Biosciences)
- 5ml FACS tubes (BD Falcon)

P5 MSCs were used for flow cytometric analysis. Cells were detached using 0.25x Trypsin/EDTA, centrifuged and washed with Stain Buffer (1x PBS, 1% FBS, and 0.09% Sodium Azide) and resuspended at a concentration of 5 x 10<sup>6</sup> cells/ml. Multicolour analysis was carried out using a Human MSC Analysis Kit, to minimize the number of cells for each assay, and to create a simple protocol for multiple sample analysis. Cells were incubated with individual or a cocktail of antibodies in separate tubes, as indicated in **Table 2.3**. Single stained controls were included for the first sample run (tubes 1-4). For all subsequent samples only tubes 4-6 were set up. Once the antibodies had been added to the cells, the samples were incubated in the dark for 30 minutes. The reaction was stopped by adding 500µl of Stain Buffer, and samples were spun at 1,000 rpm for 5 minutes. The cell pellet was resuspended in 500µl of Stain Buffer and centrifuged again. The cells were resuspended in 500µl of Stain Buffer and transferred to FACS tubes, and kept on ice until samples were run on the flow cytometer.

Tube	Antibody	Antibody volume	Volume of cells
1	CD90	5µl	100µl
2	CD105	5µl	100µl
3	CD73	5µl	100µl
4	Unstained	-	100µl
5	MSC Positive Isotype Control Cocktail	20µl	100µl
	PE MSC Negative Isotype Control Cocktail	20µl	
6	MSC Positive Cocktail	20µl	100µl
	PE MSC Negative Cocktail	20µl	

**Table 2.3. Antibodies added to each tube for detection of cell surface markers on MSCs.** PE; phycoerythrin.

### 2.3.2 Analysis of cells on the flow cytometer

Flow cytometric analysis was carried out using the FACS Aria II from Becton Dickinson (BD Biosciences). The FACSDiva software Version 6.1.2 (BD Biosciences) was used to analyse the data. The flow cytometer has 5 lasers; UV (355nm), Violet (405nm), Blue (488nm), Yellow/Green (561nm) and Red (640nm), for which there are assigned filters for each laser to detect the emitted wavelength from each fluorescent dye (**Table 2.4**). Logarithmic side scatter (SS) and forward scatter (FS) was used to detect MSCs. Once established the MSC population was gated and labelled as P1. First the isotype control cocktail sample was run to set the APC, FITC, PerCP-Cy5.5 and PE gate at 2% positive, to account for non-specific binding of the antibodies. The percentage of positive cells was recorded. Each sample was run until ten thousand events were recorded. The WinMDI software (Purdue University) was used to generate histograms from the data.

Antibody	Fluorescent dye	Laser	Filter
Anti-Human CD90	APC	640nm (Red)	670nm
Anti-Human CD105	PerCP-Cy5.5	561nm (Yellow/green)	710nm
Anti-Human CD73	FITC	488nm (Blue)	530nm
Anti-Human CD34	PE	561nm (Yellow/green)	582nm
Anti-Human CD11b			
Anti-Human CD19			
Anti-Human CD45			
Anti-Human HLA-DR			

**Table 2.4. Details of the antibodies, their attached fluorescent dye, lasers and specific filters present in the FACSria II flow cytometer to detect the emitted wavelength from each dye.** APC; allophycocyanin, PerCP-Cy5.5; Peridinin chlorophyll protein with cyanine dye, FITC; fluorescein isothiocyanate, PE; phycoerythrin.

### 2.3.3 Flow cytometry for Nile red staining

- Nile red (Sigma-Aldrich). 1mg/ml stock solution of Nile red was made in acetone, and kept in the dark at 4°C.
- 4% paraformaldehyde; 4g of paraformaldehyde (PFA; Sigma-Aldrich) was added to 50ml PBS in a beaker on a hot plate, and allowed to dissolve. The solution was cooled and filtered. The volume was made to 100ml, adjusted to pH 6.9 and frozen into working aliquots. 1% PFA was made by diluting it in PBS.
- 5ml FACS tubes (BD Falcon)

Nile red (9-diethylamino-5H-benzo[*a*]phenoxazine-5-one) was used to quantify lipid droplets within MSC-derived adipocytes. Cells were trypsinized and centrifuged at 1,500 rpm for 5 minutes. Media was discarded and 200µl of PBS was added, and transferred to a 96 well plate. 100µl of 1% PFA was added to the well, and incubated for 10 minutes at 4°C. The plate was centrifuged at 13,000 g for 1 minute and supernatant discarded. Nile red was diluted to get a 1:2000 working dilution which was added to each well, and incubated for 20 minutes at 4°C in the dark. 150µl of PBS was added to each well, and centrifuged at 13,000 g for 1 minute. This step was repeated. 300µl of PBS was added, cells resuspended and transferred to FACS tubes. Samples

were analysed using the flow cytometer (CyAn ADP, Dako Cytomation, Beckman Coulter) and data analysed using the Summit software V4.3.02 (Beckman Coulter). First a control sample (MSCs incubated with Nile red) were run to set the FL1 FITC gate at 2% positive, to account for non-specific binding of Nile red. The percentage of positive cells was recorded.

#### **2.3.4 Nile Red staining in 6 well plate**

- 4',6-Diamidino-2-Phenylindole, Dilactate (DAPI; Invitrogen).

The same experimental steps were followed as in described in **Section 2.2.9** however cells were not trypsinized. After Nile Red incubation, 5mg/ml stock of DAPI was diluted to 1:10,000 in PBS and incubated for 1 minute. The cells were washed twice with PBS, and once in dH<sub>2</sub>O. The cells were visualised using the Evos fl microscope (Advanced Microscopy Group) using the GFP and DAPI filters.

### **2.4 Cellular assays**

#### **2.4.1 Measurement of intracellular Ca<sup>2+</sup>**

- Tyrode solution (6mM KCl, 135mM NaCl, 5mM Na pyruvate, 1mM MgCl<sub>2</sub>, 10mM Glucose, 10mM HEPES, 0.33mM NaH<sub>2</sub>PO<sub>4</sub>, 1.3mM CaCl<sub>2</sub>. The pH was adjusted to 7.4 by the addition of 1M NaOH).
- Angiotensin II (Merck Millipore). Prepared 1mg/ml stock in dH<sub>2</sub>O.
- Carbachol (Merck Millipore). Prepared 100mg/ml stock in dH<sub>2</sub>O.
- Potassium Chloride (KCl; Sigma-Aldrich). Prepared 1M stock in dH<sub>2</sub>O.
- 13mm circular coverslips (Thermo Scientific)
- Fura-2, AM, cell permeant (Invitrogen)
- Pluronic acid (Sigma-Aldrich)

Fura-2 AM is a cell permeable, ratio-metric calcium indicator used to measure intracellular calcium. Upon crossing the cell membrane, intracellular non-specific esterases cleave off the esters, resulting in Fura-2 free acid, which

is impermeable. When  $\text{Ca}^{2+}$  binds Fura-2 it is excited at 340 nm. The unbound form of Fura-2 is excited at 380 nm, and emits at 510nm regardless of  $\text{Ca}^{2+}$  binding. Upon  $\text{Ca}^{2+}$  flux into the cell, Fura-2 binds to  $\text{Ca}^{2+}$ , and causes an increase in fluorescence at 510nm by increased excitation at 340nm. However a decrease in fluorescence occurs due to reduced excitation at 380nm. The ratio of the emissions is directly related to the amount of intracellular calcium.

For experiments, cells were seeded onto 13mm coverslips. A 2mM Fura-2 solution was prepared by resuspending in DMSO containing 5% Pluronic acid. Medium was removed from the wells, and washed with pre-warmed Tyrode solution. To each well, 2ml of Tyrode solution was added. Fura-2 was added at a final concentration of 5 $\mu\text{M}$ . The plate was covered in foil and incubated for 45 minutes. During the incubation, solutions and agonists were prepared. 100nM Angiotensin II, 100 $\mu\text{M}$  carbachol and 60mM KCl was prepared in 100ml Tyrode solution. Coverslips were placed into a diamond shaped perfusion chamber, located on a stage of a Nikon Eclipse TE2000-E microscope. The chamber was maintained at an approximate temperature of 37°C using the TC-344b dual auto temperature controller. Cells were perfused using an Ismatec ms REGLO peristaltic pump at a rate of 3ml/min with Tyrode solution until a steady state was reached. Cells were then perfused with Tyrode solution supplemented with Angiotensin II, carbachol or KCl. Cells were recorded for 1 minute in Tyrode solution, followed by four minutes with Tyrode solution containing the agonist. The fluorescence was recorded by a Hamamatsu Camera Controller. The Velocity software was used to analyse the data. Firstly regions of interest were drawn around individual cells. Next the background value was subtracted. Traces were determined for individual cells to calculate the Fura-2 340/380 ratio.

#### **2.4.2 Cell Contraction Assay**

- Calcein, AM, cell-permeant dye (Invitrogen)
- Carbachol (Merck Millipore). Prepared 100mg/ml stock in  $\text{dH}_2\text{O}$ .
- Tyrode solution; as detailed previously in **Section 2.4.1**.

The cell contraction assay was carried out on MSCs, differentiated SMCs, aoSMCs and HeLa-S3 cells described earlier. Cells were seeded at  $3 \times 10^3$  cells/cm<sup>2</sup>. After 48 hours the assay was carried out. Firstly calcein solution was prepared, by dissolving 50µg into 250µl of DMSO+ 5% pluronic acid. The vial was covered with foil to protect the solution from light. Cell culture medium was removed, and washed once with pre-warmed Tyrode solution. 0.5ml of Tyrode solution was added to each well followed by 5µl of calcein. The plate was incubated at 37°C for 15 minutes in the dark. Cells were washed twice and loaded onto the Nikon Eclipse Ti-E microscope platform, surrounded by an environmental chamber at 37°C, 5% CO<sub>2</sub>.

Automated positions were set in each well, to ensure the camera took an image of the same cells before and after treatment with carbachol. Once the positions had been set, 100µM carbachol was added carefully to each well. Images were obtained before the addition of carbachol, and every minute for 20 minutes after the addition of carbachol. Phase-contrast and FITC channels were used. The Nikon JOBS software collected the data from the experiments. Image J (<http://imagej.nih.gov/ij/>) was used to calculate the cell surface area at 0 minutes (no treatment) and 10 minutes (after carbachol treatment), which was expressed as a percentage change in cell surface area.

### **2.4.3 Scratch assay**

MSCs and differentiated SMCs were seeded into 6 well plates at  $1 \times 10^4$  cells/cm<sup>2</sup> and  $4 \times 10^4$  cells/cm<sup>2</sup>, respectively. Upon confluency, a pipette tip was used to make a scratch the length of the well. The angle of the tip was held at approximately 30 degrees, in order to keep the scratch width limited. Cells were washed twice with pre-warmed medium and loaded onto the Nikon Eclipse Ti-E microscope platform, surrounded by an environmental chamber at 37°C, 5% CO<sub>2</sub>. Water was added to the surrounding reservoir to prevent extreme evaporation of the medium. Automated positions were set along the scratch at 10x magnification, and imaged for 24 and 72 hours for MSCs and differentiated SMCs, respectively. Images of at least 3 different scratch areas were acquired per well, every 30 minutes. The Nikon JOBS software was used to acquire the

data. Image J was used to analyse the data. The cell covered area was determined between 0-24 hours (0-72 hours for differentiated SMCs). The linear phase of cell surface covered area was determined for each genotype group. In addition, using Image J the distance between the two wound edges was calculated at 5 different points, along the wound edge. This was calculated at 0, 6, 9, 12 and 24 hours. To obtain the actual distance migrated by the cells, the difference between the distance at 0 hours and at the hour of interest was calculated.

## **2.5 Protein methods**

### **2.5.1 Immunofluorescence staining**

- 22mm circle coverslips (Fisher Scientific)
- 4% paraformaldehyde, described previously in **Section 2.3.3**
- 10x TBS; 6g of Tris Base and 22g of NaCl was dissolved in 250ml dH<sub>2</sub>O. The pH was adjusted to 7.6 with 1M HCl
- 1x TBS; 10x TBS was diluted 1:10 with dH<sub>2</sub>O
- 0.2% saponin; 0.2g saponin (Sigma-Aldrich) in 100ml dH<sub>2</sub>O. Stored at 4°C in foil.
- Wash buffer; 0.1% Triton X-100 (Sigma-Aldrich) in 1x TBS
- Dilution/blocking buffer; 0.1% Triton X-100 and 2% bovine serum albumin (BSA; Sigma-Aldrich) in 1x TBS
- Monoclonal Anti-Actin,  $\alpha$ -Smooth Muscle antibody (Sigma-Aldrich)
- Monoclonal Anti-Calponin antibody (Sigma-Aldrich)
- Monoclonal Anti-Myosin (Smooth) antibody (Sigma-Aldrich)
- Anti-Mouse IgG (Fc specific)-FITC antibody (Sigma-Aldrich)
- Fluoroshield Mounting Medium (Abcam)
- 4',6-Diamidino-2-Phenylindole, Dilactate (DAPI; Invitrogen). 2ml of dH<sub>2</sub>O was added to give a 5mg/ml DAPI stock solution.

Coverslips were sterilized by treatment with 100% ethanol, air-dried and washed with sterile 1x PBS. Coverslips were coated with Collagen I Rat Protein, Tail and seeded with cells as described in **Section 2.2.15**. After 3 and 6 days,

MSCs and differentiated SMCs were washed twice with 1x PBS. 1ml of 4% paraformaldehyde was added to each well for 20 minutes and incubated at 4°C. Cells were washed three times in 1ml TBS, for two minutes on a rocker. 0.2% saponin solution was added to each well for 10 minutes on a rocker. Cells were washed three times with wash buffer, for 5 minutes, on a rocker. The concentration of the primary antibody required (**Table 2.5**), was made by diluting the antibody in dilution buffer. 1ml of diluted antibody was added and incubated at 37°C for 1 hour in the dark. The cells were washed three times for five minutes on a rocker. 1ml of the diluted secondary antibody was added and incubated at 37°C for 1 hour in the dark. Wells were washed twice. A 5mg/ml stock of DAPI was diluted 1:10,000 in PBS and incubated for 1 minute. The cells were washed twice with PBS, and once in ddH<sub>2</sub>O. Cells were mounted onto a glass slide using the Fluoroshield Mounting Medium. Slides were viewed using the Evos fl microscope using the GFP and DAPI filters.

<b>Antibody</b>	<b>Dilution</b>
Monoclonal Anti-Actin, $\alpha$ -Smooth Muscle antibody	1:800
Monoclonal Anti-Calponin antibody	1:500
Monoclonal Anti-Myosin (Smooth) antibody	1:100
Anti-Mouse IgG (Fc specific)–FITC antibody	1:400

**Table 2.5. Details of the antibody dilutions for immunofluorescence.**

### 2.5.2 Western blotting

- Protein extraction buffer (50mM HEPES (pH 7.4), 50mM KCl, 1mM NaF, 1mM MgCl<sub>2</sub>, 1mM EGTA, 0.1% Triton-X-100). Stored at 4°C. 50 $\mu$ l of PhosSTOP (20x; Roche) and cOmplete mini (20x; Roche) Phosphatase Inhibitor Cocktail was added to 1ml of protein extraction buffer.
- NuPAGE<sup>®</sup> Novex<sup>®</sup> 10% Bis-Tris Protein Gels, 1.0 mm and 1.5mm, 10 well (Invitrogen)
- XCell SureLock<sup>®</sup> Mini-Cell (Invitrogen)

- Amersham™ Full-Range Rainbow™ Molecular Weight Markers (GE Healthcare)
- NuPAGE® LDS Sample Buffer (4X; Invitrogen)
- Protran® Nitrocellulose Membrane (GE Healthcare)
- DL-dithiothreitol (DTT; Sigma-Aldrich)
- NuPAGE® MOPS SDS Running Buffer (20X; Invitrogen)
- NuPAGE® Transfer Buffer (20X; Invitrogen)
- Methanol (Fisher Scientific)
- Blotting paper, pure cellulose (Sigma-Aldrich)
- XCell II™ Blot Module (Novex, Life Technologies)
- Phosphate Buffered Saline (PBS) tablets (Sigma-Aldrich)
- Tween® 20 (Sigma-Aldrich)
- Skim Milk Powder (Sigma-Aldrich)
- Ponceau S Solution (Sigma-Aldrich)
- Rabbit polyclonal anti-ADAMTS7 (prodomain) antibody (Abcam)
- Rabbit polyclonal anti-ADAMTS7 (spacer domain) antibody (Abcam)
- Mouse monoclonal anti-FLAG M2 antibody (Sigma-Aldrich)
- Donkey ECL IgG, HRP-linked antibody (GE Healthcare)
- Sheep ECL prime IgG, HRP-linked antibody (GE Healthcare)
- Amersham™ ECL™ Prime Western Blotting Detection reagent (GE Healthcare)
- 3K Filter Units (Amicon Ultra 0.5ml centrifugal filters; EMD Millipore)
- 10K Filter Units (Amicon Ultra 15ml centrifugal filters; EMD Millipore)
- 50mM Ammonium Bicarbonate pH 7.6 (Sigma-Aldrich)
- Pierce™ BCA Protein Assay Kit (Thermo Scientific)
- Albumin from Bovine Serum (BSA; Sigma-Aldrich)

### **2.5.2.1 Preparation of cell lysate**

Cells were grown in serum free medium for 24 hours. A T75 flask of cells was placed on ice and washed with ice-cold PBS. 0.5ml of ice-cold protein extraction buffer was added to each flask. Using a cold cell scraper, adherent cells were scraped off the dish, and transferred to a pre-cooled 1.5ml eppendorf

tube. Samples were sonicated on ice, twice for 20 seconds. Samples were centrifuged at 13,000 rpm for 15 minutes at 4°C. The supernatant was carefully removed, transferred to a new tube and stored at -80°C. The remaining pellet was discarded.

### **2.5.2.2 Concentration of conditioned media**

Cells were grown for 24 hours in serum-free medium. Conditioned media was removed and centrifuged at 1,500 rpm for 5 minutes at 4°C, to remove any cell debris. All subsequent centrifugation steps were carried out at 4°C. 500µl of 50mM ammonium bicarbonate was added to the 3K Amicon Ultra 0.5ml centrifugal filters and spun at 13,000 rpm for 10 minutes. The filtrate was discarded. 450µl of sample was added to the column and spun at 13,000 rpm for 20 minutes. This step was repeated until the entire sample was processed. The filter was washed three times with ammonium bicarbonate. The filter unit was inverted into a new collection tube, and centrifuged at 13,000 rpm for 10 minutes. The filter unit was turned the correct way, and 50µl of ammonium bicarbonate was added, and incubated for 2 minutes. The filter unit was turned upside down and centrifuged at 13,000 rpm for 10 minutes. The filter unit was discarded.

Use of the 10K Amicon Ultra 15ml centrifugal filters, first required a wash with 15ml of ammonium bicarbonate at 4,000 g for 10 minutes. The filtrate was discarded, and conditioned media was added to the filter, and centrifuged at 4,000 g for 20 minutes. The filter was washed three times with ammonium bicarbonate. The last wash step required centrifugation for 30 minutes. To recover the concentrate, the sample was pipetted out of the filter unit.

### **2.5.2.3 Pierce™ BCA Protein Assay Kit**

The Pierce™ BCA Protein Assay Kit was used to measure the amount of protein in each sample, to ensure an equal amount of protein was loaded for Western blotting following the manufacturer's instructions. The absorbance was

measured at 562 nm on the BioTek ELx800 micro plate reader (BioTek) and the KC Junior software (BioTek).

#### 2.5.2.4 Western Blotting

The NuPAGE gel system was used to resolve proteins from cell lysates and conditioned media. To each 0.5ml tube, the components detailed in **Table 2.6** were added. Samples were incubated at 95°C for 5 minutes, and centrifuged briefly to collect the sample.

Components	Volume
Sample (20µg)	x
NuPAGE <sup>®</sup> LDS Sample Buffer (4x)	8.75µl
DTT (1M)	0.7 µl
dH <sub>2</sub> O	To 35µl

**Table 2.6. Western Blot components for a 35µl sample.**

Samples were resolved on NuPAGE<sup>®</sup> Novex<sup>®</sup> 10% Bis-Tris Protein Gels. 5µl of Full-Range Amersham Rainbow Marker was loaded into the first well. The gel was run for 55 minutes at 200v in 1x MOPS buffer. The XCell II<sup>™</sup> Blot Module was used to transfer protein to a nitrocellulose membrane. 6 blotting pads, 2 pieces of filter paper and nitrocellulose membrane were pre-soaked in 1x Transfer Buffer for at least 2 hours at 4°C. The transfer sandwich was arranged by placing 3 blotting pads down onto the negative cathode core, followed by filter paper, gel, nitrocellulose membrane, filter paper and 3 blotting pads. The positive anode core was placed on top and the sandwich was placed into the XCellSureLock<sup>®</sup> Mini-Cell. The transfer module was filled with 1x Transfer Buffer. The outer chamber was filled with cold dH<sub>2</sub>O. Transfer was carried out at 35v for 1 hour and 25 minutes.

The nitrocellulose membrane was removed from the sandwich and rinsed with PBST (1x PBS with 0.1% Tween-20). Ponceau S solution was added to the membrane and incubated for 5 minutes on a rocker. DH<sub>2</sub>O was

used to remove residual Ponceau S. An image of the membrane was taken using the ImageQuant LAS 4000 system and software. Measuring protein stained by Ponceau S was used as a loading control. The membranes were rinsed with PBST to remove Ponceau S solution and blocked with blocking buffer (PBST+5% milk powder) for 1 hour on a rocker. Membranes were incubated overnight at 4°C with the primary antibody. Details of the antibodies are listed in **Table 2.7**. The following day membranes were washed 3 times in PBST for 5 minutes, on a rocker. Next membranes were incubated with the secondary antibody for 2 hours, followed by 3 washes. For protein detection, membranes were incubated for 1 minute in ECL™ Western Blotting Detection Reagents and visualised using the ImageQuant LAS 4000 system. The ImageQuant TL software was used to quantify protein.

<b>Antibody</b>	<b>Dilution</b>
Rabbit polyclonal anti-ADAMTS7 (prodomain) antibody	1:1000
Rabbit polyclonal anti-ADAMTS7 (spacer domain) antibody	1:1000
Donkey ECL IgG, HRP-linked antibody	1:5000
Mouse monoclonal anti-FLAG M2 antibody	1:1000
Sheep ECL prime IgG, HRP-linked antibody	1:15000

**Table 2.7. Details of the antibody dilutions used for Western Blotting.**

## 2.6 Statistical analysis

All data from experiments was analysed in Microsoft Office Excel. GraphPad Prism 6.00 (GraphPad software Inc.) was used to generate all graphs. Results are shown as mean  $\pm$  Standard Deviation (SD). SD was chosen as it shows the variation in the individual samples. Statistical significance of the data was assessed by a Student's t-test when the data was normally distributed. A one-way Analysis of Variance (ANOVA), following the appropriate post-test was used to compare two or more groups. The Spearman's rank correlation coefficient was used to assess the relationship between two variables. A p-value <0.05 was considered statistically significant.

# **Chapter 3 - Isolation and characterisation of mesenchymal stem cells**

### 3.1 Introduction

CAD-related genetic variants identified in GWASs require a genotype-specific model to study them. MSCs are a potential cell type to produce genotype-specific disease models, as they can differentiate into CAD-relevant cell types; they promise a new paradigm in studying the functional mechanisms of CAD-related genetic variants. This chapter describes the establishment of a MSC bank.

#### 3.1.1 Mesenchymal stem cells

MSCs are a type of adult stem cell, described by Friedenstein *et al.*, over 40 years ago. These cells have also been referred to as mesenchymal progenitor cells or marrow stromal cells. In this thesis, the cells will be referred to as mesenchymal stem cells.

The increased interest in MSCs over the last two decades has resulted in many inconsistencies and ambiguities in defining their characteristics. Typically, the bone marrow has been used as the primary source for obtaining MSCs (Colter *et al.*, 2000). However, MSCs can be isolated from many other tissue sources including dental pulp, tendons, adipose tissue and the umbilical cord (da Silva Meirelles *et al.*, 2006). Different groups have used different isolation and expansion methods for MSCs that have slight, yet sometimes significant differences. To address these problems the Mesenchymal and Tissue Stem Cell Committee of the International Society of Cellular Therapy proposed the minimal criteria required to characterise human MSCs (Dominici *et al.*, 2006; **Table 3.1**).

Minimal criteria to characterise MSCs	
• Adherence to plastic under standard culture conditions	
• Phenotype: Positive ( $\geq 95\%+$ )	Negative ( $\leq 2\%+$ )
	CD105
	CD73
	CD90
	CD45
	CD34
	CD14 or CD11b
	CD79 $\alpha$ or CD19
	HLA-DR
• <i>In vitro</i> differentiation; adipocytes, chondrocytes and osteoblasts	

**Table 3.1. Summary of the minimal criteria to characterise MSCs (Dominici *et al.*, 2006).**

### 3.1.1.1 Plastic adherence

Firstly, MSCs must be able to adhere to plastic under standard culture conditions. MSC subsets from common and rare sources, have all exhibited this property (Colter *et al.*, 2000; Zhang *et al.*, 2004). It is possible to maintain and potentially expand MSCs in culture without adherence (Baksh *et al.*, 2003). However these methods need an extremely specific culture environment. If these cells were kept under more standardized conditions, they would be required to exhibit plastic adherence to be classed as a MSC population (Dominici *et al.*, 2006).

### 3.1.1.2 Cell surface markers

The second criteria cells should meet, is the expression of certain cell surface markers. To date no specific markers have been found to be expressed exclusively by MSCs, so a group of cell surface markers are used to characterise MSCs. More than 95% of the population should be positive for the expression of CD73 (known as ecto 5' nucleotidase), CD105 (known as endoglin) and CD90 (known as Thy-1). In addition, the MSC population should be negative (less than 2% of the population) for expression of CD45, CD34, CD14 or CD11b, CD79a or CD19 and HLA-DR. These markers are tested to ensure the MSC population does not include other cells likely to be present in

the population. CD45 and CD34 are haematopoietic markers; the latter is a marker of primitive haematopoietic progenitor cells and endothelial cells. CD14 and CD11b are found on macrophages and monocytes, and these cells are likely to be included during MSC isolation, primarily from bone marrow isolates. Also B cells may attach to MSCs, therefore B cells markers; CD79a and CD19 are used. For macrophages, monocytes and B cells only one cell surface marker is required. Finally MSCs should be negative for HLA-DR expression, except under stimulation by certain cytokines, such as IFN $\gamma$ . These markers represent the minimal requirement and alone do not stringently characterise MSCs, so additional markers can be used (Dominici *et al.*, 2006). Additional positive markers are CD166, ICAM-1, CD29, CD44, CD71, Stro-1, CD106 and extra negative markers include markers for the co-stimulatory molecules CD40, CD86 or CD80 and the adhesion molecules; CD31, CD56 or CD18 (Haynesworth *et al.*, 1992; Sordi *et al.*, 2005; Le Blanc *et al.*, 2003; Pittenger *et al.*, 1999). CD146 is another additional marker, and has been suggested to correlate with MSC differentiation potential (Russell *et al.*, 2010). Different laboratories utilize different sets of antibodies; therefore it is difficult to directly compare results from different groups. A comparison of reports from different studies showed that there is not a subset or a single marker that can define MSCs (Zipori, 2009).

It is possible to observe variable expression of the cell surface markers on MSCs due to the disparity in tissue source, species, isolation and culture methods (Javazon *et al.*, 2004; Baddoo *et al.*, 2003). For example, CD34 is a negative marker for MSCs, but some studies have shown variable expression of this marker on murine MSCs. Of importance to note are the external influences that may impact the expression of cell surface markers, such as factors released by neighbouring cells during early passages (Zvaifler *et al.*, 2000).

### **3.1.1.3 Trilineage differentiation**

The last and most unique characteristic of MSCs is their trilineage differentiation ability towards mesodermal lineages. These cells must differentiate into adipocytes (fat cells), chondrocytes (cartilage cells) and

osteoblasts (bone cells) *in vitro* (Dominici *et al.*, 2006; Friedenstein *et al.*, 1974; **Figure 3.1**).

In order to differentiate MSCs into adipocytes, cells are treated with indomethacin, insulin, dexamethasone and isobutyl methyl xanthine. Adipocyte cells produce lipid vacuoles within the cell, and express peroxisome proliferator-activated receptor gamma (PPAR $\gamma$ ), lipoprotein lipase and adipocyte protein 2 (aP2; Pittenger *et al.*, 1999). Lipid vacuoles stain positive for Oil Red O staining, demonstrating successful differentiation.

To induce differentiation of MSCs into chondrocytes, cells are cultured at high densities, to form a pellet or micromass culture. Cells are incubated in medium containing transforming growth factor- $\beta$  (TGF- $\beta$ ), dexamethasone, proline, pyruvate, ascorbate-2-phosphate and glutamax (Mackay *et al.*, 1998). Glycosaminoglycans and collagen type II are produced in chondrocytes, a characteristic feature of articular cartilage; therefore Toluidine Blue staining against these molecules is confirmation of successful chondrogenic differentiation (Pittenger *et al.*, 1999).

The third lineage MSCs must differentiate into are osteoblasts. The cells undergo treatment with ascorbic acid, dexamethansone and glycerophosphate. Upon treatment, MSC-derived osteoblasts aggregate or form nodules, and express increased amounts of alkaline phosphatase (Pittenger *et al.*, 1999). Alizarin red is used to stain the bone nodules to confirm their presence.

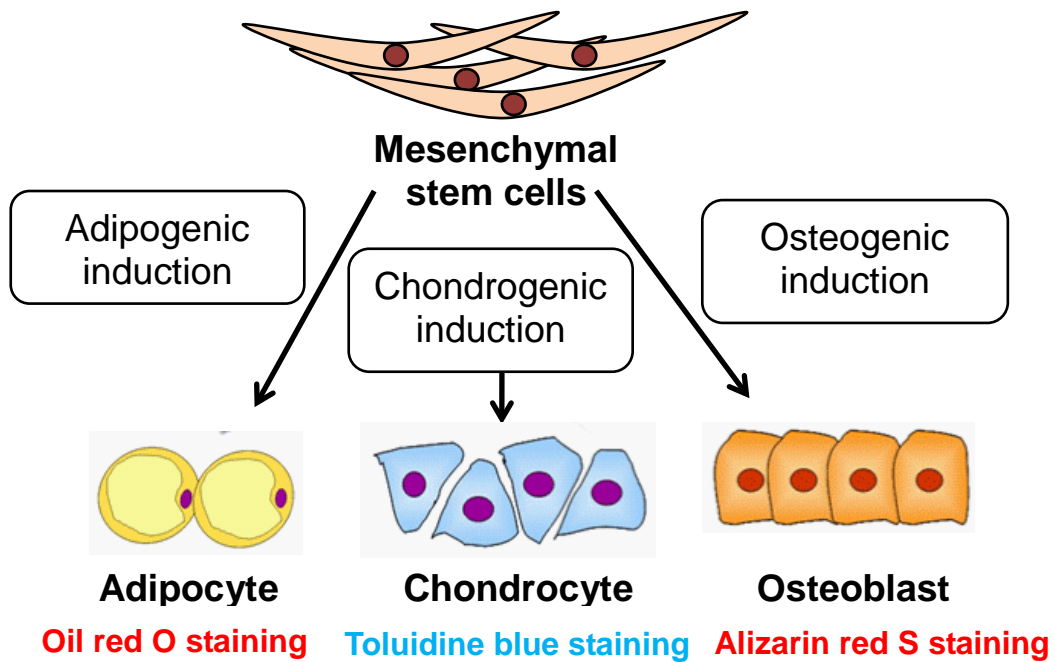


**Figure 3.1. Schematic diagram of the trilineage differentiation of MSCs into adipocytes, chondrocytes and osteoblasts upon treatment with specialised differentiation mediums. To confirm adipocyte differentiation cells are positive for Oil Red O staining. Toluidine blue staining is confirmation of successful differentiation to chondrocytes. Alizarin Red staining is used to stain the bone nodules to confirm their presence within osteoblast cells.**

### 3.1.2 Aims and objectives

The first aim of this project was to isolate and characterise MSCs from donated umbilical cord samples to establish an MSC bank. The morphology and phenotype of the cells were investigated to ensure they were MSCs, for use in subsequent experiments.

The objectives were:

- Isolate and culture MSCs from umbilical cords
- Characterise MSCs;
  - Determine MSC morphology and adherence to plastic
  - Expression of certain cell surface markers (positive for CD105, CD73 and CD90 and negative for CD45, CD34, CD11b, CD19 and HLA-DR)
  - Assess *in vitro* differentiation of MSCs into three common lineages; adipocytes, chondrocytes and osteoblasts.
- Genotype DNA from MSCs using the Axiom™ Genome-Wide UKB WCSG Genotyping Array, to determine the genotypes for CAD-associated SNPs

## 3.2 Results

### 3.2.1 Isolation, culture and morphology of MSCs

An explant method was used to isolate MSCs from 120 human umbilical cord samples, which varied in length between seven and twenty centimetres. WJ tissue was extracted from the umbilical cord for each donor, diced into explant fragments and plated into 6-well plates. Plastic adherent MSCs were observed migrating from the explant fragments over a period of time (**Figure 3.2**). The time taken for migration of MSCs from the tissue explants was variable. The earliest migration of MSCs from donor tissue was seen after 7 days, the longest migration was observed at 6 weeks. Upon confluency of MSCs around tissue fragments (**Figure 3.2F**), the cells were subcultured. MSCs were successfully isolated from 114 samples, yielding a 95% success rate for the explant method.

Freshly isolated cells displayed a fibroblast-like appearance characteristic of MSCs (**Figure 3.3**). Red blood cells (often a contaminant in MSC culture) were absent, upon observation of MSCs in primary culture. This is due to the plastic adherent property of MSCs, as frequent media changes removed non-adherent cells, whereas MSCs remained attached. After subculturing and seeding cells at a density of  $5 \times 10^3$  cells/per  $\text{cm}^2$ , MSCs reached confluency after 5-7 days. Cells were maintained in culture and MSCs from each donor were banked at different passages (P1-P5).

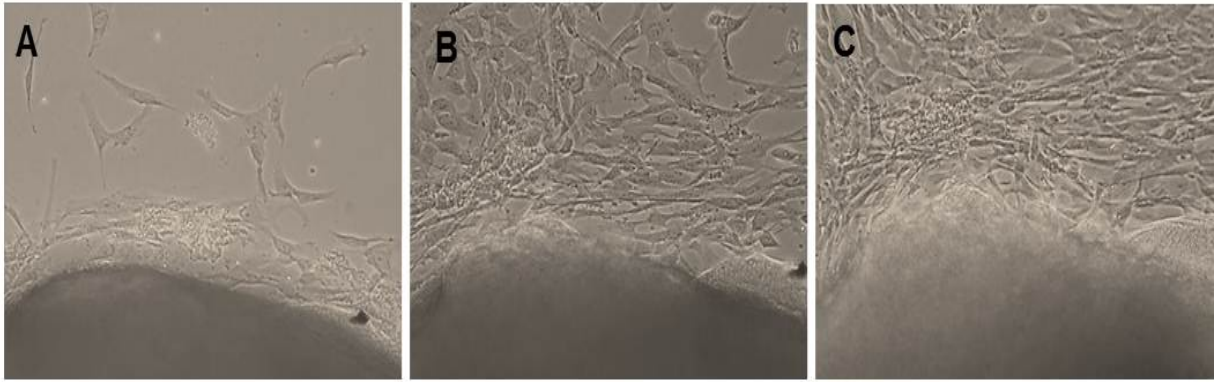


**Figure 3.2. Representative images of the migration of MSCs from Wharton's jelly (WJ) of human umbilical cord using the explant method. (A) First appearance of the migration of MSCs from the tissue explant fragments at day 7. (B) The continuous migration of MSCs from the explant fragments. (C) At day 11 the cells reached confluency around the tissue fragments. Magnification x10.**

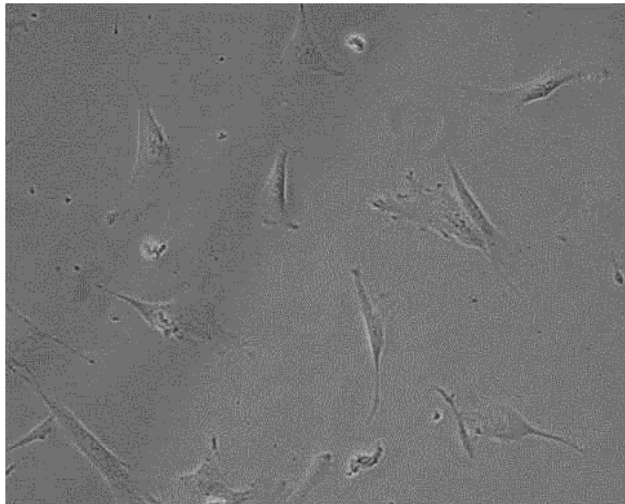


**Figure 3.3. Morphology of MSCs isolated from Wharton's jelly (WJ) of the umbilical cord.** Freshly isolated MSCs (passage 0; P0) exhibited a fibroblast-like appearance and adhered to tissue culture plastic. **Magnification x20.**

Human umbilical cord-derived MSCs were purchased from ATCC and were used as a positive control. MSCs that I isolated from different donors exhibited a similar morphology to the positive control (**Figure 3.4**). Both cell populations exhibited fibroblast-like cells, with thin cell processes protruding from the small cell body, creating a spindle-like appearance. Large irregular

shaped nuclei were observed within the body of each cell. The shared morphology of the MSCs isolated from WJ and the human umbilical cord-derived MSCs purchased from ATCC, suggested the successful isolation of MSCs from human umbilical cords.

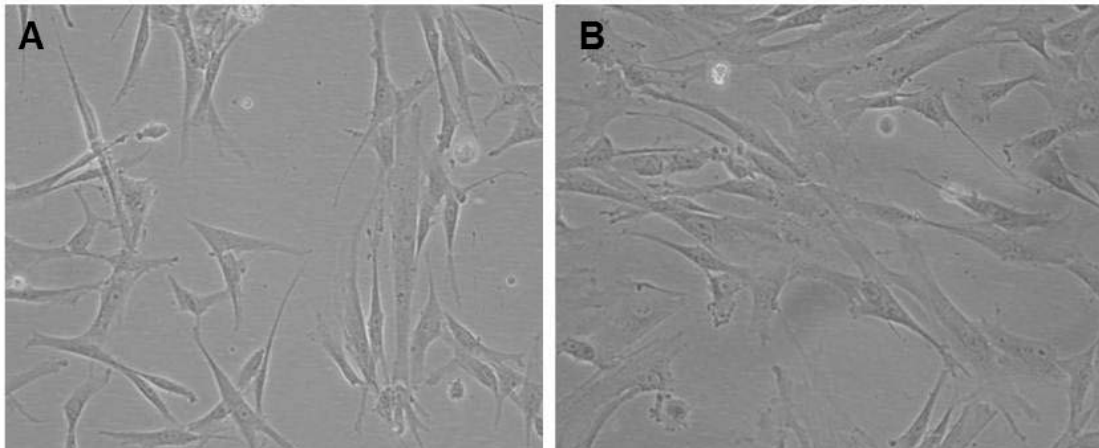


**Figure 3.4. Comparison of the morphology of MSCs isolated from Wharton's jelly (WJ) and human umbilical cord-derived MSCs purchased from ATCC. (A) Third passage (P3) MSCs isolated from WJ at 30% confluency. (B) P3 human umbilical cord-derived MSCs purchased from ATCC at 40% confluency. Both MSC populations exhibited a fibroblast-like morphology. Magnification x20.**

### 3.2.2 Morphological heterogeneity

In primary culture, morphological heterogeneity of MSCs was observed. The main cell phenotype exhibited was the typical fibroblast-like appearance (**Figure 3.5A**). In addition to a fibroblast-like morphology, approximately 5% of cells were flat with a large cytoplasmic area and had the appearance of intracellular stress fibres. In addition, the morphology of MSCs was affected by cell density, as cells in a confluent culture appeared more slender with a narrower cell body (**Figure 3.5B**).

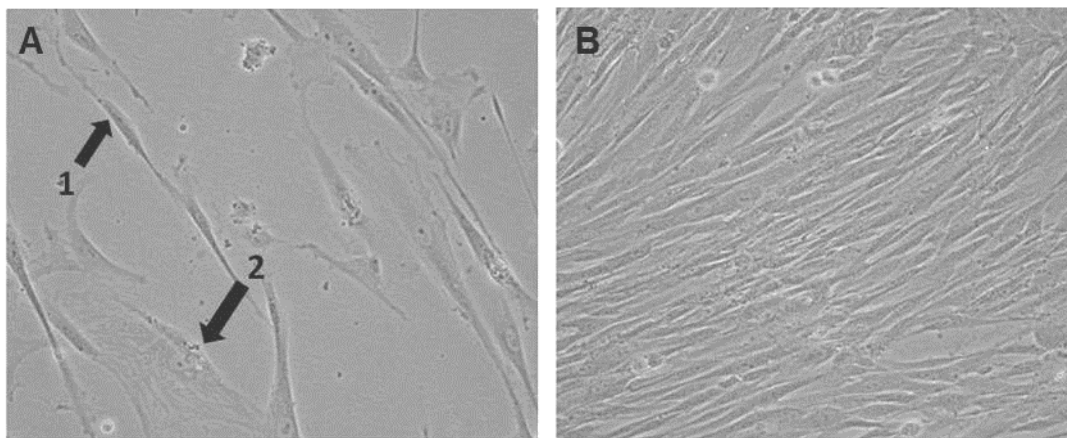


**Figure 3.5. Morphological heterogeneity of MSCs.** (A) Cell phenotypes observed were; (1) Fibroblast-like, slender cells. (2) Wide, flat cytoplasmic cells with the appearance of stress fibres. (B) MSCs that reached 100% confluency were more slender in their appearance, with a narrower cytoplasm. **Magnification x20.**

### 3.2.3 Population doubling time

The population doubling time (PDT) is the time taken for a given cell population to double in number. P3 cells taken from three different donors were seeded at a density of  $1 \times 10^4$  cells/cm<sup>2</sup> and counted when MSCs reached confluency. PDT was measured by using the equation  $PDT = \text{culture time (CT)} / \text{population doubling number (PDN)}$ . PDN was determined by using the equation  $PDN = \log(N_1/N_0) \times 3.31$ , where  $N_0$  = number of cells at the start of culture time,  $N_1$  = number of cells at the end of culture time. The mean PDT for MSCs was  $37.29 \pm 2.91$ .

### 3.2.4 Growth curve

A growth curve was plotted for MSCs from three different donors to analyse their growth kinetics (**Figure 3.6**). Cells were seeded at  $6 \times 10^3$  cells/cm<sup>2</sup>, and every two days the cell number was determined by cell counting using Trypan Blue. MSCs had a lag (adaptation) phase of 0-2 days. During the next 10 days MSCs rapidly proliferated (log phase). At day 12 MSCs reached a plateau phase, where cellular contact inhibition occurred and cells stopped multiplying.

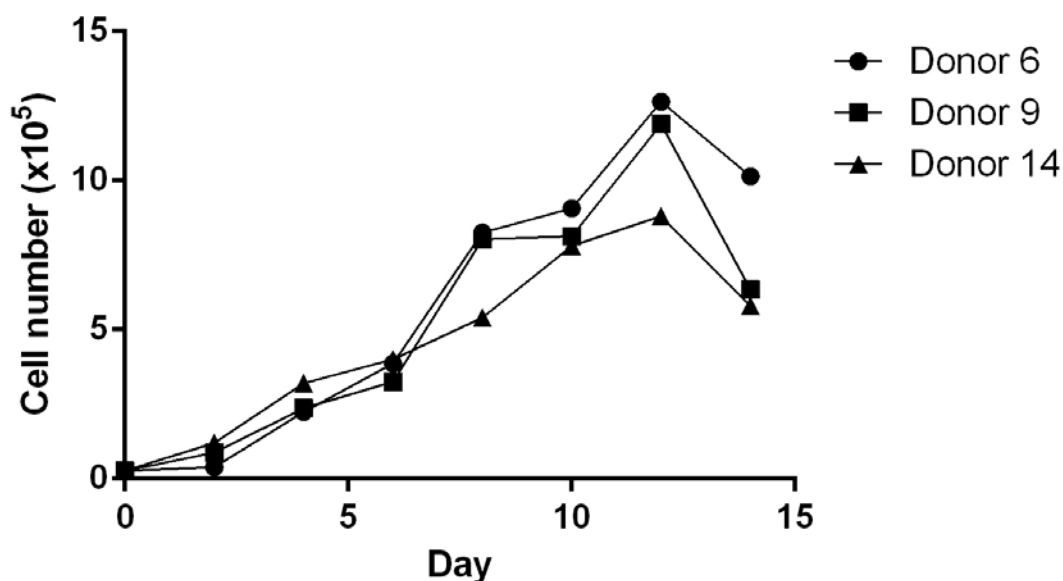


**Figure 3.6. Growth curve of MSCs.** MSCs from Donor 6, 9 and 14 were seeded at a density of  $6 \times 10^3$  cells/cm<sup>2</sup> and cell number determined every 2 days. MSCs possessed a lag (adaptation phase), log and plateau phase.

### 3.2.5 Characterisation of MSCs

The Mesenchymal and Tissue Stem Cell Committee of the International Society of Cellular Therapy (2006) proposed the minimal criteria for defining MSCs; **(1)** adherence to plastic under standard culture conditions **(2)** expression of certain cell surface markers (positive ( $\geq 95\%$ +) for CD105, CD73 and CD90 and negative ( $\leq 2\%$ +) for CD45, CD34, CD14 or CD11b, CD79 $\alpha$  or CD19 and HLA-DR **(3)** *In vitro* differentiation into three common lineages; adipocytes, chondrocytes and osteoblasts.

#### 3.2.5.1 Cell surface marker expression

First the cell surface marker expression was analysed by flow cytometry. A Human MSC Analysis Kit was used to create a simple protocol for multicolour analysis and to minimise the number of cells required for each assay. Human umbilical cord-derived MSCs were purchased from ATCC, and had already been tested to be positive for CD29, CD44, CD73, CD90, CD105, and CD166

and negative for CD14, CD31, CD34, and CD45. These cells were used as a positive control to set up a protocol on the flow cytometer. Firstly, the MSC population was identified by measuring two parameters; forward scatter (FS) and side scatter (SS). FS is a measure of cell size and SS is a measure of cell granularity. Measurement of these two parameters enabled the MSC population to be gated, and were subsequently defined as 'P1' (**Figure 3.7**). Cells within this region were used for subsequent cell surface marker analysis. Events representing cell debris appeared towards the origin of the graph, whereas cell aggregates exhibited both high FS and SS values.

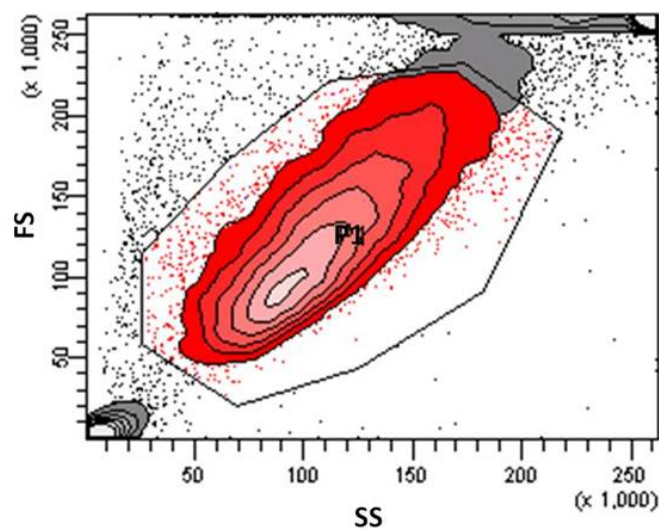


**Figure 3.7. Representative contour plot of the MSC population.** Cells were identified by their forward scatter (FS; Y axis) and side scatter (SS; X axis) and defined as 'P1'. The P1 population was used to measure cell surface marker expression.

To establish the protocol, single stained controls were set up as compensation controls (**Table 2.3**), to account for overlap in emission between different fluorescent dyes that were detected by different band pass filters. The software was able to apply the relevant compensation to each dataset.

For every sample that was analysed using the flow cytometer, two controls were included; these were (1) unstained cells and (2) cells incubated with isotype controls. Unstained cells accounted for any auto fluorescence emitted from the cells. Isotype controls measured the non-specific binding signal emitted by the primary antibodies. MSCs were incubated with an

antibody cocktail for; CD90, CD105, CD73, CD34, CD11b, CD19, CD45 and HLA-DR and analysed on the flow cytometer. Representative histograms show when MSCs were incubated with the isotype antibody cocktail (red histogram) low non-specific background for CD73 (**Figure 3.8A**) and CD90 (**Figure 3.8B**) was observed. However MSCs displayed a slightly higher signal for CD105 (**Figure 3.8C**), suggesting greater non-specific binding of the antibody. Upon incubation of MSCs with the antibody cocktail, 100%, 100% and 99.8% of the cell population on their surface displayed CD73 (**Figure 3.8A**), CD90 (**Figure 3.8B**), and CD105 (**Figure 3.8C**), respectively. The five negative markers (CD34, CD11b, CD19, CD45 and HLA-DR) were attached to the same PE fluorescent dye; therefore they were measured in the same channel. Only 0.2% of the MSC population displayed the negative markers (**Figure 3.8D**).

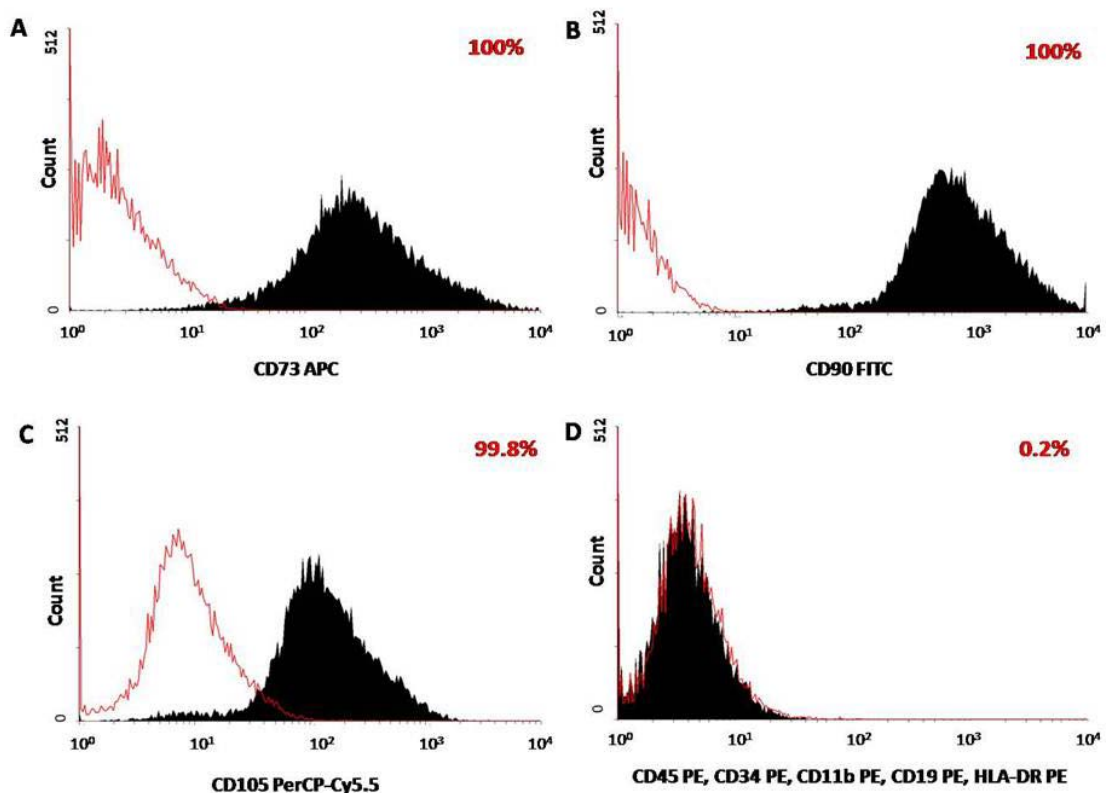


**Figure 3.8. Human umbilical cord-derived MSCs purchased from ATCC analysed using flow cytometry for the expression of cell surface markers.** Data shown is representative of 10,000 events and was analysed using WinMDI software. Isotype control cocktail (red histograms) show low non-specific background signal for each antibody. MSCs were positive for (A) CD73 (B) CD90 and (C) CD105. Cells were negative for (D) CD45, CD34, CD11b, CD19 and HLA-DR.

Next P5 MSCs derived from WJ, from six different donors were characterized by flow cytometry. Cells were positive for three markers; CD105, CD90 and CD73. CD45, CD34, CD11b, CD19 and HLA-DR were not detected on the cell surface of MSCs (**Table 3.2**). These results demonstrate the explant method and culture methods used, yielded a MSC population that expressed a characteristic surface profile.

	<b>CD105</b>	<b>CD90</b>	<b>CD73</b>	<b>Negative markers (CD34, CD45, CD11b, CD19, HLA-DR)</b>
<b>Mean</b>	99.8	99.8	99.6	0.2
<b>SD</b>	0.16	0.14	0.28	0.10

**Table 3.2. MSCs isolated from WJ analysed using flow cytometry for the expression of cell surface markers.** MSCs were positive for CD73, CD90 and CD105. Cells were negative for CD45, CD34, CD11b, CD19 and HLA-DR (n=6).

### 3.2.5.2 Trilineage differentiation

To investigate the trilineage differentiation potential of MSCs, specific differentiation mediums were used to differentiate MSCs into adipocytes, chondrocytes and osteoblasts.

#### 3.2.5.2.1 Adipogenic differentiation

P5 MSCs were cultured in adipogenic differentiation medium for 14 days, to induce differentiation of MSCs towards the adipogenesis pathway. Negative control samples were MSCs cultured in complete medium. After 14 days, MSCs cultured in adipogenic differentiation medium had differentiated into adipocytes. MSC morphology had altered from a fibroblast-like morphology to a wide triangular shaped appearance (**Figure 3.9B**). The adipocytic phenotype was confirmed by the appearance of intracytoplasmic lipid droplets, stained with Oil Red O. In the undifferentiated control samples, MSCs did not exhibit lipid droplets (**Figure 3.9A**).

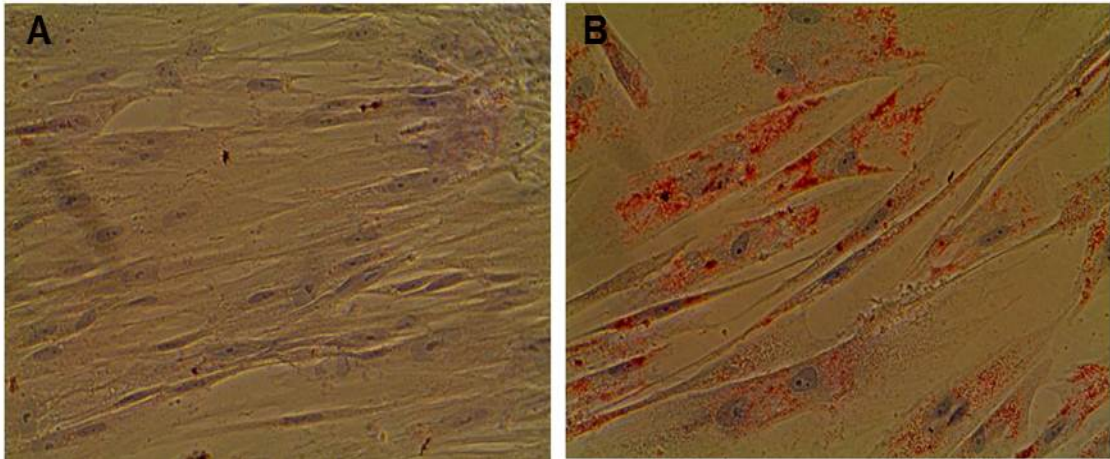


**Figure 3.9. Representative images of adipogenic differentiation of MSCs (n=5).** (A) In control samples (undifferentiated MSCs); lipid droplets were not detected. (B) MSCs cultured in adipogenic differentiation medium for 14 days. Intracellular lipid-rich vacuoles were present, demonstrated by Oil Red O staining. Cells were counterstained with Mayer's hematoxylin. **Magnification x40.**

### 3.2.5.2.2 Chondrogenic differentiation

P5 MSCs were cultured with chondrogenic differentiation medium using a pellet cultural system, to induce MSC differentiation towards the chondrogenesis pathway. As a negative control MSCs were maintained in complete medium. After 24 hours, treatment with chondrogenic medium resulted in an increase in cell pellet size. After 28 days the micromass pellet was harvested, and 4 $\mu$ M sections were obtained. Sections were stained with Toluidine Blue, which is a dye that stains glycosaminoglycans found in cartilage tissue. MSCs subjected to the complete medium did not form a clear pellet and stained blue for Toluidine Blue (**Figure 3.10A**). MSCs treated to the chondrogenic differentiation medium had differentiated into chondrocytes. Cells formed a pellet, and deposited extracellular matrix which stained purple after Toluidine blue staining. Within the pellet chondrocytic lacunae were observed. Surrounding the pellet were MSCs that had not differentiated (stained blue; **Figure 3.10A**).

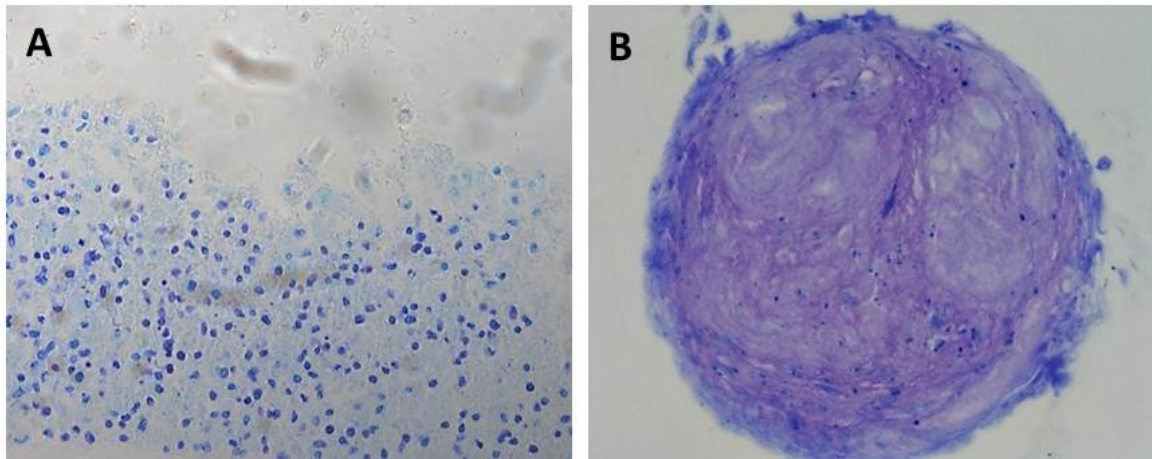


**Figure 3.10. Representative images of the chondrogenic differentiation of MSCs (n=3).** (A) In control samples MSCs did not form a pellet and stained blue (B) MSCs cultured in chondrogenic medium for 28 days formed a pellet and stained purple for cartilaginous extracellular matrix, demonstrated by Toluidine blue. **Magnification x20.**

#### **3.2.5.2.3 Osteogenic differentiation**

MSCs at P5 were treated with osteogenic differentiation medium for 28 days, to induce differentiation of MSCs into osteoblasts. In parallel, MSCs were grown in complete medium, as a negative control. MSCs grown in osteogenic differentiation medium differentiated into osteoblast-like cells. Alizarin Red S is a dye that binds to calcium salts. Calcium deposition was seen after staining with Alizarin Red S (**Figure 3.11B**). In the control samples (undifferentiated MSCs) calcium phosphate was absent (**Figure 3.11A**).

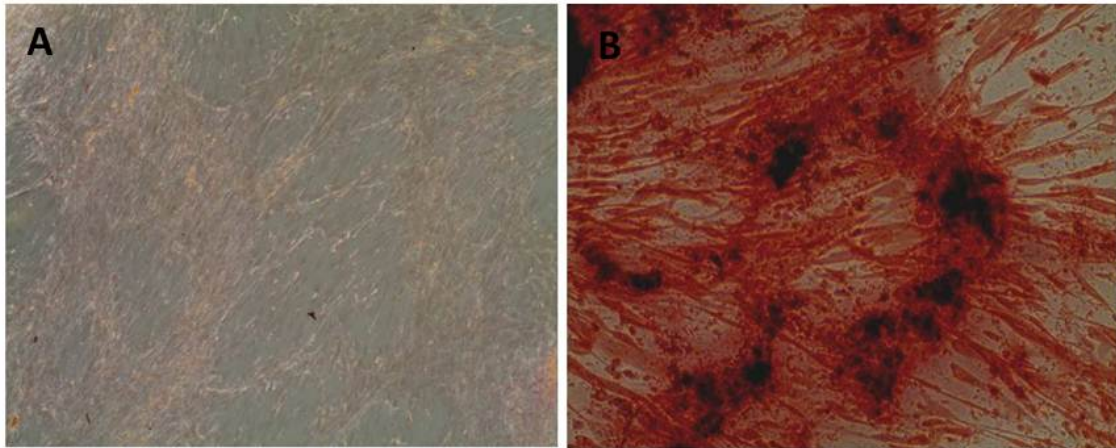


**Figure 3.11. Representative images of osteogenic differentiation of MSCs (n=5).** (A) Control sample (undifferentiated MSCs) did not stain positive for calcium. (B) MSCs were cultured in osteogenic differentiation medium for 28 days. Mineralised bone nodules were formed, demonstrated by positive Alizarin Red S staining. **Magnification x20.**

### 3.2.6 Genotyping of MSC bank

The objective was to genotype the entire MSC bank (114 donors), to determine the genotypes of each donor for CAD-associated SNPs. Genomic DNA was extracted from MSCs from 114 donors and run on a 0.8% agarose gel to verify the quality of the DNA (**Figure 3.12**). DNA was diluted, plated and sent to Affymetrix for genotyping. The Axiom™ Genome-Wide UKB WCSG Genotyping Array was used, which consisted of 845,487 probesets that covered 825, 928 SNPs. For some SNPs on the array there was more than one probe to interrogate a particular SNP. In this instance SNP quality control (QC) metrics were used to sort the best probe for each SNP. Of the 825,928 SNPs 97.5% passed the SNP QC metrics. Therefore data was analysed for 805,128 SNPs.

Of the 114 DNA samples sent, 2 failed the array, so 98.2% of the samples were successfully genotyped. The quality of each individual sample was determined using Dish QC (DQC). DQC is the recommended QC metric for the array; it measures how well the distribution of the signal values is separated from the background values. A value of 0 indicates no separation, whereas a value of 1 indicates perfect separation, the threshold is 0.82 for each sample. Samples had a DQC value  $\geq 0.82$  and a call rate of  $\geq 97\%$ , therefore samples

were passed. Hardy-Weinberg equilibrium (HWE) was calculated for each CAD-associated variant. All variants, met the 0.05 threshold (rs1561198 was borderline significant), therefore the population was in HWE.

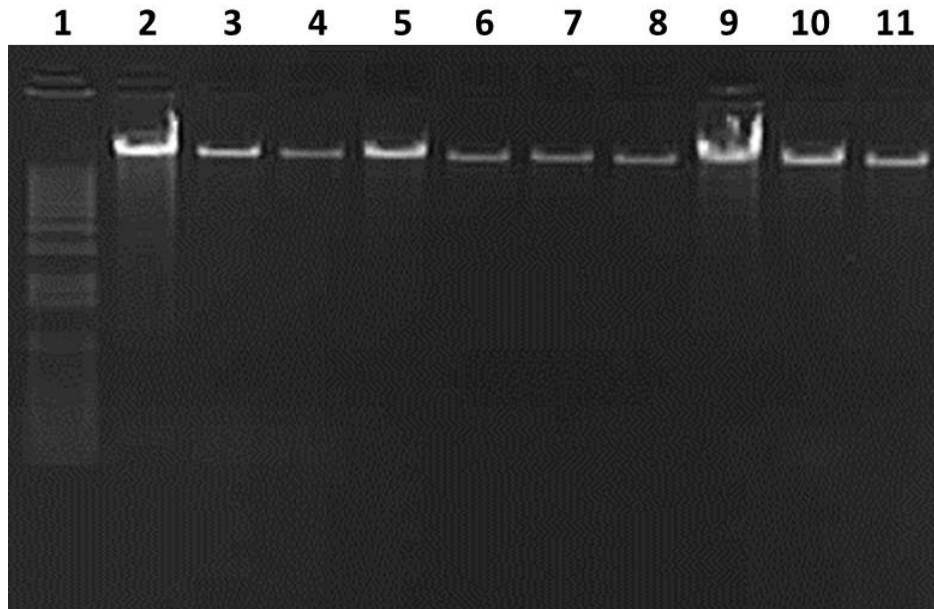


**Figure 3.12.** Analysis of MSC DNA, visualised by gel electrophoresis on 0.8% agarose gel. Lane 1: HyperLadder™ 1kb, lane 2-11: MSC DNA of acceptable quality.

50 known loci associated with CAD were annotated for the samples (**Table 3.3**). Two loci; rs7692387 (GUCY1A3) and rs4252120 (PLG) were not on the platform and therefore were not analysed. Cluster plots were created using the Affymetrix® Genotyping Console™ (GTC) version 4.2 and the Affymetrix® Power Tools (APT) version 1.16.1. This was to ensure the samples had good cluster resolution, and to determine any ambiguous samples (**Appendix S1**).

The minor allele frequencies (MAFs) were calculated for the MSC population. The MAFs were also noted for a CEU population reported by the Single Nucleotide Polymorphism Database (dbSNP; [www.ncbi.nlm.nih.gov/SNP/](http://www.ncbi.nlm.nih.gov/SNP/)). The MAF of many variants in the MSC population differed greatly to that reported for the CEU population from dbSNP. For

example, in the MSC population rs599839 had a MAF of 0.22, but in the dbSNP CEU population, a MAF of 0.33 was reported, which resulted in an 11% difference. It is important to note, that the umbilical cords were donated from individuals of unknown ethnicity. The highest allele frequency was 50% (rs2252641; ZEB2-AC074093.1) and the lowest allele frequency was 1% (rs3798220; SLC22A3-LPAL2-LPA). The MSC bank provided coverage ( $n \geq 3$ ) for 37 CAD-associated SNPs. Genotyping of the MSC bank provides a useful resource, as it will enable the selection of genotype-specific donors, to generate homozygous major and homozygous minor groups to investigate CAD-associated SNPs.

Chr.	Nearest gene(s)	SNP	Genotype			MAF		HWE p-value
			Homozygote major	Heterozygote	Homozygote minor	MSCs	CEU	
1	PCSK9	rs11206510	80 (TT)	31 (TC)	1 (CC)	0.15	0.16	0.28
1	PPAP2B	rs17114036	87 (AA)	22 (AG)	1 (GG)	0.11	0.11	0.76
1	SORT1	rs599839	67 (AA)	41 (AG)	4 (GG)	0.22	0.33	0.45
1	IL6R	rs4845625	42 (CC)	48 (CT)	22 (TT)	0.41	0.46	0.22
1	MIA3	rs17465637	59 (CC)	41 (CA)	12 (AA)	0.29	0.27	0.24
2	APOB	rs515135	81 (GG)	28 (GT)	3 (TT)	0.15	0.23	0.76
2	ABCG5-ABCG8	rs6544713	57 (CC)	47 (CT)	8 (TT)	0.28	0.26	0.69
2	VAMP5-VAMP8-GGCX	rs1561198	38 (GG)	45 (GT)	28 (TT)	0.45	0.49	0.05
2	ZEB2-AC074093.1	rs2252641	26 (TT)	60 (TC)	26 (CC)	0.5	0.46	0.45
2	WDR12	rs6725887	87 (TT)	24 (TC)	1 (CC)	0.12	0.14	0.64
3	MRAS	rs9818870	85 (CC)	26 (CT)	1 (TT)	0.13	0.16	0.52
4	EDNRA	rs1878406	77 (CC)	30 (CT)	5 (TT)	0.18	0.14	0.36
5	SLC22A4-SLC22A5	rs273909	86 (AA)	26 (AG)	0 (GG)	0.12	0.12	0.16
6	PHACTR1	rs9369640	41 (AA)	52 (AC)	19 (CC)	0.4	0.42	0.72
6	PHACTR1	rs12526453	47 (CC)	50 (CG)	15 (GG)	0.36	0.39	0.77
6	ANKS1A	rs17609940	68 (GG)	41 (GC)	3 (CC)	0.21	0.21	0.27
6	KCNK5	rs10947789	65 (TT)	44 (TC)	3 (CC)	0.22	0.22	0.16
6	TCF21	rs12190287	47 (CC)	50 (CG)	15 (GG)	0.36	0.42	0.77
6	SLC22A3	rs2048327	56 (TT)	43 (TC)	13 (CC)	0.31	0.33	0.29
6	SLC22A3-LPAL2-LPA	rs3798220	110 (TT)	2 (TC)	0 (CC)	0.01	0.01	0.92
7	HDAC9	rs2023938	94 (TT)	17 (TC)	1 (CC)	0.08	0.13	0.81
7	BCAP29	rs10953541	61 (CC)	45 (CT)	6 (TT)	0.25	0.25	0.53
7	ZC3HC1	rs11556924	55 (CC)	44 (CT)	13 (TT)	0.31	0.43	0.36
8	LPL	rs264	86 (GG)	23 (GA)	3 (AA)	0.13	0.13	0.35
8	TRIB1	rs2954029	35 (AA)	48 (AT)	28 (TT)	0.47	0.38	0.17
9	CDKN2BAS1	rs3217992	42 (CC)	58 (CT)	12 (TT)	0.37	0.37	0.22
9	CDKN2BAS1	rs1333049	29 (GG)	65 (GC)	18 (CC)	0.45	0.49	0.07

9	ABO	rs579459	66 (TT)	44 (TC)	2 (CC)	0.21	0.2	0.08
10	KIAA1462	rs2505083	42 (TT)	53 (TC)	17 (CC)	0.39	0.43	0.97
10	CXCL12	rs2047009	32 (TT)	48 (TG)	30 (GG)	0.49	0.45	0.18
10	CXCL12	rs501120	77 (TT)	32 (TC)	3 (CC)	0.17	0.13	0.88
10	LIPA	rs11203042	35 (CC)	57 (CT)	20 (TT)	0.43	0.49	0.7
10	LIPA	rs1412444	52 (CC)	45 (CT)	15 (TT)	0.33	0.37	0.3
10	CYP17A1, CNNM2, NT5C2	rs12413409	96 (GG)	16 (GA)	0 (AA)	0.07	0.08	0.42
11	PDGFD	rs974819	57 (CC)	47 (CT)	4 (TT)	0.25	0.22	0.13
11	ZNF259, APOA5-A4-C3-A1	rs964184	77 (CC)	33 (CG)	2 (GG)	0.17	0.12	0.47
12	SH2B3	rs3184504	35 (CC)	55 (CT)	22 (TT)	0.44	0.45	0.96
13	FLT1	rs9319428	50 (GG)	51 (GA)	11 (AA)	0.33	0.27	0.7
13	COL4A1-COL4A2	rs4773144	28 (AA)	61 (AG)	23 (GG)	0.48	0.42	0.33
13	COL4A1-COL4A2	rs9515203	63 (TT)	37 (TC)	11 (CC)	0.27	0.27	0.12
14	HHIPL1	rs2895811	41 (TT)	51 (TC)	20 (CC)	0.41	0.42	0.55
15	ADAMTS7	rs3825807	31 (AA)	51 (AG)	29 (GG)	0.49	0.39	0.39
15	FURIN-FES	rs17514846	30 (AA)	59 (AC)	23 (CC)	0.47	0.44	0.54
17	SMG6	rs216172	50 (GG)	49 (GC)	13 (CC)	0.33	0.33	0.85
17	RAI1-PEMT-RASD1	rs12936587	38 (AA)	56 (AG)	18 (GG)	0.41	0.47	0.73
17	UBE2Z	rs46522	29 (TT)	64 (TC)	19 (CC)	0.46	0.49	0.11
19	LDLR	rs1122608	77 (GG)	29 (GT)	6 (TT)	0.18	0.26	0.16
19	ApoE-ApoC1	rs2075650	81 (AA)	30 (AG)	1 (GG)	0.14	0.16	0.32
19	ApoE-ApoC1	rs445925	90 (GG)	21 (GA)	1 (AA)	0.1	0.11	0.85
21	Gene desert (KCNE2)	rs9982601	84 (CC)	26 (CT)	2 (TT)	0.13	0.21	0.99

**Table 3.3. Summary of the genotypes for 50 CAD-associated SNPs in the MSC bank (114 donors).** Shown are the calculated minor allele frequencies (MAFs) for the MSC bank and the MAFs for a CEU population from the single nucleotide database (dbSNP). All SNPs were in Hardy-Weinberg equilibrium. Chr; chromosome, MAF; minor allele frequency, CEU; Utah residents with western and northern Europe ancestry, HWE; Hardy-Weinberg equilibrium.

### 3.3 Discussion

In this project I explored the use of MSCs as a prospective cell type to study CAD-related genetic variants. MSCs are multipotent; and have been reported to differentiate into CAD-relevant cells, and therefore have the potential to be utilized to investigate the functional mechanisms CAD-related variants act through in specific cell types.

The first aim of this project set out to reproduce a method to isolate MSCs from WJ from the umbilical cord and investigate their characteristic features. The explant method, has been used by many research groups, and was employed to isolate MSCs, based on the ability of the cells to migrate out of WJ tissue onto the plastic surface. MSCs were successfully isolated from 114 out of 120 umbilical cords collected. This represented 95% harvesting efficiency, demonstrating the explant method is sufficient to harvest MSCs. The cells were very similar in appearance to human umbilical cord-derived MSCs purchased from ATCC. Both populations exhibited a fibroblast-like appearance, as thin cell processes were observed protruding from the small cell body. MSCs also displayed morphological heterogeneity, as some cells appeared as wide, flat cytoplasmic cells. This observed morphological heterogeneity is consistent within the literature (Pevsner-Fischer *et al.*, 2011; Haasters *et al.*, 2009; Karahuseyinoglu *et al.*, 2007). The relationship between morphology and cellular function is still unclear.

Upon successful isolation of MSCs from WJ, additional characteristic features of MSCs were investigated. To determine the proliferation rate of MSCs, the PDT was calculated. The mean PDT of P3 MSCs was 37 hours. Kim *et al.*, (2011) reported a PDT of 21 hours for P3 MSCs isolated from WJ. The difference in PDTs may be due to the density at which the MSCs were seeded. I seeded MSCs at a cell density of  $1 \times 10^4$  cells/cm<sup>2</sup>, whereas Kim *et al.*, (2011) seeded cells at  $5 \times 10^3$  cells/cm<sup>2</sup>. It has previously been shown MSCs seeded at a higher density have a lower proliferation rate, in comparison to MSCs seeded at a lower density (Both *et al.*, 2007), thereby accounting for the difference in PDTs. Furthermore, the PDT for MSCs isolated from WJ was lower than the PDT reported for bone marrow-derived MSCs (Lu *et al.*, 2006), which indicates

MSCs from WJ proliferate faster than bone marrow-derived MSCs. Growth curve analysis showed MSCs grew in a characteristic pattern which included three phases; lag phase, the time taken for cells to recover from subculturing, log phase, where the cell number increased exponentially, and plateau phase, where cells became confluent and stopped proliferating. This characteristic pattern has also been observed by other investigators (Wei *et al.*, 2008; Qiao *et al.*, 2008).

The morphology alone does not confirm the successful isolation of MSCs and therefore additional criteria must be met. In 2006 The Mesenchymal and Tissue Stem Cell Committee of the International Society of Cellular Therapy proposed the minimum criteria the cell population must meet, in order to classify them as MSCs. Firstly, MSCs must be adherent to plastic. Secondly, MSCs must display and be positive ( $\geq 95\%$ ) for CD105, CD73 and CD90 and negative ( $\leq 2\%$ ) for CD45, CD34, CD14 or CD11b, CD79 $\alpha$  or CD19 and HLA-DR (Dominici *et al.*, 2006). Cell surface marker expression of MSCs from six different donors was analysed and quantified using the flow cytometer. MSCs were more than 95% positive for CD105, CD73 and CD90 and less than 2% positive for CD45, CD34, CD11b, CD19 and HLA-DR. The negative markers represent cells MSCs are likely to be contaminated with haematopoietic cells; macrophages, monocytes and B cells. The lack of expression of the negative markers demonstrated the explant method yielded a pure population of MSCs that expressed a characteristic surface profile. The same methodology of isolation was applied to all umbilical cord samples to harvest MSCs, therefore cell surface marker expression was analysed on six different donors, as a quality control across the samples.

The third criterion MSCs must meet is the potential to differentiate into three lineages; adipocytes, chondrocytes and osteoblasts (Dominici *et al.*, 2006). After 14 days, MSCs treated with adipogenic differentiation medium exhibited intra-cytoplasmic lipid droplets, which stained positive with Oil Red O staining. Next MSCs were cultured for 28 days with chondrogenic differentiation medium using a pellet cultural system to induce chondrogenic differentiation. Toluidine Blue staining of the harvested sections was successful, as Toluidine blue stained glycosaminoglycans, which are found in cartilage tissue.

Undifferentiated MSCs did not form a pellet, except MSCs from Donor 9, and did not stain purple suggestive of the lack of the deposition of extracellular matrix. Lastly, MSCs were treated with osteogenic differentiation medium to induce differentiation into osteoblasts. After 28 days, cells deposited calcium which was positively stained by Alizarin Red S staining. Overall these results are demonstrative of the multipotent potential of MSCs, to differentiate into three common lineages.

Of importance to note is that the trilineage differentiation of MSCs was heterogeneous. This was seen within MSCs from the same donor and between MSCs from different donors. During adipogenic differentiation, all the cells from one donor did not display the same number and size of lipid vesicles. In the same well, some cells displayed a more mature morphology (larger lipid droplets), whereas other cells displayed no lipid droplets. This heterogeneity appeared in patches in the well. It was also apparent that, MSCs from different donors which were seeded at the same time, and at the same density, displayed different levels of adipogenic differentiation. Certain donors showed a greater quantity of lipid stained cells in comparison to cells from other donors. Also certain individuals showed a greater number of mature adipocytes, as larger lipid droplets were displayed.

For chondrogenic differentiation the heterogeneity was less apparent, as the differentiation success was observed at the pellet and not at the cellular level. Yet, it was still seen that within the chondrogenic pellet from certain donors, a more intense staining of extracellular matrix was observed, and a lower proportion of undifferentiated MSCs around the pellet was seen.

Osteogenic differentiation of MSCs was also heterogeneous. Differentiated cells from certain donors displayed a more intense staining of calcium deposition in certain areas within the well. As observed with adipogenic differentiation, cells from particular donors displayed a greater degree of calcium deposition than cells from other donors.

My results demonstrate the heterogeneous nature of MSCs. Researchers have investigated MSC heterogeneity at the clonal level. They observed when single MSCs derived from a mother colony were selected and differentiated into osteoblasts, there was variability in this differentiation

between different colonies, as some had differentiated but some had not (DiGirolamo *et al.*, 1999).

There are many plausible reasons for the heterogeneity in MSC differentiation. The heterogeneity observed in MSCs from the same donor, may be due to more multipotent MSCs within the population, differentiating more quickly upon treatment with the induction medium, and releasing certain cytokines influencing neighbouring cells to differentiate. The differences in the multipotent potential of MSCs within a population may be as a result of extensive *ex vivo* culturing, as long term culture associates with changes in gene expression and DNA methylation (Wagner *et al.*, 2008; Bork *et al.*, 2010; Izadpanah *et al.*, 2008), altering the phenotype of cells. An alternative explanation is the observed heterogeneity may simply reflect the diverse repertoire of MSC subpopulations that exist *in vivo*. To support this notion, heterogeneity of osteogenic differentiation is seen under *in vivo* conditions (Kuznetsov *et al.*, 1997).

A hierarchical model of MSC heterogeneity has been proposed. A study was carried out, 185 cultures of bone marrow-derived MSCs were analysed. Analysis of the colonies showed chondrogenic-adipogenic or osteogenic-adipogenic differentiation did not occur, in addition to adipogenic or chondrogenic differentiation (Muraglia *et al.*, 2000), suggesting a hierarchical structure of MSC differentiation. They propose a model where adipogenic differentiation is lost first from the cells, followed by a loss of chondrogenic differentiation ability, leaving MSCs with the sole ability for osteogenic differentiation. However it is possible that osteogenic differentiation is favoured by *in vitro* culturing and expansion conditions. A study showed bone marrow-derived MSC clones with osteogenic-adipogenic and adipogenic-chondrogenic differentiation abilities were not observed, suggesting culture conditions favour osteogenesis (Banfi *et al.*, 2000). Analogous to the hierarchical model, a random hierarchical model has been suggested. A study reported that MSC clones have tripotent differentiation ability and all combinations of bi- and mono-potent clones were observed. The investigators report that all mono- and bi-potent MSCs were possible. Tripotent cells lose differentiation ability leading to bi-potent cells and subsequently monopotent cells (Russell *et al.*, 2010). It is important to note, these studies were conducted on bone marrow-derived

MSCs, and MSCs from other regions within the body may follow an alternative model of heterogeneity.

An explanation for the variability observed between MSCs from different donors, may be due to events that occur before the birth of the baby. It has been shown that low birth weight and a shorter pregnancy resulted in a higher degree of osteogenic differentiation of MSCs (Penolazzi *et al.*, 2009). Therefore differences in the length of pregnancy and birth weight between donors may result in differences in MSC differentiation potential *in vitro*.

In summary the characterisation of MSCs demonstrated their immunophenotype was homogenous, but the ability to differentiate into three common lineages was not homogenous. True MSCs are tripotent, however only some plastic-adherent MSCs were multipotent, suggesting WJ-derived MSCs were a heterogeneous population of cells with diverse lineage commitment.

The final objective was to genotype DNA from MSCs, to determine the genotypes for CAD-associated SNPs. MSCs were subcultured up to P5 from each donor, cryopreserved and transferred to liquid nitrogen for long-term storage, to form a MSC bank. The intention of the bank was to deposit MSCs from different donors (114 in total), for whom the genotypes for various CAD-related genetic variants were known. To this end, DNA was extracted from each donor, plated and sent to Affymetrix for genotyping. Of the 114 DNA samples, 2 failed the array, so 112 samples were successfully genotyped and information extracted for the 50 CAD-associated SNPs. The MAFs for SNPs were determined in the MSC population, so individuals homozygous major, heterozygous and homozygous minor for each variant was known. For some variants, the MAF in the MSC bank differed more than 5% when compared to a CEU population detailed on dbSNP. It is important to note, that the umbilical cords were donated from individuals of unknown ethnicity. Samples were collected from the Leicester Royal Infirmary Hospital. Leicester is an ethnically diverse city, therefore is highly likely that the 114 samples consisted of individuals from different ethnicities, and is not a 100% Caucasian population. This may explain the differences observed in MAFs of the MSC bank and the CEU population on dbSNP. For example, rs12190287 (minor allele; G) had a

MAF of 0.36 in the MSC bank. It had a MAF in the CEU dbSNP population of 0.42. But in a sub-saharan African (YRI) population on dbSNP the minor allele was less common in the population (MAF=0.04). Therefore if donors present in the MSC bank were of sub-saharan African origin, the MAFs calculated for the MSC population would be skewed. The notion that the MSC bank was not comprised of a 100% Caucasian population, may translate into functional differences when studying genetic associations that differ by ethnicity e.g. 9p21.

### **3.3.1 Conclusion**

In conclusion, MSCs were successfully isolated and expanded from WJ from 114 umbilical cords. MSCs met the International Society of Cellular Therapy criteria; cells adhered to plastic, expressed the characteristic cell surface profile and differentiated into three common lineages. DNA from 112 donors underwent successful genotyping for 50 CAD-associated variants. Future work for investigating a specific CAD variant will include the selection of MSCs from the MSC bank based on their genotype for that specific variant.

# **Chapter 4- Analysis of a variant associated with body mass index**

## 4.1 Introduction

Obesity is a term that describes an individual with abnormal or excessive fat accumulation. It is a very common problem, affecting approximately 1 in 4 adults, and 1 in 5 children (aged 10-11) in the UK. Since 1980, obesity has more than doubled worldwide. In 2014, there were more than 1.9 billion overweight adults, of which 600 million were obese. In most countries being overweight and obese kills a greater number of people than being underweight (World Health Organisation, 2015). It has a negative effect on an individual's health, resulting in increased health problems or reduced life expectancy. Obesity is a major risk factor, for many diseases, including cardiovascular disease, type 2 diabetes mellitus, hypertension, stroke, metabolic syndrome and certain forms of cancer (Must *et al.*, 1999). Therefore factors that affect the development of obesity may also predispose to these diseases.

Many lifestyle changes have made obesity an epidemic problem, such as inactive lifestyle, unhealthy diet, eating habits, medical problems and social and economic issues. In addition to lifestyle factors, obesity has a genetic basis, where the contribution of the heritability is between 40-70% (Maes *et al.*, 1997; Zaitlen *et al.*, 2013).

Body mass index (BMI) is a measure of being overweight and obese. It is defined by the weight (kg) of a person divided by the square of the body height ( $m^2$ ), and is expressed in units of  $kg/m^2$ . The World Health Organisation define that a BMI equal to or greater than  $25kg/m^2$  is overweight, and a BMI equal to or greater than  $30kg/m^2$  is classed as obese. BMI can also predict the risk of other health complications.

The identification of the genetic determinants for BMI will lead to a greater understanding of the biology underpinning obesity. GWASs have been conducted to determine genetic determinants of BMI. The first study was conducted in 2007, where SNPs at the fat mass and obesity associated (*FTO*) gene were strongly associated with BMI (Frayling *et al.*, 2007). Following this study, four more GWASs were published over the next three years identifying an additional 9 loci that reached genome wide significance ( $p \leq 5 \times 10^{-8}$ ); *KCTD15*, *ETV5*, *MTCH2*, *SH2B1*, *NEGR1*, *BDNF*, *GNPDA2*, *TMEM18* and *MC4R* (Loos

*et al.*, 2008; Willer *et al.*, 2008; Thorleifsson *et al.*, 2009; Scuteri *et al.*, 2007). The majority of these genes are present or act in the central nervous system, suggesting its involvement in the predisposition to obesity (Willer *et al.*, 2008).

These ten loci only accounted for a small fraction of the variation in BMI. In attempt to identify additional variants associated with BMI, the Genetic Investigation of Anthropometric Traits (GIANT) consortium carried out a meta-analysis using 46 different studies in Stage 1 which included 123,865 individuals. Stage 2 examined 125,931 additional individuals from another 34 studies. 14 previously identified susceptibility loci were confirmed and 18 novel loci were identified. The allele frequencies ranged from 4-87% (Speliotes *et al.*, 2010).

Additional studies have discovered another 34 loci that associated with BMI at the  $p \leq 5 \times 10^{-8}$  significance level (Wen *et al.*, 2012; Okada *et al.*, 2012; Heard-Costa *et al.*, 2009). The most recent study was conducted in up to 339,224 individuals from 125 different studies, the largest GWAS to date. 97 BMI-associated loci were identified, of which 56 were novel genomic regions (Locke *et al.*, 2015). The investigation of BMI-associated loci will highlight new pathways, and expand our understanding of the biological processes involved in obesity.

In this chapter, I focussed on a BMI-associated variant identified in a GWAS. Speliotes *et al.*, (2010) identified rs3810291 to be significantly ( $p=1.64 \times 10^{-12}$ ) associated with BMI. They annotated this variant to the *TMEM160* locus, however the SNP sits in the 3'UTR of zinc finger CCCH-type containing 4 (*ZC3H4*) gene. The A allele is the BMI increasing allele and has a frequency of 67% in the population. To identify potential candidate genes, each BMI-associated loci was functionally annotated for quantitative trait loci (eQTL) in the brain, blood, liver, lymphocyte and adipose tissue (Speliotes *et al.*, 2010; Emilsson *et al.*, 2008). It was demonstrated rs3810291 was the most significant SNP associated with the *ZC3H4* gene transcript in adipose tissue ( $n=701$ ;  $p=9 \times 10^{-9}$ ).

There are a number of ways SNPs that sit within non-coding regions of the genome may affect gene expression. For example, if a SNP sits in the 3'

UTR of a gene, it is susceptible to micro RNA (miRNA) regulation. A miRNA is a small non-coding RNA that can post-transcriptionally regulate mRNAs at the 3' UTR. So the introduction of a SNP in the 3' UTR may affect binding of a miRNA and cause differential gene expression between genotype groups. It is probable that rs3810291 affects expression, by altering the binding of a miRNA, to alter *ZC3H4* expression.

#### 4.1.1 ZC3H4

*ZC3H4* encodes a member of a family of CCCH zinc finger domain-containing proteins. *ZC3H4* contains 1 to 2 proline-rich domains, which may mediate protein-protein interactions (Liang *et al.*, 2008). Overall, it is a poorly characterised protein. High *ZC3H4* expression levels have been seen in high energy expense tissues such as the muscle, brown adipose tissue, aorta and heart, indicating this gene may be involved in fatty acid metabolism (Liang *et al.*, 2008).

The mouse homolog of *ZC3H4* is *BWQ1* on chromosome 7. *BWQ1* has been identified as a body weight QTL in mice (Suto *et al.*, 1998). Suto and Sekikawa (2004) further characterised this locus and showed it was significantly associated with body weight gain in the KK mouse (polygenic model for noninsulin-dependent diabetes mellitus with moderate obesity). It is plausible that *ZC3H4* is the functional gene at this region.

#### 4.1.2 Aims and objectives

The aim of this chapter was to, as a proof of principle, differentiate genotype-specific MSCs for rs3810291 into adipocytes, to recapitulate the effects of rs3810291 on *ZC3H4* expression.

The objectives were:

- Measure the heterogeneity of adipogenic differentiation of MSCs
- Separate differentiated adipocytes from MSCs
- Investigate the effect of rs3810291 on *ZC3H4* gene expression in MSCs and MSC-derived adipocytes
- Analyse other reported eQTLs in MSCs and MSC-derived adipocytes

## 4.2 Results

### 4.2.1 Heterogeneity of adipogenic differentiation

In Chapter 3 it was observed that the adipogenic differentiation of MSCs was heterogeneous, both within and between donors. So, the first objective was to investigate this heterogeneity further, as it was hypothesised that variability in the level of differentiation between donors may mask the effects of the BMI-associated variant under investigation. I studied MSCs from ten different donors, which had been selected on the basis of their genotype for a BMI-associated variant (5 subjects in each genotype group (discussed later in this section)).

Upon treatment with the STEMPRO<sup>®</sup> Adipogenesis Differentiation Kit MSCs stopped proliferating. During the 14 day treatment their morphology altered from a fibroblast-like appearance to a more rounded morphology, with the presence of intracellular lipid droplets. Oil Red O, a dye frequently used to detect neutral lipids and lipid droplets was used to stain intracellular lipids in differentiated adipocytes. The phenotype of the cells varied greatly between cultures from different donors (**Figure 4.1**). Some cultures displayed cells with a rounder appearance (Donor 60), while others exhibited an elongated appearance (such as Donor 37). In addition, cells from some donors (e.g. Donor 60) were present with numerous small intracellular droplets. Whereas other cell cultures (e.g. Donor 39), showed fewer cells positive for lipid, but cells that had stained contained larger lipid droplets. As observed in Chapter 3, all the cells from one donor did not display the same number and size of lipid vesicles. Some cells displayed larger lipid droplets, whereas other cells displayed no lipid droplets. The appearance of a mature adipocyte is defined by the presence of a single unilocular lipid droplet. This phenotype was not observed in any of the cultures from the ten different donors. This finding suggests that even though MSCs were able to differentiate into adipocytes, this transition did not result in vast numbers of mature adipocytes. Overall, these results suggest the differentiation of MSCs into adipocytes is a variable process within and between cells from different donors.

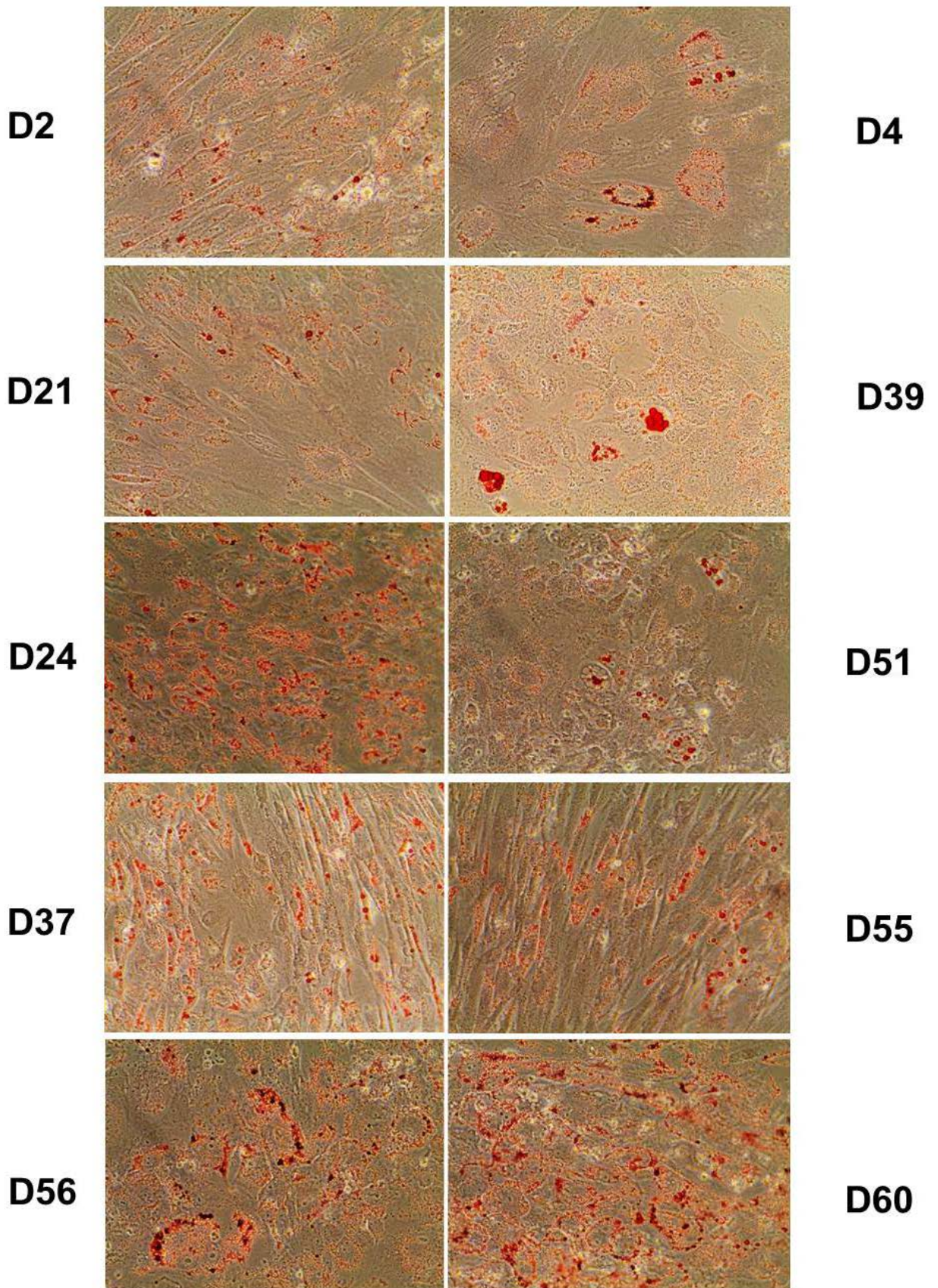


**Figure 4.1. Representative images of adipogenic differentiation of MSCs from 10 different donors. Heterogeneity was seen within and between donors. Intracellular lipid droplets were demonstrated by Oil Red O staining. Magnification x40.**

Oil Red O stained intracellular lipid droplets efficiently, but it did not provide quantitative information on the level of lipid and cellular heterogeneity in each cell population. Nile red (9-diethylamino-5H- benzo[alpha]phenoxazine-5-one; Greenspan *et al.*, 1985) is a lipophilic stain which fluoresces brightly when it intercalates with lipid droplets, and is used to locate and quantitate lipids within a cell. Fluorescent microscopy showed Nile red stained lipid droplets within differentiated adipocytes, which were absent in MSCs (**Figure 4.2**).

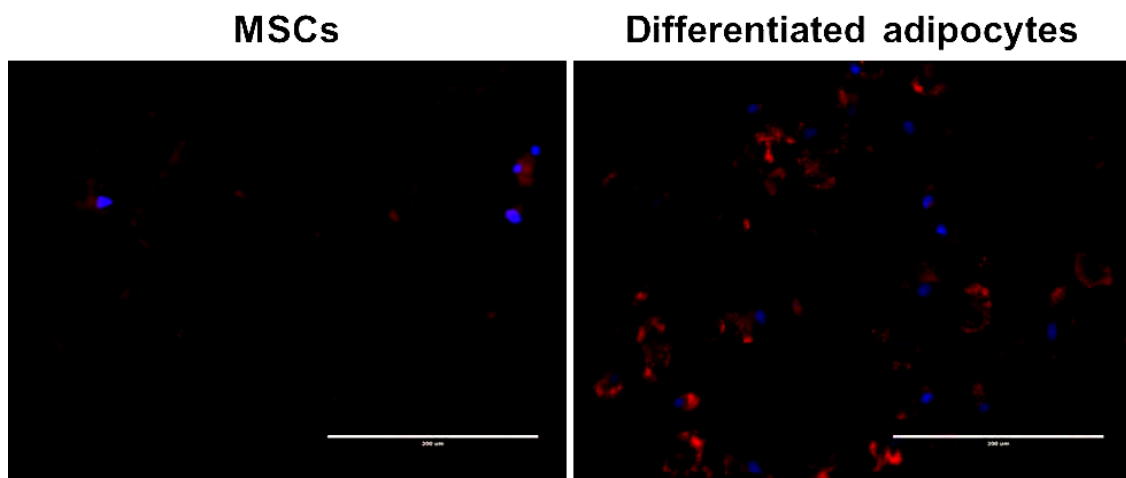


**Figure 4.2. Representative images of Nile red staining of MSCs and differentiated adipocytes.** Nile red enabled the visualisation of lipid droplets within the cell. DAPI was used to counterstain the nucleus (n=3). Bars show 200μM.

Next Nile red staining was used in conjunction with flow cytometry, to provide quantitative information about the cell population. MSCs from Donor 55, 56 and 65 were subjected to adipogenic differentiation medium, and on day 14 cells were run on the flow cytometer (**Figure 4.3**). First a control sample (MSCs incubated with Nile red) were ran to set the FL1 FITC gate at 2% positive, to account for non-specific binding of Nile red. Subsequently, differentiated adipocytes from Donor 55, 56 and 65 were ran on the flow cytometer, and were 35.9, 40.4 and 47.6% positive for Nile red, respectively. This finding suggested a heterogeneous cell population was present after adipogenic differentiation of MSCs. Side scatter (SS) is a measure of cell granularity and has been used as a parameter to quantify adipogenic differentiation, as adipocytes contain fat, it

makes them more granular (Schaedlich *et al.*, 2010). There was no difference in SS between MSCs and differentiated adipocytes (**Figure 4.5**).

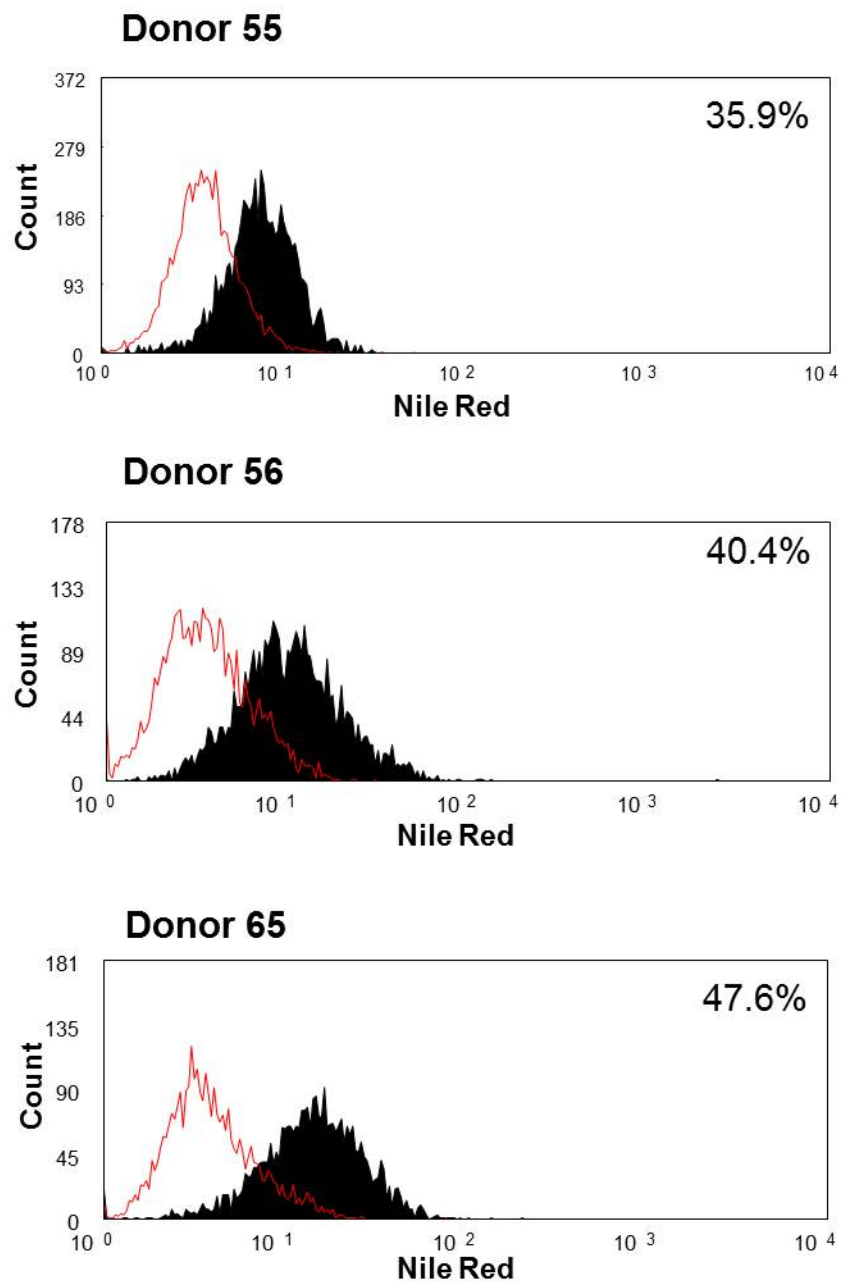


**Figure 4.3. Flow cytometry of MSCs treated to adipogenic differentiation medium.** MSCs from Donor 55, 56, 65 were cultured with adipogenic differentiation medium. On day 14, cells were stained with Nile red and run on the flow cytometer. Data shown is representative of 10,000 events and was analysed using the Summit V 4.3 software. MSCs are indicated by the red histogram. Differentiated adipocytes (black histogram) from Donor 55, 56 and 65, were 35.9%, 40.4% and 47.6% positive for Nile red, respectively.

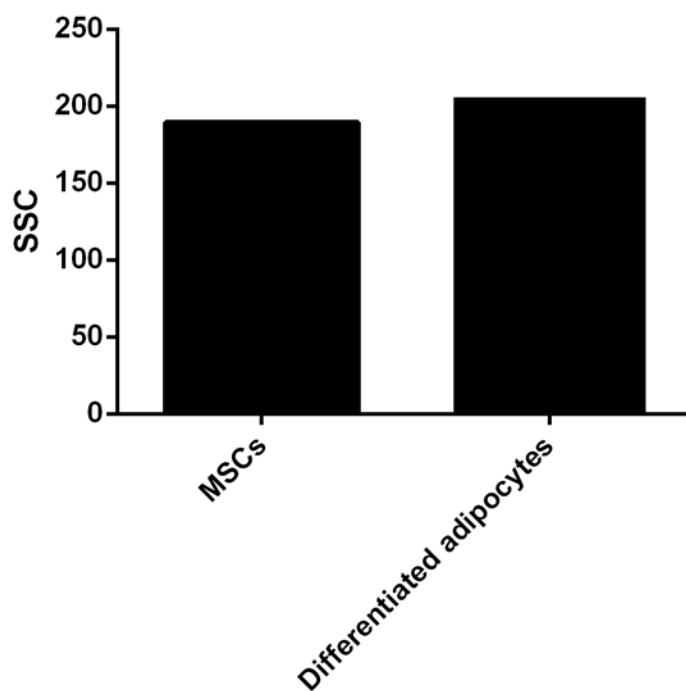


**Figure 4.4. Side scatter analysis of MSCs and differentiated adipocytes.** Side scatter (SS) is measure of cell granularity. There was no increase in SS after adipogenic differentiation of MSCs (n=3).

#### 4.2.2 Separation of differentiated adipocytes from MSCs

As the adipogenic differentiation of MSCs from different donors was variable, a method was sought to separate differentiated adipocytes from MSCs. Unfortunately adipocytes do not have a single unique cell surface marker, so a magnetic bead separation technique could not be used. In addition, I did not have access to a flow cytometer with cell sorting capabilities, so cells that were positive for Nile red could not be separated by fluorescence.

Density centrifugation was an alternative approach taken to separate adipocytes from a heterogeneous population containing MSCs. This method involved centrifuging cells, taking volumes from different levels of the supernatant and plating into new plates. As adipocytes have a buoyant property, they will be located at the top of the supernatant. However, after 24 hours, fat cells were not seen in any of the wells.

Next a ceiling culture technique was applied to try and separate adipocytes from MSCs. Firstly, 3T3-L1 cells, which are a well characterised adipocyte cell model were differentiated. They exhibited a higher number of cells with larger intracellular lipid droplets (**Figure 4.5**), indicating the population was more buoyant than MSC-derived adipocytes. 3T3-L1 differentiated adipocytes were trypsinized, the flask completely filled with medium, and incubated, to allow for lipid filled adipocytes to float and adhere to the top of the flask, and the undifferentiated 3T3-L1 cells to sink and adhere to the bottom of the flask. Many attempts were made with this method. At 4 and 72 hours, only a few differentiated adipocytes had attached to the top of the flask (**Figure 4.6**). This method was repeated with MSC-derived adipocytes, however the separation of adipocytes was not observed.

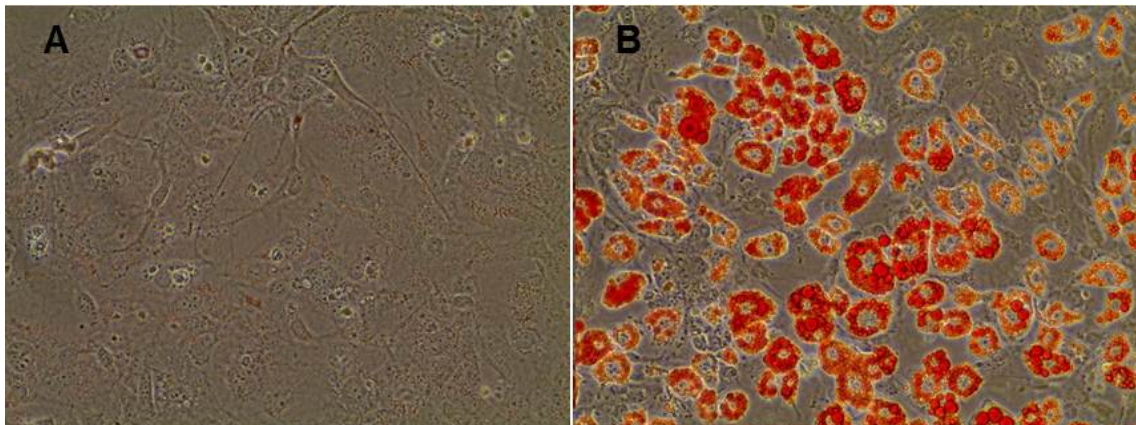


**Figure 4.5. Representative image of the differentiation of 3T3-L1 into adipocytes, upon induction with adipogenic differentiation medium. (A)** In 3T3-L1 cells lipid droplets **were** not detected. **(B)** 3T3-L1 cells cultured in adipogenic differentiation medium displayed intracellular lipid droplets when stained with Oil Red O (n=3; **Magnification x40**).

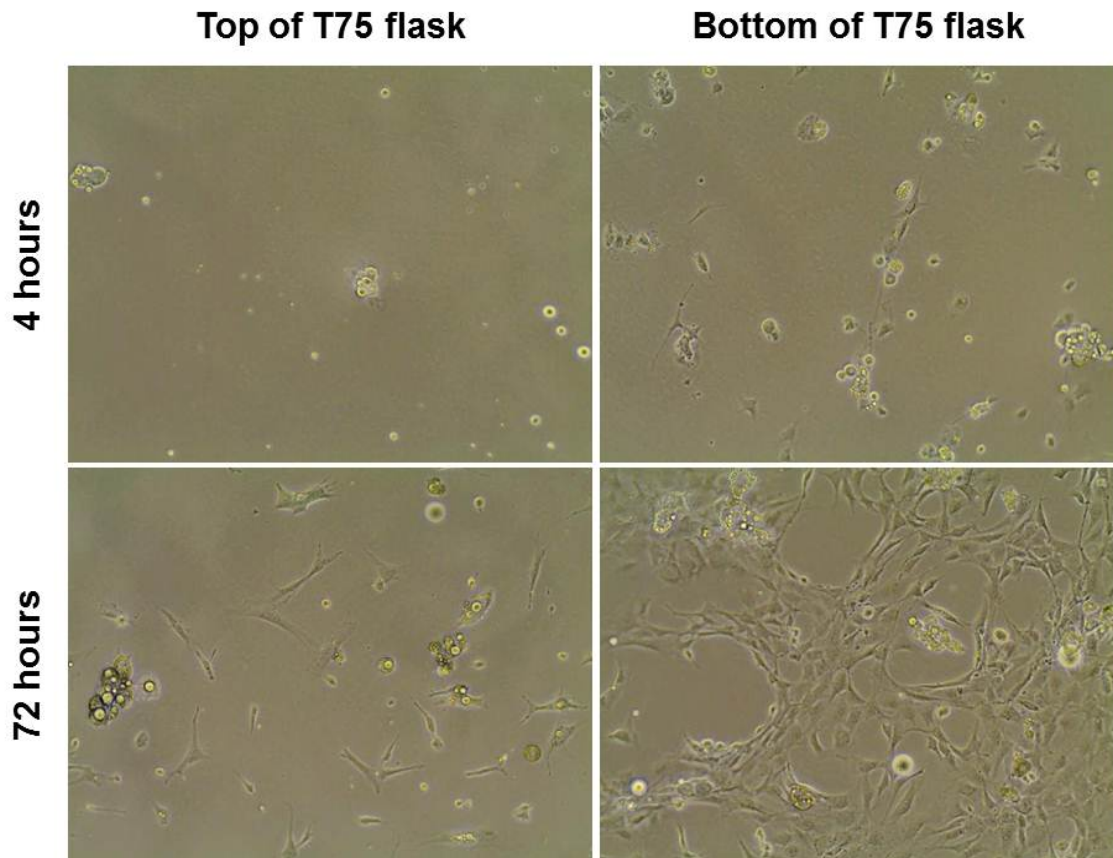


**Figure 4.6. Attempt at ceiling culture separation of differentiated adipocytes.** 3T3-L1 cells were differentiated into adipocytes, and subjected to a ceiling culture separation method to separate mature adipocytes. Images were obtained 4 and 72 hours after cell detachment. **Magnification x40.**

In summary, these results suggest that the differentiation of MSCs into adipocytes yielded partially differentiated cells which were heterogeneous in their morphology and lipid content. As the separation of adipocytes from non-differentiated cells was not possible, I accounted for this variation by measuring adipogenesis markers.

#### 4.2.3 Gene expression of adipogenic markers

To measure the efficiency of differentiation, I analysed the expression of genes associated with adipogenesis. Peroxisome proliferator activated receptor (PPAR $\gamma$ ) increases upon adipogenesis (Nolte *et al.*, 1998; Janderová *et al.*, 2003; Neubauer *et al.*, 2004; Sekiya *et al.*, 2004). Upon ligand stimulation,

PPAR $\gamma$  forms a heterodimer with retinoid-X receptor which binds DNA and activates transcription (Nolte *et al.*, 1998). Fatty acid binding protein 4 (FABP4) is a late marker of adipogenesis. FABP4 acts in adipocytes to metabolise and transport fatty acids, amongst other roles (Furuhashi & Hotamisligil, 2008).

Quantitative PCR techniques were performed to quantify the levels of PPAR $\gamma$  and FABP4 gene expression in MSCs and MSC-derived adipocytes. First qPCR products were run on an agarose gel to ensure single amplicons, which also showed a noticeable increase of PPAR $\gamma$  and FABP4 upon adipogenic differentiation of MSCs (**Figure 4.7**). Next, MSCs from ten different donors were treated to adipogenic differentiation medium, and on day 14 RNA was extracted, cDNA synthesised and qPCR was performed. This experiment was conducted on three separate occasions on MSCs from the same ten donors to determine the reproducibility of adipogenic differentiation. Preliminary qPCR experiments used  $\beta$ -actin as a normalisation control, however it was demonstrated that adipocytes showed a significant reduction in  $\beta$ -actin expression in comparison to MSCs (data not shown). 36B4 (also known as ribosomal protein large P0 (RPLP0)) was alternatively used as a housekeeping gene, as its expression remained relatively constant across all the samples.

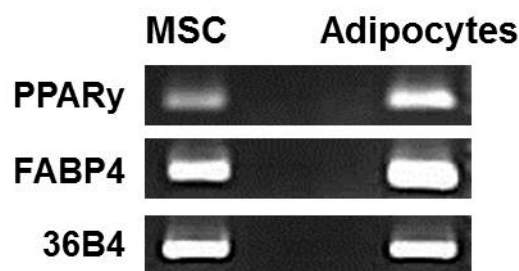


**Figure 4.7. Representative agarose gel electrophoresis of qPCR products of adipocyte-specific genes in MSCs and differentiated adipocytes.** Products were visualised by gel electrophoresis on 1.5% agarose gel. Lane 1; MSCs, Lane 2; differentiated adipocytes. 36B4 was used as the housekeeping gene. Adipocytes show an increase in expression of PPAR $\gamma$  and FABP4.

Experiment 1 showed *PPAR $\gamma$*  expression varied greatly between adipocytes from different donors, as it ranged from 6.3 to 48- fold increase compared to MSCs (**Figure 4.8**). In Experiment 2, *PPAR $\gamma$*  expression varied from 4 to 19.7- fold. In Experiment 3, fold changes relative to MSCs ranged from 1.9 to 14.2 for *PPAR $\gamma$*  expression.

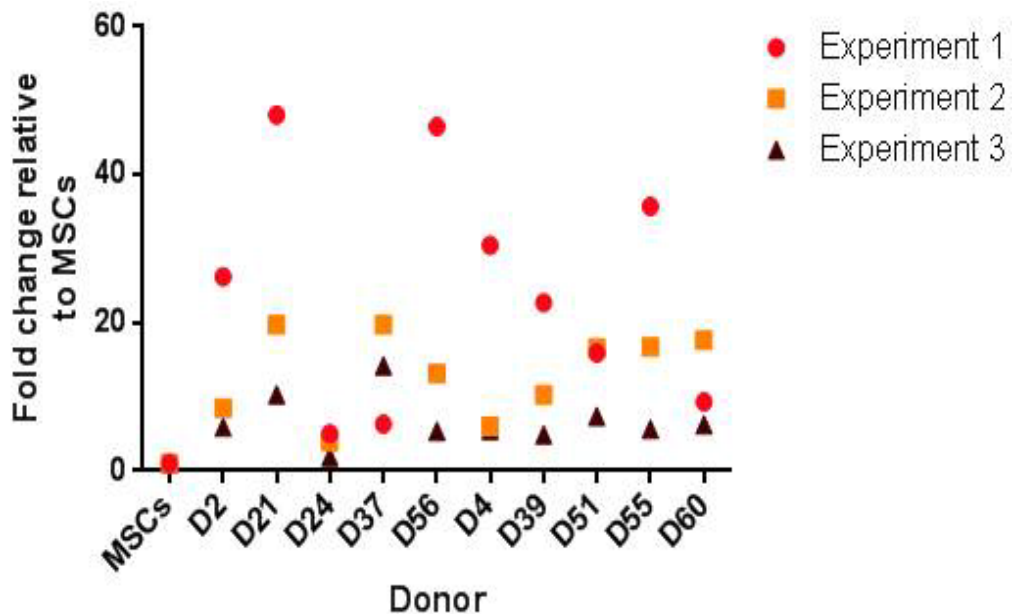


**Figure 4.8. Measurement of an adipogenic marker, peroxisome proliferator activated receptor (*PPAR $\gamma$* ) in differentiated adipocytes.** MSCs from ten different donors on three separate occasions (Experiment 1, Experiment 2 and Experiment 3) were differentiated into adipocytes, following a 14 day treatment with adipogenic differentiation medium. Gene expression of *PPAR $\gamma$*  was measured. Samples were normalised to *36B4*.

In addition analysis of *PPAR $\gamma$*  expression in cells, from the same donor, on three separate occasions showed inter-assay variation. For example, cells from Donor 2 in Experiment 1, Experiment 2 and Experiment 3 showed a 26.2, 8.4 and 5.9- fold change in *PPAR $\gamma$*  expression, respectively. To determine whether there was a relationship in the increase in *PPAR $\gamma$*  expression between different experiments a scatter graph was plotted. *PPAR $\gamma$*  gene expression for adipocytes from ten different donors in three separate experiments did not correlate (**Figure 4.9**). These results demonstrated the large variability in adipogenic differentiation of MSCs from the same donor. Experiments 2 and 3

were conducted 4 months after Experiment 1 was carried out, and may explain why the findings from Experiment 1 did not correlate with Experiment 2 and 3.

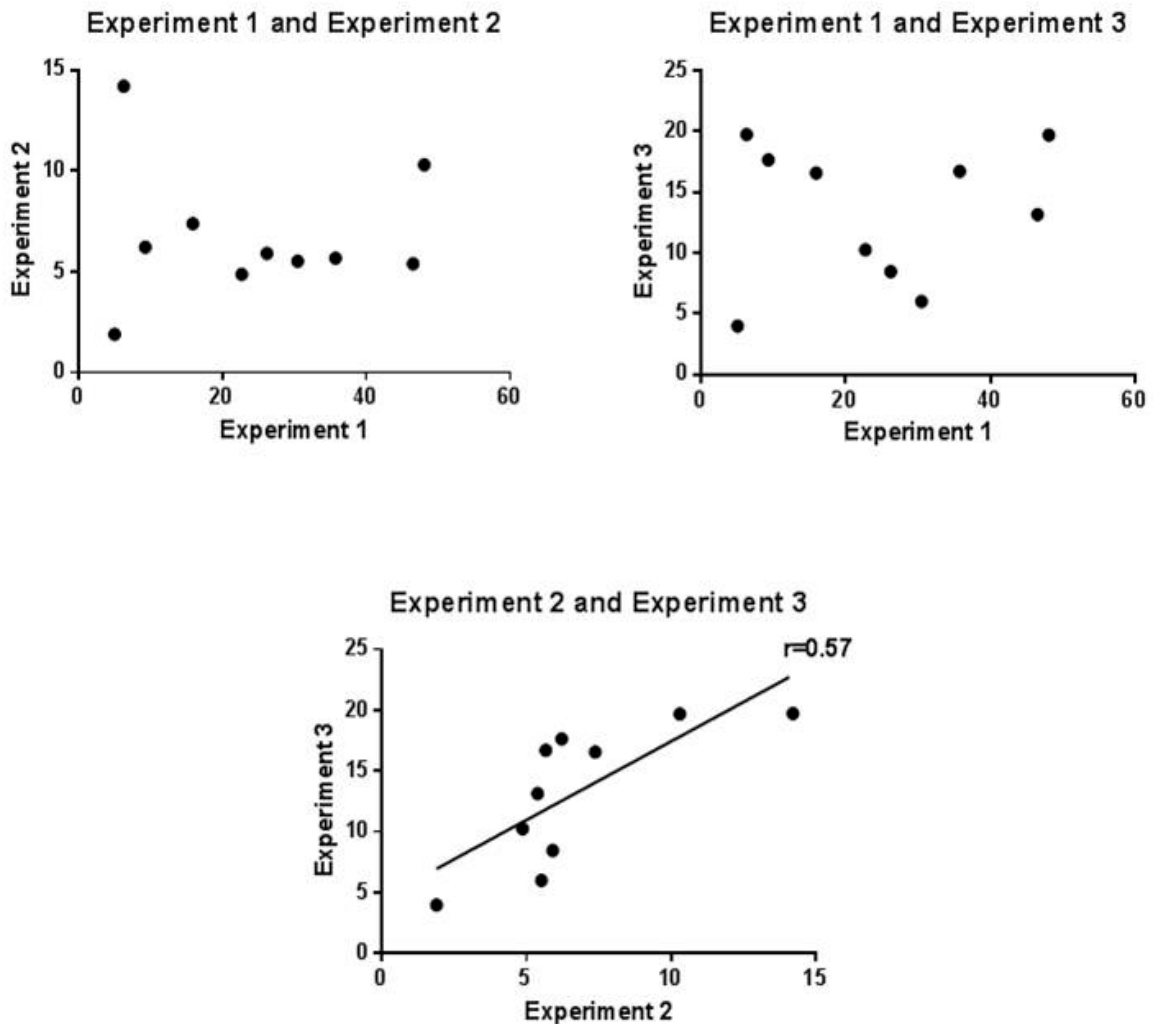


**Figure 4.9. Spearman's Correlation of *PPAR* $\gamma$  expression between Experiment 1, 2 and 3.** No correlation was observed between Experiment 1 and 2, and between Experiment 1 and 3. Poor correlation was observed between Experiment 2 and 3.

Next *FABP4* (a late marker of adipogenesis) was investigated. Expression of *FABP4* also varied greatly in cells from the ten different donors, the change in expression varying between 1 and 55- fold in Experiment 1, 0 to 5.6- fold in Experiment 2 and 0 to 8 fold in Experiment 3 (**Figure 4.10**). The inter-assay variation observed upon *PPAR* $\gamma$  measurement was also seen with *FABP4*. For example, cells from Donor 2 showed a 36, 5.6 and 4.8 -fold change

in *FABP4* expression relative to MSCs in Experiment 1, Experiment 2 and Experiment 3, respectively. These results suggest large variability in the adipogenic differentiation of MSCs derived from the same donor.

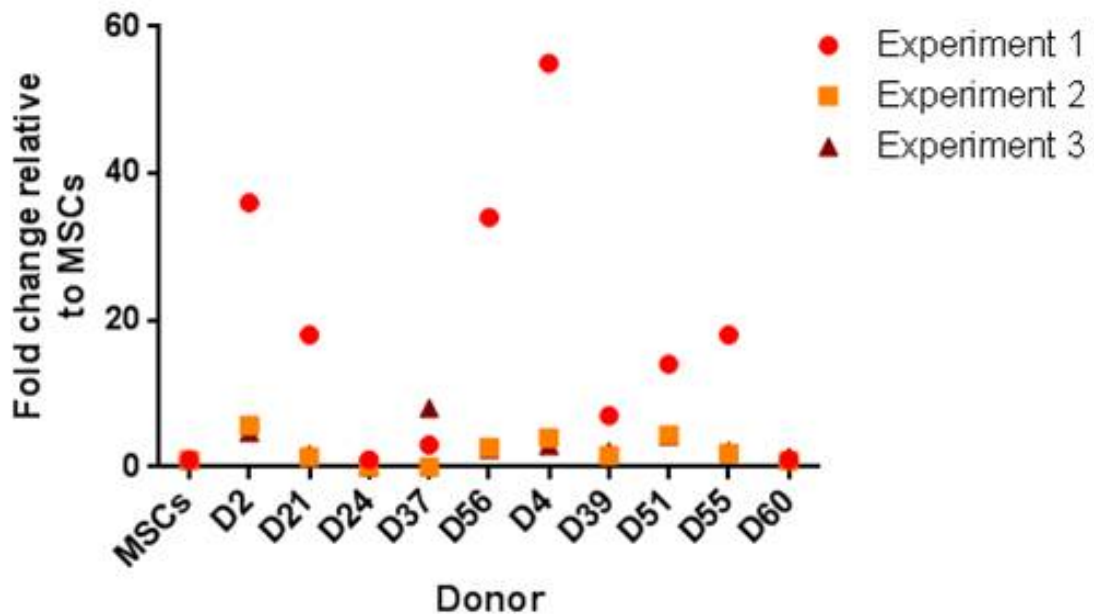


**Figure 4.10. Measurement of the late adipogenic marker, fatty acid binding protein 4 (*FABP4*) in differentiated adipocytes.** MSCs from ten different donors on three separate occasions (Experiment 1, Experiment 2 and Experiment 3) were differentiated into adipocytes, following a 14 day treatment with adipogenic differentiation medium. Gene expression of the adipogenic marker; *FABP4* was measured. Samples were normalised to *36B4*.

To investigate whether there was a relationship between *PPAR $\gamma$*  and *FABP4* expression in Experiment 1, 2 and 3 in the ten different donors, a scatter graph was plotted. *PPAR $\gamma$*  and *FABP4* gene expression correlated in Experiment 1 ( $r=0.76$ ,  $p=0.01$ ), but not in Experiment 2 ( $r=0.25$ ,  $p=0.5$ ) and Experiment 3 ( $r=0.44$ ,  $p=0.2$ ; **Figure 4.11**). These results suggest that *PPAR $\gamma$*  (early marker) and *FABP4* (late marker) do not correlate in their expression after a 14 day adipogenic differentiation treatment. Earlier histological results demonstrated that the majority of the adipocyte population were not terminally differentiated, which is supported by the finding that some donors (e.g. Donor 24 and 60) did not show an increase in *FABP4* expression, therefore this marker would not be suitable to assess the level of adipogenic differentiation in

our samples. However *PPAR $\gamma$*  expression was consistently up-regulated in MSC-derived adipocytes across all ten donors in all three experiments.

In summary, results from this section show it was possible to measure the level of adipogenesis of MSCs, but to obtain a pure population of mature adipocytes using density centrifugation or ceiling culture was not successful. I therefore decided for future experiments to use *PPAR $\gamma$*  gene expression to account and normalise for the variation in differentiation in MSC-derived adipocytes.

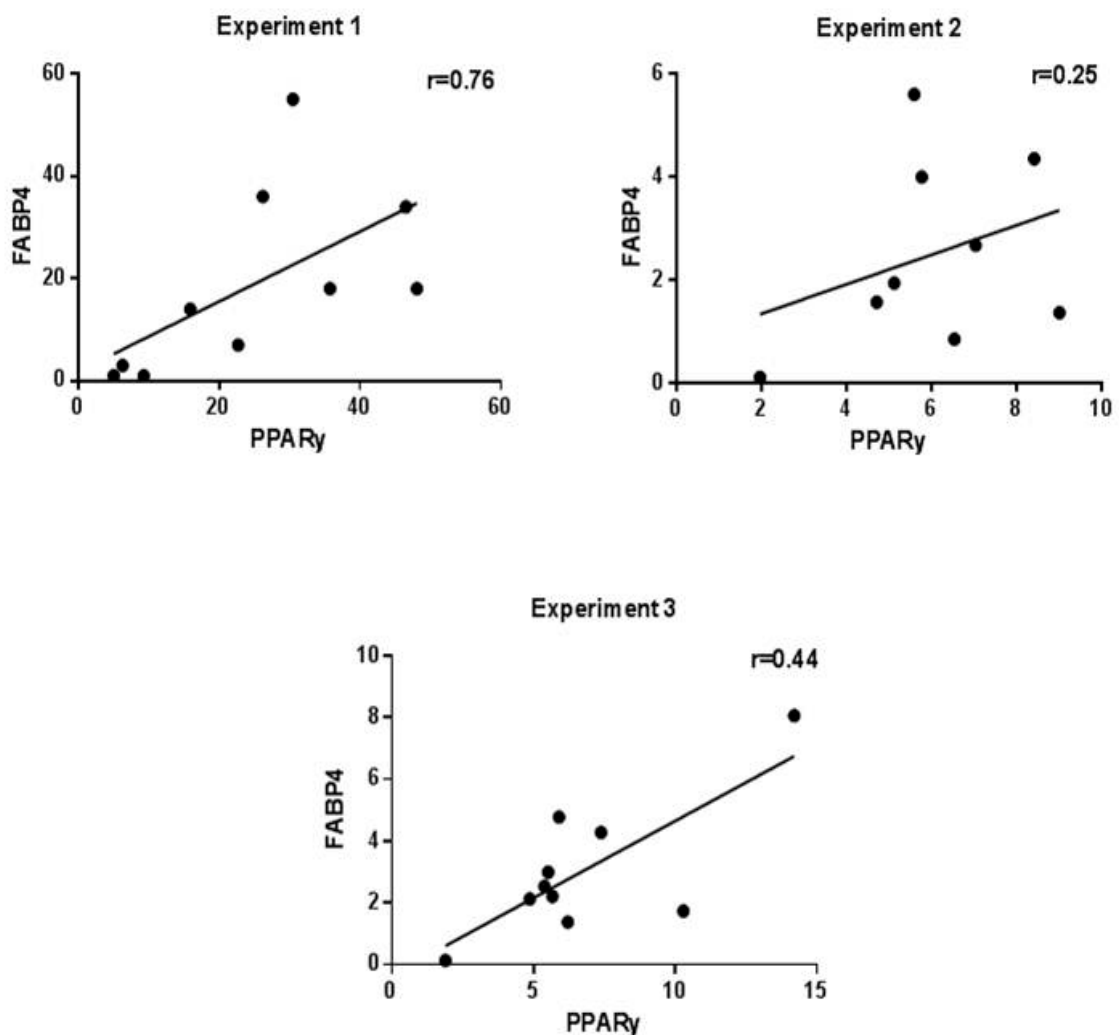


**Figure 4.11. Evaluation of the correlation between the gene expression of two adipogenesis markers.** Spearman's Correlation values were determined for *PPAR $\gamma$*  and *FABP4* gene expression in Experiment 1 ( $r=0.76$ ,  $p=0.01$ ), Experiment 2 ( $r=0.25$ ,  $p=0.5$ ) and Experiment 3 ( $r=0.44$ ,  $p=0.2$ ) overall showed poor correlation.

#### 4.2.4 Analysis of rs3810291 on ZC3H4 gene expression

In order to test the MSC bank as a research tool for the study of complex traits I performed a proof of principle study. I investigated if MSC-derived adipocytes could replicate an eQTL finding reported in a previous study. I chose to focus on a variant identified by Speliotes *et al.*, (2010) which was significantly ( $p=1.64 \times 10^{-12}$ ) associated with BMI. This locus (rs3810291) was further annotated in a gene expression database for adipose tissue (Emilsson *et al.*, 2008), where they analysed transcripts from 701 individuals. rs3810291 was identified as the most significant SNP for the ZC3H4 gene transcript in adipose tissue ( $p=9 \times 10^{-9}$ ).

First, the MSC bank was genotyped for rs3810291. At this stage, whole genome genotyping on DNA from the MSC bank had not been undertaken. A Taqman<sup>®</sup> SNP Genotyping assay was used to genotype the MSC bank for rs3810291. DNA underwent a 45 cycle PCR reaction and allelic discrimination was determined by quantifying the fluorescence emitted from the VIC and FAM allele specific reporter probes using the ViiA 7<sup>™</sup> software v1.1 (**Figure 4.12**). The genotyping results are summarised in **Table 4.1**, the genotypes of 3 samples could not be determined. The minor allele frequency (MAF) of the MSC population was 0.31, which is in line with a CEU population reported on dbSNP. The observed genotype distribution in 111 samples agreed with Hardy-Weinberg equilibrium ( $\chi^2=0.58$ ,  $p=0.45$ ). Successful genotyping of the cohort enabled the next experimental step, investigating the expression of ZC3H4 in differentiated adipocytes.

SNP	Genotype			MAF	
	Homozygote major allele	Heterozygotes	Homozygote minor allele	Local cohort	HapMap CEU
<b>rs3810291</b>	51 (AA)	51 (AG)	9 (GG)	0.31	0.32

**Table 4.1. Summary of the genotype of 111 donors for rs3810291.** The number of homozygote majors, heterozygotes and homozygote minors are displayed. The minor allele frequency (MAF) was calculated for the MSC population. Also displayed is the MAF for a population of Utah residents with western and northern Europe ancestry (CEU) from the Single Nucleotide Polymorphism database (dbSNP).

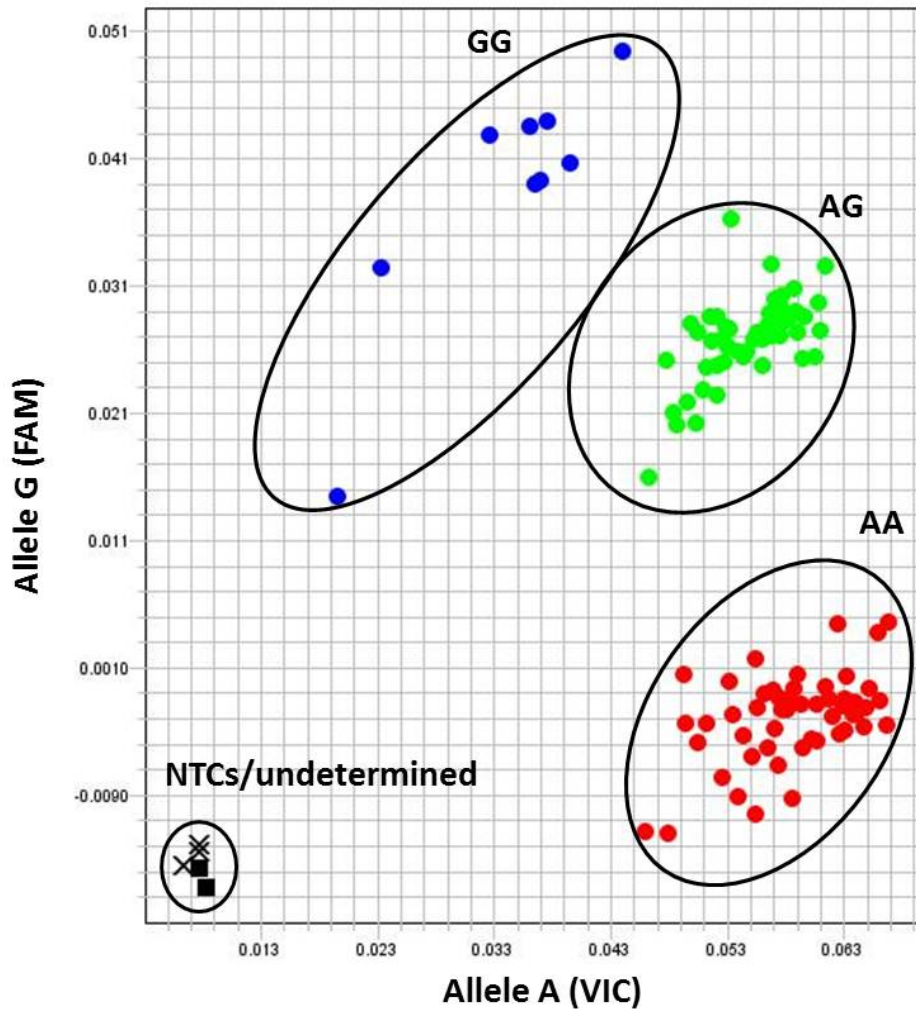


**Figure 4.12. Allelic discrimination plot for rs3810291.** The FAM reporter probe (allele G) is shown on the Y axis and the VIC reporter probe (allele A) is shown on the X axis. The blue and red dots are homozygotes, the green dots are heterozygote individuals. No template controls (NTCs; black dots) clustered toward the origin of the graph. Black crosses (x) are samples that did not cluster.

Quantitative PCR was used to measure *ZC3H4* expression in MSCs and differentiated adipocytes in 10 individuals who were selected based on their genotype for rs3810291 (5 of each genotype group). The expression of *ZC3H4* in differentiated adipocytes was normalised against *PPAR $\gamma$*  expression, to account for the variation in adipogenic differentiation between donors. There was no significant difference in *ZC3H4* expression between homozygote majors (AA) and homozygote minors (GG) in MSCs or differentiated adipocytes (**Figure 4.13**). However a trend (41% difference in gene expression) between

genotypes was seen in differentiated adipocytes, donors with the GG genotype showed reduced expression of *ZC3H4* (but the standard error was large). When *ZC3H4* expression was not corrected for *PPAR $\gamma$*  levels, the same trend was observed, however the GG genotype showed a smaller decrease of 23% when compared to the AA genotype. In MSCs a trend of a 7% difference in gene expression was observed between genotype groups.

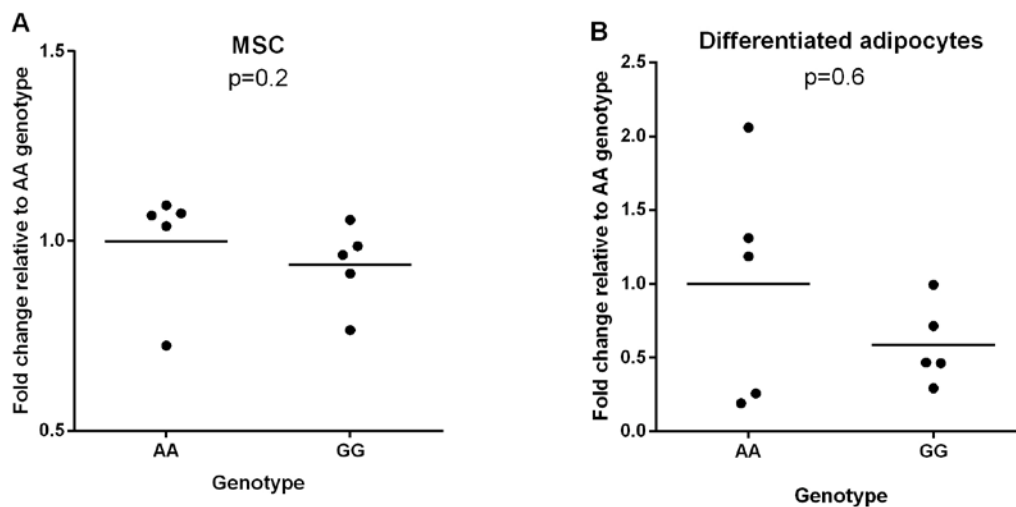


**Figure 4.13. *ZC3H4* expression in homozygote majors (AA) and homozygote minors (GG) for rs3810291.** No effect of rs3810291 on gene expression in (A) MSCs (B) differentiated adipocytes. Samples were normalised to *36B4*. Expression of *ZC3H4* in differentiated adipocytes were further normalised to *PPAR $\gamma$*  to account for variation in adipogenic differentiation. Data was analysed using a Student's t-test (n=5 each genotype group).

A power calculation was conducted on the gene expression data from the 10 donors to determine if the study was adequately powered. The mean and Standard Deviation (SD) was used to calculate the power of the current study, which was 20.03%. A subsequent calculation showed, in order to provide the study with 80% power, 32 donors were required in each genotype group to validate the difference in *ZC3H4* expression seen between homozygote majors and homozygote minors for rs3810291. **Table 4.1** shows that there were 51 donors who were homozygous major, but only 9 donors who were homozygous minor, therefore this study could not be extended.

#### 4.2.5 Analysis of rs4929949 and rs10840106 on *TRIM66* gene expression

In addition to rs3810291, Speliotes *et al.*, (2010) identified 8 other BMI-associated SNPs that affected expression of 17 nearby genes in adipose tissue. Speliotes *et al.*, also noted the most significant SNP (peak SNP) associated with the gene transcript in adipose tissue. I looked at a number of these SNPs to establish if they were present on the Axiom™ Genome-Wide UKB WCGS Genotyping Array, to determine which variants could be investigated in differentiated adipocytes from the MSC bank. rs4929949, rs10840106 and rs713586 were taken forward, as genotype information was available for these variants. rs4929949 (BMI-associated SNP;  $p=0.002$ ) and rs10840106 (peak SNP;  $p=1.1 \times 10^{-71}$ ) were significantly associated with *TRIM66*, rs713586 (BMI-associated SNP;  $p=3.5 \times 10^{-4}$ ) was associated with *POMC* expression even after conditional analyses were performed. The expression of *TRIM66* and *POMC* was investigated in MSCs and differentiated adipocytes. *TRIM66* was expressed in MSCs and adipocytes (**Figure 4.14**). *POMC* was detected at very low levels in both cell types (even after 45 cycles); therefore rs713586 was not taken forward for analysis.

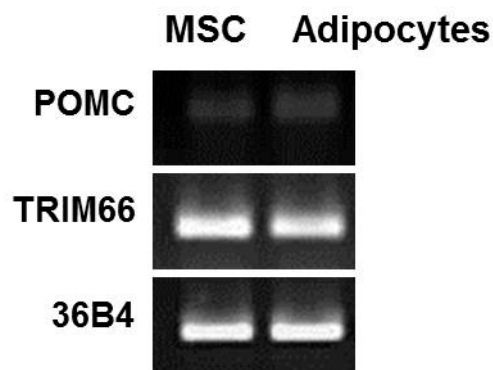


**Figure 4.14. Representative agarose gel electrophoresis of qPCR products for *POMC* and *TRIM66* in MSCs and differentiated adipocytes.** Products were visualised by gel electrophoresis on a 1.5% agarose gel. Lane 1 shows MSCs, Lane 2 shows differentiated adipocytes. Both cells types did not express *POMC* but did express *TRIM66*. *36B4* was used as the housekeeping gene.

MSCs were selected and differentiated based on their genotype for rs4929949 and rs10840106, and *TRIM66* gene expression was analysed by qPCR. Expression of *TRIM66* was normalised to *PPAR $\gamma$*  as described before. Rs4929949 (BMI-associated SNP) did not have an effect on *TRIM66* expression in MSCs and differentiated adipocytes. rs10840106 (peak SNP) significantly associated with *TRIM66* expression in MSCs ( $p=0.0002$ ) and differentiated adipocytes ( $p=0.0002$ ), where homozygote minors (TT) showed a significant increase in expression compared to homozygote majors (CC; **Figure 4.15**).

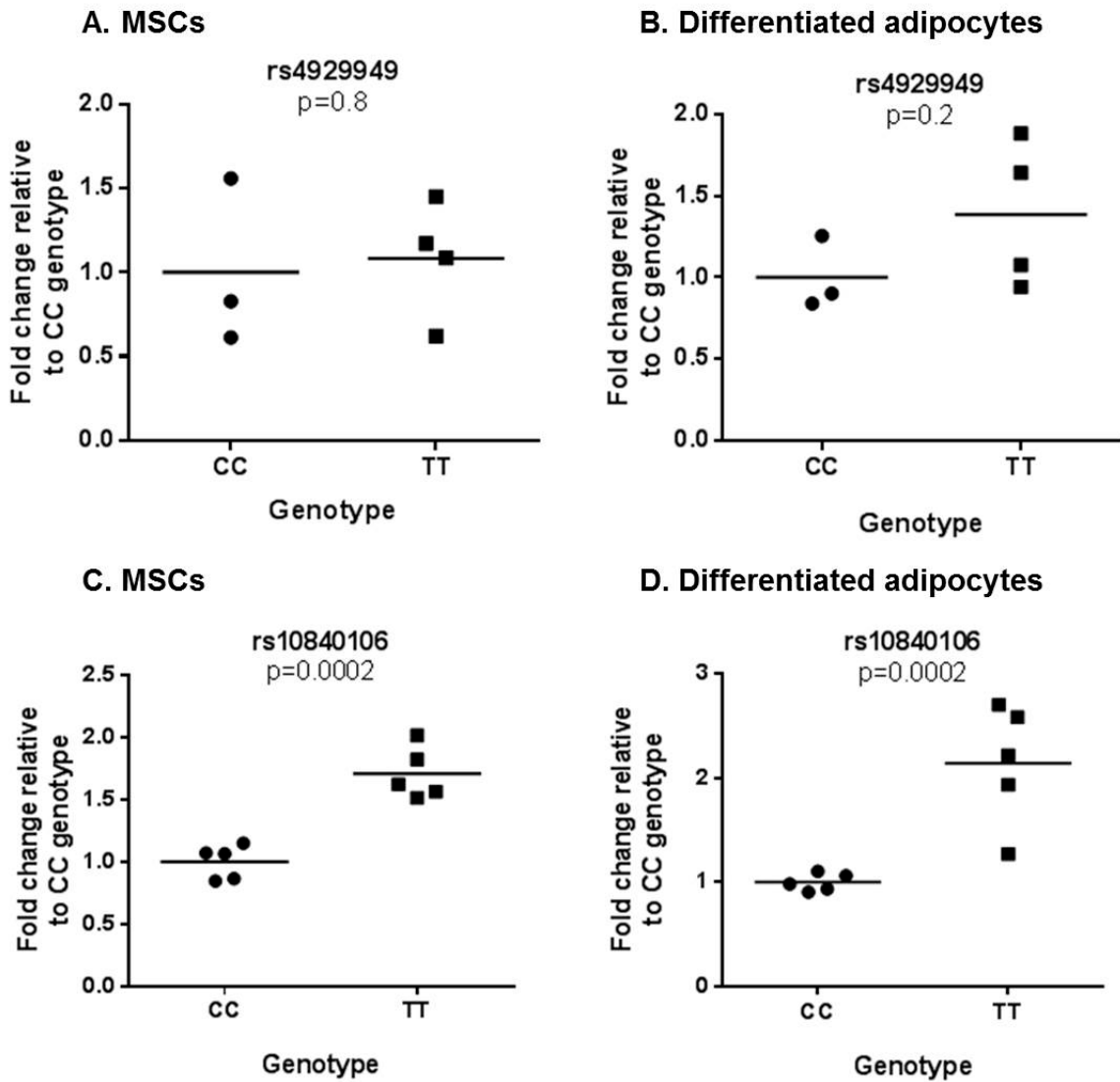


**Figure 4.15. *TRIM66* expression in homozygote (CC) and homozygote minors (TT) for rs4929949 and rs10840106.** No effect of rs4929949 on gene expression in (A) MSCs (B) differentiated adipocytes. Homozygote minors (TT) for rs10840106 showed a significantly increased level of *TRIM66* gene expression in (C) MSCs and (D) differentiated adipocytes. Samples were normalised to *36B4*. Expression of *TRIM66* in differentiated adipocytes were further normalised to *PPAR $\gamma$*  to account for variation in adipogenic differentiation. Data was analysed using a Student's t-test (n=4 and n=5 each genotype group for rs4929949 and rs10840106, respectively).

### 4.3 Discussion

Speliotes *et al.*, (2010) carried out a GWAS to identify additional variants associated with BMI. 18 novel loci were identified, for which they annotated in a gene expression database for adipose tissue to identify eQTLs (Emilsson *et al.*, 2008). For this chapter, advantage was taken of this finding, as MSCs were able to differentiate into adipocytes. So the aim was, as a proof of principle, to use MSC-derived adipocytes to recapitulate the eQTL effect of one of the loci reported in adipocytes.

The ability of MSCs to differentiate into adipocytes was initially characterised in Chapter 3, where differences between donors in the adipogenic differentiation ability were seen. In this chapter the adipogenic differentiation of MSCs was studied in more detail, and attempts were made to quantify the differentiation efficiency. It was hypothesised that the effect of a variant in a small sample size could be quite subtle, and may be masked by variable factors such as the differentiation efficiency. In Chapter 3 and in this chapter, Oil Red O staining was used to visualise the lipid content in MSC-derived adipocytes, as this is the most common staining method used. The absorbance of Oil Red O in a sample can be measured; however this only provides an overall level of the amount of dye in a sample (Platt & El-Sohemy, 2009).

Nile Red is a dye that intercalates with lipid and fluoresces. It was used in combination with flow cytometry, to enable the quantification of lipid within the population. MSC-derived adipocytes were analysed using the flow cytometer, where variation in the percentage of lipid stained cells was seen, ranging from 35.9-47.6%. SS can be analysed using the flow cytometer, it is a measure of a cells' granularity. Adipocytes are more granular than MSCs, as they contain fat (Schaedlich *et al.*, 2010). Overall no difference was seen in SS between MSCs and adipocytes. This may be due to the loss of more buoyant adipocytes during the centrifugation steps before samples were ran on the flow cytometer.

As adipogenic differentiation of MSCs was variable, the next objective was to obtain a pure population of differentiated adipocytes. Unfortunately I did not have access to a flow cytometer with cell sorting capabilities, so cells that were positive for Nile Red could not be separated, to try and obtain a pure

population. Also magnetic bead separation techniques could not be used, as at the time of the experiments there was not a unique cell surface marker for adipocytes. Since Ussar *et al.*, (2014) identified the amino acid transporter (ASC-1) as a specific cell surface protein for human white adipocytes. Using antibodies against this cell surface marker, in conjunction with magnetic beads would provide a unique approach for identifying and separating adipocytes from a population. Alternatively, magnetic beads (MicroBeads from Miltenyi Biotec) are available for MSCs (isolation of CD105 positive cells) which are used to isolate MSCs from bone marrow aspirates. Using this technique to remove MSCs from the differentiated adipogenic population would be inaccurate, as the population is heterogeneous, and most likely consists of a population with a mixture of phenotypes. There may have been cells that produced lipid droplets but still partially expressed MSC cell surface markers. It remains to be addressed at what stage cells lose expression of MSC cell surface markers upon differentiation.

MSC-derived adipocytes could not be separated from MSCs by density centrifugation or ceiling techniques. Both techniques which utilize the buoyancy of adipocytes have often been applied to isolate adipocytes from adipose tissue (Zhang *et al.*, 2000; Ebke *et al.*, 2014; Toda *et al.*, 2009). This finding suggested that MSC-derived adipocytes did not take on a mature phenotype, due to the absence of a significant population of buoyant cells; a property of mature adipocytes. Previous findings have shown MSCs derived from the umbilical cord display a reduced ability to differentiate into adipocytes (Karahuseyinoglu *et al.*, 2007; Bieback *et al.*, 2004; Kern *et al.*, 2006), which may explain why differentiation did not induce mature adipocytes.

There are many approaches which may be utilised to obtain “better” adipocytes to use to study CAD-related genetic variants. In my experiments, I used passage 5 MSCs; however MSCs from a lower passage may have been more suitable to use. It has been shown as passage number increases, the differentiation potential decreases (Kretlow *et al.*, 2008). Secondly, MSCs may have benefited from a longer exposure with the adipogenic differentiation medium, to induce a more mature adipocyte population. Thirdly, over-expression of key drivers of adipogenic differentiation may increase the maturity

and efficiency of differentiation. Inducible expression of *PPARG2* in iPSC-derived mesenchymal progenitor cells produced white adipocytes at high efficiencies (85-90%; Ahfeldt *et al.*, 2012). Fourthly, using adipose-derived MSCs may be a more superior cell source to use. Adipose-derived MSCs have been shown to have a greater ability to differentiate into adipocytes, when compared to MSCs isolated from bone marrow, periosteum and skeletal muscle (Sakaguchi *et al.*, 2005). A limitation of our study is the lack of a positive control; human pre-adipocytes, which can be differentiated into adipocytes, could have been used as a comparison against MSC-derived adipocytes.

Many groups have used MSCs for the study of adipogenesis. These human cell-based models have provided a great insight into the mechanisms of adipogenesis; however they are limited by proliferative potential, reduced differentiation potential with passaging, and inconsistent differentiation potential (Pacini, 2014). The latter is what was observed in our experiments. The MSC population exhibited donor-to-donor and intra-population differentiation heterogeneity, which has also been observed by other groups (Phinney *et al.*, 1999; Phinney, 2012; Russell *et al.*, 2010).

It was demonstrated that adipogenic differentiation of MSCs was variable, and adipocytes could not be separated. So a measure to account for the variability of the adipogenesis of MSCs was sought. *PPAR $\gamma$*  and *FABP4*, are early and late markers of adipocytes, respectively. The increase of *PPAR $\gamma$*  and *FABP4* have previously been shown to mirror the adipogenic development of MSCs (Janderová *et al.*, 2003; Neubauer *et al.*, 2004; Sekiya *et al.*, 2004; Qian *et al.*, 2010). Results demonstrated that upon a 14 day treatment with adipogenic differentiation medium *PPAR $\gamma$*  and *FABP4* expression increased. But for *FABP4* this was not seen in cells across all ten donors. This finding further suggested that the differentiated adipocytes were not mature, or only a small number of adipocytes in the cell population were mature, but not enough to be reflected in the global gene expression. RNA was isolated at one time point (day 14), which may not have been the most suitable time point to analyse *FABP4*, which is one of the best adipogenic markers (Sekiya *et al.*, 2004). A longer differentiation period (21-28 days) may have been required to induce a mature phenotype. As *PPAR $\gamma$*  is an early marker and was consistently

upregulated across all ten donors, this marker was used in subsequent experiments.

The level of *PPAR $\gamma$*  expression of cells from ten different donors did not correlate between Experiment 1, Experiment 2 and Experiment 3. For Experiment 1, overall the fold-change in *PPAR $\gamma$*  expression was higher than for Experiment 2 and 3. MSCs from the same donor and different donors gave different outcomes under identical differentiation conditions, as the same passage of MSCs and seeding density was used. It suggested that adipogenic differentiation was not reproducible. Intrinsic factors (such as the epigenetic state of individual lines) may lead to bias of MSCs from different donors. It has been shown that CpG methylation profiles within and between donors are not uniform (Noer *et al.*, 2007). It is hypothesised that an uneven methylation profile stems at CpG sites as a result of age, health-related factors and environmental factors (Yatabe *et al.*, 2001; Hoffman & Carpenter, 2005). An environmental factor may be the culture conditions MSC are grown and differentiated in. The non-reproducibility of adipogenic differentiation is a novel finding for this thesis, and is an important step in the broader picture of using MSC-derived adipocytes in disease modelling. It highlights the barriers that are needed to be overcome to develop a better cellular model to investigate complex traits/diseases.

As a proof of principle, a BMI-associated variant (rs3810291) was investigated to try and recapitulate its effects on *ZC3H4* expression that were reported by Speliotes *et al.*, (2010). There was no significant effect of the rs3810291 genotype on expression in MSCs and MSC-derived adipocytes. However a trend was observed, homozygote minors (GG) showed reduced *ZC3H4* expression compared to homozygote majors (AA). Where a larger difference (43%) was seen in differentiated adipocytes, compared to MSCs (7%). rs3810291 sits in the 3' UTR of *ZC3H4*, and the minor G allele has been predicted to create a binding site for the mir-502-3p. Mir-502-3p is a microRNA (miRNA), which is a small non-coding RNA that can post-transcriptionally regulate mRNAs at the 3'UTR. Mir-502-3p and *ZC3H4* are both expressed in adipocytes (Estep *et al.*, 2010). It is hypothesised that rs3810291 affects expression, by the binding of mir-502-3p to the minor G allele, to reduce *ZC3H4* expression. It is important to add that Speliotes *et al.*, (2010) annotated loci for

eQTLs in a gene expression database with a large sample size (701 individuals; Emilsson *et al.*, 2008; Zhong *et al.*, 2010), which may have been difficult to replicate in a much smaller sample size (10 individuals). So my study may have benefited from a larger sample size, also indicated by the power calculation that was performed. It showed 32 donors were required in each genotype group for rs3810291 to validate the difference seen in *ZC3H4* expression.

Caution must be taken in assuming that the *ZC3H4* eQTL is the intermediate phenotype between rs3810291 and BMI. As the eQTL with *ZC3H4* was relatively weak ( $p=9 \times 10^{-9}$ ) compared to the association between rs3810291 and BMI ( $p=1.64 \times 10^{-12}$ ).

Two other variants that were significant known eQTLs in adipose tissue were investigated. Speliotes *et al.*, (2010) showed rs4929949 (BMI-associated SNP) had a significant effect on *TRIM66* gene expression, even after conditional analyses on the most significant SNP (peak SNP) for the gene transcript ( $p=0.002$ ). rs4929949 did not significantly affect *TRIM66* gene expression in our cohort. This is mostly likely due to the reduced effect of rs4929949 on *TRIM66* expression, after conditioning on the peak SNP. The most significant SNP for *TRIM66* (peak SNP; rs10840106,  $p=1.1 \times 10^{-71}$  after conditioning on the BMI SNP), showed an increased expression in homozygote minors (TT), compared to homozygote majors (CC) in MSCs and differentiated adipocytes. There was a greater difference in expression between homozygote majors and homozygote minors in adipocytes (2.4-fold) than MSCs (1.6-fold), suggesting the effect of the variant was larger in adipocytes. The direction of the effect was not reported by Speliotes *et al.*, (2010), and a literature search did not reveal any further information. So it was not possible to confirm if the direction of the effect for rs10840106 that I observed was concurrent with the literature. It is of importance to note, that rs10840106 was a significant eQTL for *TRIM66* expression in other tissues apart from adipose. These included blood, omental fat and liver tissue. This suggests that this eQTL is probably not cell-type specific and may explain why I saw a significant genotype effect in MSCs. *TRIM66* is located on chromosome 11p15.4, and its protein has been poorly characterised. It may function as a transcription repressor, which is thought to

be by recruiting deacetylase activity to mediate its repressive effects (Khetchoumian *et al.*, 2004).

When investigating eQTLs, it is important to understand as much about the genetic architecture that affects the gene under investigation. For example, if the variance in gene expression is completely explained by one variant, then recapitulating the effect is an easier challenge. If the variance in gene expression is explained by multiple genetic variants, then recapitulating an effect is a difficult process. A signal will be harder to deduce because of the variable genetic background of different donors, which will produce noise in the experiment. It is likely that the variation in *TRIM66* gene expression is predominantly explained by rs10840106, which is why a significant difference was seen in a small sample size.

#### **4.3.1 Conclusion**

This chapter sought to test the feasibility of using a MSC approach to investigate functional variants identified from GWASs. The aim was to recapitulate the effects of a reported SNP (rs3810291), on *ZC3H4* gene expression in differentiated adipocytes. As the differentiation was variable and not reproducible between and within donors, the separation of differentiated adipocytes was conducted. However, ceiling culture and density centrifugation techniques were not successful and did not enable adipocytes to be separated. So a measure to account for the variability of the adipogenesis of MSCs was sought. *PPAR $\gamma$*  gene expression was used to account for the differences in adipogenic differentiation between donors.

Two additional variants that were reported to affect the expression of nearby genes were investigated. Of the two variants, I was only able to repeat the effects of rs10840106 on *TRIM66* gene expression in MSCs and differentiated adipocytes. This result shows that MSCs and their differentiated counterparts demonstrated a reported association of a genotype effect on gene expression.

# **Chapter 5- Hepatogenic and smooth muscle cell differentiation of MSCs**

## 5.1 Introduction

Large-scale genetic studies have identified many variants associated with CAD. Functional variants that cause phenotypic changes are likely to be tissue specific. For example, it has been hypothesised that some of the risk variants exert their functional effects within the liver (e.g. rs12740374 at 1p13). It has also been proposed that other variants e.g. 9p21 risk variants exert their effects in SMCs. In order to use MSCs to model and study CAD would require their differentiation into functional hepatocytes and SMCs. This chapter describes the differentiation of MSCs into hepatocytes and SMCs.

### 5.1.1 Hepatocytes

The liver is the largest internal organ in the human body. Hepatocytes are the predominant cell type in the liver, as they make up approximately 80% of the total mass (Goyak *et al.*, 2010). The main function of hepatocytes is to metabolise lipoproteins and glucose, and synthesise and detoxify proteins. Hepatocytes are polygonal in shape, and contain a large quantity of organelles that are involved in metabolic and secretory functions. For example, hepatocytes contain smooth and rough endoplasmic reticulum abundantly, in order to synthesise large amounts of protein and lipids for export.

MSCs can be differentiated into hepatocytes *in vitro*. Within the literature there are two general approaches taken by researchers to induce hepatogenic differentiation. The first approach is to expose MSCs to a continuous cocktail of growth factors (Aurich *et al.*, 2006; Kang *et al.*, 2006; Stock *et al.*, 2010). The second approach is a sequential exposure of different growth factors. The latter approach has been reported as a more efficient method, as the treatment mirrors the secretion pattern of growth factors during liver embryogenesis *in vivo* (Duncan, 2000; Kinoshita & Miyajima, 2002; Zaret, 2002).

During the early stage of hepatogenic differentiation using the sequential exposure approach, hepatocyte growth factor (HGF), epidermal growth factor (EGF) and nicotinamide are used. HGF and EGF stimulate hepatocyte functions such as albumin and urea production (He *et al.*, 2003). Also HGF and EGF are

involved in the long term maintenance of human hepatocytes in their differentiated form (Runge *et al.*, 2000). Nicotinamide is involved in the proliferation of rat hepatocytes and appearance of small hepatocyte colonies *in vitro* (Mitaka *et al.*, 1999). It has also been shown to enhance the maturation of fetal liver cells *in vitro* (Sakai *et al.*, 2002). In the maturation stage of hepatogenic differentiation oncostatin M (OSM) and dexamethasone are used. OSM belongs to the IL6 family of cytokines, and aids the progression of hepatocytes to maturity (Schmidt *et al.*, 1995). Dexamethasone induces hepatic nuclear factor 4 (HNF-4) and CCAAT/enhancer-binding protein alpha (C/EBP- $\alpha$ ) expression. These are transcription factors vital for hepatocyte differentiation (Michalopoulos *et al.*, 2003). Insulin-Transferrin-Selenium (ITS) is commonly used throughout the differentiation steps. During the induction step, it maintains the survival of the cells as a monolayer.

#### **5.1.1.1 Markers of hepatogenic differentiation**

Upon hepatogenic differentiation, hepatogenic specific genes are switched on and upregulated indicating the function and state of maturation. Detailed below are the hepatogenic markers used in this thesis.

*AFP* and *CK19* are early markers of hepatogenic differentiation. The *AFP* gene encodes alpha fetoprotein, which is a 70 kDa glycoprotein produced by the liver and the yolk sac, during fetal development (Jiang *et al.*, 1997). *CK19* encodes cyto-keratin 19, a 40kDa protein. It is one of the first proteins detected in primitive hepatic progenitor cells (Nishikawa *et al.*, 2005).

*ALB* and *PCK1* are markers of mature hepatocytes. *ALB* encodes albumin, a 65 kDa serum protein. It is almost exclusively made by liver cells and secreted into the bloodstream. *PCK1* encodes Phosphoenolpyruvatecarboxykinase 1, a 69 kDa cytosolic enzymatic protein. It is highly expressed in the liver and is involved in gluconeogenesis, a process whereby glucose is produced (Tontonoz *et al.*, 1995). There are other genes that can be used as hepatogenic markers such as *CK18* and *CYP3A4*.

### **5.1.1.2 Functionality of differentiated hepatocytes**

Hepatocytes carry out several important functions. Functional assessment can indicate the degree of hepatogenic differentiation, and the quality of the differentiated cells. One of the functions of hepatocytes is to synthesise glucose and store it as glycogen (Bechmann *et al.*, 2012). They can also synthesise urea and coagulation factors, and proteins involved in the inflammatory response (De Bartolo *et al.*, 2006; Pless *et al.*, 2006; Chen *et al.*, 1998). Hepatocytes take up bilirubin, and are also involved in the transport of lipids and cholesterol (Runge *et al.*, 2000; Liu *et al.*, 1999). Hepatocytes detoxify ammonia, so ammonium secretion is another functional marker (Takagi *et al.*, 2000). To be able to induce CYP-dependent monooxygenases involved in drug metabolism is a key functional parameter for adult hepatocytes (Rogiers & Vercruysse, 1993). Measuring any of these processes is vital for indicating the functionality of differentiated hepatocytes.

### **5.1.2 Smooth muscle cells**

SMCs are another cell type of interest to study CAD-related genetic variants in. SMCs are the cellular components found in the walls within numerous tissues around the body, such as the gastrointestinal tract and respiratory tract. SMCs are also found in blood vessels (termed vascular SMCs). SMCs give the vessel wall structure; they surround the endothelial cell layer and regulate the diameter of the vessel through contraction and dilation to maintain blood pressure. SMCs are also involved in other functions such as vascular remodelling during exercise, pregnancy or vascular injury (Owens *et al.*, 2004). SMCs are different from skeletal and cardiac muscle cells, as they differ in contractile protein expression, for example alpha-smooth muscle actin ( $\alpha$ SMA; Owens, 1995).

SMCs occur in two states; contractile and synthetic, and exhibit plasticity as they have the ability to switch between the two states. Contractile and synthetic SMCs exhibit different features e.g. morphology, expression of specific genes, migration and proliferation potential. These features are

dependent on local cues and conditions, for example, cell origin, cell to cell and cell to matrix interactions, and mechanical forces (Owens, 1998). The switch from contractile to synthetic phenotype, involves re-entering the cell cycle and releasing ECM proteins (Owens, 1995; Mahoney & Schwartz, 2005). This switch is involved in the development of vascular diseases such as hypertension and atherosclerosis (Yoshida & Owens, 2005; Beamish *et al.*, 2010).

MSCs are able to differentiate into SMCs. There is evidence that supports the role of MSCs in SMC differentiation *in vivo*. It has been demonstrated that a MSC population are destined to commit to a SMC lineage, which suggests that putative mesenchymal smooth muscle cell progenitors may exist (Kashiwakura *et al.*, 2003). In embryonic development, during angiogenesis, MSCs are recruited to newly formed tubes. Cells differentiate into synthetic SMCs characterised by high proliferation and migration rates and production of ECM proteins (Jain, 2003; Gaengel *et al.*, 2009; Carmeliet, 2003). After birth SMCs take on a contractile phenotype, to play an important role in vessel stabilisation (Dempsey *et al.*, 1994).

The literature suggests transforming growth factor beta 1 (TGF- $\beta$ 1) is the key growth factor to induce SMC differentiation, via the Notch signalling pathway (Kurpinski *et al.*, 2010). TGF- $\beta$ 1<sup>-/-</sup> mice die from vascular defects at E10.5-E11.5 (Dickson *et al.*, 1995). Different groups have taken different approaches using TGF- $\beta$ 1 to induce stem cells into SMCs. A combination of TGF- $\beta$ 1 and heparin has been used on MSC intermediates derived from iPSCs (Bajpai *et al.*, 2012). Alternatively TGF- $\beta$ 1 alone has been used (Gong & Niklason, 2008), or TGF- $\beta$ 1 and ascorbic acid (Narita *et al.*, 2008).

Platelet derived growth factor BB (PDGF-BB) is another growth factor that has been studied for its involvement in SMC differentiation. However its effects on SMC differentiation are inconsistent within the literature. Some groups demonstrate PDGF-BB induces differentiation of MSCs into SMCs (Jain, 2003). Whereas other research groups have shown that PDGF-BB mediates the switch from a contractile to synthetic phenotype, as it decreases SMC

markers expression and increases migration and proliferation of SMCs (Sörby & östman, 1996; Uchida *et al.*, 1996).

### 5.1.2.1 Markers of SMC differentiation

A necessary step when studying cellular differentiation is to determine the upregulation of gene-sets that contribute to the functions of the differentiated cell and the state of maturation. Many different gene markers have been used in studying SMC differentiation. Detailed below are the markers used in this thesis.

Alpha smooth muscle actin ( $\alpha$ SMA) is an early marker of SMCs, and is the first known protein expressed during embryonic development (Frid *et al.*, 1992; Hungerford *et al.*, 1996). It is encoded by the *ACTA2* gene and its protein is 42 kDa. It is the most abundant protein, as it makes up 40% of total protein in SMCs (Fatigati & Murphy, 1984). It is a less specific marker, as it has been found to be transiently expressed in immature skeletal and cardiac myocytes (Ruzicka & Schwartz, 1988; Sawtell & Lessard, 1989). It is also expressed in tumours, and by endothelial cells and myofibroblasts upon treatment with TGF- $\beta$ 1 (Arciniegas *et al.*, 1992; Marotti *et al.*, 1993). Other markers need to be considered, as  $\alpha$ SMA expression is not conclusive by itself.

Smooth muscle protein 22-alpha (SM22 $\alpha$ ) is 22 kDa and is a less characterised protein. It is encoded by the *TAGLN* gene. It is expressed specifically in visceral and vascular SMCs. It is expressed abundantly, and its protein structure is related to calponin (Lawson *et al.*, 1997; Shapland *et al.*, 1993). It induces the development of actin networks. SM22 $\alpha$  has three different isoforms of which the alpha isoform is the most abundantly expressed (Owens, 1995; Faggin *et al.*, 1999).

Calponin expression is a mid-marker and more specific, as it is almost exclusive to SMCs (Owens, 1995). It is encoded by the *CNN1* gene and its protein is 28-34 kDa. Calponin has been proposed to be a regulator of contraction because it interacts with F-actin and tropomyosin, in a calcium

independent manner. It also interacts with calmodulin but in a calcium dependent manner. Calponin has many isoforms, including H-calponin (high molecular weight) and L-calponin (low molecular weight).

Smooth muscle myosin heavy chain (SM-MHC) is a marker for a mature contractile phenotype. It is encoded by the *MYH11* gene. It is exclusive to SMCs, as it has never been identified in non-SMCs *in vivo*. During embryogenesis, SM-MHC is the only specific marker (Miano *et al.*, 1994). Myosin is ~500 kDa and contains two 200 kDa heavy chains and four 15-26 kDa light chains. It consists of two regions; a head and a tail. Myosin uses the tail region to aggregate with filaments and bind with actin. It uses the head region to bind to ATP. For contraction to occur, energy is released from ATP in the form of ADP and phosphate, so myosin can bind to actin, to induce contraction.

Smoothelin is a 59 kDa SMC marker. Smoothelin is also a marker of contractile mature SMCs and is encoded by the *SMTN* gene (van der Loop *et al.*, 1996). There are two major isoforms of smoothelin; Smoothelin A (59 kDa) expressed in visceral SMCs and smoothelin B (110 kDa) expressed in vascular SMCs (Kramer *et al.*, 1999). Knowledge about smoothelin function is limited. To date the literature suggests it is involved in the contractile apparatus (van Eys *et al.*, 2007).

#### **5.1.2.2 Smooth muscle cell contraction**

The main function of SMCs is to contract, which is initiated by the binding of various agonists to cell surface receptors to activate the contraction mechanism. The receptors are coupled to a heterotrimeric G protein, which increases phospholipase C activity. Phospholipase C produces two secondary messengers; inositol triphosphate (IP<sub>3</sub>) and diacylglycerol (DG). IP<sub>3</sub> binds to receptors on the sarcoplasmic reticulum, which causes a release of Ca<sup>2+</sup>. DG and Ca<sup>2+</sup> stimulates protein kinase C (PKC), which results in the phosphorylation of target proteins. Ca<sup>2+</sup> can also enter the cell via receptor-operated Ca<sup>2+</sup> channels. Ca<sup>2+</sup> binds to calmodulin, which together activates

Myosin light-chain (MLC) kinase to phosphorylate the 20 kDa myosin light chain. The myosin light chain interacts with actin and causes cross-bridge cycling to occur, causing the cells to shorten, resulting in cellular contraction (Webb, 2003).

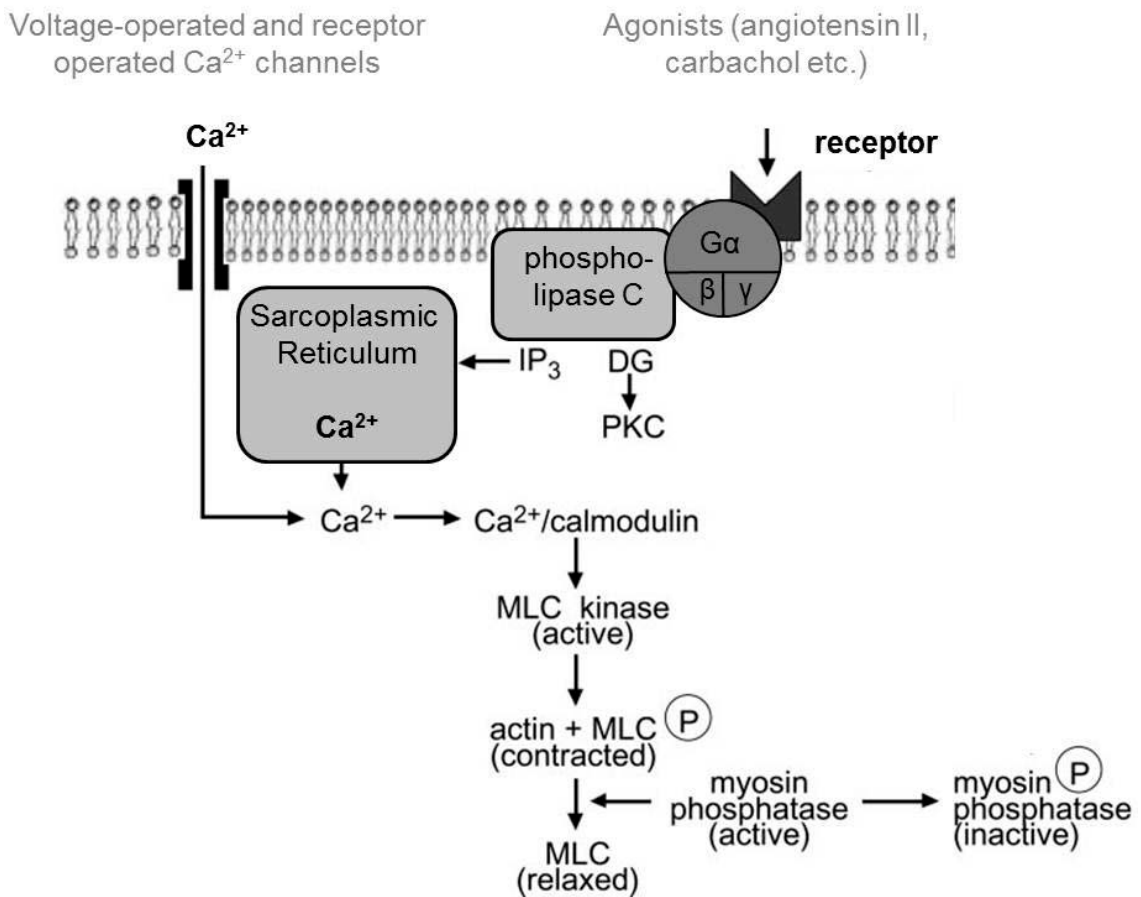


**Figure 5.1. Schematic diagram of the details of contraction** (adapted from Webb, 2003). DG; Diacylglycerol, IP<sub>3</sub>; inositol triphosphate, PKC; protein kinase C, MLC; myosin light-chain.

### **5.1.3 Aims and objectives**

The third aim of this project was to differentiate MSCs into CAD-relevant cell types; hepatocytes and SMCs. The investigation of their morphology and phenotype, upon differentiation was required to determine if MSCs had differentiated.

The objectives were:

- Assess differentiation of MSCs into hepatocytes
  - Determine differentiated hepatocyte morphology
  - Characterise differentiated hepatocytes
- Assess differentiation of MSCs into SMCs
  - Determine differentiated SMC morphology
  - Characterise differentiated SMCs

## 5.2 Results

### 5.2.1 Hepatogenic differentiation of MSCs

#### 5.2.1.1 Morphology

Within the literature there are two general approaches taken by researchers to induce hepatogenic differentiation; 1) continuous exposure to growth factors or 2) a sequential exposure to different growth factors. The latter approach has been suggested as a more efficient method for differentiation, as the growth factor exposure mirrors the secretion pattern during liver embryogenesis *in vivo*. Therefore MSCs were exposed to a sequential exposure of different cytokines. **Figure 5.2** is a schematic diagram of the 23 day method for hepatogenic differentiation. MSCs were seeded at  $1.5 \times 10^4$  cells/cm<sup>2</sup>, to produce a confluent layer of cells after 24 hours. It has been shown that confluency of MSCs is important for the efficiency of the differentiation, to enable cell-to-cell contact for intracellular communication to occur (Lee *et al.*, 2004). The pre-treatment step was serum free, to hinder cell proliferation, prior to induction of differentiation. During the differentiation, half of the wells were treated to a cytokine cocktail mixture without the addition of FBS (referred to as HD+0% FBS). The other half were treated to a cocktail mixture and 1% FBS (referred to as HD+1% FBS). Hepatogenic differentiation took 23 days, which was a prolonged time for cells to be in culture, without subculturing. This is the reason 1% FBS was added, to ensure cells stayed alive.

At day 0, MSCs were 100% confluent and exhibited a spindle-like morphology (**Figure 5.3A and Figure 5.4A**). At day 5, MSCs had been treated to the differentiation medium, where cells displayed a slightly flatter morphology (**Figure 5.3B and Figure 5.4B**). At day 8, cells started to take on a slightly more rounded morphology. During the maturation step (**Figure 5.3D, E and Figure 5.4D, E**), cells appeared more cuboidal, for cells treated with HD+0% FBS. Cells treated to HD+1% FBS had not altered their morphology drastically from their flatter morphology. By day 23, cells began to look like hepatocytes (**Figure 5.3F and Figure 5.4F**). They had a cuboidal appearance, and contained

cytoplasmic granules. Approximately 90% of the population took on this appearance. Cells treated with the HD+1% FBS were more confluent by day 23, yet they still displayed a polygonal shape (**Figure 5.4F**). Overall, MSCs exposed to the 23 day hepatogenic differentiation treatment, altered in morphology from a spindle-like appearance to a cuboidal-like appearance.

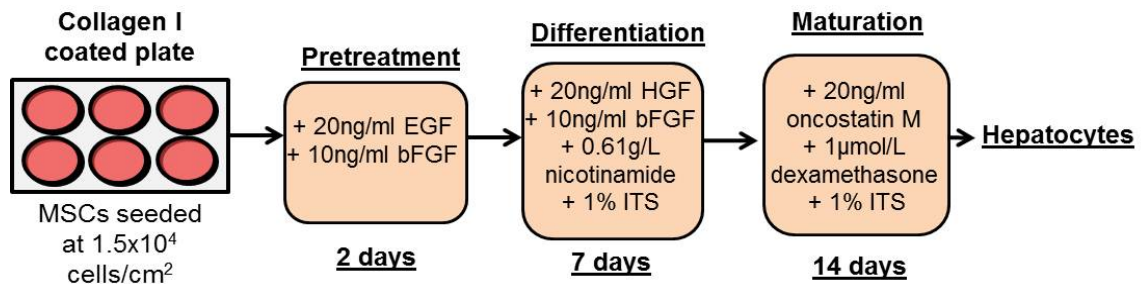


**Figure 5.2. Schematic diagram of the method used for the hepatogenic differentiation of MSCs.**

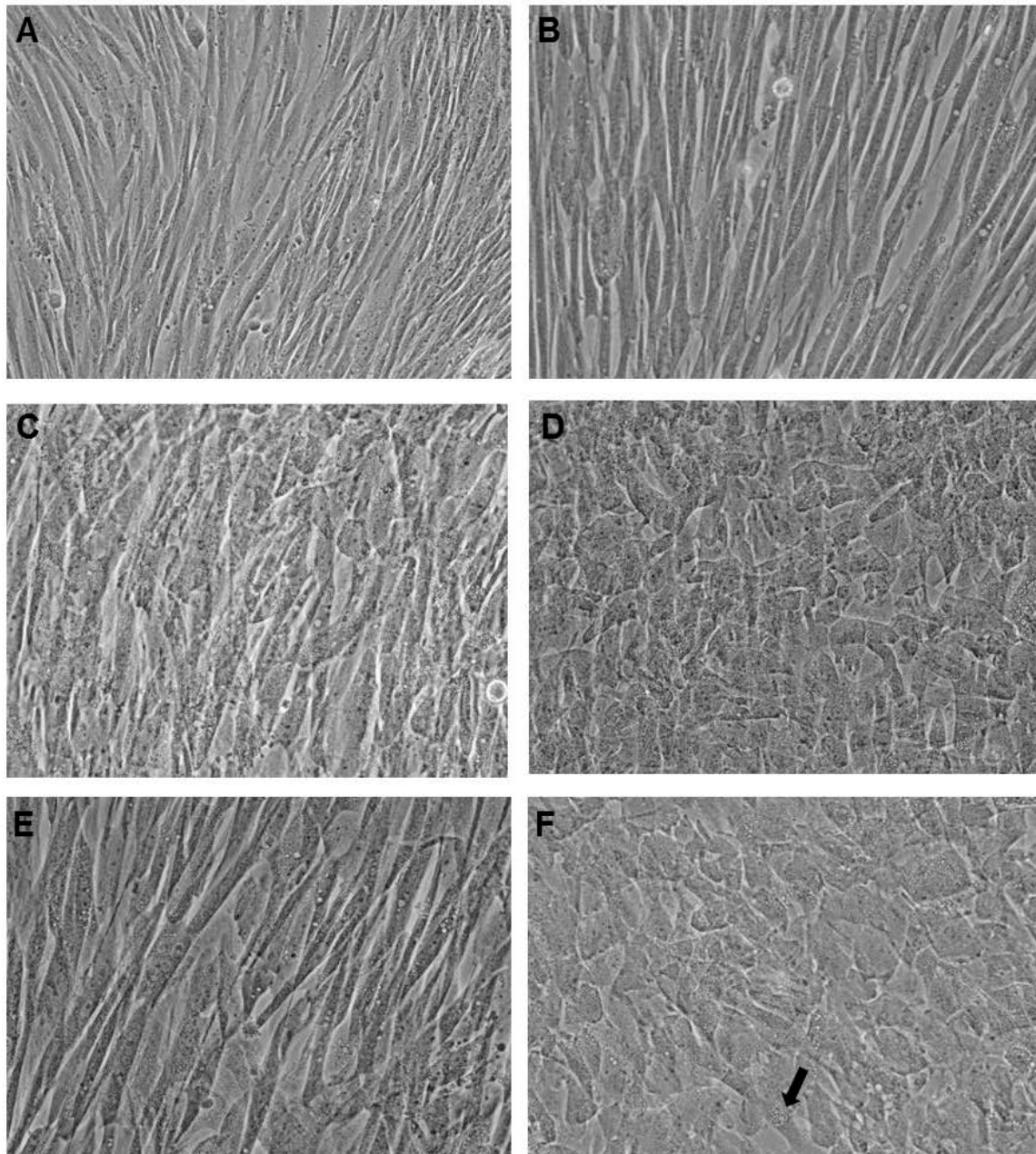


**Figure 5.3. Representative images of the morphology of MSCs treated to hepatogenic differentiation medium with 0% FBS (HD+0% FBS).** (A) Day 0; MSCs exhibited a fibroblast-like morphology (B) Day 5; cells displayed a flattened morphology (C) Day 8; cells altered to a polygonal appearance (D, E) Day 12 and 18; differentiated cells further took on a cuboidal appearance (F) Day 23; hepatocyte-like cells retained the polygonal shape, and also contained cytoplasmic granules (black arrow; n=3). **Magnification x20.**

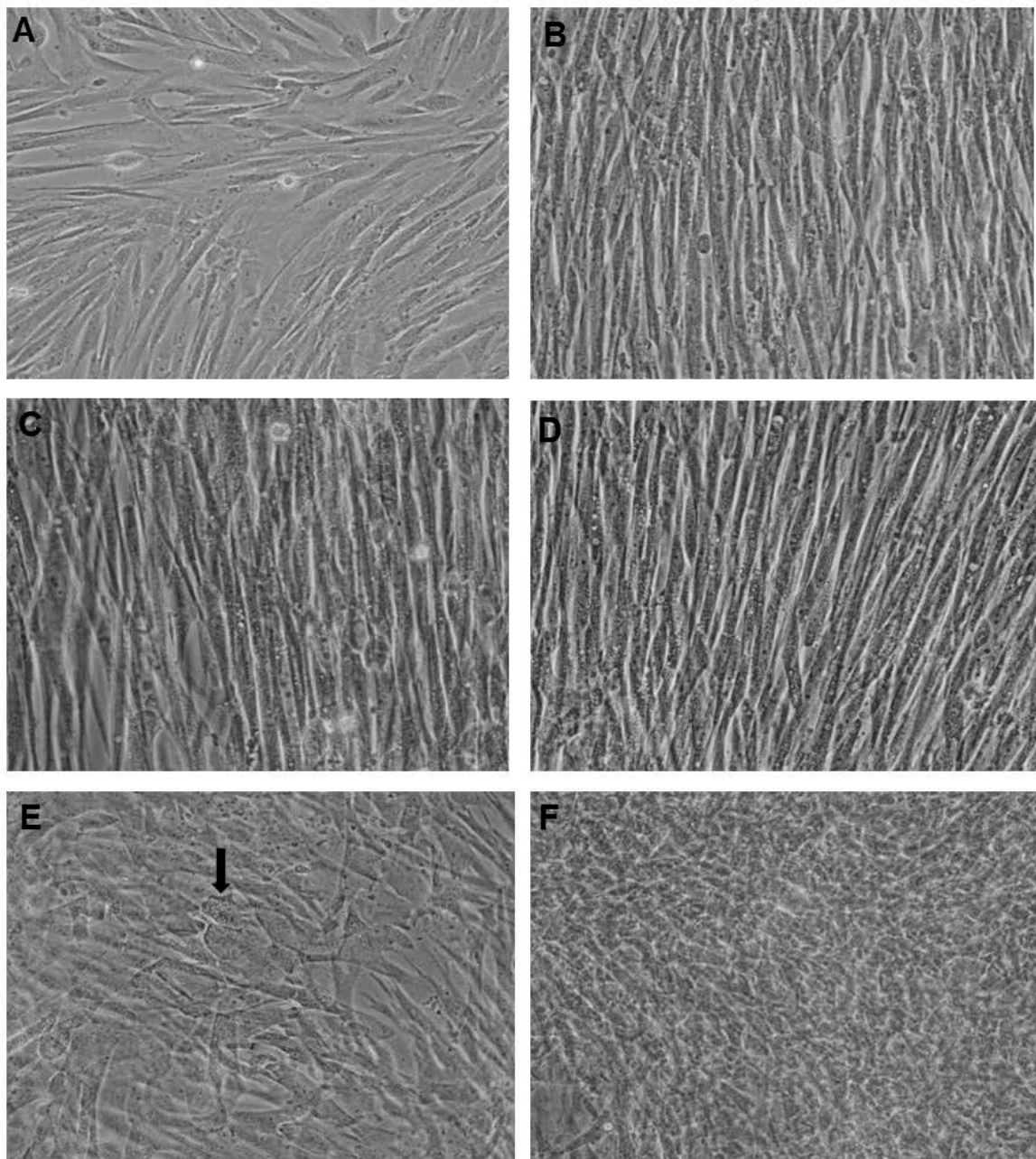


**Figure 5.4. Representative images of the morphology of MSCs treated to hepatogenic differentiation medium with 1% FBS (HD+1% FBS). (A)** Day 0; MSCs exhibited a fibroblast-like morphology **(B, C)** Day 5 and 8; cells displayed a flattened morphology **(D)** Day 12; cells still displayed a rectangular shape **(E)** Day 18; some cells took on a cuboidal appearance containing cytoplasmic granules (black arrow). **(F)** Day 23; cells became very confluent (n=3). **Magnification x20.**

### 5.2.1.2 Gene expression of hepatogenic markers

To investigate if the change in morphology during hepatogenic differentiation was associated with the increase in expression of hepatogenic gene markers qPCR was conducted. The expression of two early and late hepatogenic markers was analysed. Total RNA was extracted at day 23 and cDNA synthesised. Undifferentiated MSCs were used as a control for the differentiation, and HepG2s were used as a positive control. Experiments were carried out on MSCs isolated from Donor 6, 9 and 14, as these were cells that displayed a characteristic cell surface marker expression and differentiated into the three common lineages; adipocytes, chondrocytes and osteoblasts (described in Chapter 3).

MSCs were analysed individually for hepatogenic differentiation treatment (HD+0% FBS or HD+1% FBS). MSCs from Donor 6 showed a ~2 fold increase in *AFP*, but the expression was not at the same level as HepG2s (3314-fold; **Figure 5.5A**). MSCs from Donor 6 did not show an increase in expression for *CK19*, *ALB* and *PCK1* (**Figure 5.5D, G, and J**). Overall MSCs from Donor 9 did not show a large increase in gene expression for *AFP* (1.6-fold), *CK19* (0.37-fold), *ALB* (1.4-fold) and *PCK1* (1.5-fold; **Figure 5.5B, E, H and K**). However MSCs from Donor 14, showed an increase in expression of all four genes. For *AFP*, cells showed an 8.1-fold increase with the HD+1% FBS treatment (**Figure 5.5C**). However, gene expression was not at the same level as HepG2s (5,165-fold). For *CK19*, the HD+0% FBS caused a decrease in expression, but the HD+1% FBS caused a 3.3-fold increase in *CK19* expression, which was equivalent to the expression of HepG2s (3.1-fold; **Figure 5.5F**). HD+1% FBS medium caused a 7.1-fold increase in *ALB* expression; however HepG2s showed an 11,736-fold increase (**Figure 5.5I**). *PCK1* is a late marker of hepatocytes, and was also investigated. Exposure to HD+0% FBS and HD+1% FBS, saw a 12.4-fold and 10.4-fold increase, respectively. HepG2s showed a 31.4-fold change in *PCK1* expression compared to MSCs (**Figure 5.5L**).

In summary, I investigated to see if the expression of hepatogenic marker genes increased upon exposure to hepatogenic differentiation medium.

The expression of MSCs from three different donors was analysed, only cells from one donor showed a clear increase in expression of the four genes upon HD+1% FBS treatment. Yet, they did not express the markers as highly as the positive control, HepG2s.

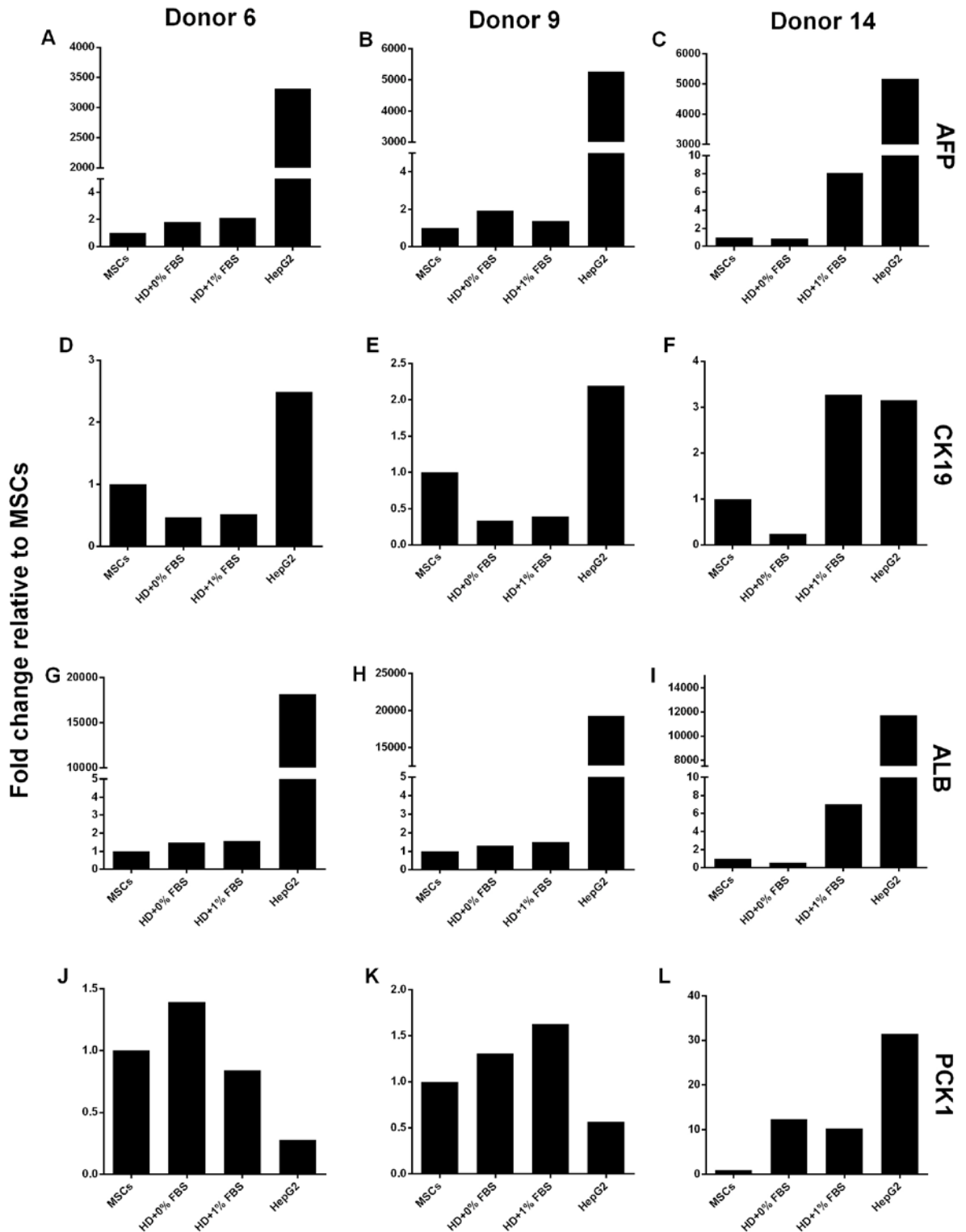


**Figure 5.5. Gene expression of hepatogenic markers upon treatment of MSCs from Donor 6, 9 and 14 with hepatogenic differentiation medium.** Gene expression of (A-C) *AFP* (D-F) *CK19*, (G-I) *ALB*, and (J-L) *PCK1* after the 23 day treatment, demonstrated by qPCR. Untreated MSCs and HepG2s were used as controls. Samples were normalised to  $\beta$ -actin.

### 5.2.2 Smooth muscle cell differentiation of MSCs

Next, the differentiation of MSCs into SMCs was attempted. The literature suggested TGF- $\beta$ 1 is the key growth factor to induce SMC differentiation (Kurpinski *et al.*, 2010). Reduced serum has also been suggested to aid SMC differentiation (Wanjare *et al.*, 2012).

As a preliminary experiment MSCs were seeded at  $8 \times 10^3$  cells/cm<sup>2</sup> onto collagen I coated 6 well plates, and grown until 70% confluency. Collagen Type I has been shown to promote contractile SMCs (Thyberg & Hultgårdh-Nilsson, 1994). Cells were treated to SMC differentiation medium which contained 10ng/ml TGF-B1 and 1% FBS for 12 days. Quantitative PCR was used to measure the expression of *ACTA2*, *CNN1* and *SMTN*; an early, mid and late marker, respectively. After twelve days an increase in gene expression was seen for *ACTA2* (11.1-fold; **Figure 5.6A**), *CNN1* (4-fold; **Figure 5.6B**) and *SMTN* (1.8-fold; **Figure 5.6C**). As an increase in gene expression was observed for SMC markers, a detailed 20 day time course was carried out, to study the gene expression over a longer period of time. Also to determine if a higher level of expression for the mature marker, *SMTN* could be induced.

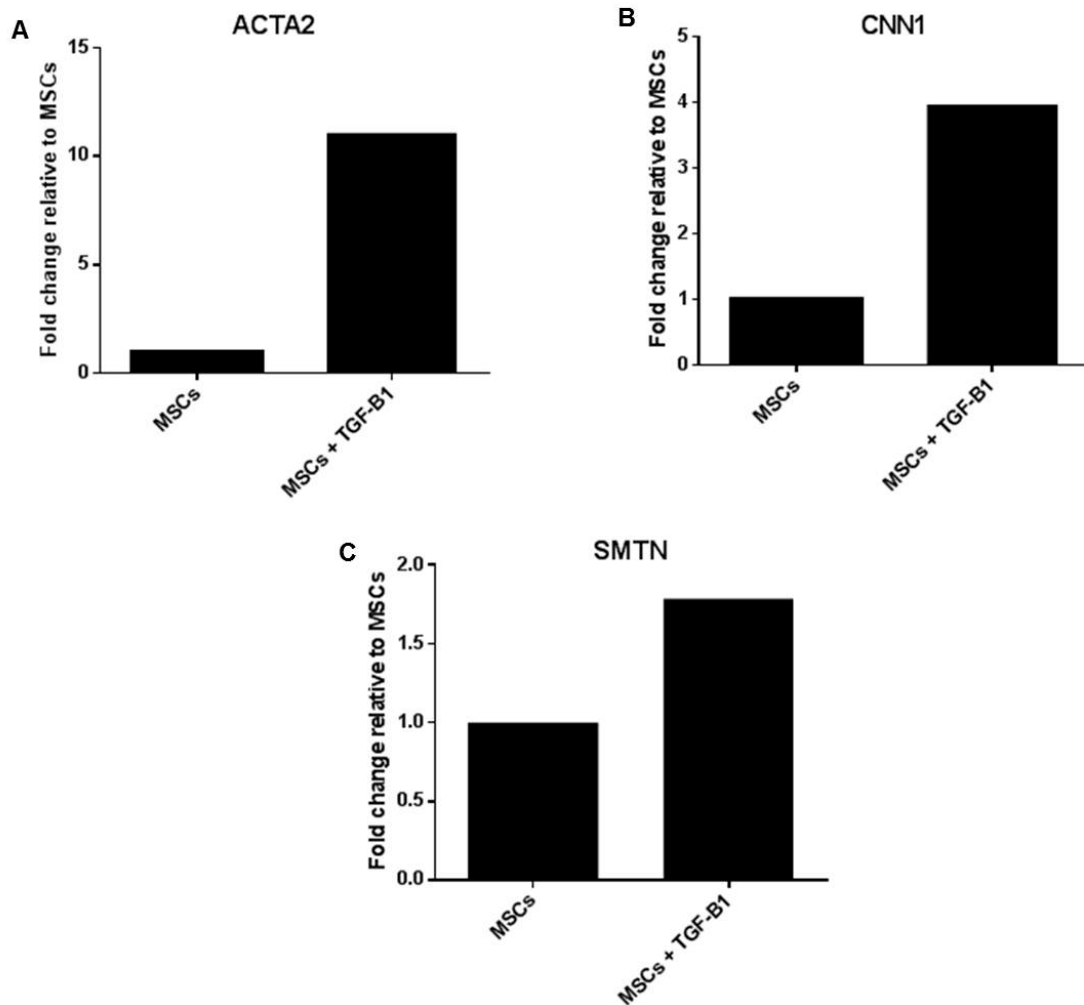


**Figure 5.6. Preliminary experiment: Upregulation of smooth muscle cell markers upon treatment of MSCs with 10ng/ml TGF- $\beta$ 1 and 1% FBS.** Increase in gene expression of (A) *ACTA2* ( $\alpha$ -smooth muscle actin), (B) *CNN1* (calponin) and (C) *SMTN* (smoothelin) during the 12 day treatment, demonstrated by qPCR. Samples were normalised to  $\beta$ -actin (n=1).

### 5.2.2.1 Morphology

As previously stated, MSCs were treated to SMC differentiation medium (containing 10ng/ml TGF- $\beta$ 1 and 1% FBS). The morphology of the cells was documented during the 20 day time course. MSCs at day 0 exhibited a fibroblast-like morphology. Upon treatment to the SMC differentiation medium, the morphology of MSCs altered to that of a more spread-out and myoblast-like morphology. In cells, intracellular fibres were apparent after day 6 (**Figure 5.7B**), which remained until day 20 (**Figure 5.7D**). Cells also became confluent

over this time period. Differentiated cells were split at 1:2 ratio, to observe the morphology more clearly (**Figure 5.8A and B**). Differentiated cell had a larger cell surface area than MSCs. More than 90% of the cells had taken on this morphology. Subculturing the cells also showed that differentiated SMCs appeared to proliferate slowly.

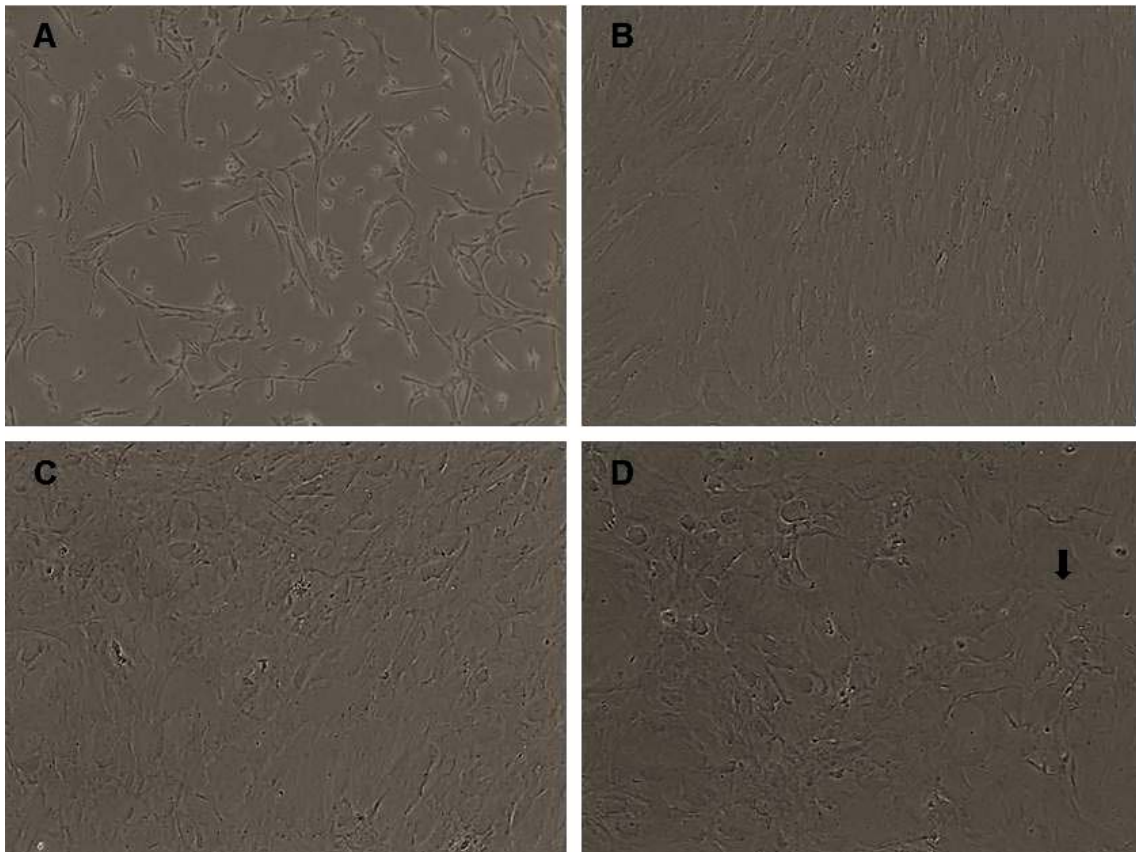


**Figure 5.7. Morphology of MSCs differentiated into SMCs. (A)** Day 0; MSCs exhibited a fibroblast-like morphology (**B-D**) Day 6-20; differentiated cells displayed intracellular stress fibres (indicated by black arrow). **Magnification x20.**

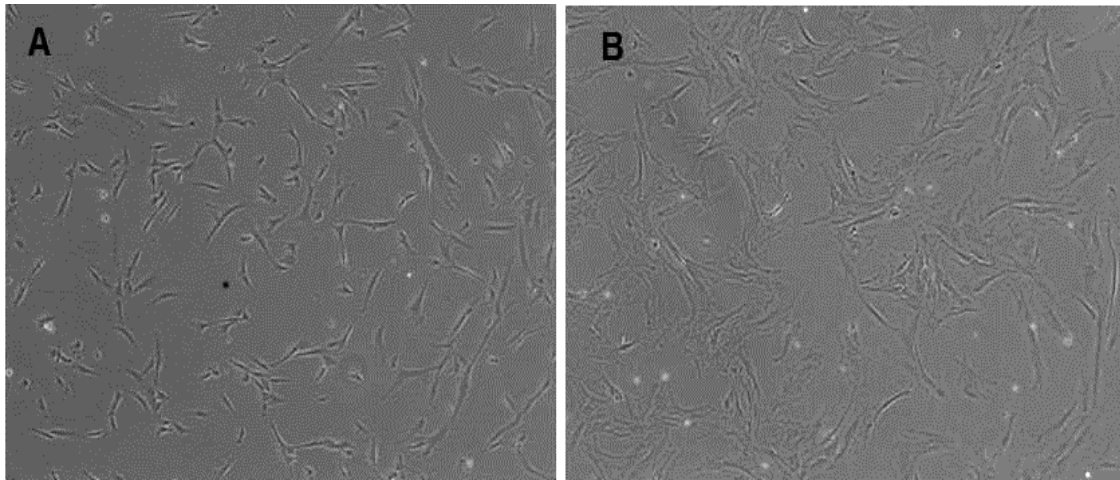


**Figure 5.8. Morphology of MSCs differentiated into SMCs after 1:2 split.** (A) MSCs displaying fibroblast-like morphology (B) differentiated SMCs, more spread out morphology with appearance of stress fibres. **Magnification x20.**

#### 5.2.2.2 Gene expression of SMC markers

To quantify the effects of TGF- $\beta$ 1 on MSCs, and the induction of SMC differentiation, qPCR was used to measure the expression of SMC markers. *TAGLN* and *MYH11* were also analysed, in addition to *ACTA2*, *CNN1* and *SMTN* which were used in the preliminary experiment. MSCs were used as a control. After a 3 day treatment with SMC differentiation medium, qPCR showed an increase in expression of *ACTA2* (18.8-fold; **Figure 5.9A**), *TAGLN2* (4.1-fold; **Figure 5.9B**) and *CNN1* (7.2-fold; **Figure 5.9C**). *ACTA2*, *TAGLN* and *CNN1* are early and mid-markers of SMCs and their upregulation remained constant from day 3-20. Aortic SMCs (aoSMCs) were used as a positive control. Differentiated SMCs showed similar levels of expression as aoSMCs for *TAGLN2*. However, for *ACTA2* and *CNN1* differentiated SMCs showed higher levels than aoSMCs. Aortic SMCs were used at P5 and above. Next the gene expression of two SMC late markers; *SMTN* and *MYH11* were investigated. MSCs treated to SMC differentiation medium did not show an increase in expression of *SMTN* or *MYH11* (**Figure 5.10A and B**). The expression of Kruppel-like factor 4 (*KLF4*), which is a good indicator of stem cell-like capacity, was also investigated. After day 3, cells showed a 3.7-fold decrease of *KLF4*

gene expression. After day 6, cells showed a 6.5-fold decrease, which remained constant until day 20 (**Figure 5.11**).

Bajpai *et al.*, (2012) showed that when iPSCs were differentiated to SMCs through MSC intermediates, using different SMC medium compositions, TGF- $\beta$ 1 (10ng/ml) and heparin (30 $\mu$ g/ml) induced the highest expression of the late marker *MYH11*. Therefore heparin was added to the SMC differentiation medium to see if the expression of one of the late markers (*SMTN*) could be induced. *ACTA2* and *CNN1* increased in expression at day 3, showing a 2.2-fold and 2-fold increase, respectively (**Figure 5.12A and B**). However at day 6, *CNN1* decreased in expression to 1.4-fold. *SMTN* did not increase in expression over the 20 day time period (**Figure 5.12C**). *KLF4* did not show a clear decrease in expression (**Figure 5.13D**). Treatment with additional heparin to the SMC differentiation medium did not enhance the differentiation, or induce expression of mature SMC markers.

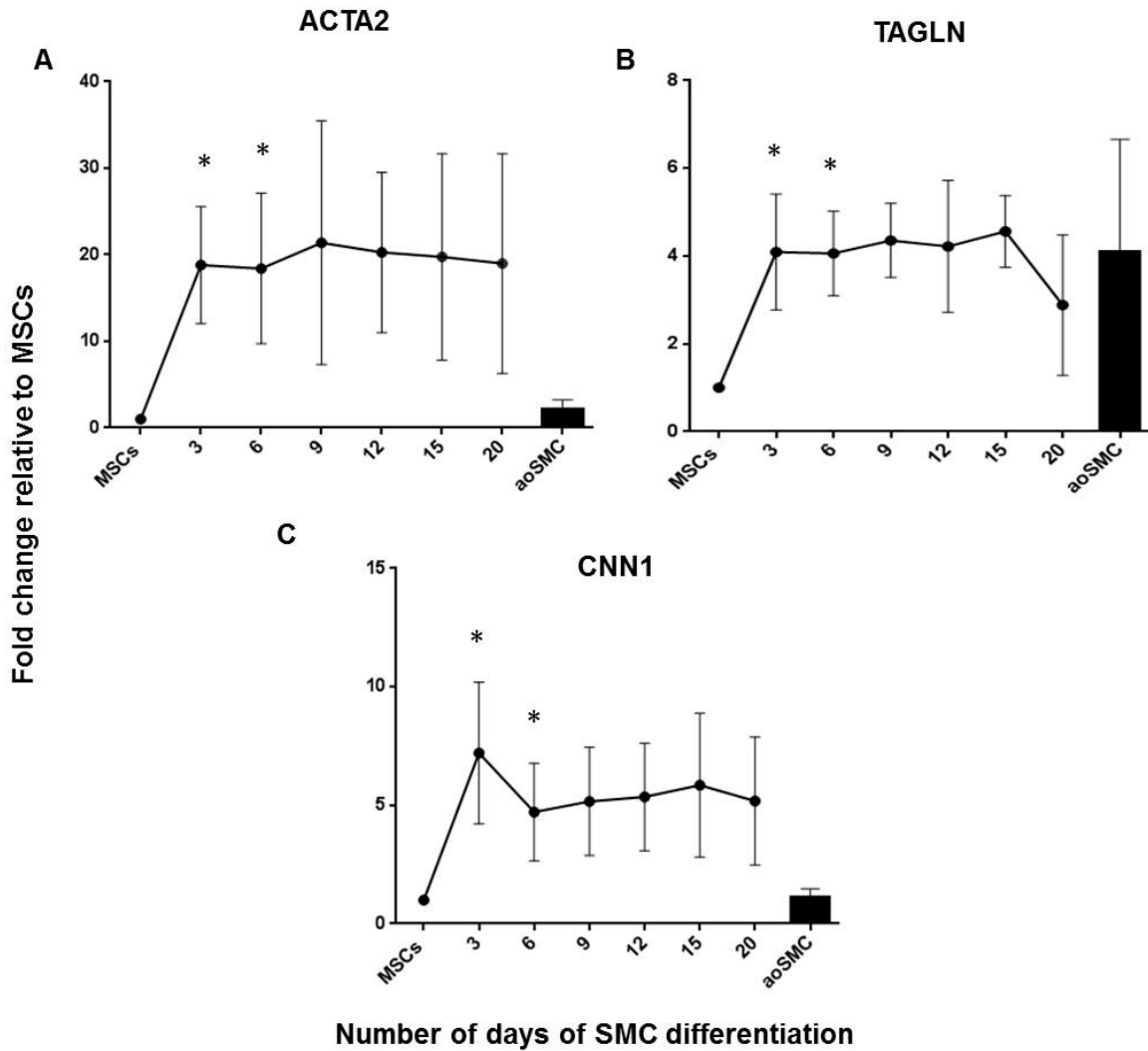


**Figure 5.9. Upregulation of smooth muscle cell markers upon treatment of MSCs with 10ng/ml TGF- $\beta$ 1 and 1% FBS.** Increase in gene expression of (A) *ACTA2* ( $\alpha$ -smooth muscle actin), (B) *TAGLN* (transgelin) and (C) *CNN1* (calponin) during the 20 day treatment, demonstrated by qPCR. Untreated MSCs and aoSMCs were used as controls. Samples were normalised to  $\beta$ -actin. Data is shown as mean  $\pm$  Standard Deviation (SD; n=3). Data was analysed using a Student's t-test (\*p<0.05 vs control cells).

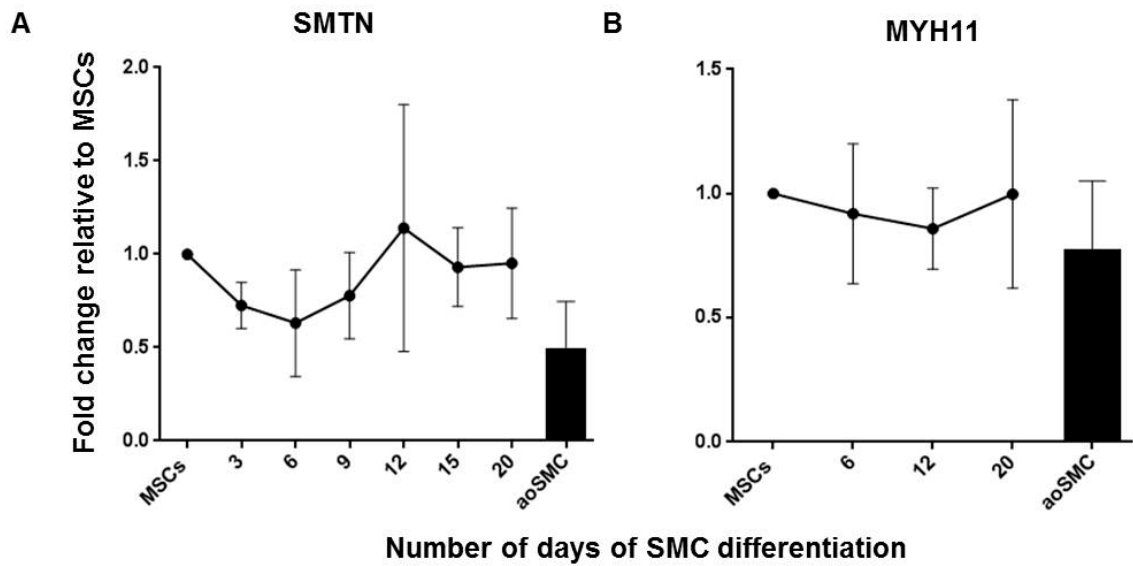


**Figure 5.10. No upregulation of late smooth muscle cell markers upon treatment of MSCs with 10ng/ml TGF- $\beta$ 1 and 1% FBS. (A) *SMTN* (Smoothelin) and (B) *MYH11* (myosin, heavy chain 11, smooth muscle) during the 20 day treatment, demonstrated by qPCR. Samples were normalised to  $\beta$ -actin. Untreated MSCs and aoSMCs were used as controls. Data is shown as mean  $\pm$  Standard Deviation (SD; n=3).**

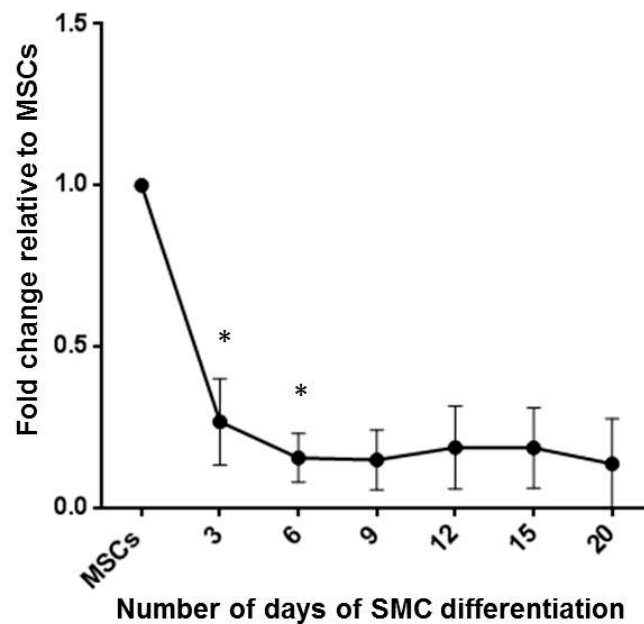


**Figure 5.11. Downregulation of the Kruppel-like factor 4 (*KLF4*) transcription factor. A decrease in *KLF4* expression during the 20 day SMC differentiation treatment with 10ng/ml TGF- $\beta$ 1 and 1% FBS. Samples were normalised to  $\beta$ -actin. Untreated MSCs were used as a positive control. Data is shown as mean  $\pm$  Standard Deviation (SD; n=3). Data was analysed using a Student's t-test (\*p<0.05 vs control cells).**

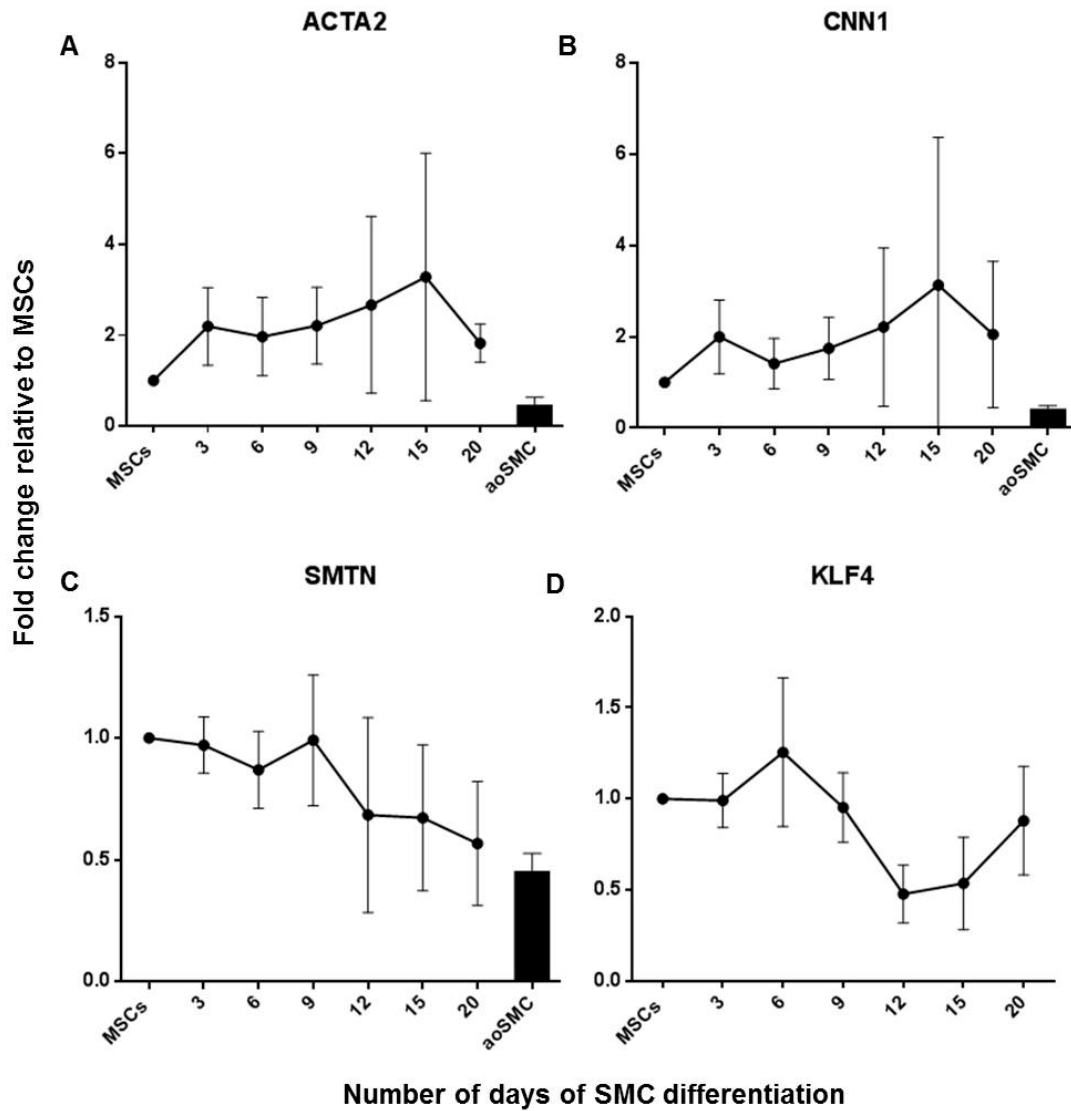


**Figure 5.12. Gene expression of vascular smooth muscle cell markers upon treatment of MSCs with SMC differentiation medium + 30µg/ml heparin.** Gene expression of (A) *ACTA2* (B) *CNN1* (C) *SMTN* and (D) *KLF4* during the 20 day treatment, demonstrated by qPCR. Untreated MSCs and aoSMCs were used as controls. Samples were normalised to  $\beta$ -actin. Data is shown as mean  $\pm$  Standard Deviation (SD; n=3).

### 5.2.2.3 Protein expression of SMC markers

It is important to confirm changes in gene expression at the protein level. The protein expression was analysed by immunofluorescence. Gene expression analysis of SMC markers showed that treatment with SMC differentiation medium for 3 days was significant to induce SMC differentiation. Therefore immunofluorescence of  $\alpha$ -SMA and calponin was carried out at day 3 and 6.

MSCs displayed hardly any expression of  $\alpha$ -SMA and calponin. Upon treatment with SMC differentiation medium, cells stained positively for both proteins (**Figure 5.13 and 5.14**). Protein expression for  $\alpha$ -SMA and calponin was higher at day 6 than day 3, where > 90% of the cells were positive for expression. So all subsequent experiments conducted on differentiated SMCs were done so after a SMC differentiation treatment for 6 days. A negative control was included, where incubation of the primary antibody was omitted.

The analysis of SM-MHC expression was attempted. However a suitable positive control cell was not found to use to optimise the antibody for experiments.

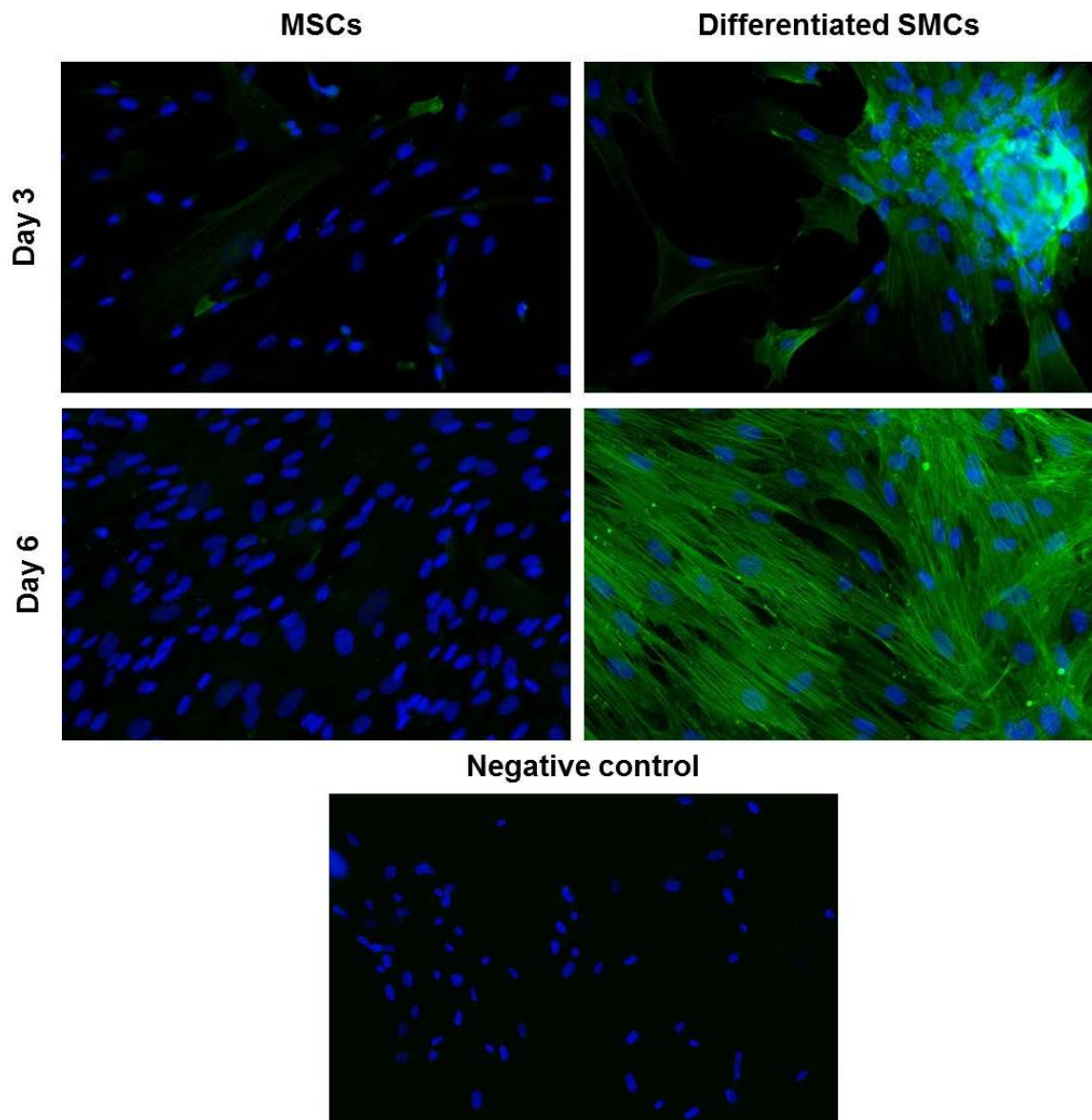


**Figure 5.13. Representative images of immunofluorescence analysis of  $\alpha$ -SMA upon treatment of MSCs with 10ng/ml TGF- $\beta$ 1 and 1% FBS.** Alpha smooth muscle actin ( $\alpha$ -SMA) was expressed in differentiated SMCs after day 3 and 6 of SMC differentiation treatment. Untreated MSCs were used as a negative control. A negative control was included, incubation with the primary antibody was omitted (n=3). **Magnification x20.**

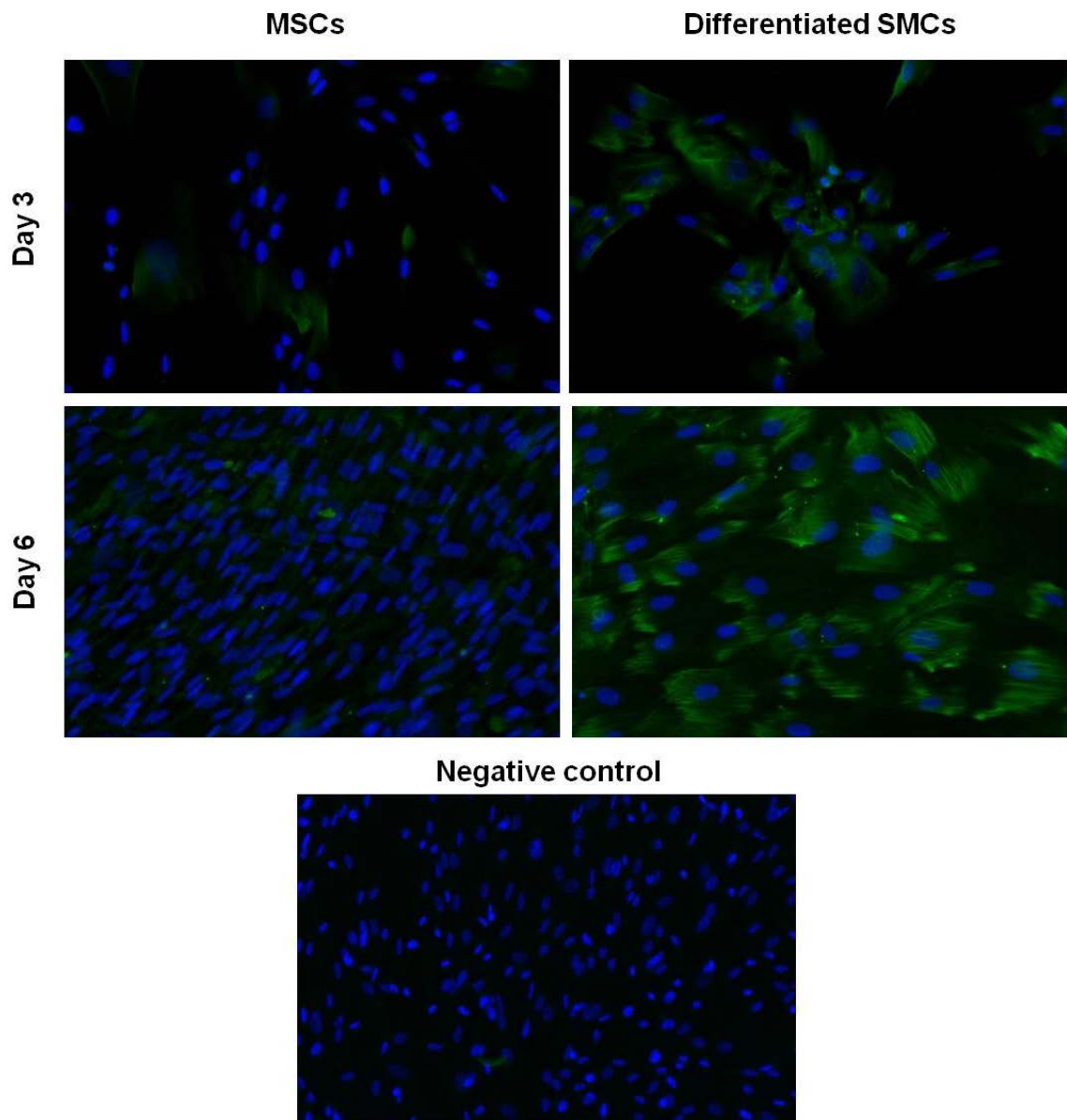


**Figure 5.14. Representative images of immunofluorescence analysis of calponin upon treatment of MSCs with 10ng/ml TGF- $\beta$ 1 and 1% FBS.** Calponin was expressed in differentiated SMCs after day 3 and day 6 of SMC differentiation treatment. Untreated MSCs were used as a control. A negative control was included, incubation with the primary antibody was omitted (n=3). **Magnification x20.**

#### 5.2.2.4 Calcium imaging

Next, the functionality of differentiated SMCs was investigated. The main function of a contractile SMC is to contract. Calcium transients within a cell are an indication of cell contraction, therefore it was sought to investigate this.

Aortic SMCs were used as a positive control to set up the experiment, and to investigate the response to various known agonists and depolarisation agents that induce intracellular calcium signalling. Cells were incubated with Fura-2, a high affinity, intracellular calcium indicator (**Figure 5.15**), and loaded onto a microscope stage into a diamond shaped perfusion chamber, and perfused with Tyrode solution until a steady state was reached. For each recording, aoSMCs were first perfused with Tyrode solution for 1 minute, and then Tyrode solution with the addition of Angiotensin II, Carbachol, or KCl. Angiotensin II induced a single  $\text{Ca}^{2+}$  transient approximately after 60 seconds (**Figure 5.16A**). Carbachol also produced a single  $\text{Ca}^{2+}$  transient after 30 seconds of perfusion with the agonist (**Figure 5.16B**). KCl failed to induce any transients (**Figure 5.16C**). Overall aoSMCs produced clear  $\text{Ca}^{2+}$  transients upon exposure to different agonists.

MSCs and differentiated SMCs were investigated to determine if they were able to produce  $\text{Ca}^{2+}$  transients under the same experimental conditions. Upon Angiotensin II exposure, cells from Donor 6, 9 and Donor 14 showed an effect. MSCs and differentiated SMCs from each donor showed a single  $\text{Ca}^{2+}$  transient approximately 90 seconds after exposure (**Figure 5.17A, 5.18A and 5.19A**). Cells from Donor 9 showed a prolonged de-polarisation upon exposure to carbachol (**Figure 5.18B**). Donor 6 and 14 showed a response to carbachol that was very similar to its response to Angiotensin II (**Figure 5.17B and 5.19B**). KCl was able to induce a response in cells from Donor 9 and Donor 14 (**Figure 5.18C and 5.19C**) and MSCs from Donor 6 (**Figure 5.17C**).

Overall, differentiated SMCs were able to produce clear  $\text{Ca}^{2+}$  transients upon exposure to Angiotensin II, Carbachol and KCl. MSCs were also able to produce calcium transients when exposed to these agonists and depolarising agent.

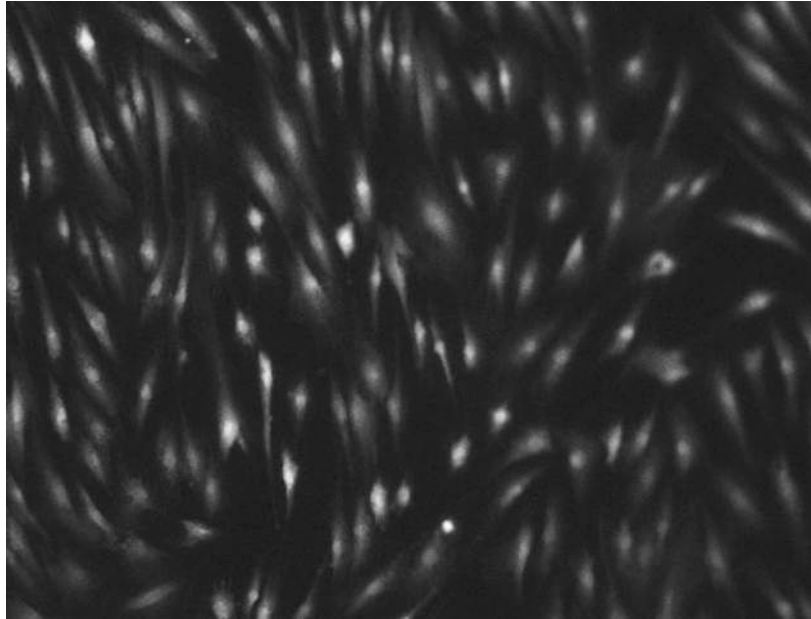


**Figure 5.15. Aortic SMCs loaded with  $\text{Ca}^{2+}$  indicator dye Fura-2. Magnification 10x.**

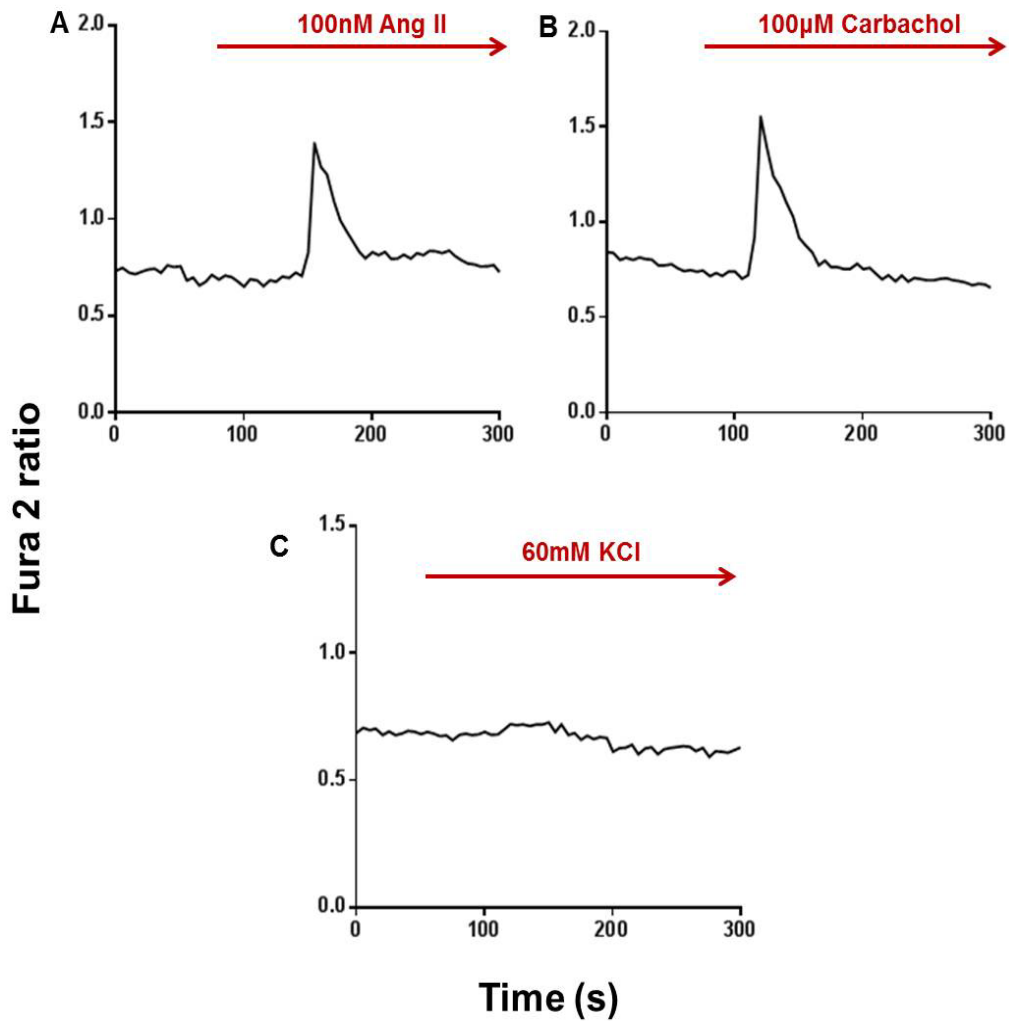


**Figure 5.16. Representative traces of the effects of Ang II, Carbachol and KCl on aoSMCs.** AoSMCs were perfused for 60 seconds with Tyrode solution, followed by perfusion with the agonist. AoSMCs produced  $\text{Ca}^{2+}$  transients in response to (A) Ang II (B) Carbachol. Aortic SMCs did not show a response to (C) KCl (n=10). Ang; Angiotensin.

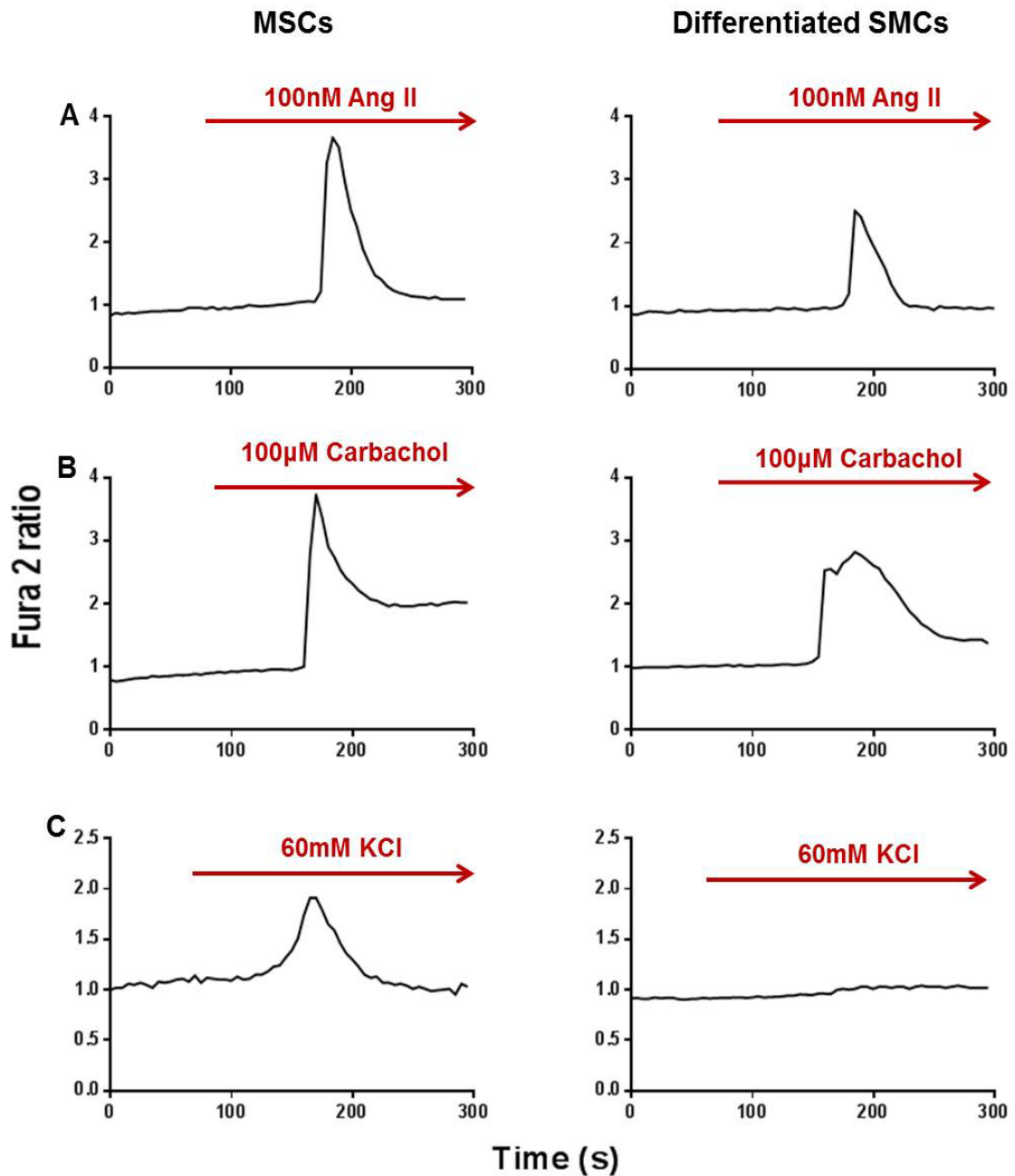


**Figure 5.17. Representative traces of the effects of Ang II, Carbachol and KCl on MSCs and differentiated SMCs from Donor 6.** Cells were perfused for 60 seconds with Tyrodes solution, followed by perfusion with the agonist. Cells produced  $\text{Ca}^{2+}$  transients in response to (A) Ang II (B) carbachol. MSCs produced a response to (C) KCl, however differentiated SMCs did not (n=10). Ang; Angiotensin.

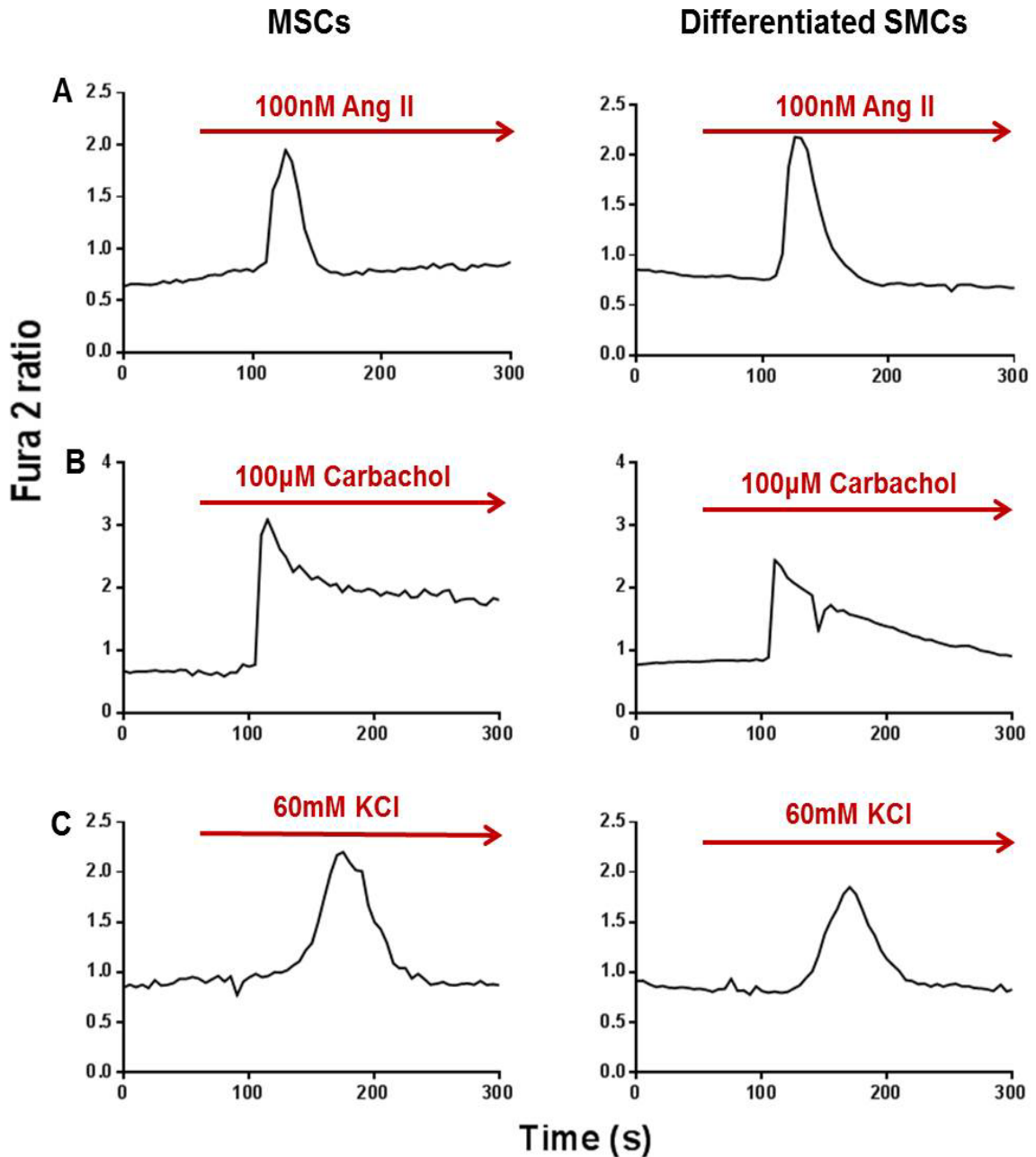


**Figure 5.18. Representative traces of the effects of Ang II, Carbachol and KCl on MSCs and differentiated SMCs from Donor 9.** Cells were perfused for 60 seconds with Tyrode solution, followed by perfusion with the agonist. MSCs and differentiated SMCs produced  $\text{Ca}^{2+}$  transients in response to (A) Ang II (B) Carbachol (C) KCl (n=10). Ang; Angiotensin.

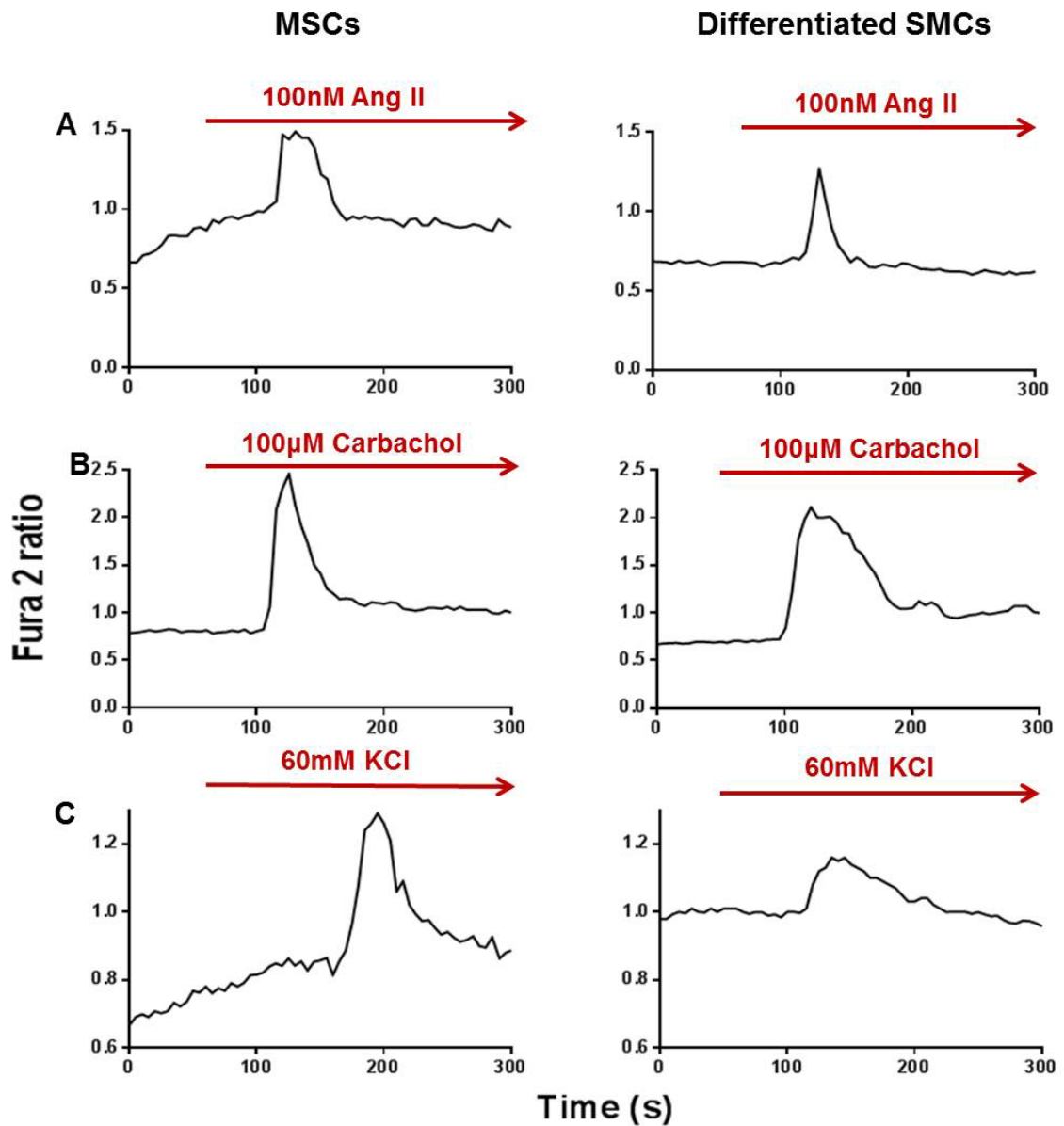


**Figure 5.19. Representative traces of the effects of Ang II, Carbachol and KCl on MSCs and differentiated SMCs from Donor 14.** Cells were perfused for 60 seconds with Tyrode solution, followed by perfusion with the agonist. Cells produced  $\text{Ca}^{2+}$  transients in response to (A) Ang II (B) Carbachol (C) KCl (n=10). Ang; Angiotensin.

### 5.2.2.5 Cell contraction

The production of calcium transients is a prerequisite for cellular contraction. As MSCs and differentiated SMCs were able to give rise to calcium transients, it was investigated to determine if the cells could contract. Aortic SMCs were used as a positive control, and first tested to see if carbachol caused a change in cell surface area, which is a measure of contraction. Aortic SMCs were loaded with calcein AM to determine the cytoplasmic region. Cells were placed onto a Nikon microscope stage with an environmental chamber. Half of the wells seeded with aoSMCs were not treated to an agonist; the remaining wells were treated to 100uM carbachol. Images were obtained before and after treatment. **Figure 5.20A and B** illustrates aoSMCs treated to carbachol showed a response. Image J was used to determine the change in cell surface area. Aortic SMCs showed approximately a 5-10% change in cell surface area upon carbachol treatment (**Figure 5.21**); suggesting carbachol was able to induce cellular contraction. Upon this finding carbachol was used to investigate whether MSCs and differentiated SMCs could contract.

For contraction, HeLa-S3 cells were used as a negative control. Carbachol did not cause HeLa-S3 cells to contract, concluded by no change in cell surface area (**Figure 5.22**). MSCs derived from three different donors were studied, which showed variable responses to carbachol. MSCs from Donor 9 showed no response to carbachol. However, MSCs from Donor 6 and Donor 14 showed a contractile response, as there was a 25% and 10% decrease in cell surface area, respectively. The response was widely variable, as the change in cell surface area for MSCs varied from 0.25% to 49%. Differentiated SMCs from Donor 6, Donor 9 and Donor 14 showed no change in cell surface area, suggesting the cells did not contract (**Figure 5.22 and 5.20C, D**).

Overall the results suggest that MSCs were able to differentiate into immature SMCs. Differentiated SMCs morphologically looked like SMCs. Quantitative PCR results suggest MSCs differentiated into immature SMCs, as they expressed early and mid-markers (*ACTA2*, *TAGLN* and *CNN1*), but not late markers (*MYH11* and *SMTN*). The finding that *KLF4* decreased in expression upon SMC differentiation treatment, suggests MSCs moved away

from a stem cell-like state and towards a defined lineage. Cells displayed certain functional abilities, such as the production of  $\text{Ca}^{2+}$  transients. However, differentiated cells were unable to contract; a characteristic feature of mature SMCs.

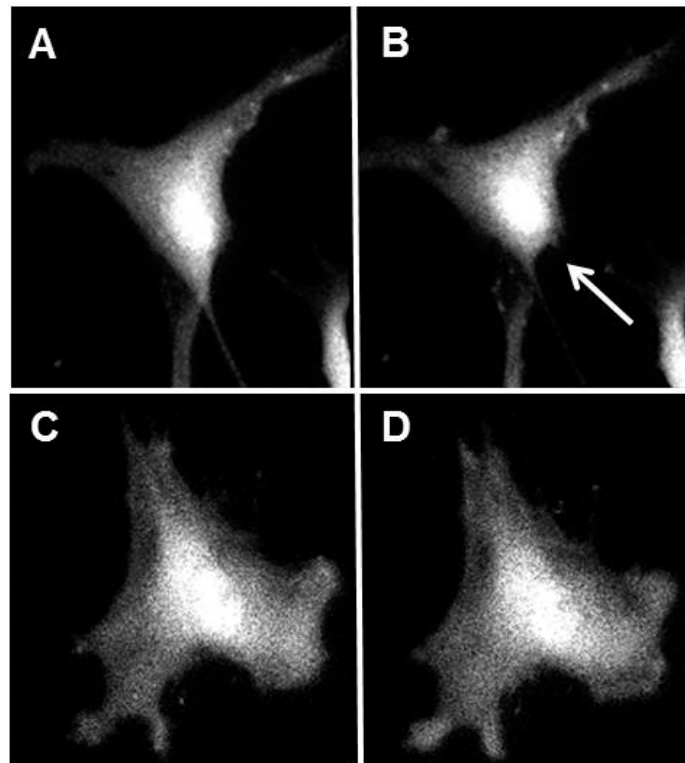


**Figure 5.20. Representative images of the contractile response of aoSMCs and differentiated SMCs. (A)** aoSMCs before and **(B)** aoSMCs after 10 minute 100 $\mu\text{M}$  carbachol treatment. White arrow shows contracted region. **(C)** Differentiated SMCs before and **(D)** after 10 minute carbachol treatment. Differentiated cells did not contract.

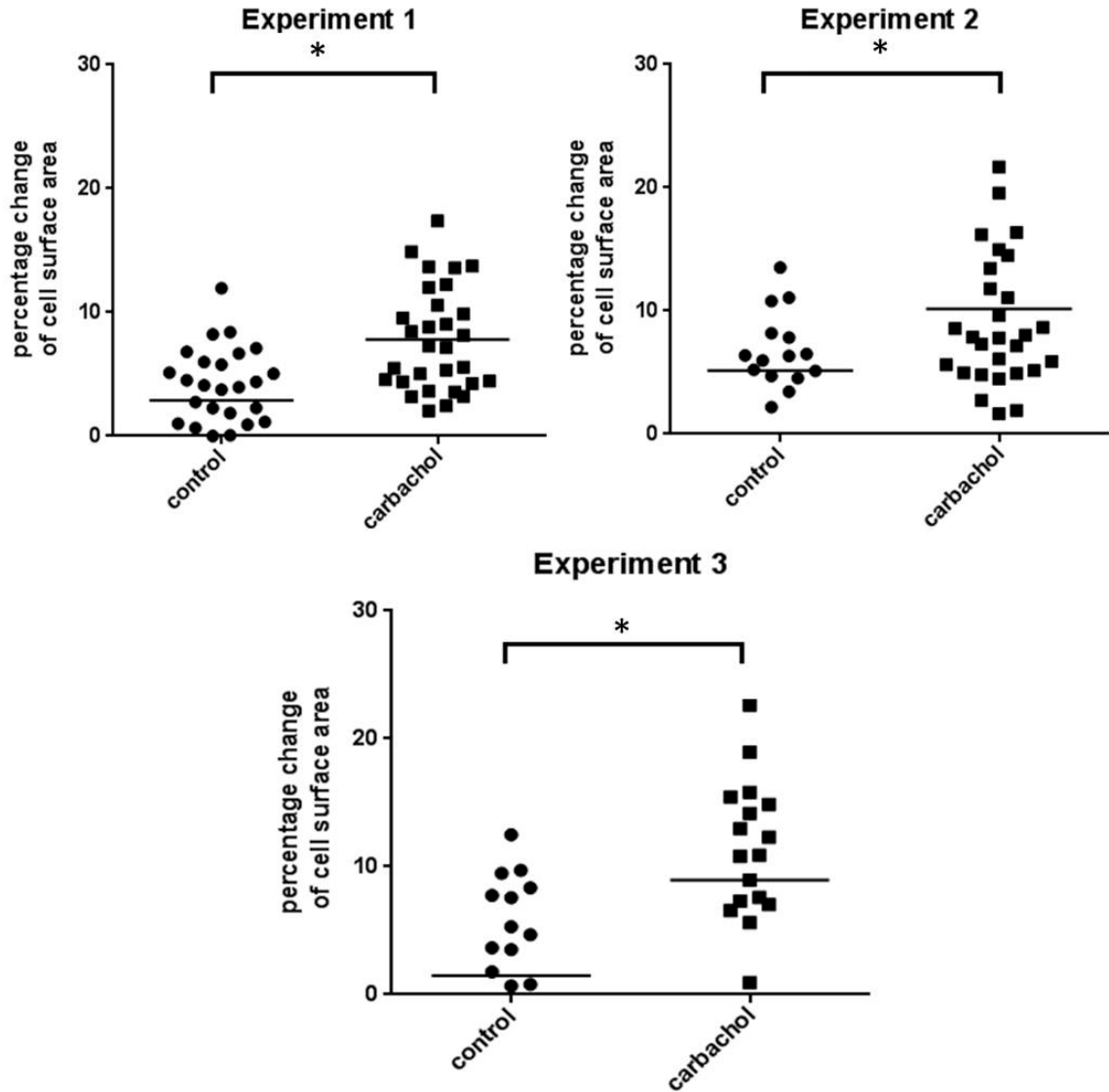


**Figure 5.21. Contractile response of aoSMCs in response to carbachol treatment.** Aortic SMCs displayed a contractile ability upon 100 $\mu$ M carbachol treatment. There was an approximate 10% change of cell surface area after 10 minutes (n=25). Data was analysed using Student's t-test, using untreated aoSMCs as the control (\*p<0.05 vs control cells).

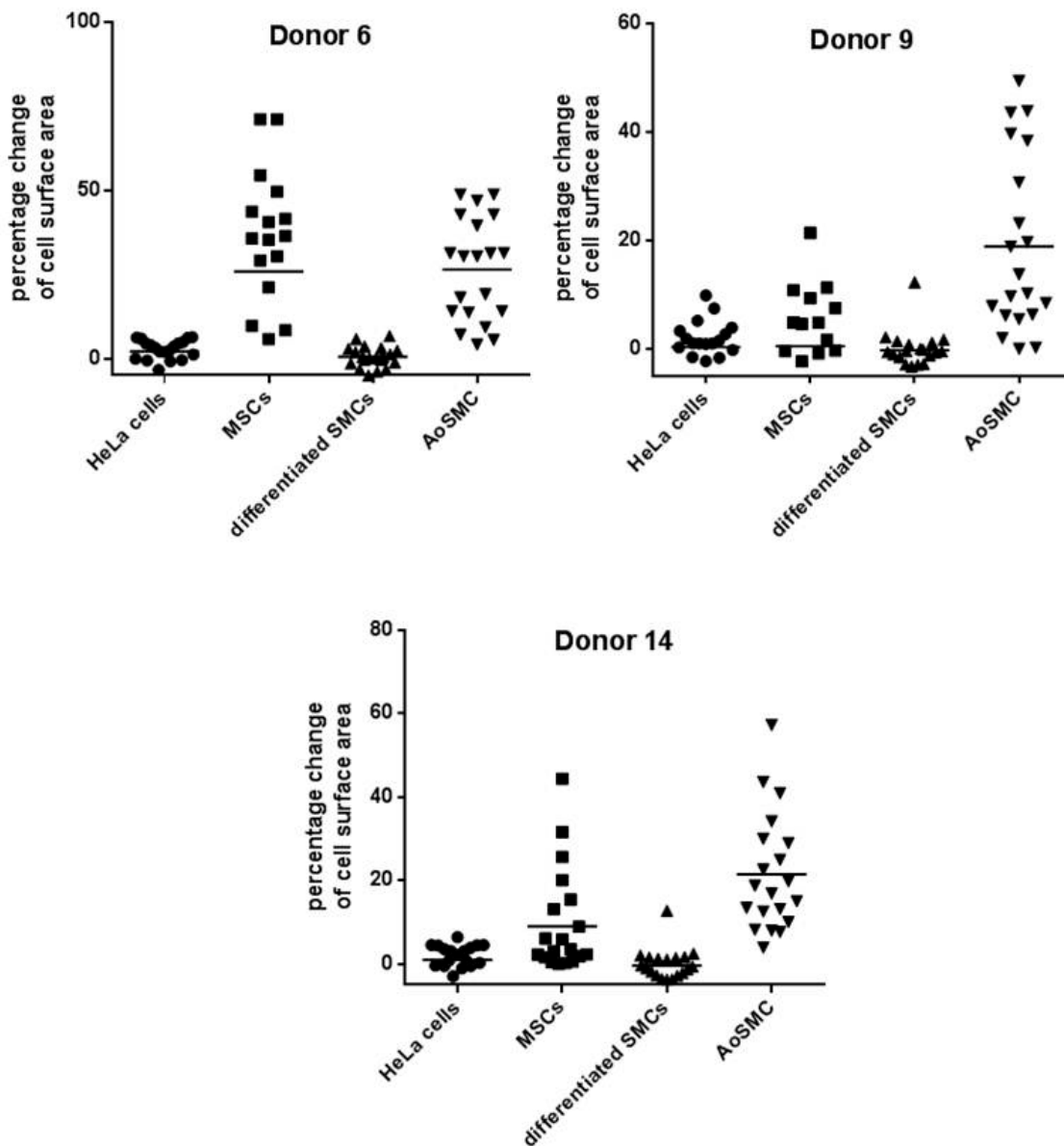


**Figure 5.22. Contractile response of HeLa cells, MSCs, differentiated SMCs and aoSMCs in response to carbachol treatment.** Cells were treated to 100 $\mu$ M carbachol and data analysed after 10 minutes (n=20). HeLa and aoSMCs were negative and positive controls, respectively.

### 5.3 Discussion

To explore the use of MSCs for disease modelling of CAD risk variants required determination of the ability of MSCs, to become CAD-relevant cell types. For a long time, adult stem cells have been thought to have a differentiation potential restricted to their germ layer or tissue of origin. However, recent studies have shown that adult stem cells have a greater potential for differentiation than previously thought. MSCs can differentiate into endodermal-derived cells, such as hepatocytes. This feature makes MSCs an attractive model to use to study CAD-related variants, as many of the risk variants may exert their functional effects within the liver. On this basis, the first objective was to differentiate MSCs into hepatocytes.

The current literature suggested a sequential approach (where cells are exposed sequentially to growth factors and cytokines), was an efficient method as it mirrors liver embryogenesis *in vivo* (Duncan, 2000; Kinoshita & Miyajima, 2002; Zaret, 2002). A method made available by Cyagen Bioscience for their OriCell™ Human Mesenchymal Stem Cell Hepatogenic Differentiation Medium was used. The method did not state the concentrations for each growth factor, so the concentrations reported by Campard *et al.*, (2008) were used, where they differentiated WJ-derived MSCs.

MSCs treated to hepatogenic differentiation medium, after 23 days more than 90% of MSCs had altered in morphology from a fibroblast to a hepatocyte-like appearance. Differentiated cells had become cuboidal, with cytoplasmic granules present. These morphological changes were coincident with existing reports detailing hepatogenic differentiation of MSCs (Lee *et al.*, 2004; Schwartz *et al.*, 2002). Next, it was investigated to see if differentiated cells increased expression of hepatogenic markers to complement the change in the morphology observed. Overall, across MSCs from three different donors investigated, there was no change in gene expression after 23 days. However, upon analysis of individual donors, Donor 14 did show an increase for all four hepatogenic genes investigated, albeit not at the same level as HepG2s (positive control). These results demonstrate that the effect of the hepatogenic differentiation medium was variable between donors. As a consistent

upregulation of hepatogenic markers was not observed, it was very unlikely the cells were functional; therefore cells were not investigated further using functional assays.

One of the initial aims of this thesis was to use MSC-derived hepatocytes to conduct a proof of principle study using one of the most characterised CAD loci. The 1p13 locus associates with CAD (Samani *et al.*, 2007), where the functional variant rs12740374 at this genomic region is responsible for differential expression of *SORT1*, specifically in the liver (Musunuru *et al.*, 2010). It has been shown that the risk variant causes a decrease in *SORT1* mRNA which leads to increased risk of CAD (Musunuru *et al.*, 2010). On this basis, MSCs from genotyped donors for the functional variant rs12740374 (1p13), were going to be differentiated into hepatocytes, to confirm the differential expression of *SORT1* mRNA between different genotypes. Recapitulation of the differential expression in MSC-derived hepatocytes would have demonstrated the ability of MSC-derived cells to model CAD. However as I did not successfully differentiate MSC into hepatocytes, this proof of principle study could not be carried out.

There are many possible reasons why MSCs did not successfully differentiate into hepatocytes. One reason may be because P5 MSCs were used. Stock *et al.*, (2010) found that the potential of MSCs to differentiate into hepatocytes reduced as the cells were passaged, therefore a lower passage may have been required. Yet other researchers have shown no difference in differentiation potential between P5-13 (Lee *et al.*, 2004; Kosmacheva *et al.*, 2011). Donor age has also been shown to affect differentiation potential (Choudhery *et al.*, 2014; D'Ippolito *et al.*, 1999). Neonatal tissue was used; therefore age was not a contributing factor for the lack of differentiation.

The finding that MSCs from Donor 14 showed an increase in gene expression of hepatogenic markers, but Donors 6 and 9 did not, may be due to subtle differences in initial isolation and expansion, even though they all shared the characteristic features of MSCs such as cell surface marker expression and trilineage differentiation. These initial differences may contribute to variations in differentiation potential. For example, the diameter of the umbilical cord varied between donors. When dissecting WJ from thinner umbilical cords, tissue may

have been obtained from regions closer to the umbilical vein subendothelium, in order to obtain a sufficient quantity of tissue. The umbilical vein subendothelium is a different compartment within the umbilical cord to obtain MSCs. This may have caused heterogeneity, as the degree of trilineage differentiation of MSCs from the vein is more variable, than cells from WJ (Mennan *et al.*, 2013). Variation between donors may also be due to the cell microenvironment, which is a difficult factor to fully control. Growth factors and cytokines added to the medium, serum, cell-cell and cell-matrix interactions together play an important role in the specifics of differentiation.

Another reason why MSCs did not differentiate into hepatocytes is the cells may have needed to be cultured in hepatogenic differentiation medium for a longer period of time. Lee *et al.*, (2004) demonstrated it took 6 weeks for differentiated cells to exhibit complete functionality.

There are many differences in differentiation protocols and the initial cell population used. MSCs can be extracted from various tissues, but the main focus for differentiation into hepatocytes has been on bone marrow-derived MSCs (Aurich *et al.*, 2007; Stock *et al.*, 2010; Ayatollahi *et al.*, 2011; Lee *et al.*, 2004). There are reports of successful hepatogenic differentiation using MSCs from the umbilical cord (Kang *et al.*, 2006; Hong *et al.*, 2005; Campard *et al.*, 2008). The protocols detailed in these studies, across the two different sources, have variations in initial cell seeding density, the level of confluency at which to start hepatogenic differentiation, and length of hepatogenic differentiation. In summary, there are many differences in initial cell populations and differentiation protocols; therefore it remains very difficult to decide which protocol is most suitable and efficient.

Our second objective for this chapter was to differentiate MSCs into SMCs. SMCs reside in the vessel wall, and are involved in the disease pathology of atherosclerosis (described in Chapter 1). Many CAD-related genetic loci are thought to be functional in SMCs (e.g. 9p21, 15q25).

TGF- $\beta$ 1 is a cytokine and a member of the TGF- $\beta$  superfamily, which regulate a wide range of cellular processes such as differentiation, proliferation and migration (Massagué *et al.*, 2000; Blobel *et al.*, 2000). The literature

suggests TGF- $\beta$ 1 is the main driver for SMC differentiation where concentrations between 1-10ng/ml have been used (Narita *et al.*, 2008; Kinner *et al.*, 2002; Jeon *et al.*, 2006). 10ng/ml TGF- $\beta$ 1 was used to induce the highest response of differentiation. In the preliminary experiment, gene expression increased for three SMC markers; *ACTA2*, *CNN1* and *SMTN* after a 12 day treatment with SMC differentiation medium. The experiment was extended to 21 days and included the analysis of *TAGLN2* and *MYH11*. An increase in gene expression was observed for early and mid-markers of SMCs. But an increase of two late markers was not detected. Quantitative PCR results suggested MSCs may have become immature SMCs. To further support this data, a down-regulation was seen for a stem cell marker, *KLF4*, suggesting cells had moved away from a stem cell state towards a defined lineage.

Aortic SMCs were used as a positive control for the qPCR experiments. Differentiated SMCs showed SMC marker expression at a greater level than aoSMCs. It has been shown aoSMCs in culture lose expression of SMC-specific markers, as they are passaged (Dorai *et al.*, 2000). This may be the reason why aoSMCs were not expressing SMC genes as highly as the differentiated SMCs.

At the protein level, MSCs barely expressed  $\alpha$ -SMA and calponin, an early and-mid marker, respectively. However, differentiated SMCs did express both proteins, more than 90% of the cell population were positive for expression. The up regulation of  $\alpha$ -SMA and calponin, two contractile proteins suggested cells had contractile properties. The analysis of the late SMC protein marker; SM-MHC was attempted, however a positive control cell was not found, as aoSMCs were negative for expression, therefore SM-MHC analysis was not conclusive.

The primary function of SMCs is to contract. A prerequisite for contraction is the production of  $Ca^{2+}$  transients in the cell. Two different agonists were tested; angiotensin II, carbachol and the depolarisation agent; KCl. Angiotensin II signalling occurs through membrane bound heterotrimeric G-protein coupled receptor (GPCR; Wynne *et al.*, 2009). Carbachol is a muscarinic agonist, which also acts through GPCRs (Billington & Penn, 2002). Both agonists exert their effects on  $Ca^{2+}$  through the same mechanism to

induce contraction (described in **Section 5.1.2.2**). KCl does not use GPCR activation to increase cytosolic  $\text{Ca}^{2+}$ . Instead it activates voltage-gated  $\text{Ca}^{2+}$  channels that cause membrane depolarisation, leading to an influx of  $\text{Ca}^{2+}$  (Bolton *et al.*, 1999).

It was found that differentiated SMCs had the ability to produce  $\text{Ca}^{2+}$  transients upon exposure to carbachol, angiotensin II and KCl. MSCs were also able to produce  $\text{Ca}^{2+}$  transients, suggesting MSCs expressed GPCRs and voltage-operated  $\text{Ca}^{2+}$  channels. Time-lapse microscopy was subsequently used to determine the contractile response, by measuring the change in cell surface area upon exposure to carbachol. Aortic SMCs were able to contract. MSCs showed a variable response to carbachol, which may be because MSCs are highly motile. It may have been necessary to measure the change in cell surface area of MSCs in the absence of carbachol, or use cytochalasin D which is an inhibitor of cellular contraction, to determine if the change in cell surface area observed was a result of cell movement as opposed to cell contraction. Lastly differentiated SMCs did not show a change in surface area, and therefore did not contract, further suggesting that they were immature SMCs.

Overall, the results suggest it was possible to differentiate MSCs into SMCs, albeit immature. An upregulation of early and mid-markers, but not late markers of SMCs was demonstrated. Other researchers' attempts to differentiate MSCs towards the SMC lineage, report upon stimulation, the upregulation of early and mid-markers, but not late markers of SMCs (Gong & Niklason, 2008; Narita *et al.*, 2008). These findings together suggest that MSCs may not have the ability to become fully mature SMCs. An alternative explanation is that an additional signal(s) may be required to push cells to maturity (discussed in **Section 5.3.1**). Differentiated SMCs produced  $\text{Ca}^{2+}$  transients; suggesting cells obtained GPCRs and voltage-operated  $\text{Ca}^{2+}$  channels. However, the complete contraction mechanism was not initiated, as cells did not contract.

The multipotency of MSCs may be the explanation for the lack of differentiation to a mature SMC. MSCs are able to differentiate into multiple, but limited cell types (Can & Karahuseyinoglu, 2007; Pevsner-Fischer *et al.*, 2011).

Whereas iPSCs and ESCs are pluripotent and can differentiate into any cell of the embryo proper, possessing a higher differentiation potential. It has been reported, that as MSCs are passaged, their differentiation potential is reduced. For these experiments P5 MSCs were used, which may be the reason why a mature population was not obtained. Chapter 3 and 4 describe the differentiation of MSCs into adipocytes, where similar results were observed, as the majority of MSCs differentiated into adipocytes did not take on a fully mature phenotype.

To use differentiated SMCs to model CAD requires high efficiency and good quality cells after the differentiation process. The experiments carried out produced differentiated SMCs that expressed early and mid-markers at variable levels during qPCR. Yet protein analysis, suggested MSCs differentiated with a more equal efficiency, as approximately 80-90% of cells expressed  $\alpha$ -SMA and calponin in cells from three different donors. Morphologically cells looked healthy, and still had the capacity to proliferate, albeit slowly. These findings illustrate MSCs may be a valid cell type to use to study CAD, if mature differentiated SMCs could be obtained.

### **5.3.1 Future work**

Hepatocytes are of endodermal origin whereas MSCs are derived mainly from the mesodermal lineage, and may require the modulation of MSC fate to effectively differentiate MSCs into hepatocytes. Ball *et al.*, (2014) have demonstrated by perturbing PDGF receptors or fibronectin, caused MSCs to revert towards a more multipotent state. This method could be applied to take MSCs back to a mesenchymoangioblast-like state, and then differentiate cells into hepatocytes, using a sequential differentiation.

Researchers have also taken other approaches than using the sequential differentiation method to commit MSCs to a hepatogenic lineage. Stock *et al.*, (2010) used a single step procedure, but initiated differentiation using a demethylation step with 5'-azacytidine. DNA demethylation is a major determinant during embryonic development and somatic cell reprogramming

(Wu & Zhang, 2010). So exposure to a demethylating agent should allow for a more efficient conversion to a differentiated cell type. Prasajak & Leraanansaksiri (2013) took a different approach to induce hepatogenic differentiation, by using a hypoxic environment, in addition to a two-step treatment. The hypoxic conditions resemble the normal microenvironment *in vivo*. They reported more than 80% of MSCs successfully differentiated into functional hepatocytes.

MSCs and SMCs are both of mesodermal origins, perhaps explaining why it was possible to differentiate MSCs into immature SMCs, as MSCs were more readily able to differentiate into cells of the same origin. Future work, for SMC differentiation should focus on producing mature contractile SMCs. This may include using additional growth factors in the differentiation medium such as PDGF-BB. The literature still remains controversial about the effects of PDGF-BB on SMC differentiation. However, some groups have shown it induces cells into SMCs, along with TGF- $\beta$ 1 (Jain, 2003). Evidence suggests stringent conditions may be required for use of PDGF-BB. Dandre & Owens (2004) showed PDGF-BB repressed SMC-markers in sub-confluent but not post-confluent culture. This suggests cell-cell or cell-matrix interaction affects the actions of PDGF-BB, and that high density MSC cultures should be initiated before treatment with PDGF-BB. Other avenues to achieve mature contractile MSCs are to grow cells in alternative extracellular matrices e.g. matrigel, use electrophysiological or mechanical stimulation, or the use of different culture medium (Bonnet *et al.*, 2008; Kobayashi *et al.*, 2004). The differentiation of MSCs into mature SMCs may be obtainable by combining these conditions.

To demonstrate the functionality of differentiated cells, the changes in intracellular  $\text{Ca}^{2+}$  by activating receptor-induced ion channels and voltage-operated  $\text{Ca}^{2+}$  channels was assessed. However, this analysis should be extended to obtain a more detailed understanding of the cells biophysical properties. Using patch-clamping techniques (Polder *et al.*, 2005), with selective pharmacological agents to block particular channels will enable the identification of specific calcium and potassium channels found on cells.

The recreation of SMCs from stem cells is complex, and is not completely understood. Previous groups have demonstrated significant variability of contractile marker expression upon differentiation (Lee *et al.*, 2010; Xie *et al.*, 2008). Further work is required on how to simulate the creation of functional SMCs *in vitro* efficiently and reproducibly. Ideally, development of a standardized differentiation protocol, created on a completely defined medium, is what is required for this field. The use of iPSCs as a starting cell type to generate SMCs has been investigated, where Cheung *et al.*, (2012) reported the generation of SMCs using a chemically defined method. They were able to produce origin-specific SMCs, which is advantageous when studying the impact of embryological origins on vascular disease. Other approaches have included using other intermediate populations, such as cardiac progenitor cells, to obtain vascular SMCs (Menendez *et al.*, 2011; Menendez *et al.*, 2013). Vascular SMCs have also been generated by using MSCs derived from iPSCs. But unlike Cheung *et al.*, (2012), who used PDGF and TGF- $\beta$ 1 to induce differentiation, Bajpai *et al.*, (2012) used a combination of TGF- $\beta$ 1 and heparin. Like MSCs, there are a number of different protocols for differentiating iPSCs into vascular SMCs.

This chapter describes the differentiation of MSCs into CAD-relevant cells. There is another cell type that would be of interest to differentiate MSCs into. Endothelial cells are involved in the process of atherosclerosis. CAD-related genetic variants that are only functional in endothelial cells may exist; therefore this cell type would be of importance to study. Oswald *et al.*, (2004) were the first to establish an *in vitro* protocol, using low-serum with vascular endothelial growth factor (VEGF) conditions, to obtain endothelial cells from bone marrow-derived MSCs. The cells showed characteristics of mature endothelium cells, including the presence of Weibel-Palade bodies, and expression of von Willebrand factor (vWF), vascular cell adhesion molecule 1 (VCAM-1), vascular endothelial (VE)-cadherin and VEGF receptors 1 and 2. Additionally, functional analysis of endothelial cells was determined by measuring acetylated LDL incorporation, and the formation of capillary-like structures. The differentiation of MSCs into endothelial cells may be attainable by applying this protocol used by Oswald *et al.*, (2004).

### 5.3.2 Conclusion

I was unsuccessful in differentiating MSCs into hepatocytes using a sequential treatment method. Cells morphologically resembled hepatocytes, but did not increase gene expression of any of the hepatogenic markers, therefore the cells were not investigated further using functional assays.

Next MSCs were pushed towards a SMC lineage. An increase in expression of early and mid-markers was induced, at the gene and protein level. Unfortunately expression of late markers was not seen. Differentiated SMCs produced calcium transients upon agonist exposure but did not contract, suggesting cells did not have the complete contractile machinery. The most likely reason is due to the limited potency of MSCs. Further work is required to produce mature SMCs *in vitro*.

# **Chapter 6- Functional studies on the 15q25 CAD-associated locus**

## 6.1 Introduction

Three different GWASs independently reported the A Disintegrin and Metalloproteinase with Thrombospondin Motifs 7 (*ADAMTS7*) locus on chromosome 15q25 to be associated with CAD.

One of the studies was conducted by the CARDIoGRAM consortium. Due to the limited power of previous studies to identify loci with modest effects, a larger transatlantic study was performed using individuals from 14 different GWASs, comprising of 22,233 cases and 64,762 controls (Schunkert *et al.*, 2011). All samples were of European ethnicity. A successive replication study was carried out by genotyping a further 60,738 individuals for the top associations, which reached a significance level of  $p < 5 \times 10^{-6}$ . The meta-analysis confirmed 10 previously reported genetic loci, and identified 13 new loci that were significantly associated with CAD. The non-synonymous variant rs3825807 within *ADAMTS7* was one of the novel loci significantly associated with CAD ( $p = 1.7 \times 10^{-12}$ ).

Next Reilly *et al.*, (2011) investigated the distinct genetic factors that contributed either to coronary atherosclerosis or directly with MI in individuals with existing coronary atherosclerosis. Two separate GWASs were performed. Firstly, 12,393 individuals with CAD (cases), and 7,383 individuals without CAD (controls) were genotyped to identify loci that predispose to CAD. To identify loci that contribute to MI, 5,783 individuals with CAD and MI and 3,644 individuals with CAD but not MI were compared. The rs1994016 variant at the *ADAMTS7* locus was significantly ( $p = 4.98 \times 10^{-13}$ ) associated with CAD, but not MI. This finding suggested that *ADAMTS7* may be involved in the early stages of atherosclerosis, and not thrombosis, which leads to MI. Rs1994016 and rs3825807 (identified by Schunkert *et al.*, 2011) are in high LD ( $r^2 = 0.9$ ) and are likely to reflect the same signal.

Lastly, the C4D Genetics Consortium, (2011) carried out a combined analysis on two European and two South Asian cohorts to identify additional CAD-associated loci. The combined analysis included 15,420 individuals with CAD and 15,062 controls of European and South Asian ancestry. The replication meta-analysis in 10 independent studies included 21,408 cases and

19,185 controls. 5 novel loci were associated with CAD. The variant rs4380028 at the *ADAMTS7* locus was one of the novel loci significantly associated with CAD ( $p=3.71 \times 10^{-9}$ ).

### 6.1.1 ADAMTS7

*ADAMTS7* encodes a member of the ADAMTS protein family which are secretory zinc metalloproteases. Since the discovery of ADAMTS1 in 1997 (Kuno *et al.*, 1997) the family has expanded to 19 members, which have been shown to play roles in important processes such as organ development, connective tissue organisation, coagulation, inflammation and angiogenesis.

The human *ADAMTS7* transcript is 52.3 kb and contains 24 protein-coding exons (Somerville *et al.*, 2004). The encoded protein is 1686 amino acids in length, and has a predicted molecular weight of 181 kDa. The ADAMTS family of proteins share a similar protein structure, and a characteristic feature is the presence of one or more thrombospondin type 1 repeats (TSRs; Kuno *et al.*, 1997). In addition *ADAMTS7* has a signal peptide, prodomain, metalloproteinase domain, disintegrin-like domain, cysteine-rich domain, spacer domain, mucin domain and a protease and lacunin (PLAC) domain (**Figure 6.1**).

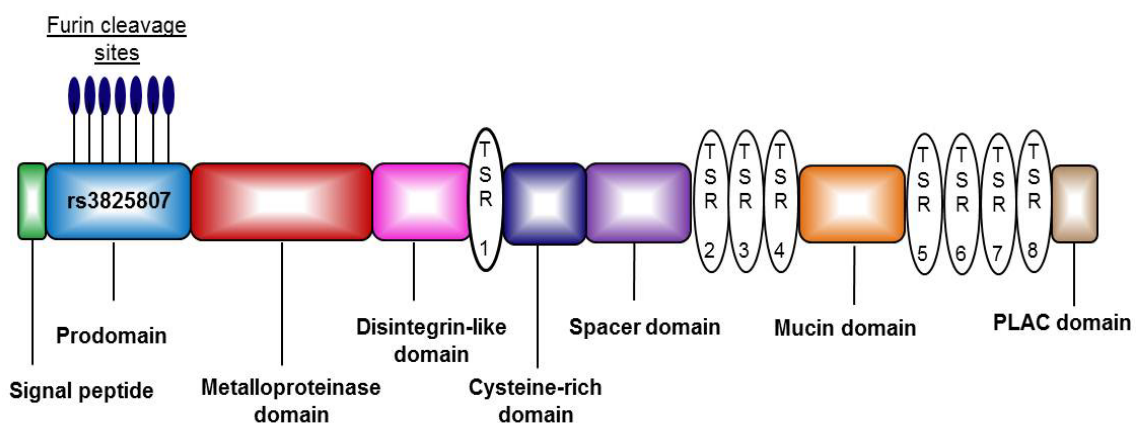


**Figure 6.1. Schematic diagram of ADAMTS7 protein.** Human ADAMTS7 is 1686 amino acids in length, and has a predicted molecular weight of 181 kDa. The variant rs3825807 locates to the prodomain.

ADAMTS7 undergoes significant post-translational modifications, which include potential conserved glycosaminoglycans (GAG) attachment sites within the mucin domain at the<sup>1006</sup>SGSG site (Brinkmann *et al.*, 1997). The mucin domain has also been predicted to be subject to O-glycosylation (when a sugar molecule is attached to serine or threonine residues; Somerville *et al.*, 2004). ADAMTS7 also has 10 N-linked glycosylation sites, whereby glycan attaches to nitrogen on asparagine or arginine side chains. Due to these various post-translational modifications, ADAMTS7 is larger than the predicted molecular weight based on the amino acid sequence. Researchers have shown full-length ADAMTS7 is ~250 kDa (Somerville *et al.*, 2004; Pu *et al.*, 2013).

As with many of the other ADAMTS proteins, the prodomain of ADAMTS7 is processed by proteolytic cleavage to activate it. Furin is a ubiquitously expressed calcium-dependent serine protease (Molloy *et al.*, 1992). It is heavily involved in the prodomain cleavage of different proteins moving through the secretory pathway (Zhou *et al.*, 1999). Furin cleaves ADAMTS7 within the prodomain (where the CAD-associated SNP lies) at furin recognition sites, to produce proteolytically active ADAMTS7. There are three furin recognition sites conserved between mouse and human; RVL<sup>58</sup>R, RVL<sup>60</sup>RKR and RQQR<sup>220</sup>, suggesting similar mechanisms of activation. There are additional furin recognition sites found in humans; RGR<sup>92</sup>ELR, RR<sup>218</sup>ER, RR<sup>229</sup>PR and RL<sup>232</sup>RR. It is suggested that ADAMTS7 prodomain processing is initiated in the Golgi apparatus and is completed at the cell surface. Upon cleavage of the prodomain on the most C-terminal furin recognition site, mature human ADAMTS7 protease is approximately 157.9 kDa (Somerville *et al.*, 2004).

*In vitro* experiments with recombinant ADAMTS7 have been conducted to determine its cellular localisation. ADAMTS7 associates with the cell membrane or extracellular matrix. Washing cells with high salt concentrations (e.g. 0.5M NaCl for 30 minutes), released more ADAMTS7 into the media, which supports the idea that ADAMTS7 localises to the cell surface (Somerville *et al.*, 2004). To further support this, other members of the ADAMTS family; ADAMTS4 and ADAMTS9 have been shown to localise at the cell surface (Somerville *et al.*, 2003; Kashiwagi *et al.*, 2004). Surface biotinylation

experiments show ADAMTS7 is transiently localised with the outer leaflet of the plasma membrane, and this interaction is thought to be mediated via the ancillary domain (Somerville *et al.*, 2004). Recent findings show ADAMTS7 co-localises at the cell membrane with cytoskeletal filaments, and markers of podosomes, which are actin-rich structures located on the outer surface of the membrane (Bauer *et al.*, 2015).

*ADAMTS7* is expressed broadly in different tissues but at low levels. Initial mouse experiments showed *ADAMTS7* (~5.5 kb) was expressed in the heart, brain, placenta, lung, liver, skeletal muscle, kidney and pancreas (Hurskainen *et al.*, 1999). In humans, it has been detected (also as a 5.5 kb transcript) in the liver, kidney, pancreas, skeletal muscles and heart (Liu *et al.*, 2006). More interestingly, immunohistochemical staining showed ADAMTS7 is expressed in the coronary artery (Wang *et al.*, 2009).

The progression of atherosclerosis is governed by pro- and anti-inflammatory cytokines that can affect ADAMTS7 expression. Also vascular injury, can initiate various stimuli that regulate ADAMTS7 expression in SMCs. IL-1 $\beta$ , PDGF-BB and TNF- $\alpha$  are pro-inflammatory cytokines and induce expression of ADAMTS7 (Wang *et al.*, 2009). Hydrogen peroxide (H<sub>2</sub>O<sub>2</sub>) is a reactive oxygen species, and also increases ADAMTS7 levels. TGF- $\beta$  is an anti-inflammatory cytokine that decreases expression of ADAMTS7. MiR-29a/b is a microRNA (miRNA; a short non-coding RNA) involved in the degradation of mRNA and inhibition of protein translation. MiR-29a/b has a target site in the 3'UTR of *ADAMTS7*, and represses mRNA and protein expression (Du *et al.*, 2012). Overall, it is suggested that ADAMTS7 levels are responsive to different inflammatory stimuli under pathological conditions.

Cartilage oligomeric matrix protein (COMP, also known as thrombospondin-5, TSP5), has been shown to interact with ADAMTS7. COMP is a 520 kDa pentameric glycoprotein, and is the fifth member of the thrombospondin gene family (Newton *et al.*, 1994). It is an extracellular matrix protein and is expressed in vertebral discs, cartilaginous joints and blood vessels. COMP was identified as the first ADAMTS7 substrate via a yeast-two hybrid system. The TSRs at the C-terminal end of ADAMTS7 are required to

interact with the EGF-like domains of COMP (Liu *et al.*, 2006). In the osteoblastic cell line MG-63, and native articular cartilage, rat ADAMTS7 co-immunoprecipitated with COMP. Experimenters carried out *in vitro* digestion assays, and discovered that recombinant ADAMTS7 in conditioned media can cleave COMP into three fragments; 100, 75 and 51 kDa upon analysis on a polyacrylamide gel (Liu *et al.*, 2006). The digestion of COMP has been implicated in diseases such as atherosclerosis.

### **6.1.2 Role of ADAMTS7 in the pathogenesis of CAD**

Vascular SMCs are a plastic cell type, with the ability to revert between a contractile and synthetic phenotype. Under physiological conditions, vascular SMCs are located in the tunica media of blood vessels, where they express a repertoire of contractile proteins and have a low proliferation and migration rate. However, during pathological conditions such as atherosclerosis or upon various environmental cues, they can switch to a synthetic/dedifferentiated phenotype with high proliferation/migration abilities and reduced expression of contractile proteins (Wang *et al.*, 2009; Owens *et al.*, 2004). Phenotypic switching of vascular SMCs is a key step during the development of atherosclerosis.

Before the discovery of the association of *ADAMTS7* with CAD from GWASs, the role of *ADAMTS7* in the vasculature had been explored. COMP is expressed in vascular SMCs (Riessen *et al.*, 2001), and it inhibits vascular SMC migration, by interacting with  $\alpha_7\beta_1$  integrin (Wang *et al.*, 2010), so COMP is important in maintaining a vascular SMC contractile phenotype. A rat balloon injury model, showed vascular injury resulted in vascular SMC migration and intima hyperplasia. This occurred by *ADAMTS7* degrading COMP in injured vessels (Wang *et al.*, 2009). *ADAMTS7* experimental over-expression enhanced vascular SMC migration, whereas small interfering RNA (siRNA) knockdown reduced migration *in vitro*. In summary the experimental evidence suggests *ADAMTS7* mediates vascular SMC migration by cleaving COMP to remove its inhibitory effect on vascular SMCs.

Pu *et al.*, (2013) investigated the association between the *ADAMTS7* locus (rs3825807) and CAD. They observed in the Bruneck Study Cohort the GG genotype had a protective effect for carotid atherosclerosis and that *ADAMTS7* was present in human coronary plaques. Pu *et al.*, (2013) described a possible mechanism for the casual variant (**Figure 6.2**). rs3825807 (A to G) causes a non-synonymous change, resulting in a Ser-to-Pro substitution in the prodomain of *ADAMTS7*. Vascular SMCs from individuals with the risk AA genotype had increased migratory ability, more cleaved COMP fragment in the conditioned media and more cleaved *ADAMTS7* prodomain, than the GG genotype. Overall, the functional studies showed that the Ser-to-Pro substitution affected vascular SMC migration, COMP degradation and *ADAMTS7* protein maturation, providing a biological mechanism for the association between rs3825807 and CAD.

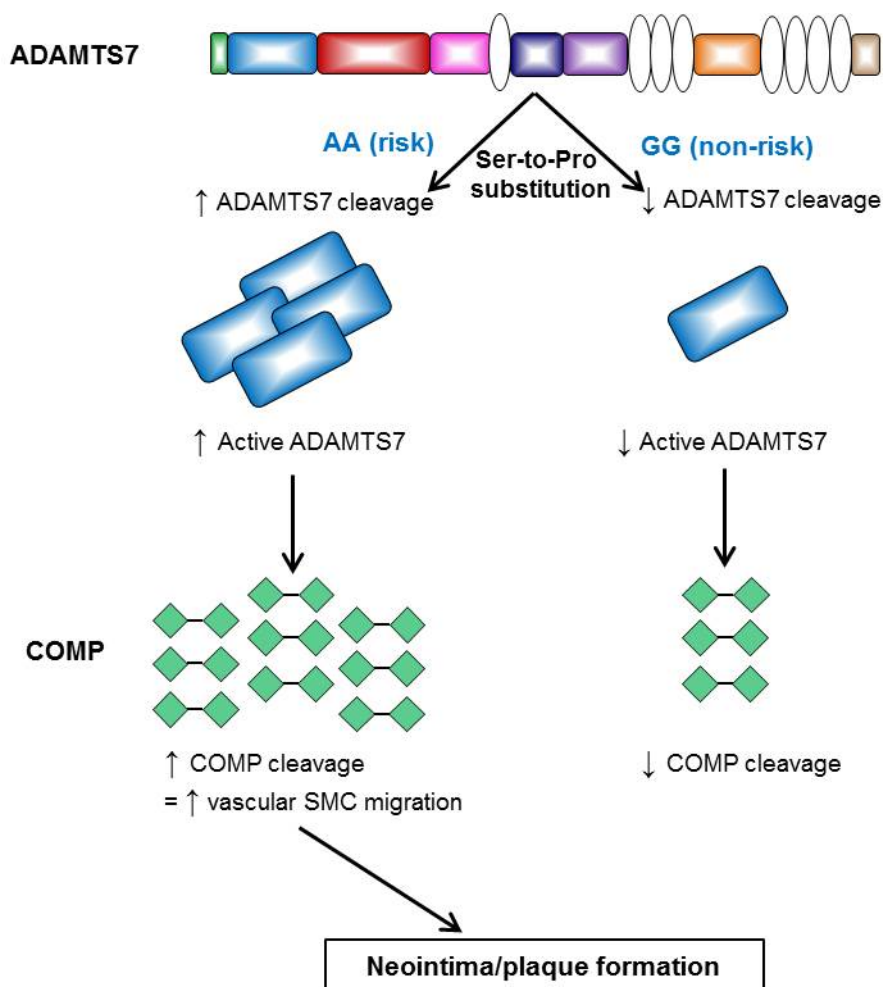


**Figure 6.2. Proposed mechanism of rs3825807 on vascular SMC migration.**

Recent *in vivo* validation has shown an association between ADAMTS7 and atherosclerosis. *ADAMTS7* knockout onto hyperlipidemic mouse models (*Ldlr*<sup>-/-</sup> and *ApoE*<sup>-/-</sup>) showed upon femoral wire injury, a decrease in neointimal formation, reduced lesion formation in aortas and aortic roots, and a decrease in vascular SMC migration upon TNF- $\alpha$  treatment (Bauer *et al.*, 2015).

A different *in vivo* rodent study of an *ADAMTS7* knockout mouse, showed after wire-injury of the carotid artery, reduced neointima formation and increased re-endothelialization occurred. Endothelial cell proliferation and migration were also greatly reduced *in vitro* and *in vivo*, via a COMP-independent mechanism. TSP1 was identified as a novel *ADAMTS7* substrate, it was demonstrated that *ADAMTS7* can bind to and degrade TSP1 in endothelial cells. This study suggested that *ADAMTS7*-mediated TSP1 cleavage may play a key role in re-endothelialization upon vascular injury (Kessler *et al.*, 2015). Overall these studies highlight the clear involvement of *ADAMTS7* in the pathology of atherosclerosis.

### 6.1.3 Aims and objectives

The final aim of this thesis was to, as a second proof of principle, differentiate MSCs with different genotypes for the functional SNP (rs3825807) into SMCs to recapitulate the effects of rs3825807 shown by Pu *et al.*, (2013) on ADAMTS7 cleavage and SMC migration *in vitro*. This will enable the demonstration of the application of MSCs as a research tool for the investigation of CAD-associated variants.

The objectives were:

- Investigate *ADAMTS7* expression in MSCs and differentiated SMCs
- Determine the effect of rs3825807 on *ADAMTS7* gene expression
- Analyse the effect of rs3825807 on ADAMTS7 prodomain cleavage and cell migration by using Western blotting and scratch assays, respectively

## 6.2 Results

### 6.2.1 *ADAMTS7* expression in MSCs and differentiated SMCs

The first objective of this chapter was to analyse *ADAMTS7* expression in MSCs and differentiated SMCs. To differentiate MSCs into SMCs, the SMC differentiation medium included 10ng/ml TGF- $\beta$ 1, which has been reported to inhibit *ADAMTS7* expression. Wang *et al.*, (2009) observed in primary human SMCs, treatment with 5ng/ml TGF- $\beta$ 1 resulted in a 50% decrease in *ADAMTS7* expression. Thus the effect of the SMC differentiation medium on *ADAMTS7* expression was investigated. MSCs were treated for 6 days with SMC differentiation medium using the protocol described in Chapter 2 (**Section 2.2.15**). An additional experimental step was included, where after the sixth day of the differentiation protocol; cells were re-seeded and were either treated for another 7 days with SMC differentiation medium without TGF- $\beta$ 1 (SMCDM-TGF- $\beta$ 1) or SMC differentiation medium with TGF- $\beta$ 1 (SMCDM+TGF- $\beta$ 1).

Total RNA was extracted from cells at day 6 and day 13 and cDNA synthesised. Undifferentiated MSCs were used as a control for qPCR experiments. MSCs and differentiated SMCs expressed *ADAMTS7*, where differentiated SMCs showed a 2.4-fold increase compared to MSCs. A subsequent SMCDM-TGF- $\beta$ 1 or SMCDM+TGF- $\beta$ 1 treatment maintained *ADAMTS7* expression (**Figure 6.3B**). *ACTA2* expression was also analysed to ensure cells had moved towards a SMC lineage. Upon removal of TGF- $\beta$ 1, a 5-fold increase was observed in *ACTA2* expression, suggesting that the differentiation of MSCs into SMCs might have improved (**Figure 6.3A**). However, these cells still did not show an upregulation of the late SMC marker; *MYH11* (data not shown). The expression of *COMP* in MSCs and differentiated SMCs was also investigated. MSCs did not express *COMP*, but *COMP* expression was detected in differentiated SMCs. As MSCs did not express *COMP*, the samples were not within linear range of the qPCR assay. For this reason, qPCR products were ran on a 1.5% agarose gel (**Figure 6.3C**). Withdrawal of TGF- $\beta$ 1, after the 6 day SMC differentiation period, drastically reduced *COMP* expression, while inclusion of TGF- $\beta$ 1 in the SMC differentiation medium, maintained *COMP* expression levels.

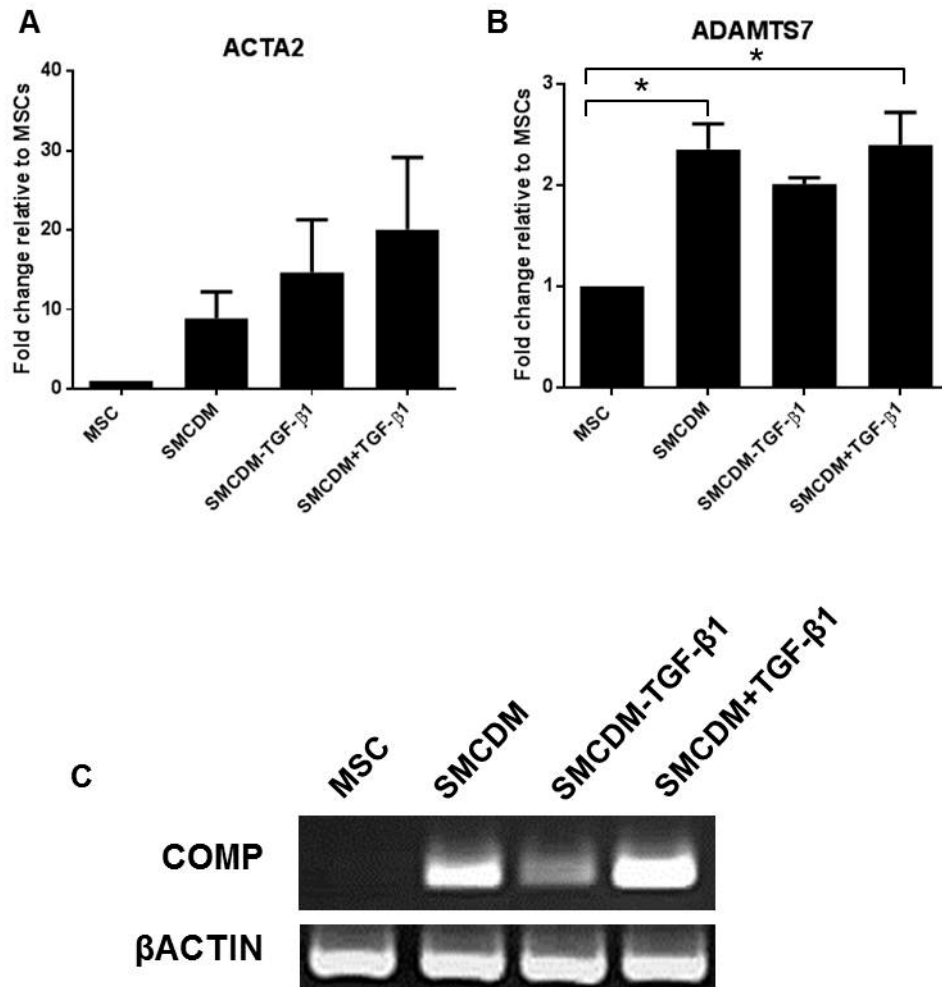


**Figure 6.3. Upregulation of *ACTA2*, *ADAMTS7* and *COMP*.** Increase in gene expression of (A) *ACTA2*, (B) *ADAMTS7* and (C) *COMP* after a 6 day treatment with smooth muscle cell differentiation medium (SMCDM). Cells were subcultured and grown and for a further 7 days in SMCDM without TGF- $\beta$ 1 (SMCDM-TGF- $\beta$ 1) and with TGF- $\beta$ 1 (SMCDM+TGF- $\beta$ 1). *COMP* products were visualised on a 1.5% agarose gel. For qPCR, MSCs were used as a control. Samples were normalised to  $\beta$ -actin. Data is shown as mean  $\pm$  Standard Deviation (SD; n=3). Data was analysed using a One-Way ANOVA with Dunnett post-test (\*p<0.05 compared to MSCs).

### 6.2.2 Analysis of rs3825807 and *ADAMTS7* expression in MSCs and differentiated SMCs

Firstly genotyping data from the results of the Axiom™ Genome-Wide UKB WCGS Genotyping Array for the MSC bank (n=112) was retrieved for rs3825807 (summary in Chapter 3; **Table 3.3**). A cluster plot was produced to

ensure the SNP had the expected cluster pattern and to highlight any anomalous samples (**Figure 6.4**).

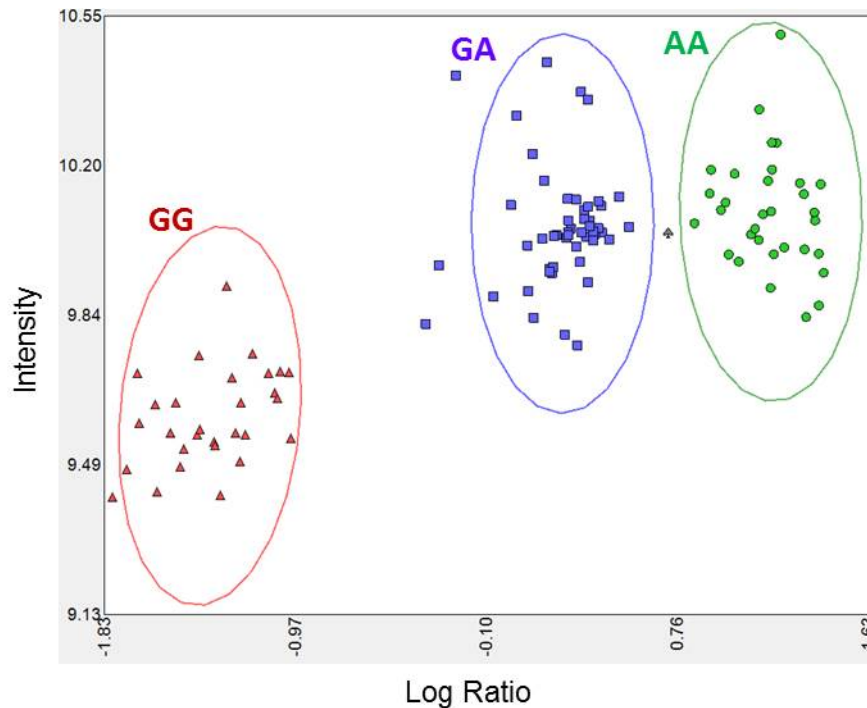


**Figure 6.4. SNP cluster plot for rs3825807 in the MSC bank (n=112).** Clustering is carried out in two dimensions. The X axis (log ratio) defines the contrast of the cluster, whereas the Y axis defines the strength of the signals from each sample. Red triangles ( $\blacktriangle$ ) are individuals with the GG genotype, purple squares ( $\blacksquare$ ) are GA genotype, and green circles ( $\bullet$ ) are individuals with the AA genotype. Grey spades ( $\spadesuit$ ) indicate no calls. Samples were clustered under the posterior model using the Affymetrix® Genotyping Console™ (GTC) version 4.2 and the Affymetrix® Power Tools (APT) version 1.16.1.

Next, MSCs from 10 donors that were selected based on their genotype for rs3825807 (5 homozygote majors and 5 homozygote minors) were differentiated into SMCs. Firstly *ACTA2* expression was analysed to verify differentiation towards a SMC lineage. The increase in *ACTA2* expression was fairly consistent between cells from different donors (between 7-10 fold increase compared to MSCs). Cells from Donor 29 and 40, showed a higher level of expression, 34-fold and 15-fold, respectively (**Figure 6.5**).

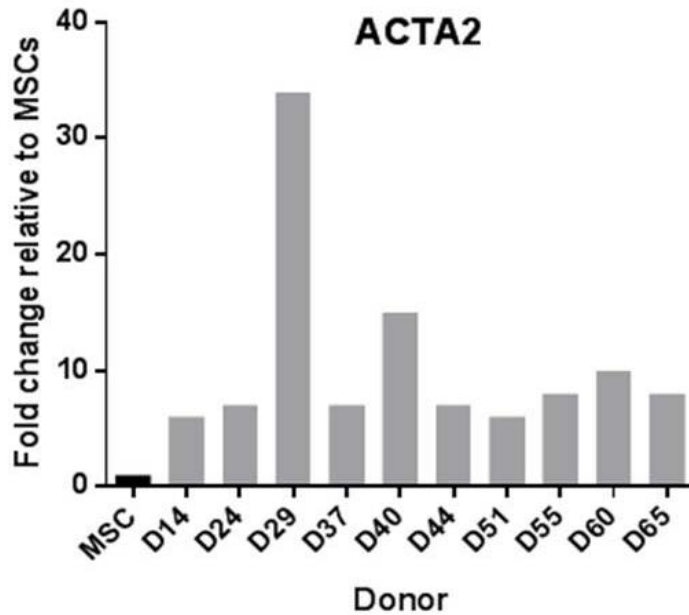


**Figure 6.5. Upregulation of *ACTA2* in differentiated SMCs from 10 different donors.** Quantitative PCR analysis after a 6 day treatment with SMC differentiation medium. There was consistency in the increase in *ACTA2* gene expression except in cells from Donor 29 and 40. MSCs were used as a control. Samples were normalised to  $\beta$ -actin.

Next the analysis of rs3825807 on *ADAMTS7* gene expression was conducted on MSCs and differentiated SMCs. In both cell types there was no association between rs3825807 and *ADAMTS7* expression (**Figure 6.6**).

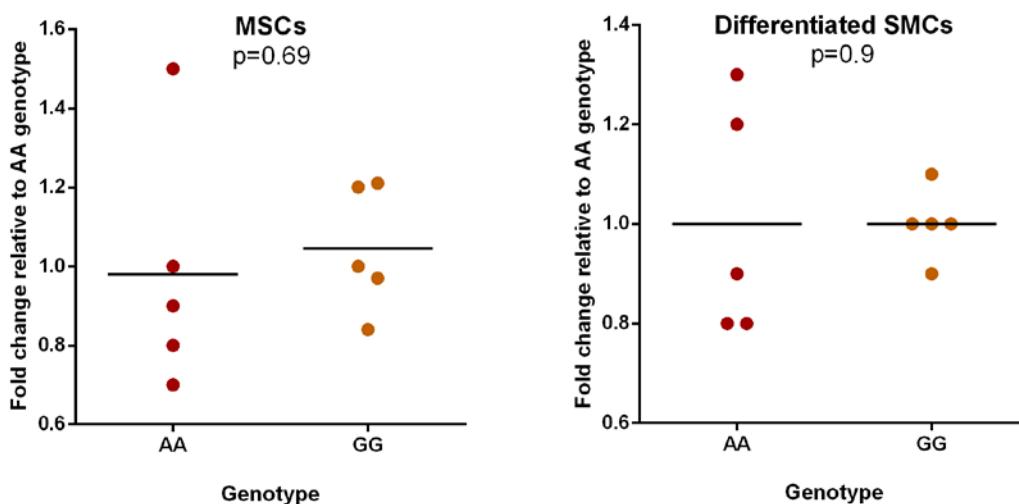


**Figure 6.6. *ADAMTS7* expression in homozygote majors (AA) and homozygote minors (GG) for rs3825807.** No effect of rs3825807 on *ADAMTS7* expression in (A) MSCs (B) differentiated SMCs. Samples were normalised to  $\beta$ -actin. Data was analysed using a Student's t-test. N=5 each genotype group.

### 6.2.3 ADAMTS7 protein expression in MSCs and differentiated SMCs

Pu *et al.*, (2013) propose that the Ser-to-Pro substitution caused by rs3825807 in the ADAMTS7 prodomain, may affect the accessibility for furin to cleave at the prodomain, as they reported an effect of rs3825807 on ADAMTS7 cleavage. To recapitulate this effect, different ADAMTS7 antibodies were used to recognise different regions of the protein. **Figure 6.7** is a schematic diagram illustrating ADAMTS7 protein structure, the location of rs3825807 and the specificity of the different antibodies. Ab45044 is a rabbit polyclonal antibody and detects full-length ADAMTS7, partially processed ADAMTS7 and the prodomain. It binds after the second furin cleavage site (RVL<sup>60</sup>RKR) between positions 80-140. So with this antibody it was possible to singly detect the prodomain fragment to investigate ADAMTS7 prodomain processing. Ab28557 is a rabbit polyclonal antibody that binds at the spacer domain.

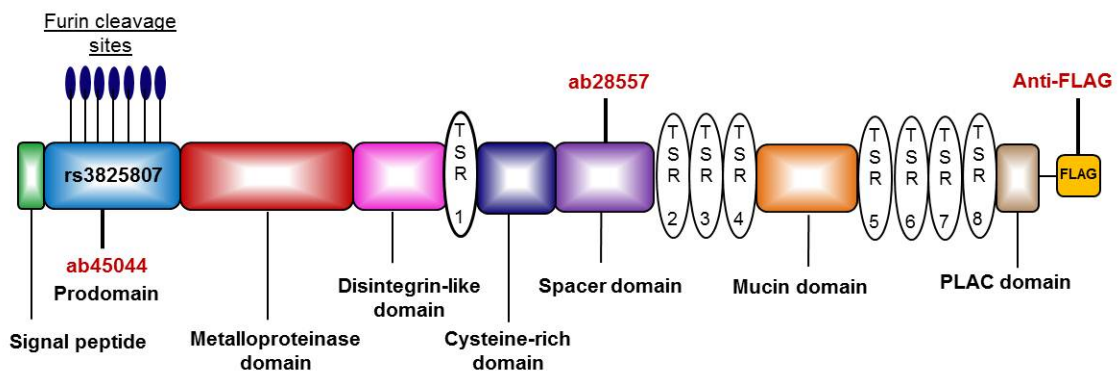


**Figure 6.7. Schematic diagram of ADAMTS7 protein and antibody specificity sites.** Human ADAMTS7 is 1686 amino acids in length, and has a predicted molecular weight of 181 kDa. The anti-ADAMTS7 antibody (ab45044) bound the prodomain, after the second furin cleavage site (RVL<sup>60</sup>RKR) between positions 80-140. The other anti-ADAMTS7 antibody (ab28557) bound in the spacer domain. The anti-FLAG antibody bound to the C-terminal FLAG tag. The variant rs3825807 was located in the prodomain.

Western blotting was conducted to determine the expression of ADAMTS7. ADAMTS7 and many ADAMTS7 fragments were detected in MSC cell lysates. Full-length ADAMTS7 was detected at ~250 kDa, a size also

reported by other researchers (Somerville *et al.*, 2004; Pu *et al.*, 2013; **Figure 6.8**). It was much larger than its predicted size of 182 kDa, most likely due to the fact that ADAMTS7 undergoes heavy post-translational modifications (Somerville *et al.*, 2004).

HEK293 cells were transiently transfected with full length ADAMTS7 containing serine at position 214 (ADAMTS7-Ser) to verify the ADAMTS7 expression pattern seen in MSCs. A mock transfection was also performed as a control. Anti-FLAG M2 a monoclonal antibody, detected the C-terminal FLAG tag, so was able to detect transfected recombinant ADAMTS7 (**Figure 6.7**). Overexpression of ADAMTS7-Ser showed similar results as endogenous ADAMTS7 in MSCs (**Figure 6.9**).

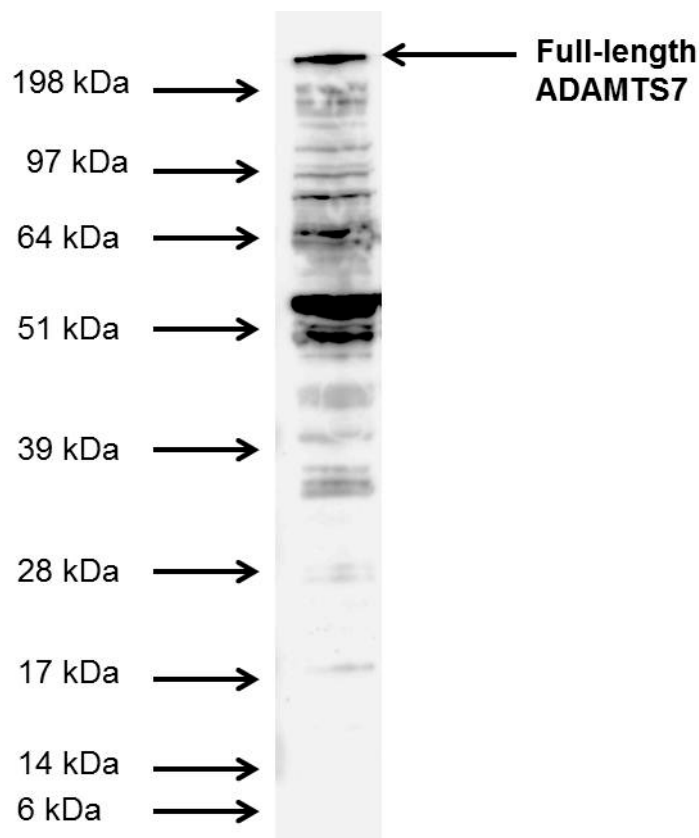


**Figure 6.8. Representative Western blot of full length ADAMTS7 and fragments in cell lysate.** MSCs were grown in serum-free medium for 24 hours. 20µg of protein was loaded onto a NuPAGE® Novex® 10% Bis-Tris Gel. Anti-ADAMTS7 prodomain antibody (ab45044) was used at 1:1000 dilution.

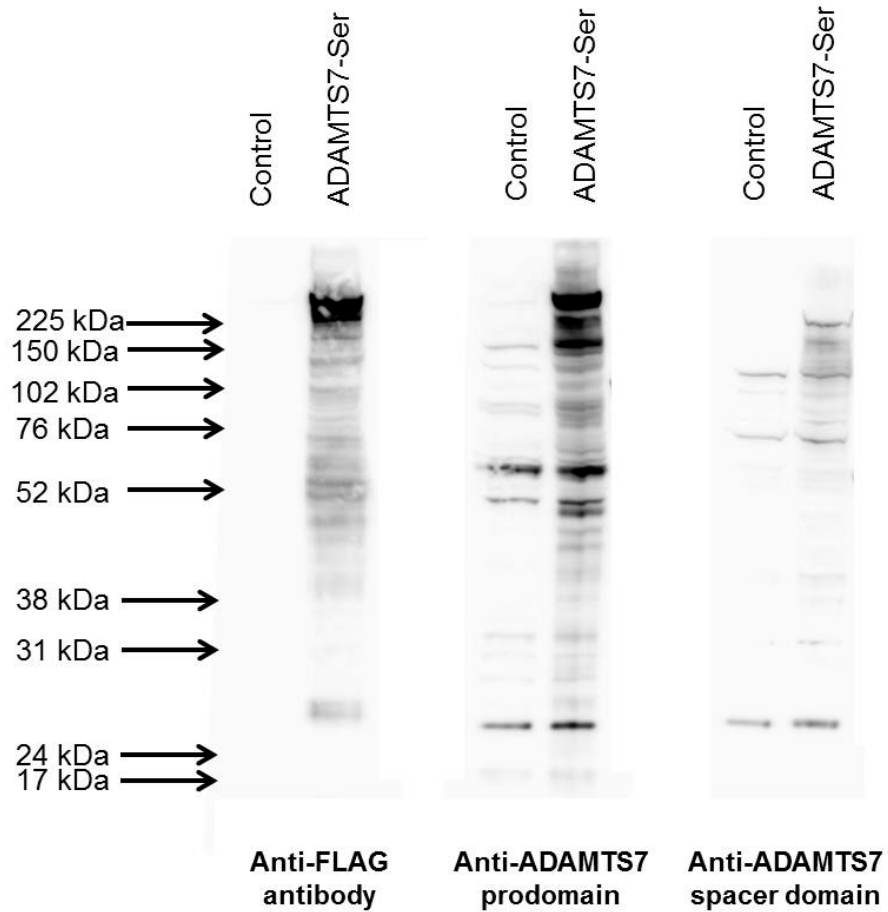


**Figure 6.9. Western blot of HEK293 cells transfected with ADAMTS7-Ser plasmid.** HEK293 cells were transfected with full length ADAMTS7 protein containing serine at position 214 and a FLAG tag at the C-terminal at position 1686. Cell lysates were collected and 20 $\mu$ g of protein was loaded onto a NuPAGE<sup>®</sup> Novex<sup>®</sup> 10% Bis-Tris Gel. Anti-FLAG antibody, anti-ADAMTS7 prodomain antibody and anti-ADAMTS7 spacer domain antibody were used.

#### 6.2.4 Analysis of rs3825807 on ADAMTS7 protein expression and processing

To re-iterate Pu *et al.*, (2013) reported rs3825807 affects ADAMTS7 processing, whereby vascular SMCs of the GG genotype had a reduced amount of cleaved ADAMTS7 prodomain in conditioned media, compared to the AA genotype.

Firstly to determine whether rs3825807 affected ADAMTS7 protein expression in MSCs and differentiated SMCs within the cell, cell lysates were collected and 20µg of protein resolved on a NuPAGE® Novex® 10% Bis-Tris Gel. There was no apparent difference in full length ADAMTS7 or fragments in individuals of the GG genotype compared to the AA genotype (**Figure 6.10**).

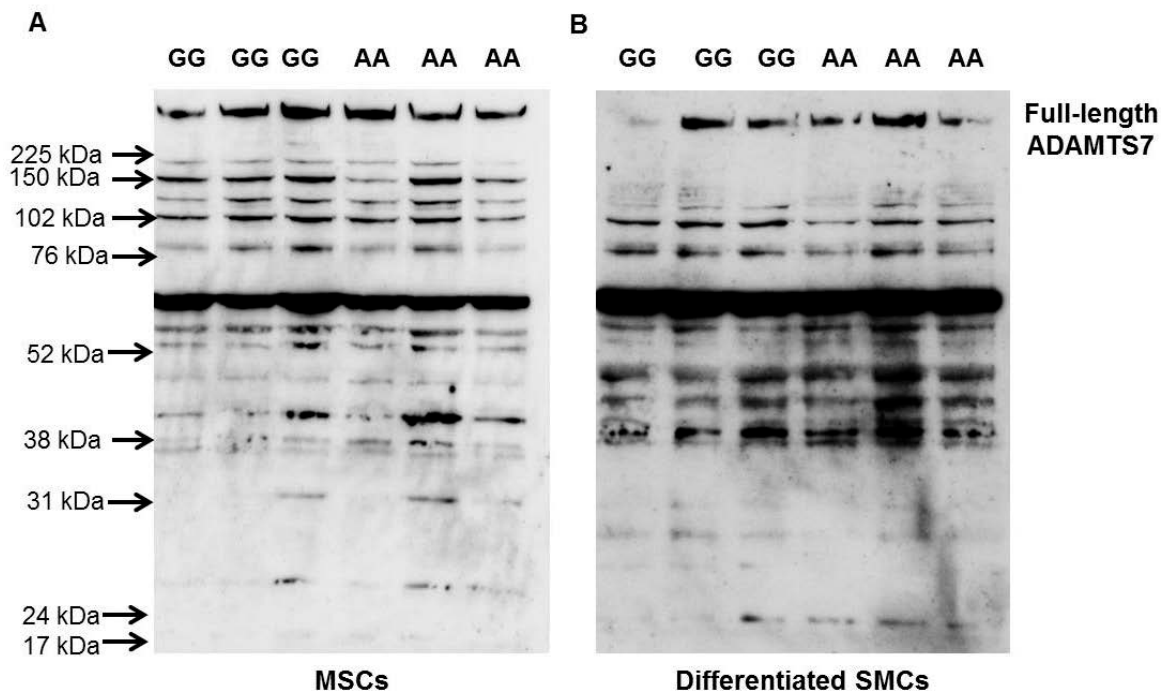


**Figure 6.10. Western blot of ADAMTS7 and fragments in MSCs and differentiated SMC lysates.** (A) MSCs and (B) differentiated SMCs were grown in serum-free medium for 24 hours, and 20µg of protein was loaded onto a NuPAGE® Novex® 10% Bis-Tris Gel. Anti-ADAMTS7 prodomain antibody was used. There was no effect of rs3825807 on full length ADAMTS7 in MSCs and differentiated SMCs (n=3 of each genotype).

Next to investigate whether rs3825807 affected ADAMTS7 prodomain cleavage, cells were treated to serum-free media for 24 hours, and media was collected and concentrated using the 10K Amicon Ultra 15ml centrifugal unit to provide a sufficient amount of protein for the detection of ADAMTS7. In preliminary Western blot experiments, ADAMTS7 prodomain was not observed when the media was concentrated at a later date than the day of collection, or when the samples had been frozen. A possible explanation is as ADAMTS7 is a secretory protein; its prodomain is most likely degraded quickly after cleavage. So conditioned media was collected, concentrated and resolved by Western blot on the same day.

A preliminary analysis of conditioned media from MSCs of the AA and AG genotype suggested more prodomain was present from individuals with the AA genotype (**Figure 6.11A**). Next, conditioned media from MSCs from three different donors of the AA and GG genotype were investigated. Protein quantification was performed, and the ADAMTS7 prodomain band intensity was normalised to Ponceau S staining, to account for unequal loading. Upon quantification, a genotype effect on the amount of prodomain in MSC conditioned media was not seen ( $p=0.9$ ; **Figure 6.11B**). A closer analysis of the Western blot revealed a number of prodomain fragments of similar size, most likely reflecting furin cleavage at the different furin recognition sites within the prodomain.

Next, conditioned media was collected from differentiated SMCs, from three donors of the AA genotype and three donors of the GG genotype. Western blot was repeated under the same conditions as the previous experiment. Upon quantification of the ADAMTS7 prodomain, a trend was observed where individuals of the GG genotype had a higher ADAMTS7 band intensity than the AA genotype, however this was not significant ( $p=0.1$ ; **Figure 6.11C**).

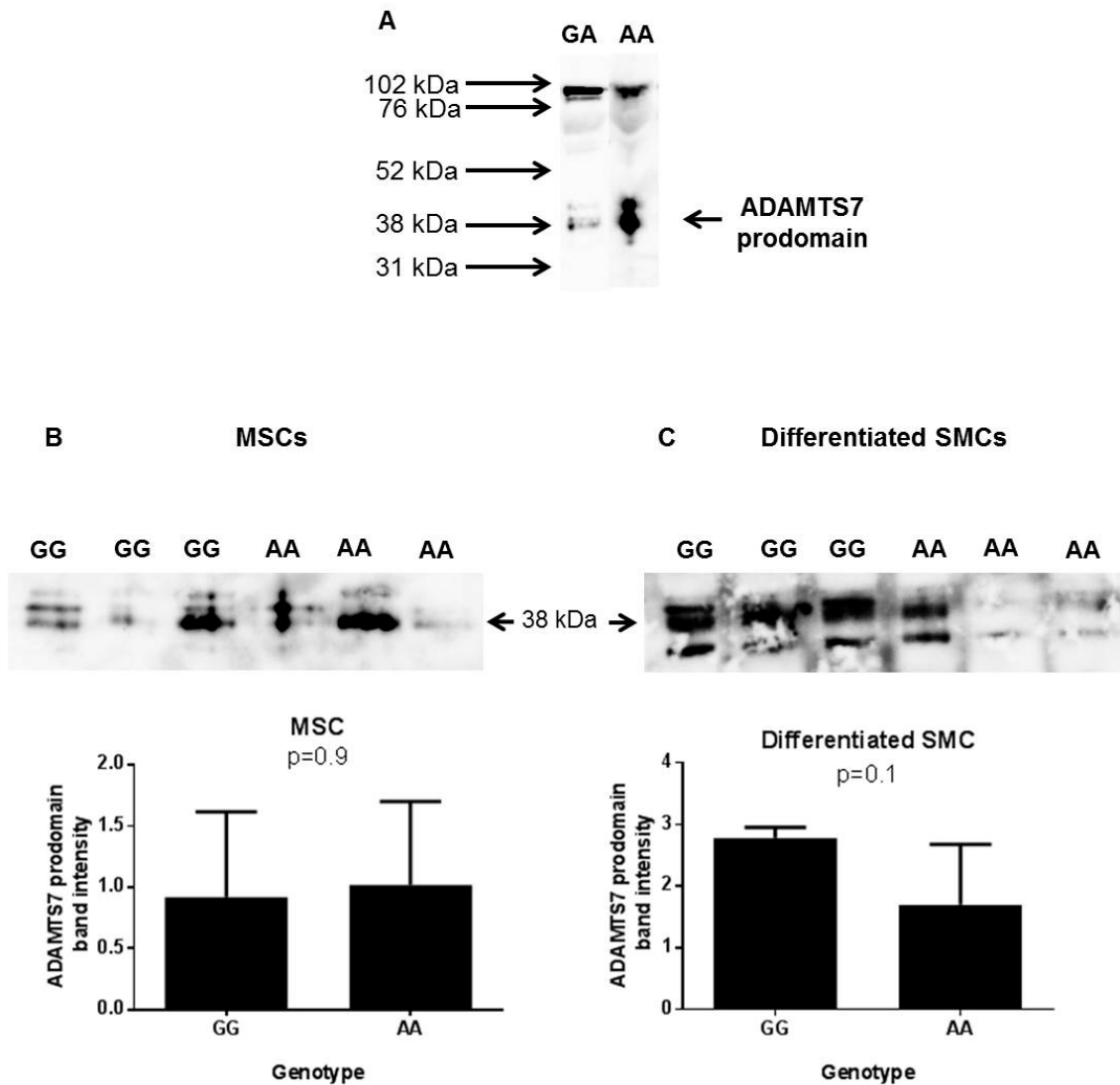


**Figure 6.11. Detection and quantification of cleaved ADAMTS7 prodomain in MSCs and differentiated SMC conditioned media.** Conditioned media was concentrated, and 20µg of protein was loaded onto a NuPAGE® Novex® 10% Bis-Tris gel. (A) Detection of ADAMTS7 prodomain in MSC conditioned media of the GA and AA genotype (n=1 of each genotype). No effect of rs3825807 on ADAMTS7 prodomain cleavage in conditioned media from (B) MSCs and (C) differentiated SMCs. Data shown by column graph is the ADAMTS7 prodomain band intensity normalised to Ponceau S staining. Data is shown as mean ± Standard Deviation (SD; n=3 of each genotype).

### 6.2.5 Analysis of rs3825807 and cell migration

Although an effect of rs3825807 on ADAMTS7 prodomain processing was not seen in conditioned media from MSCs and differentiated SMCs, further analysis of this variant was carried out. As it has been reported by Pu *et al.*, (2013) that the SNP also significantly affected vascular SMC migration. So I went on to test if I could replicate this finding.

To investigate whether the ADAMTS7 genotype had an effect on cell migration, scratch assays were performed on cells either with the GG or AA genotype for rs3825807. MSCs were seeded into 6 well plates at  $1 \times 10^4$  cells/cm<sup>2</sup>. Upon confluency, a pipette tip was used to make a scratch the length of the well. Cell migration was measured in two different ways (**Figure 6.12**). The first analysis was the measurement of the cell-covered area over 24 hours, which generated a migration curve. The linear phase of migration was the important feature of the curve, as this determined the speed of the wound closure (slope). The second analysis was the measurement of the distance the cells had migrated after 6 and 9 hours after the wound was created. The distance measured was an average of 5 different points along the wound for each image (**Figure 6.12C**).

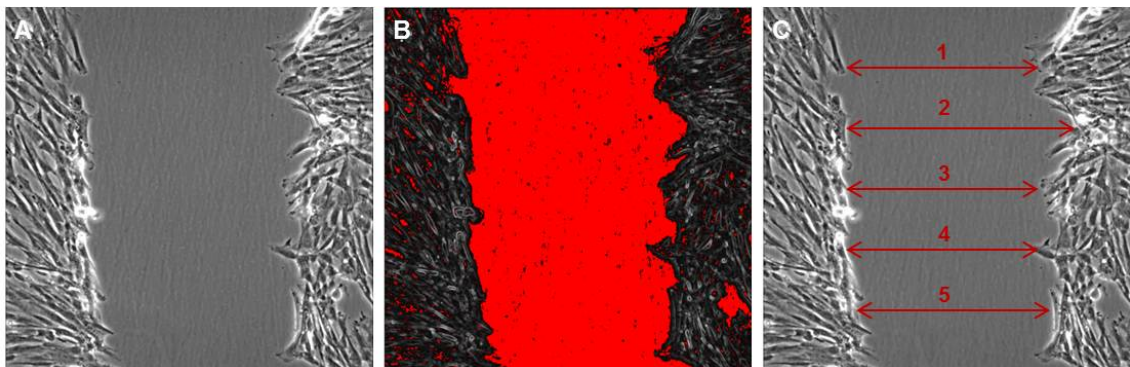


**Figure 6.12. Representative images of a scratch assay on MSCs analysed by Image J software. (A) Wound created by a P20 pipette tip. (B) Image J detected the cell-covered area (black) of the image. (C) Image J was used to calculate the distance ( $\mu\text{m}$ ) between the two sides of the scratch at 5 different points along the scratch. Magnification x10.**

The effect of rs3825807 on migration may be small, so reliability of the method was necessary. To test this, the quantification of cell migration via a scratch assay was conducted on MSCs from the same donor (Donor 9) on two different days (**Figure 6.13**). There was no significant difference ( $p=0.18$ ) in the speed of the wound closure between different days. There was also no difference in the distance cells had migrated after 6 ( $p=0.7$ ) and 9 hours ( $p=0.8$ ), suggesting the method was fairly reproducible.

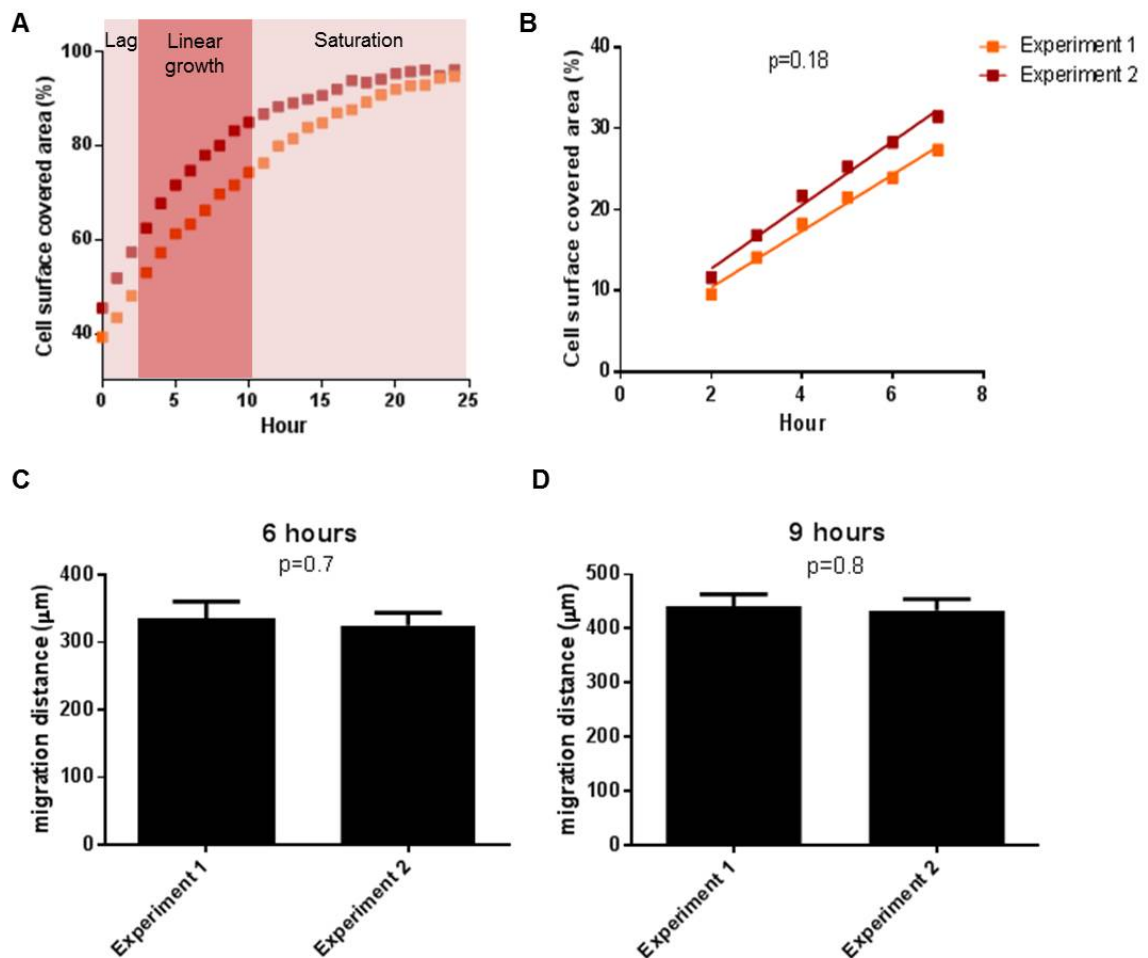


**Figure 6.13. Reproducibility of the scratch assay.** A scratch assay was conducted on MSCs from Donor 9 on different days, one week apart, to determine the reproducibility of the experiment. Cellular migration was quantified by the percentage of cell-covered area and the distance cells migrated ( $\mu\text{m}$ ). (**A**) Characteristic migration curve of a scratch assay, MSCs had a short lag phase, as the linear phase was entered rapidly and reached saturation after 20 hours (**B**) the rate MSCs migrated was determined by the linear phase, after a baseline correction was performed using the 0 hour data point. The migration distance of MSCs at (**C**) 6 hours and (**D**) 9 hours was reproducible between different experiments.

Next, the scratch assay was carried out on MSCs from 8 different donors; 4 donors with the AA genotype and 4 donors with the GG genotype. There was a non significant difference ( $p=0.4$ ) between the two genotypes for rs3825807, however it was observed that MSCs with the AA genotype migrated faster than the GG genotype (**Figure 6.14A, B**). To determine if the effect of rs3825807 could be recapitulated in SMCs, MSCs were differentiated into SMCs, and a scratch assay performed. It was observed upon differentiation the rate of migration dropped markedly. Analysis of the migration between differentiated SMCs with different rs3825807 genotypes, showed that there was no significant difference ( $p=0.6$ ) between the AA and GG genotype (**Figure 6.14C**).

A power calculation was carried out to determine if the migration study was adequately powered. The data from 8 donors was used, based on the difference between genotype groups observed at 7 hours for MSCs, and 36 hours for differentiated SMCs, as this is where the difference was the greatest (**Figure 14A, C**). The mean and SD were used to calculate the sample size. Currently the cell migration study had 16.2% and 10.6% power using data from MSCs and differentiated SMCs, respectively. Calculations showed in order to validate the difference seen between genotype groups, MSCs and differentiated SMCs, required 26 and 48 samples in each genotype group, respectively, which would provide the study with 80% power. Genotyping data showed that there were 31 donors with the AA genotype, and 29 donors with the GG genotype for rs3825807. So, additional MSC donors could have been analysed in each genotype group, however due to time constraints I was not able to extend this study.

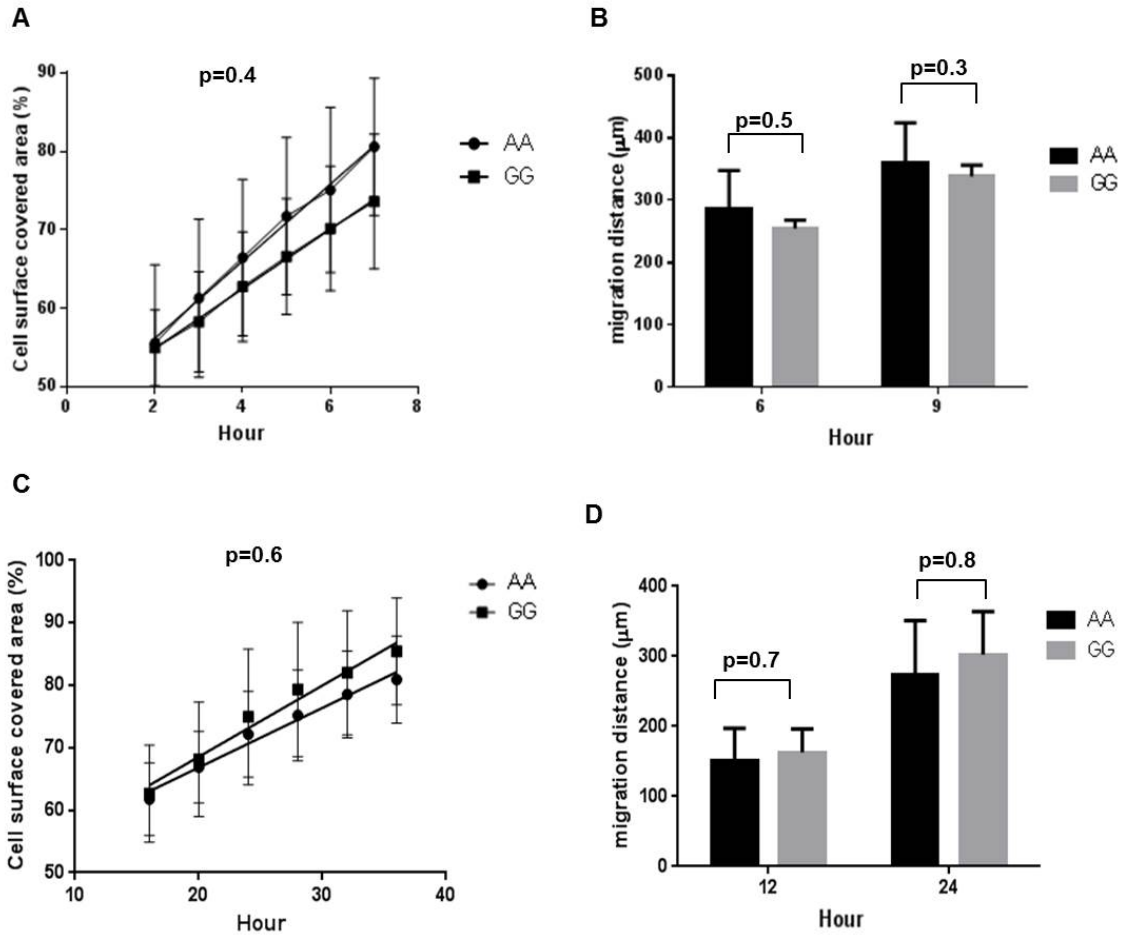


**Figure 6.14.** A scratch assay was carried out on MSCs and differentiated SMCs with the AA or GG genotype for rs3825807. For MSCs (A) the cell surface covered area between 2-7 hours and (B) the migration distance at 6 and 9 hours. For differentiated SMCs (C) the area covered by cells between 16-36 hours and (D) the migrated distance at 12 and 24 hours. Data is shown as mean  $\pm$  Standard Deviation (SD; n=4 each genotype group).

### 6.3 Discussion

Three independent GWASs have identified *ADAMTS7* to be associated with CAD. Since this discovery, researchers have aimed to understand the association of *ADAMTS7* and CAD. Mouse *ADAMTS7* knock out models have shown mouse *ADAMTS7* has a pro-atherogenic role (Bauer *et al.*, 2015; Kessler *et al.*, 2015). Recent studies assessing the effect of the CAD-associated variant, have demonstrated that rs3825807 (Ser-to-Pro substitution) affects *ADAMTS7* prodomain cleavage, COMP cleavage and vascular SMC migration *in vitro* (Pu *et al.*, 2013). The aim of this chapter was to use the *ADAMTS7* locus, as a proof of principle, to determine the use of MSCs to study CAD-related loci.

In order to recapitulate the effects of rs3825807, the expression of genes, in the proposed mechanism were investigated in MSCs and differentiated SMCs. MSCs expressed *ADAMTS7*, and upon differentiation into SMCs, expression significantly increased (2.4-fold). This result is not consistent with existing findings. The SMC differentiation medium contained TGF- $\beta$ 1, which has been shown to cause a down-regulation of *ADAMTS7* in cultured vascular SMCs (Wang *et al.*, 2009). The discrepancy may be due to the time point, at which *ADAMTS7* expression was measured. Wang *et al.*, (2009), in addition to analysing *ADAMTS7* mRNA levels, looked at *ADAMTS7* protein expression in the carotid arteries of a rat balloon injury model, and saw an initial decrease of *ADAMTS7* after 24 hours, before increasing at 4-7 days. Wang *et al.*, (2009) study on *ADAMTS7* mRNA levels in cultured vascular SMCs, do not state the time point of analysis, and may have analysed *ADAMTS7* expression at 24 hours, where protein expression does decrease as demonstrated in the experiment on *ADAMTS7* in the carotid arteries. Our study looked at gene expression after a 6 day treatment with TGF- $\beta$ 1. The primary reason to investigate *ADAMTS7* was to check the gene was still expressed upon SMC differentiation, so further analysis of the *ADAMTS7* gene and protein could be undertaken in differentiated SMCs.

*ADAMTS7* enables vascular SMC migration, by degrading the ECM protein COMP (Pu *et al.*, 2013; Wang *et al.*, 2009). So, *COMP* expression was

investigated. Interestingly MSCs did not express *COMP*, but upon SMC differentiation, *COMP* was highly expressed. *COMP* is expressed by vascular SMCs (Riessen *et al.*, 2001) and interacts with  $\alpha_7\beta_1$  integrin to keep vascular SMCs in a contractile state (Wang *et al.*, 2010). Knockdown of *COMP* by siRNAs resulted in the loss of a contractile phenotype (Wang *et al.*, 2010). The upregulation of *COMP* in differentiated SMCs, further supports our findings from Chapter 5, that upon SMC differentiation, cells had taken on a contractile SMC phenotype, albeit immature.

A later experiment for this chapter was to investigate the effect of rs3825807 on cell migration, which involved re-seeding differentiated SMCs for a scratch assay, after the 6 day SMC differentiation step. After this step, I wanted to establish if cells were still SMC-like, still expressed *ADAMTS7*, and to investigate the effect of withdrawing TGF- $\beta$ 1 from the SMC differentiation medium. After cells were subjected to the 6 day SMC differentiation treatment, they were seeded at  $4 \times 10^4$  cells/cm<sup>2</sup> into new wells, and treated for another 7 days with SMC differentiation medium without TGF- $\beta$ 1 or SMC differentiation medium with TGF- $\beta$ 1. An increase in *ACTA2* was observed, which may have been due to the change in culture conditions, as cells went from a very confluent to a less dense environment. The effect of TGF- $\beta$ 1 is dependent on the cellular environment. TGF- $\beta$ 1 is a pleiotropic factor, it binds and activates type I and II receptors to signal through SMAD- dependent and independent pathways (Shi & Massagué, 2003). The activation of these pathways depends on cell type, cell density and culture conditions (Hneino *et al.*, 2009; Orlandi *et al.*, 1994).

As *ADAMTS7* was expressed in MSCs and differentiated SMCs the effect of rs3825807 on *ADAMTS7* gene expression was investigated. There was no difference in *ADAMTS7* expression between cells with the AA and GG genotype, which is consistent with Pu *et al.*, (2013), who also saw no association of rs3825807 on *ADAMTS7* expression in vascular SMCs. Apart from rs3825807, two further SNPs; rs1994016 and rs4380028 were identified as lead SNPs in the other two GWASs (Reilly *et al.*, 2011; C4D Genetics Consortium, 2011). Rs1994016 is in strong LD ( $r^2 > 0.8$ ) with rs3825807, it locates to intron 8 of *ADAMTS7*. Rs4380028 sits in an intergenic region 7.6kb

upstream of *ADAMTS7* and is in  $r^2$  of 0.5 with rs3825807, which is suggestive that there may be more than one signal at the *ADAMTS7* locus. **Figure S2** is a graphical representation of the LD at 15q21. The first haploblock includes rs3825807 and rs1994016, the second haploblock includes rs4380028. This evidence combined with the low to moderate linkage with rs3825807 and rs1994016, suggests that rs4380028 may represent an independent signal at this locus, and may be worth investigating independently.

Rs3825807, rs1994016 and rs4380028 have been analysed in a large eQTL dataset; the Multiple Tissue Human Expression Resource (MuTHER) study (n=850). In lymphoblastoid cell lines, a significant association was seen with *ADAMTS7* expression, where the CAD risk allele associated with higher *ADAMTS7* expression (Grundberg *et al.*, 2012). But it still remains to be investigated, if eQTLs exist for *ADAMTS7* in relevant human cells and vascular tissue, such as aortic SMCs or coronary lesions.

An additional SNP at the *ADAMTS7* locus has been identified to be significantly associated with CAD. The C4D Genetics Consortium (2012) conducted a larger study comprising of 63,746 CAD cases and 130,681 controls. The study confirmed the CAD-associated *ADAMTS7* locus, however rs7173743 ( $r^2= 0.4$  with rs3825807) was identified as the lead SNP. Rs7173743 is also located 38kb upstream of *ADAMTS7* in an intergenic region.

To recapitulate the functional effects of the Ser-to-Pro (A to G) substitution in the *ADAMTS7* prodomain shown by Pu *et al.*, (2013), Western blot was carried out. Upon activation, the *ADAMTS7* prodomain is cleaved off, so by measuring the amount of prodomain indicates the level of mature *ADAMTS7*. An *ADAMTS7* antibody (ab45044) was used that specifically bound at the prodomain. An *ADAMTS7* overexpression study verified the *ADAMTS7* expression pattern seen in MSCs. Alternatively a blocking peptide experiment could have been performed or the band of interest sliced from the gel and prepared for mass spectrometry analysis. These experiments would have confirmed the specificity of the *ADAMTS7* antibody.

Western blot analysis showed genotype had no effect on the amount of cleaved *ADAMTS7* prodomain in MSC conditioned media. However in

conditioned media from differentiated SMCs, cells with the GG genotype overall had more cleaved ADAMTS7 prodomain present than cells with the AA genotype. But upon quantification, there was a non significant difference in the ADAMTS7 prodomain band intensity between the two genotypes. Western blot showed one of the donors with the AA genotype displayed more ADAMTS7 prodomain than the other two donors with the AA genotype (**Figure 6.11C**). This difference observed within AA genotype, maybe be due to rare variants within *ADAMTS7*, that also affect ADAMTS7 prodomain processing, that have not yet been discovered.

Cell migration is a key process for normal development and maintenance of an organism. It is also important in disease processes such as atherosclerosis. Upon vascular injury, SMCs and monocytes migrate into the intima space within the vessel, which results in atherosclerotic and restenotic lesion formation (Schwartz, 1997). Pu *et al.*, (2013) show rs3825807 affects cell migration of vascular SMCs *in vitro*, so I aimed to recapitulate this finding. Scratch assays were performed which reveal properties of a cells migratory behaviour. Data from the scratch assay was analysed in two different ways. Measuring the area covered by cells over time, than measuring the distance cells migrated is a more accurate analysis, as it is not affected by individual migrating cells. However, both forms of analysis were carried out. It was observed, MSCs of the AA genotype migrated faster than cells of the GG genotype, but in differentiated SMCs, the observation was reversed. However, there was a non significant effect of the rs3825807 genotype on cell migration.

A power calculation was carried out, to determine if the study was adequately powered. For MSCs, 26 individuals would have been required for 80% power, to reject the null hypothesis (there is no relationship between genotypes). For differentiated SMCs, 48 individuals would have been required for 80% power. So the cell migration study may have benefited from a larger sample number, as a smaller difference needs a larger sample group to validate it.

An explanation for why a difference in cell migration was not observed between the two genotype groups in MSCs is because MSCs do not express

COMP. The mechanism for ADAMTS7-mediated migration occurs when mature ADAMTS7 degrades COMP. So the effect of rs3825807 on cell migration would not have been seen, as there was no COMP for differential amounts of ADAMTS7 to act on and degrade.

A potential reason why the complete recapitulation of the effect of rs3825807 was not seen in differentiated SMCs is maybe due to the finding that differentiated SMCs were of an immature phenotype. Pu *et al.*, (2013) demonstrated the significant effects of rs3825807 in primary vascular SMCs. Our immature differentiated SMCs may have been of a different phenotype to vascular SMCs used by Pu *et al.*, (2013). If so, the repertoire of proteins and characteristics of the cells may have been different, and may have altered the functional effect of the variant. As an extra component may have been present in the vascular SMCs used by Pu *et al.*, (2013) that contributed to the genotype-specific effect, which was not present in differentiated SMCs.

Alternatively, rs3825807 may exert its effects on ADAMTS7 in another manner. Furin is present in virtually all cells (Thomas, 2002; Denault and Leduc, 1996), and is most likely the preferred pro-ADAMTS7 convertase (Somerville *et al.*, 2004). However, as I did not see differential ADAMTS7 processing according to genotype in MSCs and differentiated SMCs, the variant may influence ADAMTS7 in a furin-independent manner. The majority of ADAMTS prodomains have consensus sites for the attachment of N-linked oligosaccharides (Koo *et al.*, 2006), where ADAMTS7 has a single N-glycosylation site in the prodomain (Somerville *et al.*, 2004). Glycosylation is very important for a wide range of biological processes, ranging from recognition of a protein to controlling the conformation of a protein. Thus rs3825807 may affect the glycosylation of the ADAMTS7 prodomain, resulting in differences in post-translational processes, which may warrant further investigation.

It is important to note that if the effect of the variant is specific to vascular SMCs, then the efficiency of SMC differentiation may have added an additional layer of variation into the assay, and may have masked the effects of rs3825807. Immunofluorescence analysis of differentiated SMCs demonstrated

approximately >90% of cells were positive for expression of  $\alpha$ -SMA and calponin in cells from three different donors (**Chapter 5, Section 5.2.2.3**). However this is not a quantitative method. The SMC differentiation of MSCs across ten donors, showed some variability in *ACTA2* gene expression, however protein expression of SMC markers was not quantified in these cells from the ten different donors. Future work should look to quantify the level of *ACTA2* and *CNN1* markers by flow cytometry to determine the efficiency and reproducibility of the SMC differentiation protocol.

### 6.3.1 Future work

Scratch assays have many disadvantages for measuring cell migration. Creating a 'scratch' causes damage to cells, removal of the ECM components and can result in the leakage of intracellular contents, which may obscure the interpretation of the data. The wound size and shape is also very variable. This variation may mask any effects of the variant, and complicate data analysis. Alternative methods may be required to measure and quantify migration more accurately. The Boyden Chamber assay is a useful tool to study cell migration and invasion. Cells are placed into an upper compartment, which migrate through a microporous membrane into a lower compartment, which contains a chemoattractant. The cells are incubated for a period of time, and the membrane fixed and stained. The number of cells that have migrated through the membrane is determined. This method may provide an alternative approach to studying the effect of rs3825807 on migration.

It is likely the true disease-related effects of the variants are only seen under disease-specific conditions. During the progression of an atherosclerotic lesion, SMCs migrate from the tunica media into the tunica intima, which is regulated by pro-inflammatory cytokines such as TNF- $\alpha$  and PDGF-BB. This environment may need to be recreated, to capture the true effects of the variant. To support this idea, Bauer *et al.*, (2015) showed that a 24 hour TNF- $\alpha$  treatment on *ADAMTS7*<sup>-/-</sup>VSMCs compared to WT cells, showed a reduction in migration, while untreated cells showed no difference in migration. This supports the notion that the effect of *ADAMTS7* on vascular SMC phenotype is

revealed under inflammatory stress conditions. If a cytokine treatment was to be incorporated into the experimental design, it would require further characterisation of differentiated SMCs, and the determination of the effect on *ADAMTS7* expression.

Abnormal re-endothelialization is inversely correlated with neointimal formation during post-injury restenosis and atherosclerosis. Kessler *et al.*, (2015) demonstrated that *ADAMTS7* inhibits endothelial recovery upon injury, as it inhibits endothelial cell proliferation and migration, in addition to its role in vascular SMC migration. Therefore it may be important to study rs3825807 in endothelial cells, to determine if it has an effect on endothelial proliferation and migration.

### **6.3.2 Conclusion**

As a proof of concept study, I aimed to recapitulate the effect of rs3825807 on *ADAMTS7* prodomain processing and vascular SMC migration, to test the use of MSCs in modelling CAD-related variants. In MSCs and differentiated SMCs, a genotype effect of rs3825807 on *ADAMTS7* prodomain processing or cell migration was not seen. A power calculation showed larger n numbers were required for the investigation of rs3825807 on cell migration. These results suggest that MSCs as an *in vitro* model to investigate CAD-related variants may not be practical.

# **Chapter 7- Discussion**

Since 2007, many GWASs have been conducted to identify genetic variants that are associated with CAD. These studies have resulted in 50 risk loci, more than half of which are very common; being found in over 50% of the population. 35 of these variants are not associated with intermediate risk factors, or sit in or near genes with a known cardiovascular function, which suggest they act through novel biological pathways. It is important to clearly understand how changes induced by genetic variants at the DNA level, affect susceptibility genes, which can alter molecular phenotypes and subsequently result in changes in the disease trait. The race is now on to establish the mechanistic pathways that these variants act through, in order to eventually target them for therapeutic purposes.

Atherosclerosis, the underlying pathological process of CAD, involves many different cell types' e.g. endothelial cells, monocytes, vascular SMCs that are implicated in the disease pathology (discussed in Chapter 1.2; Libby *et al.*, 2011). It is hypothesised that the risk variants act in one, or more than one of these cell types to exert their effects and contribute to disease. An *in vitro* model system is required which enables *in vitro* studies to investigate the function of CAD-associated variants in different cell types, and aid in understanding the disease pathogenesis. As primary tissue-specific cells from different individuals are difficult to obtain and are not available in large quantities, developing a genotype-specific model using stem cells that have the ability to differentiate into CAD-relevant cell types, is a possible solution.

There are three types of stem cells; ESCs, iPSCs and adult stem cells. ESCs are pluripotent, and can give rise to almost any cell type in the human body. ESCs are derived from the inner cell mass of a blastocyst, which is an early-stage preimplantation embryo that is destroyed upon ESC isolation. Thus the use of ESCs is clouded by ethical issues. For this reason, using ESCs to create a cell bank is undesirable, problematic, in addition to requiring complex culture conditions to maintain ESCs. iPSCs represent an alternative stem cell to use to create genotype-specific disease models. Four transcription factors (Oct4, Sox2, Klf4 and c-Myc) are able to create pluripotent stem cells from somatic cells (Takahashi *et al.*, 2007). However the generation of iPSCs is a long, labour intensive process (takes > 1 month) with low efficiency, for example

less than 1% of transfected fibroblasts become iPSCs (Yamanaka, 2012), however non-viral reprogramming methods have achieved efficiencies of up to 4.4% (Warren *et al.*, 2010). Also the resultant cells require careful attention during culturing. To produce over 100 different iPSC lines and investigate casual variants within the course of this PhD was not practicable. However initiatives to create and bank vast numbers of iPSCs have been instigated. The UK has launched the Human Induced Pluripotent Stem Cell Initiative (HIPSCI) which aims to produce iPSCs from more than 500 healthy individuals and 500 individuals with genetic disease. A second initiative is a €55.6 million project known as StemBANCC. They intend to generate 1,500 iPSC lines from 500 patients. The aim of both projects is to use iPSCs to study the effects of genetic variation on cellular phenotypes, in addition to standardise protocols for iPSC differentiation into specific cell types (Moran, 2013). These banks will provide a great resource for disease modelling in the future.

For this thesis, we decided to approach the challenge of functionally investigating CAD-associated variants by creating a MSC bank, as they also have the ability to differentiate into CAD-relevant cell types. MSCs are easily isolated from a number of different regions within the body, and are straightforward to maintain in culture. The umbilical cord was chosen as the source of isolation over other tissues for a number of reasons. Firstly, MSCs derived from the umbilical cord are biologically younger than MSCs from other sources e.g. bone marrow-derived MSCs. Also MSCs derived from the umbilical cord from different donors are biologically the same age, whereas bone marrow donors are often from all age groups, where it has been shown that an increase in donor age associates with a decline in proliferation and differentiation of MSCs (Zaim *et al.*, 2012; D'Ippolito *et al.*, 1999). Secondly, umbilical cord-derived MSCs have a primitive nature, as they biologically lie between ESCs and adult stem cells (Pappa & Anagnou, 2009; De-Miguel *et al.*, 2009), and have been reported to have a higher capacity of pluripotency than adult stem cells, demonstrated by findings that umbilical cord-derived MSCs can give rise to cells from all three germ layers (Can & Karahuseyinoglu, 2007). Thirdly, the umbilical cord is classed as medical waste, therefore is an easily available and obtainable tissue, enabling the production of a MSC bank quickly.

To create the MSC bank, MSCs were successfully derived from 114 umbilical cord samples using the explant method. Cells were characterised according to the criteria proposed by the ISCT (Dominici *et al.*, 2006) to confirm they were MSCs. Next whole-genome genotyping was performed using the Axiom™ Genome-Wide UKB WCSG Genotyping Array, to determine the genotypes of the MSC bank for complex trait-associated variants to enable future studies into complex diseases, as the use of the MSC bank is not just limited to studying CAD-associated variants. For the MSC bank, the genotype for 50 CAD-associated SNPs were determined. 37 CAD variants could be studied in our MSC bank, as there were at least 3 donors that were homozygous for the major and minor allele. For homozygote vs heterozygote studies, 49 CAD-associated SNPs would be able to be analysed.

In order to test the MSC bank as a research tool for the study of complex traits/diseases I performed two proof of principle studies. As I showed MSCs differentiated into adipocytes, I investigated if MSC-derived adipocytes could replicate eQTL findings reported in a previous study. Speliotes *et al.*, (2010) conducted a GWAS and identified 18 genetic loci that associated with BMI, and reported the functional annotation of these loci. Several loci had cis-eQTLs in adipose tissue. I chose to focus on one of these BMI-associated loci, which centred on rs3810291, and mapped to chromosome 19q13 residing in the 3' UTR of the *ZC3H4* gene. Speliotes *et al.*, (2010) reported rs3810291 significantly associated with expression of the *ZC3H4* gene in adipose tissue. In addition, the mouse homolog of *ZC3H4* is a known body weight QTL in mice (Suto *et al.*, 1998; Suto & Sekikawa 2004); suggesting *ZC3H4* is the functional gene at this locus. I chose to look at a second locus centred on rs10840106 that maps to an intergenic region on chromosome 11p15. Speliotes *et al.*, (2010) reported rs10840106 was the peak SNP (the most significant SNP associated with the gene transcript) that associated with *TRIM66* gene expression which was also located on chromosome 11p15. It was not reported as a BMI-associated variant, however I still chose to investigate rs10840106, as it had a huge effect ( $p=1.1 \times 10^{-71}$ ) on *TRIM66* expression. The expression of both genes was investigated in MSCs and MSC-derived adipocytes. Firstly there was no significant effect of the rs3810291 genotype on *ZC3H4* expression in MSCs and

MSC-derived adipocytes. However a trend was observed in the reported direction, homozygote minors (GG) showed reduced *ZC3H4* expression compared to homozygote majors (AA). The most likely explanation for not recapitulating the effect of rs3810291 on *ZC3H4* expression is due to the variability of the adipogenic differentiation, which added variation into the assay, in addition to the small sample size used. Secondly, a significant genotype effect was revealed for rs10840106 on *TRIM66* gene expression in MSCs and differentiated adipocytes. Homozygote minors showed an increase in *TRIM66* expression, in comparison to homozygote majors. However, the direction of the effect was not reported, and this information was not available elsewhere. Speliotes *et al.*, (2010) reported rs108401016 was an eQTL for *TRIM66* in blood, omental fat and liver, in addition to adipose tissue, which suggests it was not a tissue-specific effect, and hence may explain why a significant association for this variant was observed in MSCs.

Next in order to study CAD-associated variants, I first investigated the ability of our MSC bank to differentiate into CAD-relevant cell types. Numerous reports demonstrate the ability of MSCs to differentiate into hepatocytes and SMCs (Aurich *et al.*, 2006; Kang *et al.*, 2006; Stock *et al.*, 2010; Duncan, 2000; Kinoshita & Miyajima, 2002; Zaret, 2002; Kurpinski *et al.*, 2010; Gong & Niklason, 2008; Jain, 2003).

One of the original aims of this project was to obtain MSC-derived hepatocytes to conduct a proof of principle study using one of the most characterised CAD loci (1p13). Musunuru *et al.*, (2010) demonstrated the CAD-associated variant rs12740374 was responsible for the differential expression of *SORT1*, specifically in the liver. So, my aim was going to be to differentiate MSCs from genotyped donors into hepatocytes, to recapitulate the effect of rs12740374 on *SORT1* expression, to overall demonstrate the feasibility of using MSC-derived cells to model CAD. In an attempt to obtain hepatocytes, MSCs were exposed sequentially to growth factors and cytokines (detailed in **Chapter 5, Figure 5.2**). After the 23 day hepatogenic differentiation protocol, MSCs altered in morphology to a hepatocyte-like appearance, but did not show an up-regulation of hepatogenic markers, therefore these cells were not taken further for functional characterisation. As I was not able to successfully

differentiate MSC into hepatocytes, the *SORT1* proof of principle study could not be carried out. So I focused on a different CAD-associated variant in MSC-derived SMCs as an alternative proof of concept study.

Thus experiments were conducted to obtain SMCs. MSCs were differentiated towards a SMC lineage by a 6 day treatment with 10ng/ml TGF- $\beta$ 1 and 1% FBS. Differentiated cells expressed early and mid-SMC markers, produced calcium transients upon exposure to agonists, but did not contract, overall suggesting cells had taken on an immature SMC phenotype.

Next I went on to investigate whether MSC-derived SMCs are a suitable model to study CAD-associated loci, by attempting to replicate the effects of rs3825807 observed in vascular SMCs as a second proof of concept study. This variant is located in the prodomain of the protease ADAMTS7. It has been hypothesised that the Ser-to-Pro substitution caused by rs3825807 may reduce access of proprotein convertases such as furin, to cleave ADAMTS7 at the prodomain to produce mature ADAMTS7 in vascular SMCs. Subsequently it was shown that rs3825807 affects ADAMTS7 prodomain cleavage, vascular SMC migration and COMP cleavage (Pu *et al.*, 2013), and this is what I sought to replicate. Unfortunately the effect of rs3825807 on ADAMTS7 processing and cell migration was not recapitulated in differentiated SMCs. Pu *et al.*, (2013) reported a significant effect of the rs3825807 genotype on ADAMTS7 processing and vascular SMC migration, using a small sample size (n=5 each genotype group). A power calculation based on the migration data (n=4 each genotype group) I obtained suggested a much larger sample size was required to see a significant effect between genotype groups. The effect of rs3825807 on COMP cleavage was not investigated, as I was not able to recapitulate the primary genotype effect of rs3825807 on ADAMTS7 cleavage, which acts on COMP to cause differential vascular SMC migration between genotype groups.

It is of importance to note that the effect of disease-associated SNPs may only be seen under disease-related conditions. SMCs are a plastic cell type as they can switch between a contractile or synthetic phenotype (Owens *et al.*, 2004). Under normal physiological conditions SMCs have a low replication and migration rate, upon vascular disease, such as hypertension and

atherosclerosis; they dedifferentiate into cells with a high migration and proliferation rate (Yoshida & Owens, 2005; Beamish *et al.*, 2010). The migration of SMCs from the tunica media to the intima media occurs in intimal thickening during atherosclerosis, which is regulated by pro-inflammatory cytokines such as TNF- $\alpha$  and PDGF-BB, both of which up-regulate *ADAMTS7* (Wang *et al.*, 2009), suggesting the induction of *ADAMTS7* may be required to exert its maximal effects on cell migration. Support for this notion comes from a study by Bauer *et al.*, (2015) who showed that *ADAMTS7* knock-out vascular SMCs showed reduced migration compared to WT cells, but only under inflammatory stress conditions (24 hour treatment with TNF- $\alpha$ ). So it would be of interest, to treat genotype-specific differentiated SMCs with TNF- $\alpha$  before measuring cell migration between genotype groups. In addition, my results suggested the differentiated SMCs I obtained were more of a contractile phenotype. So it may be necessary to look at *ADAMTS7* in SMCs of a more synthetic/dedifferentiated phenotype, where the effect of the CAD-associated variant might be more apparent. Previous reports suggest that *ADAMTS7* modulates the vascular SMC phenotype and vascular SMC response upon inflammation during atherosclerosis (Wang *et al.*, 2009, Bauer *et al.*, 2015). Overall it is evident that *ADAMTS7* has a role to play in the pathology of atherosclerosis, and further investigation may pave the way for the development of novel therapeutics to target *ADAMTS7*.

Despite the huge amount of genetic data from continuous GWASs, there are many barriers to try and define the functional contributions of genetic variants in complex diseases. This thesis highlights the key challenges of using a stem cell model to investigate complex disease-associated variants. The primary research on MSCs has been focussed on their use in regenerative therapy, demonstrated by the numerous clinical trials (as there are over 400) involving MSCs. However, I am not aware of any disease models created using MSCs and to my knowledge, this project is the first attempt to use MSCs as a model to study genetic variants associated with complex disease. Results from this thesis suggest that to detect genotype driven effects using a stem cell based approach, either the phenotypic effect needs to be large or additional consistency needs to be applied to the differentiation protocols, as it creates an

additional level of variation in the experimental assay. For small phenotypic effects my findings show that larger sample sizes are required, which may not always be possible depending on the genetic variant under analysis. While the use of MSCs in disease modelling may represent a potentially useful approach, there are many considerations that need to be taken into account.

The starting population of MSCs are heterogeneous exhibiting donor-to-donor differences, which will have subsequent implications in downstream experiments. MSCs were isolated from the umbilical cord using an explant method, which may have induced heterogeneity into the population. Different quantities of cells initially migrated out of the tissue blocks from each donor, making it difficult to calculate the exact age of the MSCs. The passage number gives an approximate idea of the number of cellular divisions a population has gone through; however this is not a true measure of cell age. As a result, MSCs from different donors would consist of a population of cells that have gone through a different number of cell divisions. To further contribute to the heterogeneity, when MSCs migrated out of the explant fragments, DNA methylation and global gene expression changes would have occurred, in order for cells to adapt to the new environment (Wagner *et al.*, 2008; Bork *et al.*, 2010; Izadpanah *et al.*, 2008). Also, cellular differentiation may have arisen as MSCs moved from their *in vivo* environment, which would have resulted in a population with variable levels of mature cells (Wagner *et al.*, 2010). *In vitro* culture can also subject MSCs to stress conditions (such as high oxygen concentrations), which can lead to the accumulation of mutations, resulting in heterogeneity (Wagner *et al.*, 2010) in MSCs from different donors.

I previously showed that MSCs from different donors showed variable levels of adipogenic differentiation at the genetic and phenotypic level. MSCs are a naturally heterogeneous population (D'Ippolito *et al.*, 1999; Kretlow *et al.*, 2008), as described previously (**Chapter 3, Section 3.3**), and most likely consists of a population of cells with different abilities to differentiate. In addition, it has been shown that the perinatal environment can affect the MSC differentiation potential *in vitro*. For example, evidence suggests it is during the perinatal stage that MSCs commit to become pre-adipocytes. A study comparing MSCs from normal and diabetic mothers showed that cells from

diabetic mothers, showed an increase in adipogenic differentiation (Pierdomenico *et al.*, 2011). Another reason for the heterogeneity of MSC differentiation across donors may be due to sequence variation in receptors for cytokines that are involved in the differentiation process (Kajiwara *et al.*, 2012).

There are many reports of the differentiation of MSCs into numerous cell lineages, yet very few detail the efficiency of the differentiation, suggesting a low capability or reproducibility of MSCs to differentiate. In general, the differentiation protocols for MSCs are not well-developed, as there is great variability in the approaches reported by different research groups. For example, researchers show inconsistent results for SMC differentiation with PDGF-BB, as some groups demonstrate PDGF-BB induces differentiation of MSCs into SMCs (Jain, 2003). Whereas other researchers have shown it is more involved in the switch of SMCs from a contractile to synthetic phenotype (Sörby & östman, 1996; Uchida *et al.*, 1996). The majority of the studies on the molecular regulation of MSC differentiation have been undertaken *in vitro* studies; as their *in vivo* environment is poorly understood. So the results observed under *in vitro* differentiation protocols maybe as a result of cell culture. In addition, an *in vitro* environment is unlikely to supply all the extrinsic factors found *in vivo*. For example adipogenesis *in vivo* does not occur in a two-dimensional monolayer as carried out *in vitro*, so *in vitro* cultures maybe lacking the induction of specific cellular signalling pathways and the complex architecture required during *in vivo* differentiation (Turner *et al.*, 2014).

MSCs can be isolated from many different sources across the body, and may exhibit different responses to the same differentiation stimuli. As a protocol optimised on bone marrow-derived MSCs may not be reproducible on WJ-derived MSCs. Comparative analyses on the differentiation of MSCs isolated from different tissues have been conducted. Kern *et al.*, (2006) showed that under the same experimental conditions umbilical cord blood-derived MSCs did not differentiate into adipocytes, whereas bone marrow and adipose tissue-derived MSCs successfully differentiated. In addition, a comparison of MSCs from the bone marrow-, synovium-, periosteum-, adipose tissue-, and skeletal muscle-derived MSCs, showed they did not all exhibit the same potential for trilineage differentiation. For example, MSCs from the bone marrow, synovium,

and periosteum had a higher capacity for chondrogenesis (Sakaguchi *et al.*, 2005). Differences have also been seen between MSCs derived from different compartments within the umbilical cord. Ishige *et al.*, (2009) report that when compared for osteogenic potential, WJ-derived MSCs inefficiently differentiated compared to umbilical cord artery-, and vein-derived MSCs. However, their findings do not coincide with ours, as I showed WJ-derived MSCs successfully differentiated into osteoblasts.

The variation in the differentiation of MSCs from different donors is a major limitation and needs to be addressed. The variation makes it very hard to conclude results obtained from a disease model, as it does not quantitatively characterise differentiation methods or the resultant cultures. Our own observations showed upon adipogenic differentiation of MSCs from ten different donors, variability was seen at the genetic (mRNA expression) and cellular level (lipid droplet composition). Looking at the effects of a genetic variant in these populations, may be obscured by the variation in differentiation efficiency, especially if the gene under investigation is expressed in the differentiated cell type but not in MSCs, as the effect of the gene will be diluted by the heterogeneous population. Overall, better methods to quantitatively measure and purify (using methods such as fluorescence activated cell sorting (FACS) or magnetic bead isolation using cell-specific markers) resultant cells after the differentiation process is what is required for the stem-cell field.

The major research efforts in the stem cell field focus on iPSCs to derive required cell types. Unlike MSCs, reports on iPSC differentiation demonstrate efficiencies of cell lineage-specific differentiation. For example, Cheung *et al.*, (2012) and Rashid *et al.*, (2010) reported more than 80% of iPSCs efficiently differentiated into mature vascular SMCs and hepatocytes, respectively, so iPSCs may represent a better cell type to use. However, as seen with MSCs, differentiated iPSCs do not always fully resemble adult counterparts. For example, iPSC-derived cardiomyocytes resemble fetal cardiomyocytes based on sarcomeric morphology and ion channel structure. Also they do not form organised intracellular T-tubules, implicated in action potential propagation and calcium flux (Novak *et al.*, 2012; Gherghiceanu *et al.*, 2011; Hoekstra *et al.*, 2012).

iPSCs have been used to study diseases *in vitro*, where they have been used to model Mendelian disorders successfully. iPSCs generated from dermal fibroblasts from patients with FH have been successfully differentiated into hepatocytes, and were found to recapitulate key pathological features of FH, a deficiency in LDL receptor-mediated cholesterol uptake, and increased lipid and glycogen accumulation (Rashid *et al.*, 2010). There are numerous studies using iPSCs to model Mendelian diseases (Sterneckert *et al.*, 2014), however to my knowledge there are no reports on iPSCs being used to study the effects of disease-associated genetic variants. This further highlights the difficulties that face scientists in the post-GWAS era in developing an appropriate disease model to aid in understanding genetic variants that associate with disease.

To use the MSC bank may be feasible to study common CAD variants e.g. SNPs at *ADAMTS7*. However, for rare variants e.g. *HDAC9* there would not be enough individuals ( $n \geq 3$ ) in each genotype group for a comparative study. Also if the effect of a genetic variant is subtle or the noise caused by the genetic background masks the effects of the variant, large numbers would be required for each genotype group to observe a significant effect, which may not be possible for other typed SNPs (e.g. *EDNRA*, where there is a maximum of 5 donors in each genotype group). The variation between donors, the variation in differentiation, on top of the variation in genetic background makes investigating individual risk loci very difficult.

To overcome these problems, genome editing would be a powerful technique to apply to investigate these loci, and could be applied to loci studied in this thesis. Genome editing techniques enable the generation of an isogenic cell line pair that differs only at the genome position of interest, which allows the background variation to be controlled for. It is a relatively novel method, but has great potential as a technology to study functional variants and genes. The use of genome editing technologies combined with stem cells (such as iPSCs), as the starting cell type is a superior study design. Using genome editing methods to create the change of interest (e.g. SNP) in the iPSC genome, and then simultaneously differentiate them into CAD-relevant cell types (vascular SMCs, endothelial cells, monocytes) would allow the analysis of the CAD-associated variants in different cell types, in an isogenic system. For example, rs3825807

within *ADAMTS7* could be studied in vascular SMCs differentiated from iPSCs. This approach will certainly be used more rapidly in the field of CAD genetics.

As mentioned previously, CAD is a leading cause of morbidity and mortality worldwide. In addition, in 2011 the cost of CAD to the NHS was around £6.7 billion (British Heart Foundation, 2012), and overall costs the UK economy approximately £30 billion a year (Scarborough *et al.*, 2010). The identification of part of the genetic component of CAD (as genetic variants identified so far explain less than 10.6% of the known heritability for CAD (Deloukas *et al.*, 2013)), will aid in understanding novel pathways for CAD, and provide an opportunity to potentially aid in therapeutic intervention, in turn reducing the medical, social and economic burden caused by CAD.

From the outset of this project, the aim was to develop an *in vitro* disease model to study CAD-associated genetic variants. If we can identify the proteins that genetic variants act on, then we can gain a better understanding of the biological mechanisms contributing to the pathogenesis of CAD. For example, the identification of the CAD-associated locus at 1p13 led to the work by Musunuru *et al.*, (2010), who demonstrated that *SORT1* is a novel CAD gene, where a single variant (rs12740374) results in a change of LDL-C levels, and therefore a change in the risk of CAD. At the moment the identification of CAD risk loci have a minute impact on the clinical management of CAD. Epidemiological studies are required to determine whether genetic variants can predict disease in an individual, and if they are better to predict disease, than conventional algorithms already in use e.g. Framingham Risk Score calculator. To identify the causative genes and the respective molecular targets to develop novel therapies will be the challenge for the next few decades, which will hopefully one day be used against the fight to prevent and treat CAD.

## 7.1 Conclusion

Since the first wave of GWASs in 2007, numerous genetic loci have been discovered that associate with CAD. In this project I set out to explore the use of MSCs as a model to study CAD variants. I focussed on carrying out two

different proof-of-concept studies, using variants where the functional effect had previously been reported, not specific to CAD. Firstly previous reports showed rs3810291 associated with BMI, and acted as an eQTL for *ZC3H4* in adipose tissue. I sought to recapitulate the latter finding using MSC-derived adipocytes, but did not see a significant genotype effect. Additional analysis at a second locus (rs10840106), which had been reported to associate with *TRIM66* expression, did replicate in MSCs and MSC-derived adipocytes. Secondly I aimed to recapitulate the effects of the *ADAMTS7* locus, focusing on rs3825807 which affects *ADAMTS7* prodomain cleavage and vascular SMC migration. Unfortunately, I was not able to repeat the effect of rs3825807 in differentiated SMCs.

Overall findings from the *TRIM66* locus suggest that MSCs may be robust enough to detect the effects of variants on genetic effects such as mRNA levels. However the findings on the *ADAMTS7* locus suggest that understanding the effect of variants on cellular phenotypes is a much more complicated process. There are many technical challenges, such as ill-defined differentiation protocols, that remain to be overcome in order to successfully use MSCs to model disease. However as the differentiation protocols are improved, the practicality of using MSCs as a model will increase.

# Appendix





14. The Recipient shall collect and transport the Material under the direction of the ANCT Manager and the Material shall be responsibility of the Recipient from the time of collection.
15. This Material Transfer Agreement shall be valid for one year following the date of signature by Anthony Nolan.
16. Invoices shall be issued by Anthony Nolan following each Material collection which shall be paid by the Recipient within 30 days to the payment address notified on the invoice.
17. The Recipient is responsible for any claims or liabilities which arise from the use of the Material.

**SIGNED**  
For and on behalf of  
**Anthony Nolan**



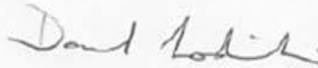
.....  
Duly Authorised Signatory

**NAME** Dr Susana G Gomez

**POSITION** Cord Blood Bank  
Lab Manager

**DATE** 26/09/2012

**SIGNED**  
For and on behalf of  
**Recipient**



.....  
Duly Authorised Signatory

**NAME** Dr David Lodwick

**POSITION** Lecturer

**DATE** 7/9/12

**Figure S1. The Anthony Nolan Cord Blood Bank Material Transfer Agreement.**

HOSPITAL NUMBER: \_\_\_\_\_ EDoB: \_\_\_\_\_

F-F1-2 Consent Form 2

INSTRUCTIONS: PLEASE PUT A TICK IN APPLICABLE BOXES  
AND ANSWER TO THE BEST OF YOUR KNOWLEDGE

	Yes	No
1 Is this a surrogate pregnancy (e.g. you are carrying the child to be raised by another couple)?		
2 Have you or the baby's biological father ever been infected by HIV, Hepatitis B or C, HTLV?		
3 Have you ever had malaria?		
<i>(Instructions for collector: If answer to 1, 2 or 3 is 'Yes' or if there is documentary evidence of these arrangements or infections, please halt process and DO NOT continue consenting and DO NOT collect)</i>		
4 Have you ever received hormones derived from the human pituitary gland (such as growth hormones, follicle stimulating hormone, Luteinising hormone, Thyroid stimulating hormone) or been a recipient of grafts (transplanted tissue) of cornea, sclera (both parts of the eye) or dura mater (part of brain / spinal cord)? If 'Yes'; please give details:		
5 Have you ever undergone infertility treatment with hCG (also known as human chorionic gonadotropin/ gonadotrophin)?		
6 Have you ever undergone brain (neuro) surgery?		
7 Have you ever been diagnosed with Creutzfeldt-Jakob disease, or variant Creutzfeldt-Jakob disease (also known as CJD, vCJD, human mad cow disease or human scrapie)?		
8 Have you ever received a transplant with tissue or organs including those from non-human (e.g. pig heart valve) origin?		
9 Have you ever been given money for sex?		
10 Have you ever injected yourself with recreational or body building drugs?		
11 Has anyone you have had sex with within the last 12 months injected themselves with recreational or body building drugs?		
12 Have you had sex with a known haemophiliac or anyone with a blood disorder?		
13 Have you had sex with a man who has ever had sex with another man?		
14 Have you had sex with anyone, no matter what their race, who has been sexually active in the parts of the world where HIV/Aids is common?		
15 Have you had sex with anyone, in the previous 12 months who may be HTLV positive, or may be a hepatitis B/C carrier?		
16 Have you had Chicken pox, shingles, or toxoplasmosis during pregnancy?		
17 In the previous 12 months, have you received a 'live' vaccine e.g. Rubella or Yellow Fever? If 'Yes'; please name/give target disease of vaccine?		
18 Have you had any acupuncture, tattoos or body piercing within the last 4 months? If 'Yes' for acupuncture; Where was this performed and what was the name of the person performing the acupuncture?		
19 Have you received a blood transfusion or blood derived product since 1980?		
20 Do you have a history of disease of unknown origin, or that could not be diagnosed?		
21 Do you or the baby's biological father have a history of rapid progressive dementia or degenerative neurological disease (e.g. Parkinson's or Alzheimer's disease), including those of unknown origin?		
22 Have you travelled abroad in the previous 12 months? If 'Yes'; which country?		
23 Were you born in or have you ever, at any time of your life lived in Africa, Central America, Asia, or the Middle East for a period longer than 6 months? If 'Yes'; which country?		
24 Do you, your sexual partner or your parents originate from: the Caribbean, Japan, South America, or Africa? If 'Yes'; which country?		

**COMMENTS**

Woman's name and signature: \_\_\_\_\_

Dedicated cord collector's name and signature: \_\_\_\_\_

Date: \_\_\_\_\_

Date sent to the ANCTC: \_\_\_\_\_

HOSPITAL NUMBER: \_\_\_\_\_

EDoB: \_\_\_\_\_

F-F1-2 Consent Form

25. In the table below, please check the boxes that apply to you and biological relatives (i.e. relatives by blood):

	YOU			BIOLOGICAL FATHER			YOUR OR THE FATHER'S BIOLOGICAL BROTHERS OR SISTERS			BABY'S MATERNAL GRANDPARENTS			BABY'S PATERNAL GRANDPARENTS			BABY'S BIOLOGICAL BROTHER OR SISTER		
Have you or your family members ever suffered from a malignant disease (Cancer) e.g. Hodgkin's lymphoma, thyroid cancer, Leukaemia etc.? <i>If 'Yes' please write the disease below</i>	Yes <input type="checkbox"/>	No <input type="checkbox"/>	Don't know <input type="checkbox"/>	Yes <input type="checkbox"/>	No <input type="checkbox"/>	Don't know <input type="checkbox"/>	Yes <input type="checkbox"/>	No <input type="checkbox"/>	Don't know <input type="checkbox"/>	Yes <input type="checkbox"/>	No <input type="checkbox"/>	Don't know <input type="checkbox"/>	Yes <input type="checkbox"/>	No <input type="checkbox"/>	Don't know <input type="checkbox"/>	Yes <input type="checkbox"/>	No <input type="checkbox"/>	Don't know <input type="checkbox"/>
Have you, or your family ever suffered from a blood disorders e.g. Glucose-6-phosphate dehydrogenase deficiency (G6PD), Spherocytosis, thalassaemia, thrombocytopenia, sickle cell disease, Chronic granulomatous disease, Hypoglobulinemia? <i>If 'Yes' please write the disease below</i>	Yes <input type="checkbox"/>	No <input type="checkbox"/>	Don't know <input type="checkbox"/>	Yes <input type="checkbox"/>	No <input type="checkbox"/>	Don't know <input type="checkbox"/>	Yes <input type="checkbox"/>	No <input type="checkbox"/>	Don't know <input type="checkbox"/>	Yes <input type="checkbox"/>	No <input type="checkbox"/>	Don't know <input type="checkbox"/>	Yes <input type="checkbox"/>	No <input type="checkbox"/>	Don't know <input type="checkbox"/>	Yes <input type="checkbox"/>	No <input type="checkbox"/>	Don't know <input type="checkbox"/>
Have you, or your family ever suffered from an autoimmune disease e.g. Arthritis, Ulcerative colitis, Crohns disease, Systemic Lupus Erythematosus (SLE), Myasthenia Gravis, Diabetes, Multiple Sclerosis? <i>If 'Yes' please write the disease below</i>	Yes <input type="checkbox"/>	No <input type="checkbox"/>	Don't know <input type="checkbox"/>	Yes <input type="checkbox"/>	No <input type="checkbox"/>	Don't know <input type="checkbox"/>	Yes <input type="checkbox"/>	No <input type="checkbox"/>	Don't know <input type="checkbox"/>	Yes <input type="checkbox"/>	No <input type="checkbox"/>	Don't know <input type="checkbox"/>	Yes <input type="checkbox"/>	No <input type="checkbox"/>	Don't know <input type="checkbox"/>	Yes <input type="checkbox"/>	No <input type="checkbox"/>	Don't know <input type="checkbox"/>
Do you or your family suffer from any metabolic/storage diseases e.g. Tay Sachs, Prophyria, Hunter syndrome, Krabbe disease? <i>If 'Yes' please write the disease below</i>	Yes <input type="checkbox"/>	No <input type="checkbox"/>	Don't know <input type="checkbox"/>	Yes <input type="checkbox"/>	No <input type="checkbox"/>	Don't know <input type="checkbox"/>	Yes <input type="checkbox"/>	No <input type="checkbox"/>	Don't know <input type="checkbox"/>	Yes <input type="checkbox"/>	No <input type="checkbox"/>	Don't know <input type="checkbox"/>	Yes <input type="checkbox"/>	No <input type="checkbox"/>	Don't know <input type="checkbox"/>	Yes <input type="checkbox"/>	No <input type="checkbox"/>	Don't know <input type="checkbox"/>
Do you or your family suffer from any 'other' diseases e.g. Cystic fibrosis, Duchene's Muscular Dystrophy Myasthenia gravis, Celiac disease? <i>If 'Yes' please write the disease below</i>	Yes <input type="checkbox"/>	No <input type="checkbox"/>	Don't know <input type="checkbox"/>	Yes <input type="checkbox"/>	No <input type="checkbox"/>	Don't know <input type="checkbox"/>	Yes <input type="checkbox"/>	No <input type="checkbox"/>	Don't know <input type="checkbox"/>	Yes <input type="checkbox"/>	No <input type="checkbox"/>	Don't know <input type="checkbox"/>	Yes <input type="checkbox"/>	No <input type="checkbox"/>	Don't know <input type="checkbox"/>	Yes <input type="checkbox"/>	No <input type="checkbox"/>	Don't know <input type="checkbox"/>

Woman's name and signature: \_\_\_\_\_

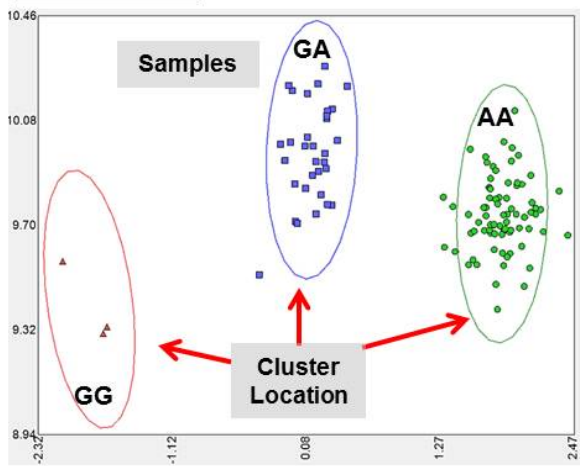
Dedicated cord collector's name and signature: \_\_\_\_\_

Date: \_\_\_\_\_

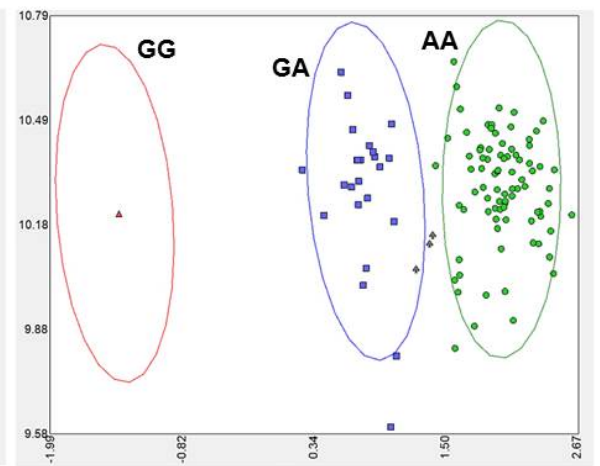
Date sent to ANCTC: \_\_\_\_\_

Figure S2. The hospital consent form completed by the baby's mother.

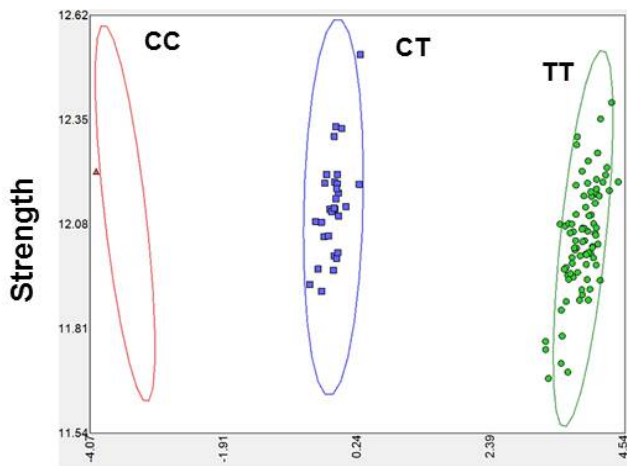
**SNP: rs599839**



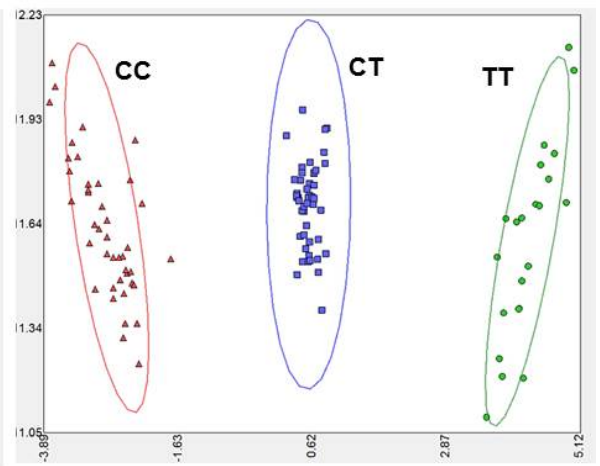
**rs17114036**



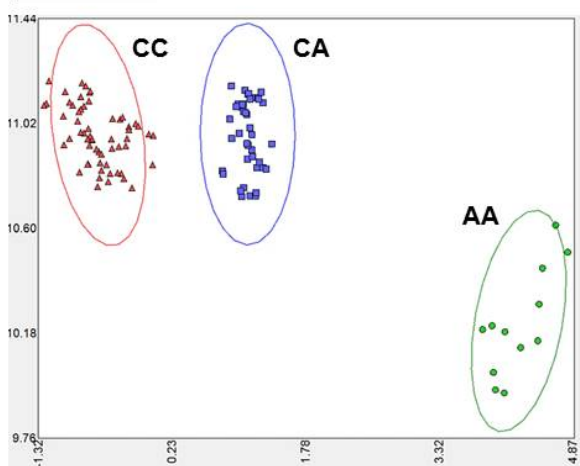
**rs11206510**



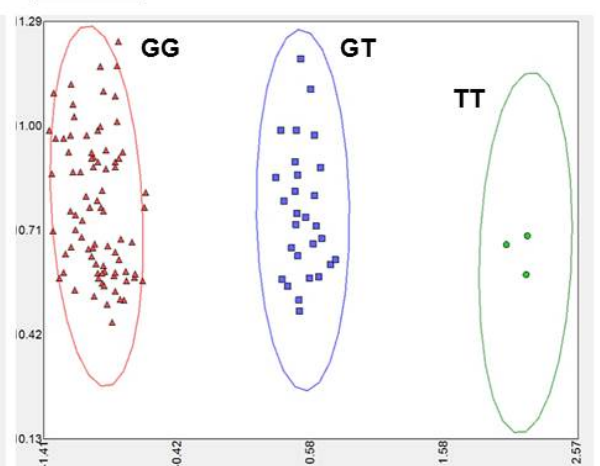
**rs4845625**



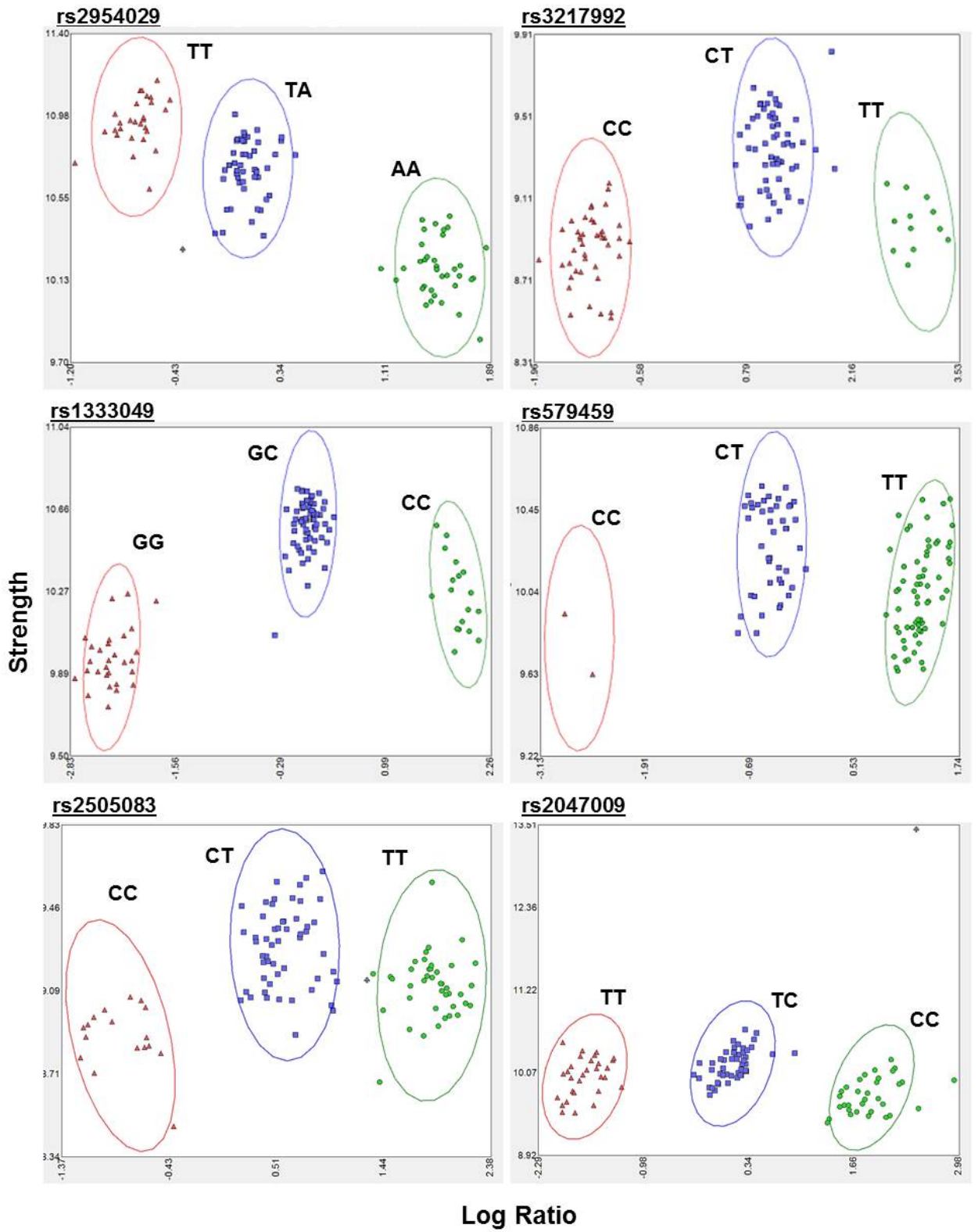
**rs17465637**



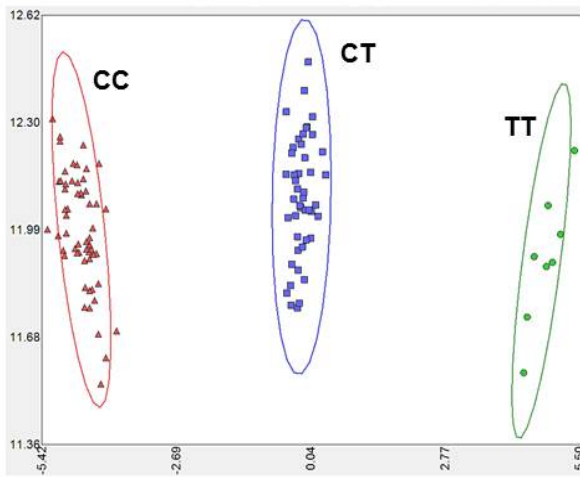
**rs515135**



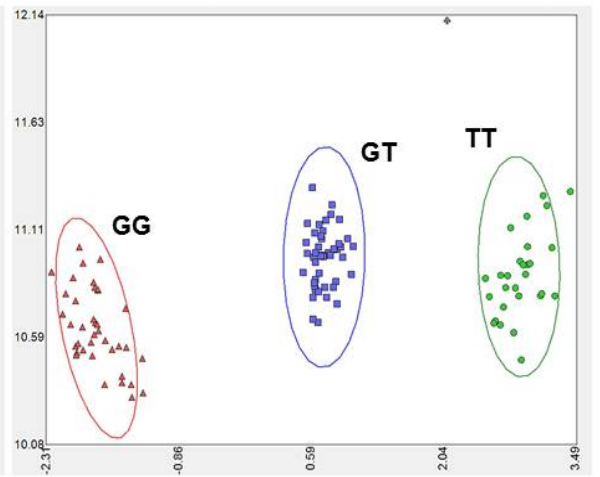
**Log Ratio**



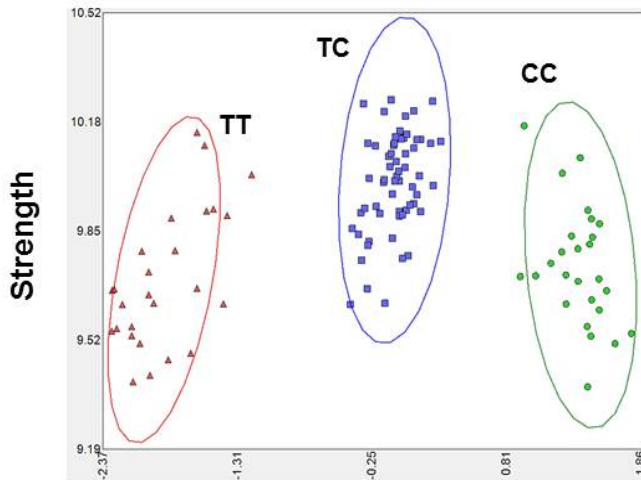
**rs6544713**



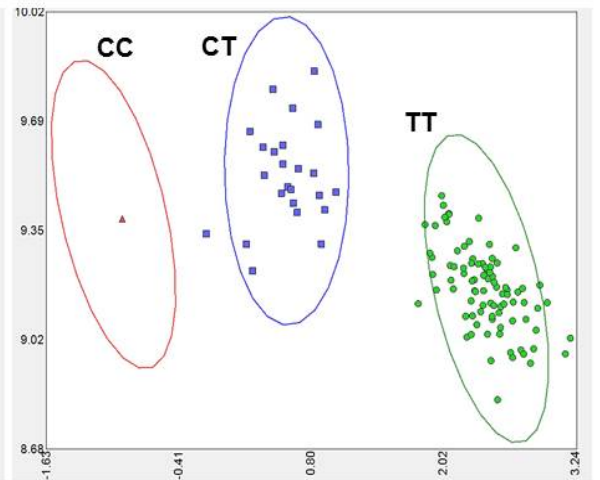
**rs1561198**



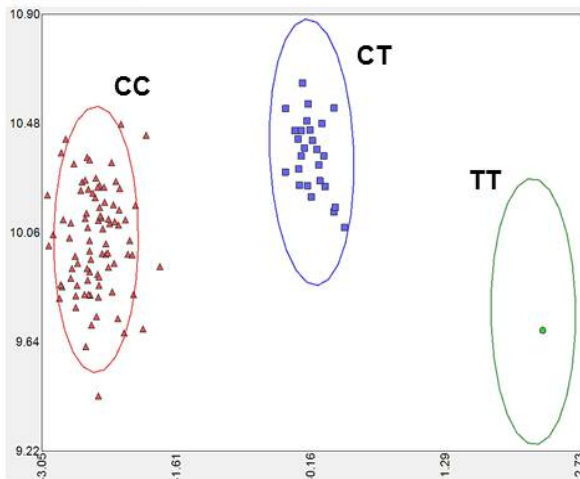
**rs2252641**



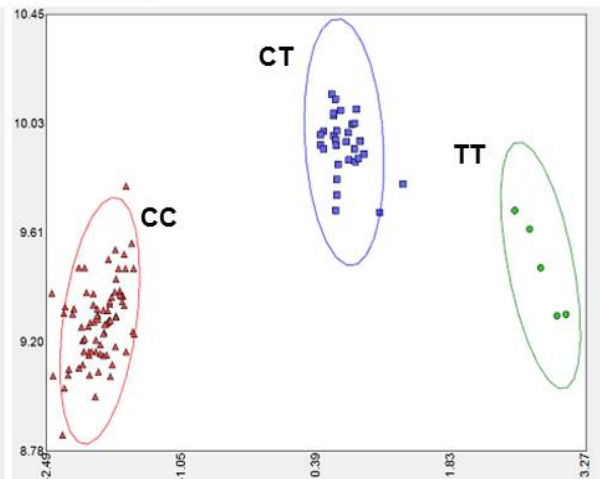
**rs6725887**



**rs9818870**

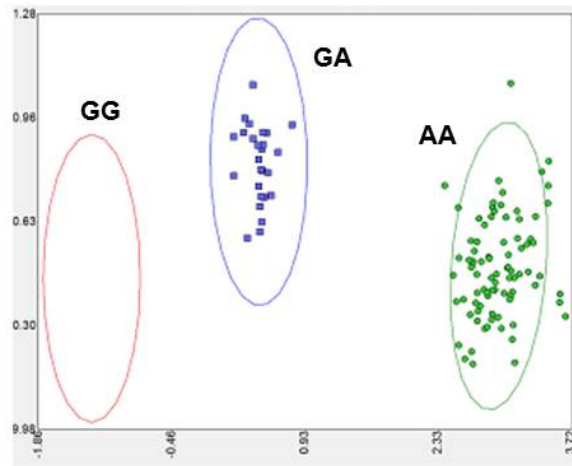


**rs1878406**

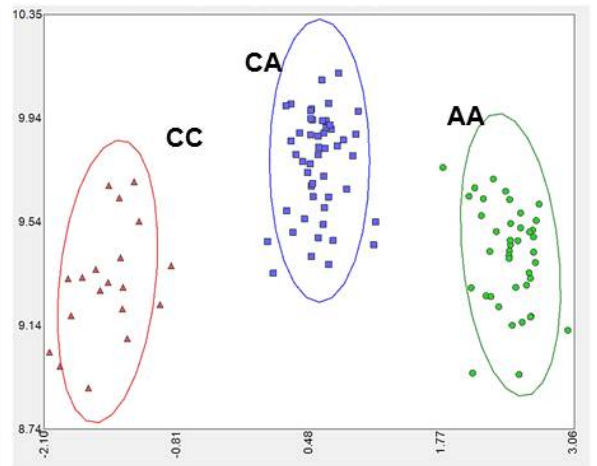


**Log Ratio**

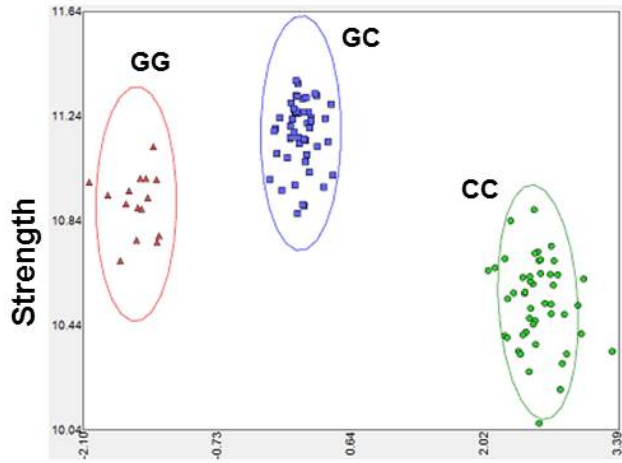
**rs273909**



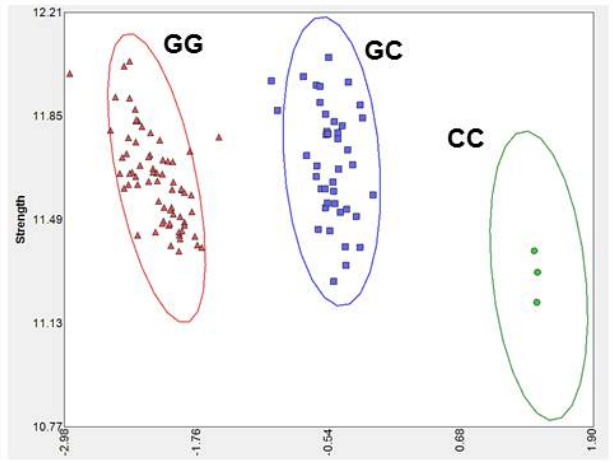
**rs9369640**



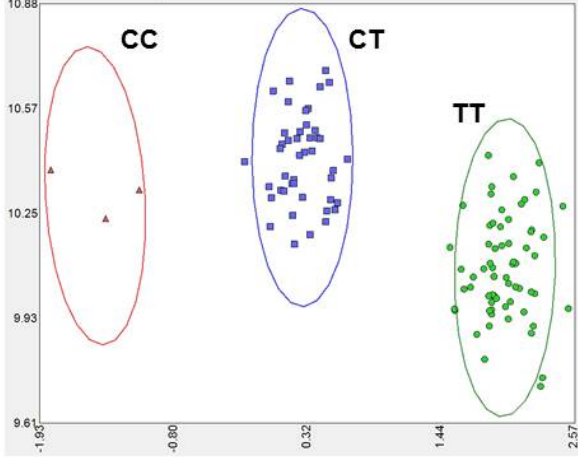
**rs12526453**



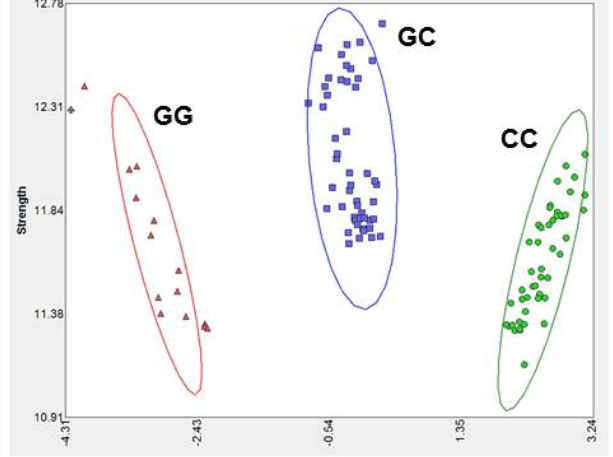
**rs17609940**



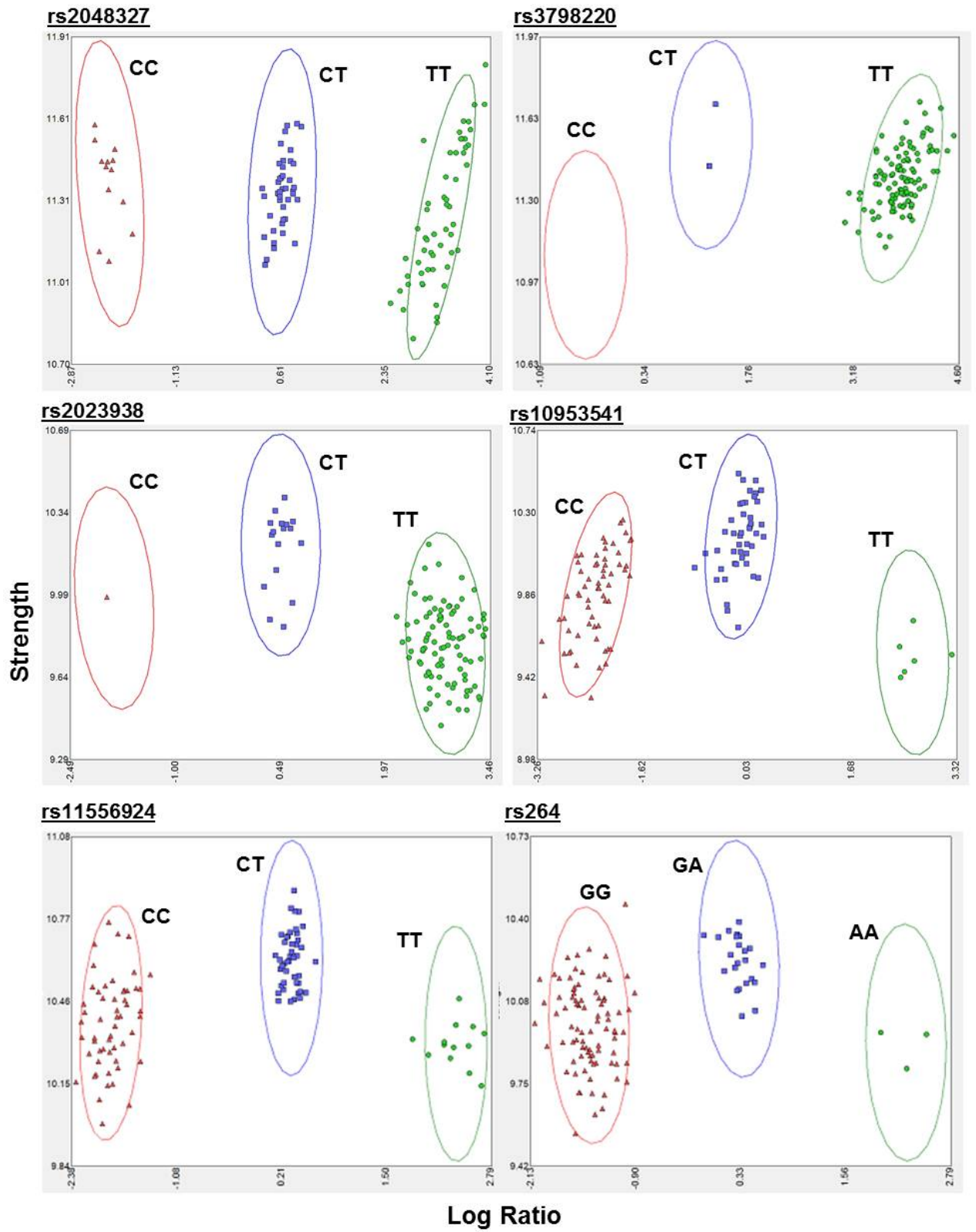
**rs10947789**

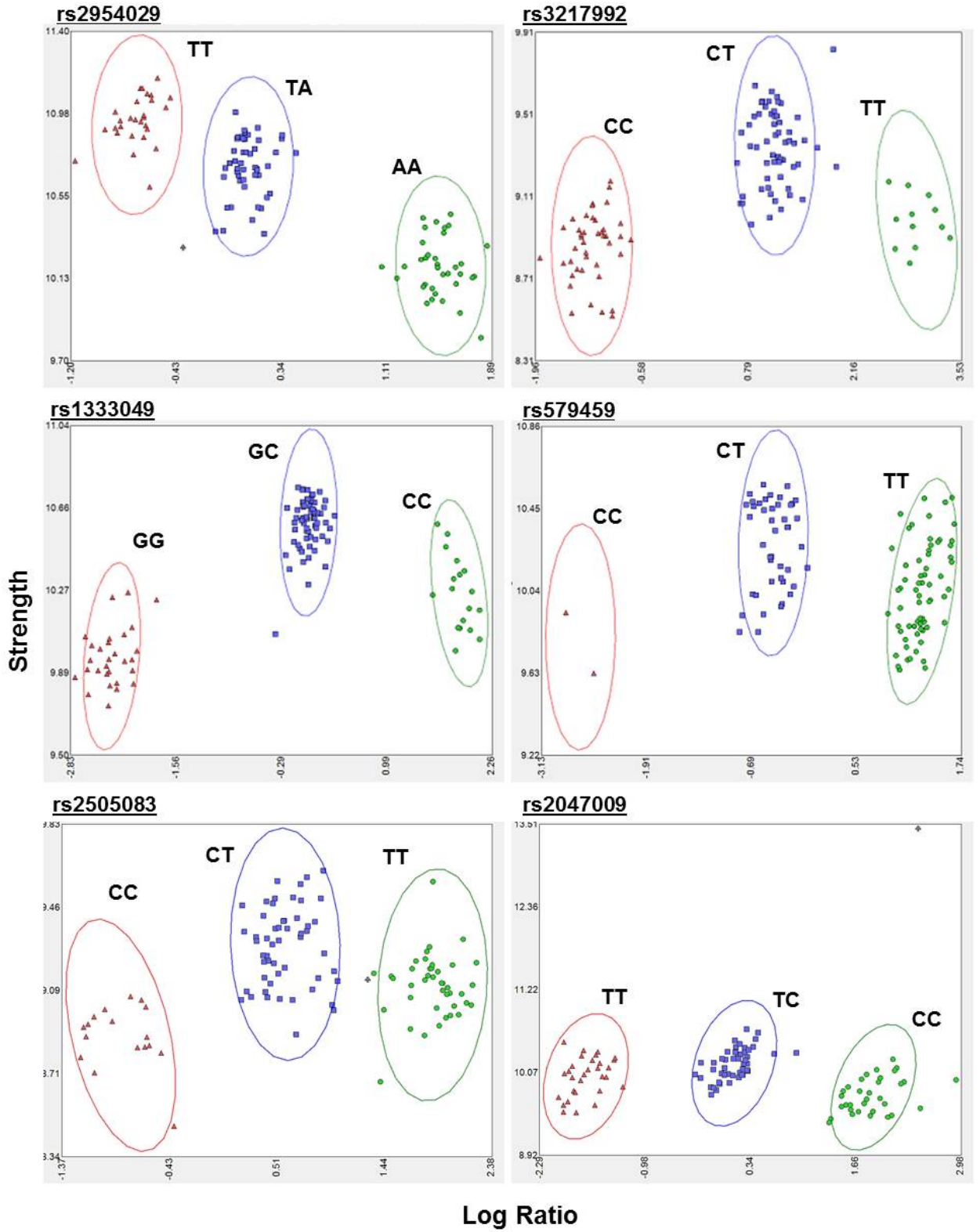


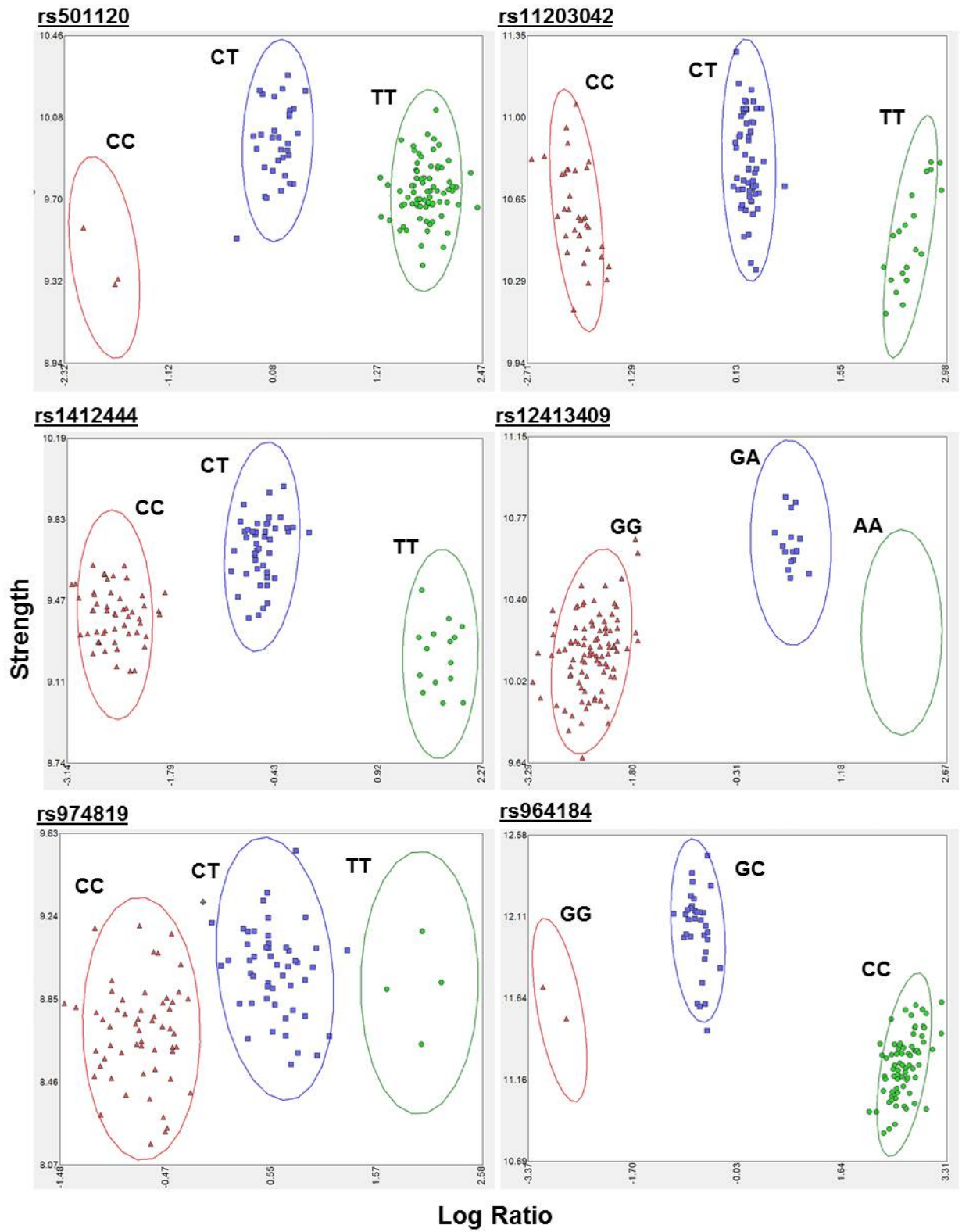
**rs12190287**

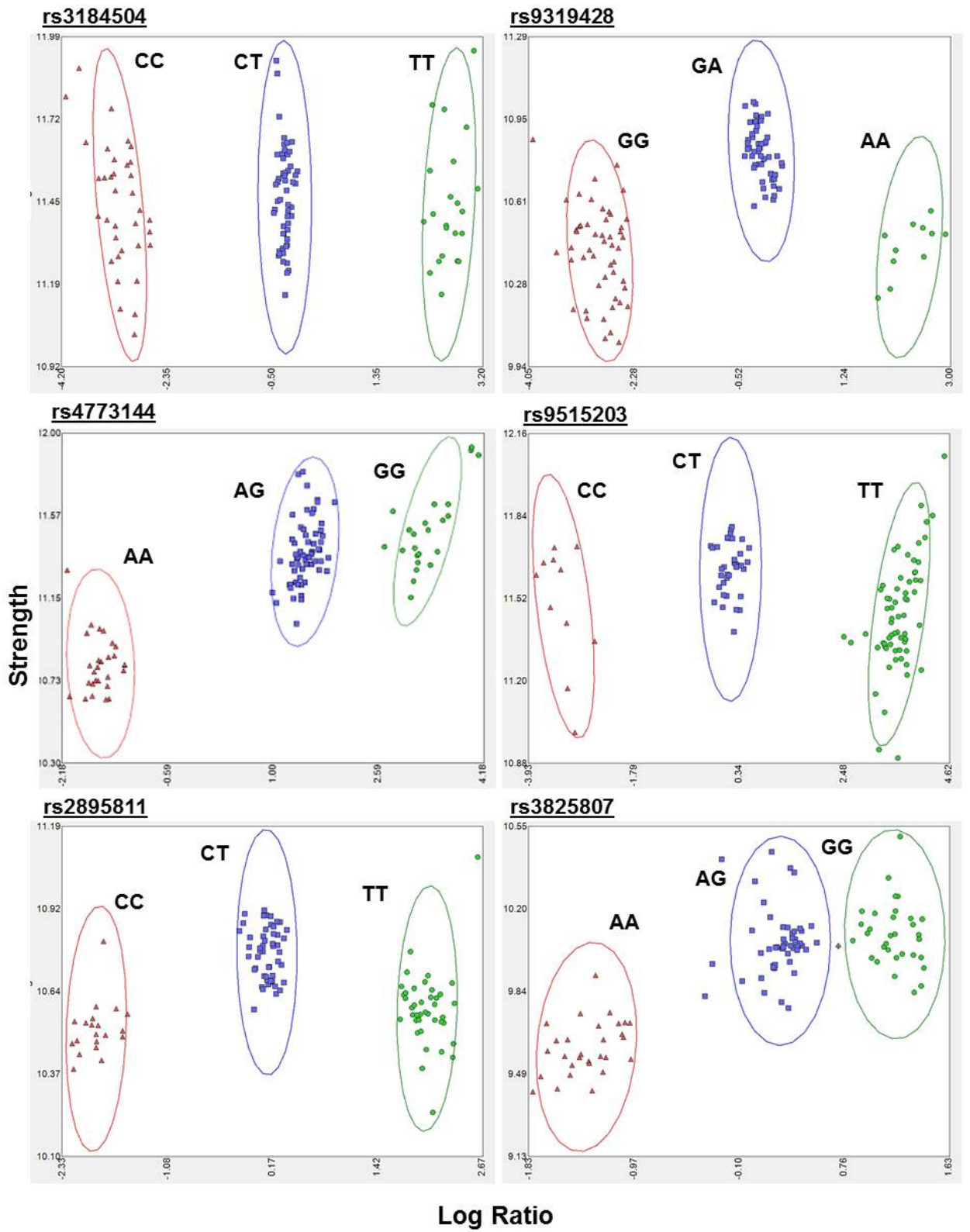


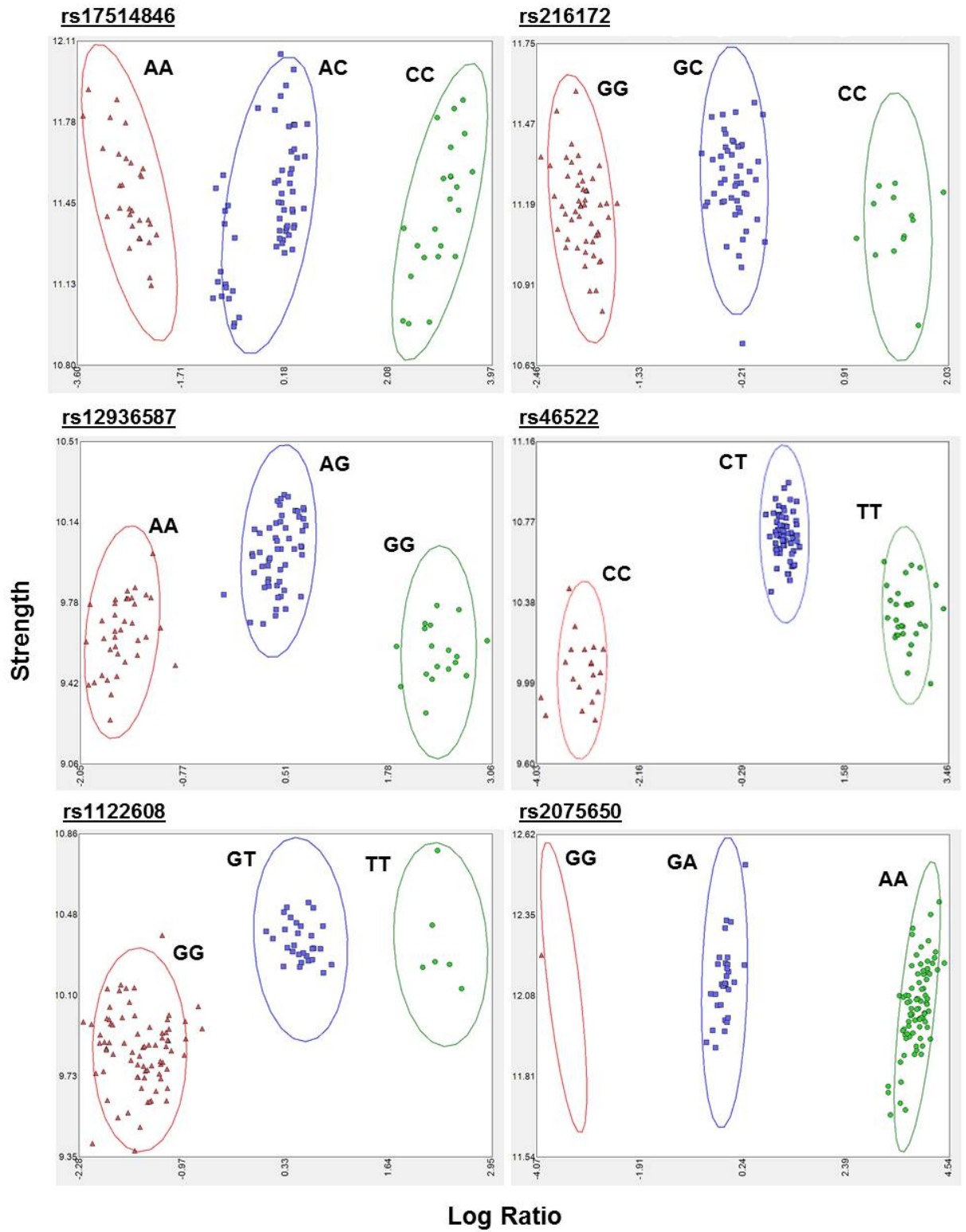
**Log Ratio**











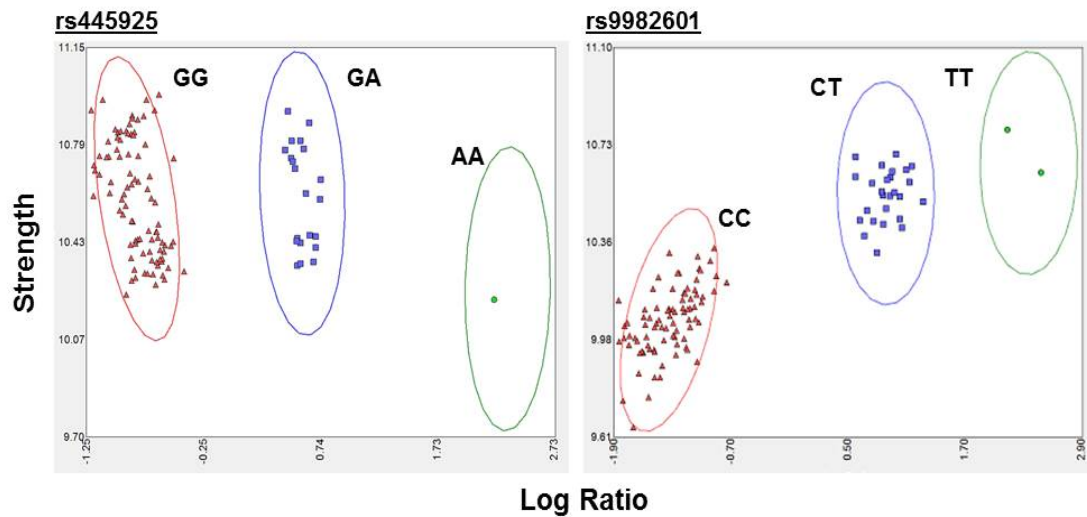


**Figure S3. SNP cluster plots for 50 CAD-associated SNPs for the MSC bank (n=112).** Clustering was carried out in two dimensions. The X axis (log ratio) defines the contrast of the cluster, whereas the Y axis defines the strength of the signals from each sample. Grey spades (♠) indicate no calls. Samples were clustered under the posterior model using the Affymetrix® Genotyping Console™ (GTC) version 4.2 and the Affymetrix® Power Tools (APT) version 1.16.1.

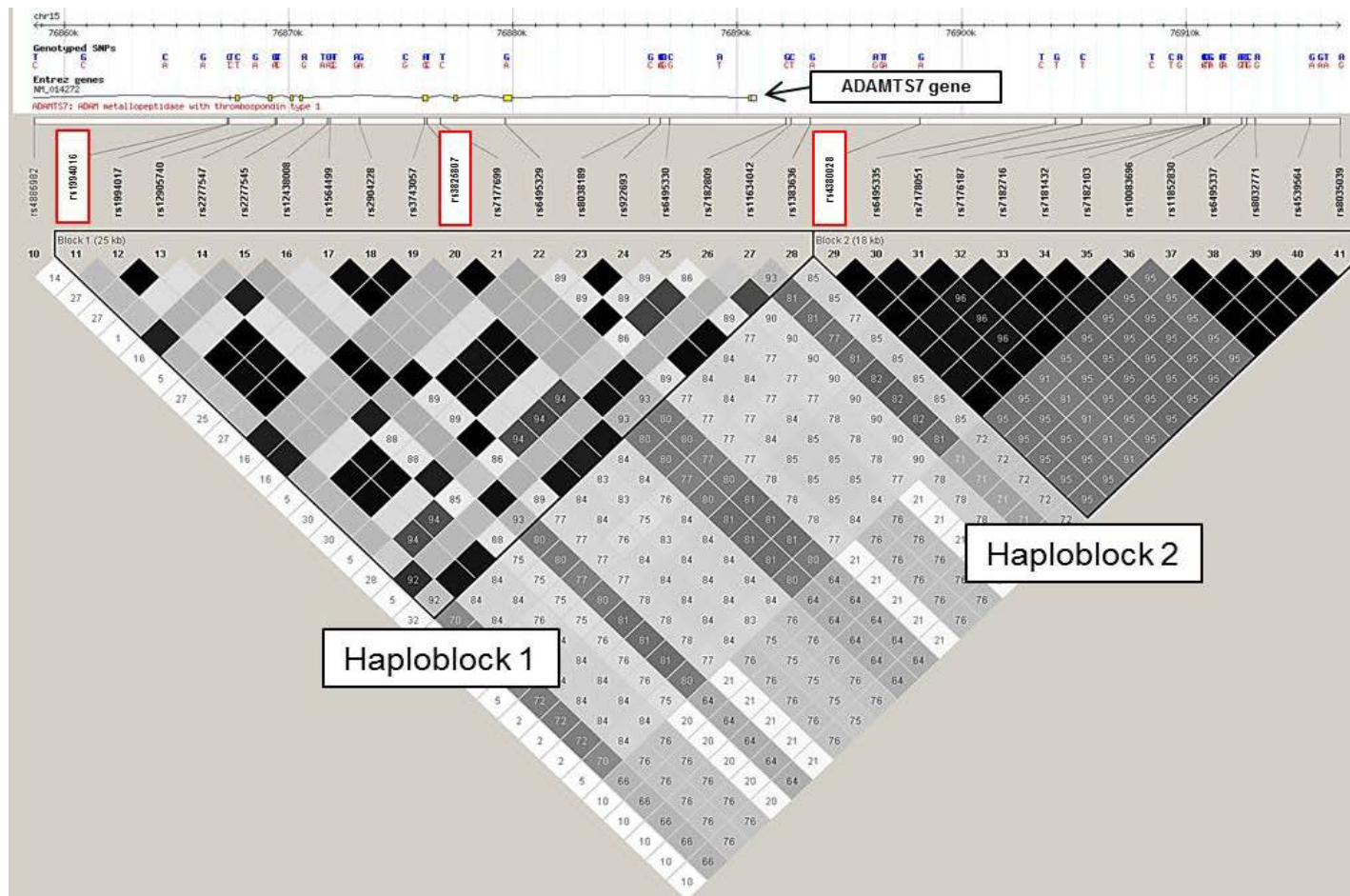


**Figure S4.** The linkage disequilibrium (LD) across *ADAMTS7*. Haploview 4.2 was used to generate the LD map, where genotype files were downloaded directly from the HapMap website (<http://www.hapmap.org>). A reference track displays the chromosomal position and the SNPs. SNPs of interest; rs382807, rs1994016 and rs4380028 are highlighted by a red rectangle. The strength of the  $r^2$  value for LD, is signified by the extent of black. The  $D'$  values are displayed in each diamond.

# References

Ahfeldt, T., Schinzel, R.T., Lee, Y., Hendrickson, D., Kaplan, A., Lum, D.H., Camahort, R., Xia, F., Shay, J., Rhee, E.P., Clish, C.B., Deo, R.C., Shen, T., Lau, F.H., Cowley, A., Mowrer, G., Al-Siddiqi, H., Nahrendorf, M., Musunuru, K., Gerszten, R.E., Rinn, J.L., Cowan, C.A., 2012. Programming human pluripotent stem cells into white and brown adipocytes. *Nature Cell Biology*. **14**, 209-219.

Almontashiri, N.A.M., Fan, M., Cheng, B.L.M., Chen, H., Roberts, R., Stewart, A.F.R., 2013. Interferon- $\gamma$  Activates Expression of p15 and p16 Regardless of 9p21.3 Coronary Artery Disease Risk Genotype. *Journal of the American College of Cardiology*. **61**, 143-147.

Ameziane, N., Beillat, T., Verpillat, P., Chollet-Martin, S., Aumont, M., Seknadji, P., Lamotte, M., Leuret, D., Ollivier, V., de Prost, D., 2003. Association of the Toll-Like Receptor 4 Gene Asp299Gly Polymorphism With Acute Coronary Events. *Arteriosclerosis, Thrombosis, and Vascular Biology*. **23**, e61-e64.

Arciniegas, E., Sutton, A.B., Allen, T.D., Schor, A.M., 1992. Transforming growth factor beta 1 promotes the differentiation of endothelial cells into smooth muscle-like cells in vitro. *Journal of Cell Science*. **103**, 521-529.

Arroyo-Espliguero, R., Avanzas, P., Jeffery, S., Kaski, J.C., 2004a. CD14 and toll-like receptor 4: a link between infection and acute coronary events? *Heart*. **90**, 983-988.

Ashton, B.A., Allen, T.D., Howlett, C.R., Eaglesom, C.C., Hattori, A., Owen, M., 1980. Formation of bone and cartilage by marrow stromal cells in diffusion chambers in vivo. *Clinical Orthopaedics and Related Research*. **151**, 294-307.

Aurich, I., Mueller, L.P., Aurich, H., Luetzkendorf, J., Tisljar, K., Dollinger, M.M., Schormann, W., Walldorf, J., Hengstler, J.G., Fleig, W.E., Christ, B., 2007. Functional integration of hepatocytes derived from human mesenchymal stem cells into mouse livers. *Gut*. **56**, 405-415.

Ayatollahi, M., Soleimani, M., Tabei, S.Z., Kabir Salmani, M., 2011. Hepatogenic differentiation of mesenchymal stem cells induced by insulin like growth factor-I. *World Journal of Stem Cells*. **3**, 113-121.

Bab, I., Ashton, B.A., Gazit, D., Marx, G., Williamson, M.C., Owen, M.E., 1986. Kinetics and differentiation of marrow stromal cells in diffusion chambers in vivo. *Journal of Cell Science*. **84**, 139-151.

Baddoo, M., Hill, K., Wilkinson, R., Gaupp, D., Hughes, C., Kopen, G.C., Phinney, D.G., 2003a. Characterization of mesenchymal stem cells isolated from murine bone marrow by negative selection. *Journal of Cellular Biochemistry*. **89**, 1235-1249.

Bajpai, V.K., Mistryotis, P., Loh, Y., Daley, G.Q., Andreadis, S.T., 2012. Functional vascular smooth muscle cells derived from human induced pluripotent stem cells via mesenchymal stem cell intermediates. *Cardiovascular Research*. **96**, 391-400.

- Baksh, D., Davies, J.E., Zandstra, P.W., 2003. Adult human bone marrow-derived mesenchymal progenitor cells are capable of adhesion-independent survival and expansion. *Experimental Hematology*. **31**, 723-732.
- Baldwin, T., 2009. Morality and human embryo research. Introduction to the Talking Point on morality and human embryo research. *EMBO Reports*. **10**, 299-300.
- Ball, S.G., Worthington, J.J., Canfield, A.E., Merry, C.L.R., Kielty, C.M., 2014. Mesenchymal Stromal Cells: Inhibiting PDGF Receptors or Depleting Fibronectin Induces Mesodermal Progenitors with Endothelial Potential. *Stem Cells*. **32**, 694-705.
- Banfi, A., Muraglia, A., Dozin, B., Mastrogiacomo, M., Cancedda, R., Quarto, R., 2000. Proliferation kinetics and differentiation potential of ex vivo expanded human bone marrow stromal cells: Implications for their use in cell therapy. *Experimental Hematology*. **28**, 707-715.
- Barnett, A.H., Eff, C., Leslie, R.D., Pyke, D.A., 1981. Diabetes in identical twins. A study of 200 pairs. *Diabetologia*. **20**, 87-93.
- Barrilleaux, B., Phinney, D.G., Prockop, D.J., O'Connor, K.C., 2006. Review: Ex vivo engineering of living tissues with adult stem cells. *Tissue Engineering*. **12**, 3007-3019.
- Bauer, R.C., Tohyama, J., Cui, J., Cheng, L., Yang, J., Zhang, X., Ou, K., Paschos, G.K., Zheng, X.L., Parmacek, M.S., Rader, D.J., Reilly, M.P., 2015. Knockout of Adamts7, a Novel Coronary Artery Disease Locus in Humans, Reduces Atherosclerosis in Mice. *Circulation*. **131**, 1202-1213.
- Beamish, J.A., He, P., Kottke-Marchant, K., Marchant, R.E., 2010. Molecular Regulation of Contractile Smooth Muscle Cell Phenotype: Implications for Vascular Tissue Engineering. *Tissue Engineering. Part B, Reviews*. **16**, 467-491.
- Bechmann, L.P., Hannivoort, R.A., Gerken, G., Hotamisligil, G.S., Trauner, M., Canbay, A., 2012. The interaction of hepatic lipid and glucose metabolism in liver diseases. *Journal of Hepatology*. **56**, 952-964.
- Benjamini, Y. & Hochberg, Y., 1995. Controlling the False Discovery Rate: A Practical and Powerful Approach to Multiple Testing. *Journal of the Royal Statistical Society. Series B (Methodological)*. **57**, 289-300.
- Berge, K.E., Tian, H., Graf, G.A., Yu, L., Grishin, N.V., Schultz, J., Kwiterovich, P., Shan, B., Barnes, R., Hobbs, H.H., 2000. Accumulation of Dietary Cholesterol in Sitosterolemia Caused by Mutations in Adjacent ABC Transporters. *Science*. **290**, 1771-1775.
- Bieback, K., Kern, S., Kluter, H., Eichler, H., 2004. Critical parameters for the isolation of mesenchymal stem cells from umbilical cord blood. *Stem Cells*. **22**, 625-634.

- Billington, C.K. & Penn, R.B., 2002. Signaling and regulation of G protein-coupled receptors in airway smooth muscle. *Respiratory Research*. **4**, 2-2.
- Blobe, G.C., Schiemann, W.P., Lodish, H.F., 2000. Role of Transforming Growth Factor  $\beta$  in Human Disease. *N Engl J Med*. **342**, 1350-1358.
- Bodzioch, M., Orso, E., Klucken, J., Langmann, T., Bottcher, A., Diederich, W., Drobnik, W., Barlage, S., Buchler, C., Porsch-Ozcurumez, M., Kaminski, W.E., Hahmann, H.W., Oette, K., Rothe, G., Aslanidis, C., Lackner, K.J., Schmitz, G., 1999. The gene encoding ATP-binding cassette transporter 1 is mutated in Tangier disease. *Nature Genetics*. **22**, 347-351.
- Bolton, T.B., Prestwich, S.A., Zholos, A.V., Gordienko, D.V., 1999. Excitation-Contraction Coupling in Gastrointestinal and Other Smooth Muscles. *Annual Review of Physiology*. **61**, 85-115.
- Bongso, A., Fong, C., Gauthaman, K., 2008. Taking Stem Cells to the Clinic: Major Challenges. *Journal of Cellular Biochemistry*. **105**, 1352-1360.
- Bonnet, P., Awede, B., Rochefort, G.Y., Mirza, A., Lermusiaux, P., Domenech, J., Eder, V., 2008. Electrophysiological maturation of rat mesenchymal stem cells after induction of vascular smooth muscle cell differentiation in vitro. *Stem Cells and Development*. **17**, 1131-1140.
- Boquest, A.C., Noer, A., Collas, P., 2006. Epigenetic programming of mesenchymal stem cells from human adipose tissue. *Stem Cell Reviews*. **2**, 319-329.
- Bork, S., Pfister, S., Witt, H., Horn, P., Korn, B., Ho, A.D., Wagner, W., 2010. DNA methylation pattern changes upon long-term culture and aging of human mesenchymal stromal cells. *Aging Cell*. **9**, 54-63.
- Both, S.K., van der Muijsenberg, A.J., van Blitterswijk, C.A., de Boer, J., de Bruijn, J.D., 2007. A rapid and efficient method for expansion of human mesenchymal stem cells. *Tissue Engineering*. **13**, 3-9.
- Boudi, B.F., 2013. Coronary Artery Atherosclerosis. Available: <http://emedicine.medscape.com/article/153647-overview#a2>
- Brinkmann, T., Weilke, C., Kleesiek, K., 1997. Recognition of Acceptor Proteins by UDP-D-xylose Proteoglycan Core Protein  $\beta$ -D-Xylosyltransferase. *Journal of Biological Chemistry*. **272**, 11171-11175.
- British Heart Foundation, 2012. Coronary Heart Disease Statistics. *A compendium of health statistics 2012 edition*. Available: [https://www.bhf.org.uk/~media/files/publications/research/2012\\_chd\\_statistics\\_compendium.pdf](https://www.bhf.org.uk/~media/files/publications/research/2012_chd_statistics_compendium.pdf)

- Brooks-Wilson, A., Marcil, M., Clee, S.M., Zhang, L., Roomp, K., van Dam, M., Yu, L., Brewer, C., Collins, J.A., Molhuizen, H.O.F., Loubser, O., Ouelette, B.F.F., Fichter, K., Ashbourne-Excoffon, K., Sensen, C.W., Scherer, S., Mott, S., Denis, M., Martindale, D., Frohlich, J., Morgan, K., Koop, B., Pimstone, S., Kastelein, J.J.P., Genest, J., Hayden, M.R., 1999. Mutations in ABC1 in Tangier disease and familial high-density lipoprotein deficiency. *Nature Genetics*. **22**, 336-345.
- Businaro, R., Tagliani, A., Buttari, B., Profumo, E., Ippoliti, F., Di Cristofano, C., Capoano, R., Salvati, B., Riganò, R., 2012. Cellular and molecular players in the atherosclerotic plaque progression. *Annals of the New York Academy of Sciences*. **1262**, 134-141.
- Campagnoli, C., Roberts, I.A.G., Kumar, S., Bennett, P.R., Bellantuono, I., Fisk, N.M., 2001. Identification of mesenchymal stem/progenitor cells in human first-trimester fetal blood, liver, and bone marrow. *Blood*. **98**, 2396-2402.
- Campard, D., Lysy, P.A., Najimi, M., Sokal, E.M., 2008. Native umbilical cord matrix stem cells express hepatic markers and differentiate into hepatocyte-like cells. *Gastroenterology*. **134**, 833-848.
- Campbell, L.A. & Kuo, C.C., 2004. Chlamydia pneumoniae - An infectious risk factor for atherosclerosis? *Nature Reviews Microbiology*. **2**, 23-32.
- Can, A. & Karahuseyinoglu, S., 2007. Concise review: Human umbilical cord stroma with regard to the source of fetus-derived stem cells. *Stem Cells*. **25**, 2886-2895.
- Caplan, A.I., 1991. Mesenchymal Stem-Cells. *Journal of Orthopaedic Research*. **9**, 641-650.
- Carlin, R., Davis, D., Weiss, M., Schultz, B., Troyer, D., 2006. Expression of early transcription factors Oct-4, Sox-2 and Nanog by porcine umbilical cord (PUC) matrix cells. *Reproductive Biology and Endocrinology*. **4**, 8-8.
- Carmeliet, P., 2003. Angiogenesis in health and disease. *Nature Medicine*. **9**, 653-660.
- Castro-Malaspina, H., Gay, R.E., Resnick, G., Kapoor, N., Meyers, P., Chiarieri, D., McKenzie, S., Broxmeyer, H.E., Moore, M.A., 1980. Characterization of human bone marrow fibroblast colony-forming cells (CFU-F) and their progeny. *Blood*. **56**, 289-301.
- Chen, H., Wu, H., Fon, C., Chen, P., Lai, M., Chen, D., 1998. Long-term culture of hepatocytes from human adults. *Journal of Biomedical Science*. **5**, 435-440.
- Cheung, C., Bernardo, A.S., Trotter, M.W.B., Pedersen, R.A., Sinha, S., 2012. Generation of human vascular smooth muscle subtypes provides insight into embryological origin-dependent disease susceptibility. *Nature Biotechnology*. **30**, 165-173.

- Choudhery, M., Badowski, M., Muise, A., Pierce, J., Harris, D., 2014. Donor age negatively impacts adipose tissue-derived mesenchymal stem cell expansion and differentiation. *Journal of Translational Medicine*. **12**, 8.
- Chow, C.K., Islam, S., Bautista, L., Rumboldt, Z., Yusufali, A., Xie, C., Anand, S.S., Engert, J.C., Rangarajan, S., Yusuf, S., 2011. Parental History and Myocardial Infarction Risk Across the World The INTERHEART Study. *Journal of the American College of Cardiology*. **57**, 619-627.
- Clarke, R., Xu, P., Bennett, D., Lewington, S., Zondervan, K., Parish, S., Palmer, A., Clark, S., Cardon, L., Peto, R., Lathrop, M., Collins, R., 2006. Lymphotoxin-Alpha Gene and Risk of Myocardial Infarction in 6,928 Cases and 2,712 Controls in the ISIS Case-Control Study. *PLoS Genet*. **2**, e107.
- Cleeman, J.I., Grundy, S.M., Becker, D., Clark, L.T., Cooper, R.S., Denke, M.A., Howard, W.J., Hunninghake, D.B., et al. 2001. Executive summary of the Third Report of the National Cholesterol Education Program (NCEP) expert panel on detection, evaluation, and treatment of high blood cholesterol in adults (Adult Treatment Panel III). *Jama-Journal of the American Medical Association*. **285**, 2486-2497.
- Cohen, J.C., Kiss, R.S., Pertsemlidis, A., Marcel, Y.L., McPherson, R., Hobbs, H.H., 2004. Multiple rare alleles contribute to low plasma levels of HDL cholesterol. *Science (New York, N.Y.)*. **305**, 869-872.
- Cohen, J.C., Boerwinkle, E., Mosley, T.H., Hobbs, H.H., 2006. Sequence Variations in PCSK9, Low LDL, and Protection against Coronary Heart Disease. *N Engl J Med*. **354**, 1264-1272.
- Colter, D.C., Class, R., DiGirolamo, C.M., Prockop, D.J., 2000. Rapid expansion of recycling stem cells in cultures of plastic-adherent cells from human bone marrow. *Proceedings of the National Academy of Sciences of the United States of America*. **97**, 3213-3218.
- Conconi, M.T., Burra, P., Di Liddo, R., Calore, C., Turetta, M., Bellini, S., Bo, P., Nussdorfer, G.G., Parnigotto, P.P., 2006. CD105(+) cells from Wharton's jelly show in vitro and in vivo myogenic differentiative potential. *International Journal of Molecular Medicine*. **18**, 1089-1096.
- Coronary Artery Disease (C4D) Genetics Consortium, 2011. A genome-wide association study in Europeans and South Asians identifies five new loci for coronary artery disease. *Nature Genetics*. **43**, 339-344.
- Coronary Artery Disease Consortium, 2009. Large Scale Association Analysis of Novel Genetic Loci for Coronary Artery Disease. *Arteriosclerosis, Thrombosis, and Vascular Biology*. **29**, 774-780.
- Cremer, P., Nagel, D., Mann, H., Labrot, B., MullerBerninger, R., Elster, H., Seidel, D., 1997. Ten-year follow-up results from the Goettingen risk, incidence and prevalence

study (GRIPS) .1. Risk factors for myocardial infarction in a cohort of 5790 men. *Atherosclerosis*. **129**, 221-230.

Critchley, J. & Capewell, S., 2004. Smoking cessation for the secondary prevention of coronary heart disease. *The Cochrane Database of Systematic Reviews*. **(1)**, CD003041.

Cybulsky, M.I. & Gimbrone, M.A., Jr, 1991. Endothelial expression of a mononuclear leukocyte adhesion molecule during atherogenesis. *Science (New York, N.Y.)*. **251**, 788-791.

da Silva Meirelles, L., Chagastelles, P.C., Nardi, N.B., 2006. Mesenchymal stem cells reside in virtually all post-natal organs and tissues. *Journal of Cell Science*. **119**, 2204-13.

Dandre, F. & Owens, G.K., 2004. Platelet-derived growth factor-BB and Ets-1 transcription factor negatively regulate transcription of multiple smooth muscle cell differentiation marker genes. *American Journal of Physiology-Heart and Circulatory Physiology*. **286**, H2042-51.

Dash, B.C., Jiang, Z., Suh, C., Qyang, Y., 2015. Induced pluripotent stem cell-derived vascular smooth muscle cells: methods and application. *The Biochemical Journal*. **465**, 185-194.

Dawber, T.R., Moore, F.E., Mann, G.V., 1957. II. Coronary Heart Disease in the Framingham Study. *American Journal of Public Health and the Nations Health*. **47**, 4-24.

Dawber, T.R., Meadors, G.F., Moore, F.E., 1951. Epidemiological Approaches to Heart Disease: The Framingham Study. *American Journal of Public Health and the Nations Health*. **41**, 279-286.

De Bartolo, L., Salerno, S., Morelli, S., Giorno, L., Rende, M., Memoli, B., Procino, A., Andreucci, V.E., Bader, A., Drioli, E., 2006. Long-term maintenance of human hepatocytes in oxygen-permeable membrane bioreactor. *Biomaterials*. **27**, 4794-4803.

Deloukas, P., Kanoni, S., Willenborg, C., Farrall, M., Assimes, T.L., Thompson, J.R., Ingelsson, E., Saleheen, D., Erdmann, J., et al. 2013. Large-scale association analysis identifies new risk loci for coronary artery disease. *Nature Genetics*. **45**, 25-33.

De-Miguel, M.P., Arnalich-Montiel, F., Lopez-Iglesias, P., Blazquez-Martinez, A., Nistal, M., 2009. Epiblast-derived stem cells in embryonic and adult tissues. *International Journal of Developmental Biology*. **53**, 1529-1540.

Dempsey, E.C., Badesch, D.B., Dobyns, E.L., Stenmark, K.R., 1994. Enhanced growth capacity of neonatal pulmonary artery smooth muscle cells in vitro: Dependence on cell size, time from birth, insulin-like growth factor I, and auto-activation of protein Kinase C. *Journal of Cellular Physiology*. **160**, 469-481.

Di Naro, E., Ghezzi, F., Raio, L., Franchi, M., D'Addario, V., 2001. Umbilical cord morphology and pregnancy outcome. *European Journal of Obstetrics Gynecology and Reproductive Biology*. **96**, 150-157.

Denault, J. & Leduc, R., 1996. Furin/PACE/SPC1: A convertase involved in exocytic and endocytic processing of precursor proteins. *FEBS Letters*. **379**, 113-116.

Dickson, M.C., Martin, J.S., Cousins, F.M., Kulkarni, A.B., Karlsson, S., Akhurst, R.J., 1995. Defective haematopoiesis and vasculogenesis in transforming growth factor-beta 1 knock out mice. *Development*. **121**, 1845-1854.

DiGirolamo, C.M., Stokes, D., Colter, D., Phinney, D.G., Class, R., Prockop, D.J., 1999. Propagation and senescence of human marrow stromal cells in culture: a simple colony-forming assay identifies samples with the greatest potential to propagate and differentiate. *British Journal of Haematology*. **107**, 275-281.

Ding, Q., Lee, Y., Schaefer, E.K., Peters, D., Veres, A., Kim, K., Kuperwasser, N., Motola, D., Meissner, T., Hendriks, W., Trevisan, M., Gupta, R., Moisan, A., Banks, E., Friesen, M., Schinzel, R., Xia, F., Tang, A., Xia, Y., Figueroa, E., Wann, A., Ahfeldt, T., Daheron, L., Zhang, F., Rubin, L., Peng, L., Chung, R., Musunuru, K., Cowan, C., 2013. A TALEN Genome-Editing System for Generating Human Stem Cell-Based Disease Models. *Cell Stem Cell*. **12**, 238-251.

D'Ippolito, G., Schiller, P.C., Ricordi, C., Roos, B.A., Howard, G.A., 1999. Age-Related Osteogenic Potential of Mesenchymal Stromal Stem Cells from Human Vertebral Bone Marrow. *Journal of Bone and Mineral Research*. **14**, 1115-1122.

Dominici, M., Le Blanc, K., Mueller, I., Slaper-Cortenbach, I., Marini, F.C., Krause, D.S., Deans, R.J., Keating, A., Prockop, D.J., Horwitz, E.M., 2006. Minimal criteria for defining multipotent mesenchymal stromal cells. The International Society for Cellular Therapy position statement. *Cytotherapy*. **8**, 315-317.

Dorai, H., Vukicevic, S., Sampath, T.K., 2000. Bone morphogenetic protein-7 (osteogenic protein-1) inhibits smooth muscle cell proliferation and stimulates the expression of markers that are characteristic of SMC phenotype in vitro. *Journal of Cellular Physiology*. **184**, 37-45.

Du, Y., Gao, C., Liu, Z., Wang, L., Liu, B., He, F., Zhang, T., Wang, Y., Wang, X., Xu, M., Luo, G., Zhu, Y., Xu, Q., Wang, X., Kong, W., 2012. Upregulation of a Disintegrin and Metalloproteinase With Thrombospondin Motifs-7 by miR-29 Repression Mediates Vascular Smooth Muscle Calcification. *Arteriosclerosis, Thrombosis, and Vascular Biology*. **32**, 2580-2588.

Duncan, S.A., 2000. Transcriptional regulation of liver development. *Developmental Dynamics*. **219**, 131-142.

Ebke, L.A., Nestor-Kalinoski, A.L., Slotterbeck, B.D., Al-Dieri, A.G., Ghosh-Lester, S., Russo, L., Najjar, S.M., von Grafenstein, H., McInerney, M.F., 2014. Tight association

between macrophages and adipocytes in obesity: Implications for adipocyte preparation. *Obesity*. **22**, 1246-1255.

Ekstrom, C.T. & Dalgaard, P., 2003. Linkage analysis of quantitative trait loci in the presence of heterogeneity. *Human Heredity*. **55**, 16-26.

Emilsson, V., Thorleifsson, G., Zhang, B., Leonardson, A.S., Zink, F., Zhu, J., Carlson, S., Helgason, A., Walters, G.B., Gunnarsdottir, S., et al. 2008. Genetics of gene expression and its effect on disease. *Nature*. **452**, 423-428.

Erridge, C., Gracey, J., Braund, P.S., Samani, N.J., 2013. The 9p21 Locus Does Not Affect Risk of Coronary Artery Disease Through Induction of Type 1 Interferons. *Journal of the American College of Cardiology*. **62**, 1376-1381.

Estep, M., Armistead, D., Hossain, N., Elarainy, H., Goodman, Z., Baranova, A., Chandhoke, V., Younossi, Z.M., 2010. Differential expression of miRNAs in the visceral adipose tissue of patients with non-alcoholic fatty liver disease. *Alimentary Pharmacology & Therapeutics*. **32**, 487-497.

Evans, M.J. & Kaufman, M.H., 1981. Establishment in culture of pluripotential cells from mouse embryos. *Nature*. **292**, 154-156.

Faggin, E., Puato, M., Zardo, L., Franch, R., Millino, C., Sarinella, F., Pauletto, P., Sartore, S., Chiavegato, A., 1999. Smooth Muscle-Specific SM22 Protein Is Expressed in the Adventitial Cells of Balloon-Injured Rabbit Carotid Artery. *Arteriosclerosis, Thrombosis, and Vascular Biology*. **19**, 1393-1404.

Fatigati, V. & Murphy, R.A., 1984. Actin and tropomyosin variants in smooth muscles. Dependence on tissue type. *Journal of Biological Chemistry*. **259**, 14383-14388.

Fischer, M., Broeckel, U., Holmer, S., Baessler, A., Hengstenberg, C., Mayer, B., Erdmann, J., Klein, G., Riegger, G., Jacob, H.J., Schunkert, H., 2005. Distinct heritable patterns of angiographic coronary artery disease in families with myocardial infarction. *Circulation*. **111**, 855-862.

Fischer, M., Mayer, B., Baessler, A., Riegger, G., Erdmann, J., Hengstenberg, C., Schunkert, H., 2007. Familial aggregation of left main coronary artery disease and future risk of coronary events in asymptomatic siblings of affected patients. *European Heart Journal*. **28**, 2432-2437.

Folkersen, L., Kyriakou, T., Goel, A., Peden, J., Malarstig, A., Paulsson-Berne, G., Hamsten, A., Franco-Cereceda, A., Gabrielsen, A., Eriksson, P., Watkins, H., Hugh Watkins PROCARDIS Consortia, 2009. Relationship between CAD Risk Genotype in the Chromosome 9p21 Locus and Gene Expression. Identification of Eight New ANRIL Splice Variants. *Plos One*. **4**, e7677.

- Fong, C.Y., Richards, M., Manasi, N., Biswas, A., Bongso, A., 2007. Comparative growth behaviour and characterization of stem cells from human Wharton's jelly. *Reproductive Biomedicine Online*. **15**, 708-718.
- Fong, C., Chak, L., Biswas, A., Tan, J., Gauthaman, K., Chan, W., Bongso, A., 2011. Human Wharton's Jelly Stem Cells Have Unique Transcriptome Profiles Compared to Human Embryonic Stem Cells and Other Mesenchymal Stem Cells. *Stem Cell Reviews and Reports*. **7**, 1-16.
- Frayling, T.M., Timpson, N.J., Weedon, M.N., Zeggini, E., Freathy, R.M., Lindgren, C.M., Perry, J.R.B., Elliott, K.S., Lango, H., et al. 2007. A Common Variant in the FTO Gene Is Associated with Body Mass Index and Predisposes to Childhood and Adult Obesity. *Science*. **316**, 889-894.
- Frid, M.G., Shekhonin, B.V., Koteliansky, V.E., Glukhova, M.A., 1992. Phenotypic changes of human smooth muscle cells during development: Late expression of heavy caldesmon and calponin. *Developmental Biology*. **153**, 185-193.
- Friedenstein, A.J., Chailakhyan, R.K., Latsinik, N.V., Panasyuk, A.F., Keilissb, I.V., 1974. Stromal Cells Responsible for Transferring Microenvironment of Hematopoietic Tissues - Cloning In vitro and Replantation In vivo. *Transplantation*. **17**, 331-340.
- Friedenstein, A. J., Petrakova, K. V., Kurolesova, A. I., Frolova, G. P., 1968. Heterotopic of bone marrow. Analysis of precursor cells for osteogenic and hematopoietic tissues. *Transplantation*. **6**, 230-47.
- Friedenstein, A. J., Piatetzky, S. II., Petrakova, K. V., 1966. Osteogenesis in transplants of bone marrow cells. *Journal of embryology and experimental morphology*. **16**, 381-390.
- Friedman, R., Betancur, M., Boissel, L., Tuncer, H., Cetrulo, C., Klingemann, H., 2007. Umbilical Cord Mesenchymal Stem Cells: Adjuvants for Human Cell Transplantation. *Biology of Blood and Marrow Transplantation*. **13**, 1477-1486.
- Frikke-Schmidt, R., Nordestgaard, B., Jensen, G.B., Tybjaerg-Hansen, A., 2004. Genetic variation in ABC transporter A1 contributes to HDL cholesterol in the general population. *Journal of Clinical Investigation*. **114**, 1343-1353.
- Furuhashi, M. & Hotamisligil, G.S., 2008. Fatty acid-binding proteins: role in metabolic diseases and potential as drug targets. **7**, 489-503.
- Gaengel, K., Genové, G., Armulik, A., Betsholtz, C., 2009. Endothelial-Mural Cell Signaling in Vascular Development and Angiogenesis. *Arteriosclerosis, Thrombosis, and Vascular Biology*. **29**, 630-638.
- Gherghiceanu, M., Barad, L., Novak, A., Reiter, I., Itskovitz-Eldor, J., Binah, O., Popescu, L.M., 2011. Cardiomyocytes derived from human embryonic and induced

pluripotent stem cells: comparative ultrastructure. *Journal of Cellular and Molecular Medicine*. **15**, 2539-2551.

Gimbrone Jr, M.A., 1999. Vascular Endothelium, Hemodynamic Forces, and Atherogenesis. *The American Journal of Pathology*. **155**, 1-5.

Girelli, D., Martinelli, N., Peyvandi, F., Olivieri, O., 2009. Genetic Architecture of Coronary Artery Disease in the Genome-Wide Era: Implications for the Emerging "Golden Dozen" Loci. *Seminars in Thrombosis and Hemostasis*. **35**, 671-682.

Goldstein, J.L. & Brown, M.S., 1973. Familial Hypercholesterolemia: Identification of a Defect in the Regulation of 3-Hydroxy-3-Methylglutaryl Coenzyme A Reductase Activity Associated with Overproduction of Cholesterol. *Proceedings of the National Academy of Sciences of the United States of America*. **70**, 2804-2808.

Gong, Z. & Niklason, L.E., 2008. Small-diameter human vessel wall engineered from bone marrow-derived mesenchymal stem cells (hMSCs). *Faseb Journal*. **22**, 1635-1648.

Gottlieb, M.S. & Root, H.F., 1968. Diabetes Mellitus in Twins. *Diabetes*. **17**, 693-704.

Grant, S.F.A., Thorleifsson, G., Reynisdottir, I., Benediktsson, R., Manolescu, A., Sainz, J., Helgason, A., Stefansson, H., et al. 2006. Variant of transcription factor 7-like 2 (TCF7L2) gene confers risk of type 2 diabetes. *Nature Genetics*. **38**, 320-323.

Greenspan, P., Mayer, E.P., Fowler, S.D., 1985. Nile red: a selective fluorescent stain for intracellular lipid droplets. *The Journal of Cell Biology*. **100**, 965-973.

Grundberg, E., Small, K.S., Hedman, A.K., Nica, A.C., Buil, A., Keildson, S., Bell, J.T., Yang, T., Meduri, E., Barrett, A., Nisbett, J., et al. 2012. Mapping cis- and trans-regulatory effects across multiple tissues in twins. *Nature Genetics*. **44**, 1084-1089.

Guillot, P.V., Gotherstrom, C., Chan, J., Kurata, H., Fisk, N.M., 2007. Human first-trimester fetal MSC express pluripotency markers and grow faster and have longer telomeres than adult MSC. *Stem Cells*. **25**, 646-654.

Gunsilius, E., Gastl, G., Petzer, A.L., 2001. Hematopoietic stem cells. *Biomedicine & Pharmacotherapy*. **55**, 186-194.

Haasters, F., Prall, W.C., Anz, D., Bourquin, C., Pautke, C., Endres, S., Mutschler, W., Docheva, D., Schieker, M., 2009. Morphological and immunocytochemical characteristics indicate the yield of early progenitors and represent a quality control for human mesenchymal stem cell culturing. *Journal of Anatomy*. **214**, 759-767.

Hamsten, A. & Eriksson, P., 2012. Quest for Genes and Mechanisms Linking the Human Chromosome 9p21.3 Locus to Cardiovascular Disease. *Circulation*. **126**, 1815-1817.

Hanna, J., Markoulaki, S., Schorderet, P., Carey, B.W., Beard, C., Wernig, M., Creighton, M.P., Steine, E.J., Cassady, J.P., Foreman, R., Lengner, C.J., Dausman, J.A., Jaenisch, R., 2008. Direct reprogramming of terminally differentiated mature B lymphocytes to pluripotency. *Cell*. **133**, 250-264.

Harismendy, O., Notani, D., Song, X., Rahim, N.G., Tanasa, B., Heintzman, N., Ren, B., Fu, X., Topol, E.J., Rosenfeld, M.G., Frazer, K.A., 2011. 9p21 DNA variants associated with coronary artery disease impair interferon-gamma signalling response. *Nature*. **470**, 264-8.

Harvald, B. & Hauge, M., 1963. Selection in Diabetes in Modern Society. *Acta Medica Scandinavica*. **173**, 459-465.

Haynesworth, S.E., Baber, M.A., Caplan, A.I., 1992. Cell-Surface Antigens on Human Marrow-Derived Mesenchymal Cells are Detected by Monoclonal-Antibodies. *Bone*. **13**, 69-80.

He, Z.P., Tan, W.Q., Tang, Y.F., Feng, M.F., 2003. Differentiation of putative hepatic stem cells derived from adult rats into mature hepatocytes in the presence of epidermal growth factor and hepatocyte growth factor. *Differentiation*. **71**, 281-290.

Heaps, C.L. & Parker, J.L., 2011. Effects of exercise training on coronary collateralization and control of collateral resistance. *Journal of Applied Physiology*. **111**, 587-598.

Heard-Costa, N., Zillikens, M.C., Monda, K.L., Johansson, Å., Harris, T.B., Fu, M., Haritunians, T., Feitosa, M.F., Aspelund, T., et al. 2009. *NRXN3* Is a Novel Locus for Waist Circumference: A Genome-Wide Association Study from the CHARGE Consortium. *PLoS Genet*. **5**, e1000539.

Heath, K.E., Day, I.N.M., Humphries, S.E., 2000. Universal primer quantitative fluorescent multiplex (UPQFM) PCR: a method to detect major and minor rearrangements of the low density lipoprotein receptor gene. *Journal of Medical Genetics*. **37**, 272-280.

Helgadottir, A., Manolescu, A., Thorleifsson, G., Gretarsdottir, S., Jonsdottir, H., Thorsteinsdottir, U., Samani, N.J., Gudmundsson, G., et al. 2004. The gene encoding 5-lipoxygenase activating protein confers risk of myocardial infarction and stroke. *Nature Genetics*. **36**, 233-239.

Helgadottir, A., Manolescu, A., Helgason, A., Thorleifsson, G., Thorsteinsdottir, U., Gudbjartsson, D.F., Gretarsdottir, S., Magnusson, K.P., et al. 2006. A variant of the gene encoding leukotriene A4 hydrolase confers ethnicity-specific risk of myocardial infarction. *Nature Genetics*. **38**, 68-74.

Helgadottir, A., Thorleifsson, G., Manolescu, A., Gretarsdottir, S., Blondal, T., Jonasdottir, A., Jonsdottir, A., Sigurdsson, A., Baker, A., Palsson, A., Masson, G., Gudbjartsson, D.F., Magnusson, K.P., Andersen, K., Levey, A.I., Backman, V.M.,

Matthiasdottir, S., Jonsdottir, T., Palsson, S., Einarsdottir, H., Gunnarsdottir, S., Gylfason, A., Vaccarino, V., Hooper, W.C., Reilly, M.P., Granger, C.B., Austin, H., Rader, D.J., Shah, S.H., Quyyumi, A.A., Gulcher, J.R., Thorgeirsson, G., Thorsteinsdottir, U., Kong, A., Stefansson, K., 2007. A common variant on chromosome 9p21 affects the risk of myocardial infarction. *Science*. **316**, 1491-1493.

Hneino, M., Bouazza, L., Bricca, G., Li, J.Y., Langlois, D., 2009. Density-Dependent Shift of Transforming Growth Factor-Beta-1 from Inhibition to Stimulation of Vascular Smooth Muscle Cell Growth Is Based on Unconventional Regulation of Proliferation, Apoptosis and Contact Inhibition. *Journal of Vascular Research*. **46**, 85-97.

Hobbs, H.H., Brown, M.S., Goldstein, J.L., 1992. Molecular genetics of the LDL receptor gene in familial hypercholesterolemia. *Human Mutation*. **1**, 445-466.

Hoekstra, M., Mummery, C.L., Wilde, A.A.M., Bezzina, C.R., Verkerk, A.O., 2012. Induced pluripotent stem cell derived cardiomyocytes as models for cardiac arrhythmias. *Frontiers in Physiology*. **3**, 346.

Hoffman, L. & Carpenter, M., 2005. Human embryonic stem cell stability. *Stem Cell Reviews*. **1**, 139-144.

Holdt, L.M., Beutner, F., Scholz, M., Gielen, S., Gaebel, G., Bergert, H., Schuler, G., Thiery, J., Teupser, D., 2010. ANRIL Expression Is Associated With Atherosclerosis Risk at Chromosome 9p21. *Arteriosclerosis Thrombosis and Vascular Biology*. **30**, 620-627.

Holdt, L.M., Sass, K., Gaebel, G., Bergert, H., Thiery, J., Teupser, D., 2011. Expression of Chr9p21 genes CDKN2B (p15(INK4b)), CDKN2A (p16(INK4a), p14(ARF)) and MTAP in human atherosclerotic plaque. *Atherosclerosis*. **214**, 264-270.

Hong, S.H., Gang, E.J., Jeong, J.A., Ahn, C.Y., Hwang, S.H., Yang, I.H., Park, H.K., Han, H., Kim, H., 2005. In vitro differentiation of human umbilical cord blood-derived mesenchymal stem cells into hepatocyte-like cells. *Biochemical and Biophysical Research Communications*. **330**, 1153-1161.

Horwitz, E.M., Le Blanc, K., Dominici, M., Mueller, I., Slaper-Cortenbach, I., Marini, F.C., Deans, R.J., Krause, D.S., Keating, A., 2005. Clarification of the nomenclature for MSC: The international society for cellular therapy position statement. *Cytotherapy*. **7**, 393-395.

Hungerford, J.E., Owens, G.K., Argraves, W.S., Little, C.D., 1996. Development of the Aortic Vessel Wall as Defined by Vascular Smooth Muscle and Extracellular Matrix Markers. *Developmental Biology*. **178**, 375-392.

Hurskainen, T.L., Hirohata, S., Seldin, M.F., Apte, S.S., 1999. ADAM-TS5, ADAM-TS6, and ADAM-TS7, Novel Members of a New Family of Zinc Metalloproteases: general features and genomic distribution of the ADAM-TS family. *Journal of Biological Chemistry*. **274**, 25555-25563.

International HapMap 3 Consortium, Altshuler, D.M., Gibbs, R.A., Peltonen, L., Altshuler, D.M., Gibbs, R.A., Peltonen, L., Dermitzakis, E., Schaffner, S.F., Yu, F., et al. 2010. Integrating common and rare genetic variation in diverse human populations. *Nature*. **467**, 52-58.

International HapMap Consortium, Frazer, K.A., Ballinger, D.G., Cox, D.R., Hinds, D.A., Stuve, L.L., Gibbs, R.A., Belmont, J.W., et al. 2007. A second generation human haplotype map of over 3.1 million SNPs. *Nature*. **449**, 851-861.

Ishige, I., Nagamura-Inoue, T., Honda, M., Harnprasopwat, R., Kido, M., Sugimoto, M., Nakauchi, H., Tojo, A., 2009. Comparison of mesenchymal stem cells derived from arterial, venous, and Whartons jelly explants of human umbilical cord. *International Journal of Hematology*. **90**, 261-269.

Izadpanah, R., Kaushal, D., Kriedt, C., Tsien, F., Patel, B., Dufour, J., Bunnell, B.A., 2008. Long-term In vitro Expansion Alters the Biology of Adult Mesenchymal Stem Cells. *Cancer Research*. **68**, 4229-4238.

Jackson, K.G., Poppitt, S.D., Minihane, A.M., 2012. Postprandial lipemia and cardiovascular disease risk: Interrelationships between dietary, physiological and genetic determinants. *Atherosclerosis*. **220**, 22-33.

Jain, R.K., 2003. Molecular regulation of vessel maturation. *Nature Medicine*. **9**, 685-693.

Janderová, L., McNeil, M., Murrell, A.N., Mynatt, R.L., Smith, S.R., 2003. Human Mesenchymal Stem Cells as an in Vitro Model for Human Adipogenesis. *Obesity Research*. **11**, 65-74.

Jarinova, O., Stewart, A.F.R., Roberts, R., Wells, G., Lau, P., Naing, T., Buerki, C., McLean, B.W., Cook, R.C., Parker, J.S., McPherson, R., 2009. Functional Analysis of the Chromosome 9p21.3 Coronary Artery Disease Risk Locus. *Arteriosclerosis Thrombosis and Vascular Biology*. **29**, 1671-1677.

Javazon, E.H., Beggs, K.J., Flake, A.W., 2004. Mesenchymal stem cells: Paradoxes of passaging. *Experimental Hematology*. **32**, 414-425.

Jeon, E.S., Moon, H.J., Lee, M.J., Song, H.Y., Kim, Y.M., Bae, Y.C., Jung, J.S., Kim, J.H., 2006. Sphingosylphosphorylcholine induces differentiation of human mesenchymal stem cells into smooth-muscle-like cells through a TGF-beta-dependent mechanism. *Journal of Cell Science*. **119**, 4994-5005.

Jiang, S.Y., Shyu, R.Y., Huang, M.F., Tang, H.S., Young, T.H., Roffler, S.R., Chiou, Y.S., Yeh, M.Y., 1997. Detection of alphafetoprotein-expressing cells in the blood of patients with hepatoma and hepatitis. *British Journal of Cancer*. **75**, 928-933.

Kajiwara, M., Aoi, T., Okita, K., Takahashi, R., Inoue, H., Takayama, N., Endo, H., Eto, K., Toguchida, J., Uemoto, S., Yamanaka, S., 2012. Donor-dependent variations in

- hepatic differentiation from human-induced pluripotent stem cells. *Proceedings of the National Academy of Sciences*. **109**, 12538-12543.
- Kang, X., Zang, W., Bao, L., Li, D., Xu, X., Yu, X., 2006. Differentiating characterization of human umbilical cord blood-derived mesenchymal stem cells in vitro. *Cell Biology International*. **30**, 569-575.
- Karahuseyinoglu, S., Cinar, O., Kilic, E., Kara, F., Akay, G.G., Demiralp, D.O., Tukun, A., Uckan, D., Can, A., 2007. Biology of stem cells in human umbilical cord stroma: In situ and in vitro surveys. *Stem Cells*. **25**, 319-331.
- Kashiwagi, M., Enghild, J.J., Gendron, C., Hughes, C., Caterson, B., Itoh, Y., Nagase, H., 2004. Altered Proteolytic Activities of ADAMTS-4 Expressed by C-terminal Processing. *Journal of Biological Chemistry*. **279**, 10109-10119.
- Kashiwakura, Y., Katoh, Y., Tamayose, K., Konishi, H., Takaya, N., Yuhara, S., Yamada, M., Sugimoto, K., Daida, H., 2003. Isolation of Bone Marrow Stromal Cell-Derived Smooth Muscle Cells by a Human SM22a Promoter: In Vitro Differentiation of Putative Smooth Muscle Progenitor Cells of Bone Marrow. *Circulation*. **107**, 2078-2081.
- Kennea, N.L. & Mehmet, H., 2002. Neural stem cells. *The Journal of Pathology*. **197**, 536-550.
- Kern, S., Eichler, H., Stoeve, J., Klueter, H., Bieback, K., 2006. Comparative analysis of mesenchymal stem cells from bone marrow, umbilical cord blood, or adipose tissue. *Stem Cells*. **24**, 1294-1301.
- Kessler, T., Zhang, L., Liu, Z., Yin, X., Huang, Y., Wang, Y., Fu, Y., Mayr, M., Ge, Q., Xu, Q., Zhu, Y., Wang, X., Schmidt, K., de Wit, C., Erdmann, J., Schunkert, H., Aherrahrou, Z., Kong, W., 2015. ADAMTS-7 Inhibits Re-endothelialization of Injured Arteries and Promotes Vascular Remodeling Through Cleavage of Thrombospondin-1. *Circulation*. **131**, 1191-1201.
- Khetchoumian, K., Teletin, M., Mark, M., Lerouge, T., Cerviño, M., Oulad-Abdelghani, M., Chambon, P., Losson, R., 2004. TIF1 $\delta$ , a Novel HP1-interacting Member of the Transcriptional Intermediary Factor 1 (TIF1) Family Expressed by Elongating Spermatids. *Journal of Biological Chemistry*. **279**, 48329-48341.
- Kiechl, S., Lorenz, E., Reindl, M., Wiedermann, C.J., Oberhollenzer, F., Bonora, E., Willeit, J., Schwartz, D.A., 2002. Toll-like Receptor 4 Polymorphisms and Atherogenesis. *N Engl J Med*. **347**, 185-192.
- Kim, J.B., Deluna, A., Mungrue, I.N., Vu, C., Pouldar, D., Civelek, M., Orozco, L., Wu, J., Wang, X., Charugundla, S., Castellani, L.W., Rusek, M., Jakubowski, H., Lusis, A.J., 2012. Effect of 9p21.3 Coronary Artery Disease Locus Neighboring Genes on Atherosclerosis in Mice. *Circulation*. **126**, 1896-1906.

- Kim, M.J., Shin, K.S., Jeon, J.H., Lee, D.R., Shim, S.H., Kim, J.K., Cha, D., Yoon, T.K., Kim, G.J., 2011. Human chorionic-plate-derived mesenchymal stem cells and Wharton's jelly-derived mesenchymal stem cells: a comparative analysis of their potential as placenta-derived stem cells. *Cell and Tissue Research*. **346**, 53-64.
- Kinner, B., Zaleskas, J.M., Spector, M., 2002. Regulation of Smooth Muscle Actin Expression and Contraction in Adult Human Mesenchymal Stem Cells. *Experimental Cell Research*. **278**, 72-83.
- Kinoshita, T. & Miyajima, A., 2002. Cytokine regulation of liver development. *Biochimica Et Biophysica Acta (BBA) - Molecular Cell Research*. **1592**, 303-312.
- Kobayashi, N., Yasu, T., Ueba, H., Sata, M., Hashimoto, S., Kuroki, M., Saito, M., Kawakami, M., 2004. Mechanical stress promotes the expression of smooth muscle-like properties in marrow stromal cells. *Experimental Hematology*. **32**, 1238-1245.
- Koo, B., Longpré, J., Somerville, R.P.T., Alexander, J.P., Leduc, R., Apte, S.S., 2006. Cell-surface Processing of Pro-ADAMTS9 by Furin. *Journal of Biological Chemistry*. **281**, 12485-12494.
- Kosmacheva, S.M., Seviaryn, I.N., Goncharova, N.V., Petyovka, N.V., Potapnev, M.P., 2011. Hepatogenic potential of human bone marrow and umbilical cord blood mesenchymal stem cells. *Bulletin of Experimental Biology and Medicine*. **151**, 142-149.
- Kramer, J., Aguirre-Arteta, A.M., Thiel, C., Gross, C.M., Dietz, R., Cardoso, M.C., Leonhardt, H., 1999. A novel isoform of the smooth muscle cell differentiation marker smoothelin. *Journal of Molecular Medicine (Berlin, Germany)*. **77**, 294-298.
- Kuno, K., Kanada, N., Nakashima, E., Fujiki, F., Ichimura, F., Matsushima, K., 1997. Molecular Cloning of a Gene Encoding a New Type of Metalloproteinase-disintegrin Family Protein with Thrombospondin Motifs as an Inflammation Associated Gene. *Journal of Biological Chemistry*. **272**, 556-562.
- Kurpinski, K., Lam, H., Chu, J., Wang, A., Kim, A., Tsay, E., Agrawal, S., Schaffer, D.V., Li, S., 2010. Transforming Growth Factor-Beta and Notch Signaling Mediate Stem Cell Differentiation into Smooth Muscle Cells. *Stem Cells*. **28**, 734-742.
- Kuznetsov, S.A., Krebsbach, P.H., Satomura, K., Kerr, J., Riminucci, M., Benayahu, D., Robey, P.G., 1997. Single-Colony Derived Strains of Human Marrow Stromal Fibroblasts Form Bone After Transplantation In Vivo. *Journal of Bone and Mineral Research*. **12**, 1335-1347.
- Kwon, J.M. & Goate, A.M., 2000. The candidate gene approach. *Alcohol Research & Health*. **24**, 164-168.
- La Rocca, G., Anzalone, R., Corrao, S., Magno, F., Loria, T., Lo Iacono, M., Di Stefano, A., Giannuzzi, P., Marasa, L., Cappello, F., Zummo, G., Farina, F., 2009. Isolation and characterization of Oct-4(+)/HLA-G(+) mesenchymal stem cells from human umbilical

cord matrix: differentiation potential and detection of new markers. *Histochemistry and Cell Biology*. **131**, 267-282.

LaFramboise, T., 2009. Single nucleotide polymorphism arrays: a decade of biological, computational and technological advances. *Nucleic Acids Research*. **37**, 4181-4193.

Lawson, D., Harrison, M., Shapland, C., 1997. Fibroblast transgelin and smooth muscle SM22 alpha are the same protein, the expression of which is down-regulated in many cell lines. *Cell Motility and the Cytoskeleton*. **38**, 250-257.

Le Blanc, K., Tammik, C., Rosendahl, K., Zetterberg, E., Ringden, O., 2003. HLA expression and immunologic properties of differentiated and undifferentiated mesenchymal stem cells. *Experimental Hematology*. **31**, 890-896.

Lee, K., Kuo, T.K., Whang-Peng, J., Chung, Y., Lin, C., Chou, S., Chen, J., Chen, Y., Lee, O.K., 2004. In vitro hepatic differentiation of human mesenchymal stem cells. *Hepatology*. **40**, 1275-1284.

Lee, M.H., Lu, K., Hazard, S., Yu, H., Shulenin, S., Hidaka, H., Kojima, H., Allikmets, R., Sakuma, N., Pegoraro, R., Srivastava, A.K., Salen, G., Dean, M., Patel, S.B., 2001. Identification of a gene, ABCG5, important in the regulation of dietary cholesterol absorption. *Nature Genetics*. **27**, 79-83.

Lee, O.K., Kuo, T.K., Chen, W.M., Lee, K.D., Hsieh, S.L., Chen, T.H., 2004. Isolation of multipotent mesenchymal stem cells from umbilical cord blood. *Blood*. **103**, 1669-1675.

Lee, T., Song, S., Kim, K.L., Yi, J., Shin, G., Kim, J.Y., Kim, J., Han, Y., Lee, S.H., Lee, S., Shim, S.H., Suh, W., 2010. Functional Recapitulation of Smooth Muscle Cells Via Induced Pluripotent Stem Cells From Human Aortic Smooth Muscle Cells. *Circulation Research*. **106**, 120-128.

LeVan, T.D., Bloom, J.W., Bailey, T.J., Karp, C.L., Halonen, M., Martinez, F.D., Vercelli, D., 2001. A common single nucleotide polymorphism in the CD14 promoter decreases the affinity of Sp protein binding and enhances transcriptional activity. *Journal of Immunology*. **167**, 5838-5844.

Liang, J., Song, W., Tromp, G., Kolattukudy, P.E., Fu, M., 2008. Genome-Wide Survey and Expression Profiling of CCCH-Zinc Finger Family Reveals a Functional Module in Macrophage Activation. *PLoS ONE*. **3**, e2880.

Libby, P., 2009. Molecular and cellular mechanisms of the thrombotic complications of atherosclerosis. *Journal of Lipid Research*. **50**, S352-S357.

Libby, P., 2002. Inflammation in atherosclerosis. *Nature*. **420**, 868-874.

Libby, P., Ridker, P.M., Hansson, G.K., 2011. Progress and challenges in translating the biology of atherosclerosis. *Nature*. **473**, 317-325.

- Liu, C., Kong, W., Ilalov, K., Yu, S., Xu, K., Prazak, L., Fajardo, M., Sehgal, B., Di Cesare, P.E., 2006. ADAMTS-7: a metalloproteinase that directly binds to and degrades cartilage oligomeric matrix protein. *The FASEB Journal*. **20**, 988-990.
- Liu, X., LeCluyse, E.L., Brouwer, K.R., Gan, L.L., Lemasters, J.J., Stieger, B., Meier, P.J., Brouwer, K.L.R., 1999. Biliary excretion in primary rat hepatocytes cultured in a collagen-sandwich configuration. *American Journal of Physiology - Gastrointestinal and Liver Physiology*. **277**, G12-G21.
- Liu, Y., Sanoff, H.K., Cho, H., Burd, C.E., Torrice, C., Mohlke, K.L., Ibrahim, J.G., Thomas, N.E., Sharpless, N.E., 2009. *INK4/ARF* Transcript Expression Is Associated with Chromosome 9p21 Variants Linked to Atherosclerosis. *PLoS ONE*. **4**, e5027.
- Lloyd-Jones, D.M., Nam, B.H., D'Agostino, R.B., Levy, D., Murabito, J.M., Wang, T.J., Wilson, P.W.F., O'Donnell, C.J., 2004. Parental cardiovascular disease as a risk factor for cardiovascular disease in middle-aged adults - A prospective study of parents and offspring. *Jama-Journal of the American Medical Association*. **291**, 2204-2211.
- Lloyd-Jones, D., Adams, R., Carnethon, M., De Simone, G., Ferguson, T.B., Flegal, K., Ford, E., Furie, K., Go, A., et al. 2009. Heart disease and stroke statistics--2009 update: a report from the American Heart Association Statistics Committee and Stroke Statistics Subcommittee. *Circulation*. **119**, 480-486.
- Locke, A.E., Kahali, B., Berndt, S.I., Justice, A.E., Pers, T.H., Day, FR., et al. 2015. Genetic studies of body mass index yield new insights for obesity biology. *Nature*. **518**, 197-206.
- Loos, R.J.F., Lindgren, C.M., Li, S., Wheeler, E., Zhao, J.H., Prokopenko, I., Inouye, M., Freathy, et al. 2008. Common variants near *MC4R* are associated with fat mass, weight and risk of obesity. *Nature Genetics*. **40**, 768-775.
- Löser, P., Schirm, J., Guhr, A., Wobus, A.M., Kurtz, A., 2010. Human Embryonic Stem Cell Lines and Their Use in International Research. *Stem Cells*. **28**, 240-246.
- Lu, L., Liu, Y., Yang, S., Zhao, Q., Wang, X., Gong, W., Han, Z., Xu, Z., Lu, Y., Liu, D., Chen, Z., Han, Z., 2006. Isolation and characterization of human umbilical cord mesenchymal stem cells with hematopoiesis-supportive function and other potentials. *Haematologica-the Hematology Journal*. **91**, 1017-1026.
- Lusis, A.J., 2000. Atherosclerosis. *Nature*. **407**, 233-241.
- Mackay, A.M., Beck, S.C., Murphy, J.M., Barry, F.P., Chichester, C.O., Pittenger, M.F., 1998. Chondrogenic differentiation of cultured human mesenchymal stem cells from marrow. *Tissue Engineering*. **4**, 415-428.
- Mackay, J. & Mensah, G.A., 2004. The Atlas of Heart Disease and Stroke. World Health Organization. Available at: [http://www.who.int/cardiovascular\\_diseases/resources/atlas/en/](http://www.who.int/cardiovascular_diseases/resources/atlas/en/)

- Maes, H.H., Neale, M.C., Eaves, L.J., 1997. Genetic and environmental factors in relative body weight and human adiposity. *Behavior Genetics*. **27**, 325-351.
- Maherali, N., Ahfeldt, T., Rigamonti, A., Utikal, J., Cowan, C., Hochedlinger, K., 2008. A High-Efficiency System for the Generation and Study of Human Induced Pluripotent Stem Cells. *Cell Stem Cell*. **3**, 340-345.
- Mahoney, W.M. & Schwartz, S.M., 2005. Defining smooth muscle cells and smooth muscle injury. *Journal of Clinical Investigation*. **115**, 221-224.
- Marenberg, M.E., Risch, N., Berkman, L.F., Floderus, B., Defaire, U., 1994. Genetic Susceptibility to Death from Coronary Heart-Disease in a Study of Twins. *New England Journal of Medicine*. **330**, 1041-1046.
- Marotti, K.R., Castle, C.K., Boyle, T.P., Lin, A.H., Murray, R.W., Melchior, G.W., 1993. Severe atherosclerosis in transgenic mice expressing simian cholesteryl ester transfer protein. *Nature*. **364**, 73-75.
- Martin, G.R., 1981. Isolation of a pluripotent cell line from early mouse embryos cultured in medium conditioned by teratocarcinoma stem cells. *Proceedings of the National Academy of Sciences of the United States of America*. **78**, 7634-7638.
- Massagué, J., Blain, S.W., Lo, R.S., 2000. TGF $\beta$  Signaling in Growth Control, Cancer, and Heritable Disorders. *Cell*. **103**, 295-309.
- Maxwell, K.N. & Breslow, J.L., 2004. Adenoviral-mediated expression of Pcsk9 in mice results in a low-density lipoprotein receptor knockout phenotype. *Proceedings of the National Academy of Sciences of the United States of America*. **101**, 7100-7105.
- McElreavey, K.D., Irvine, A.I., Ennis, K.T., McLean, W.H., 1991. Isolation, culture and characterisation of fibroblast-like cells derived from the Wharton's jelly portion of human umbilical cord. *Biochemical Society Transactions*. **19**, 29S.
- McPherson, R., Pertsemlidis, A., Kavasslar, N., Stewart, A.F.R., Roberts, R., Cox, D.R., Hinds, D.A., Pennacchio, L.A., Tybjaerg-Hansen, A., Folsom, A.R., Boerwinkle, E., Hobbs, H.H., Cohen, J.C., 2007. A common allele on chromosome 9 associated with coronary heart disease. *Science*. **316**, 1488-1491.
- Menendez, L., Kulik, M.J., Page, A.T., Park, S.S., Lauderdale, J.D., Cunningham, M.L., Dalton, S., 2013. Directed differentiation of human pluripotent cells to neural crest stem cells. *Nature Protocols*. **8**, 203–212.
- Menendez, L., Yatskievych, T.A., Antin, P.B., Dalton, S., 2011. Wnt signaling and a Smad pathway blockade direct the differentiation of human pluripotent stem cells to multipotent neural crest cells. *Proc Natl Acad Sci USA*. **108**, 19240–19245.

- Mennan, C., Wright, K., Bhattacharjee, A., Balain, B., Richardson, J., Roberts, S., 2013. Isolation and Characterisation of Mesenchymal Stem Cells from Different Regions of the Human Umbilical Cord. *BioMed Research International*. **2013**, 916136.
- Miano, J.M., Cserjesi, P., Ligon, K.L., Periasamy, M., Olson, E.N., 1994. Smooth muscle myosin heavy chain exclusively marks the smooth muscle lineage during mouse embryogenesis. *Circulation Research*. **75**, 803-812.
- Michalopoulos, G.K., Bowen, W.C., Mulé, K., Luo, J., 2003. HGF, EGF and Dexamethasone induced gene expression patterns during formation of tissue in hepatic organoid cultures. *Gene Expression*. **11**, 55-75.
- Mitaka, T., Sato, F., Mizuguchi, T., Yokono, T., Mochizuki, Y., 1999. Reconstruction of hepatic organoid by rat small hepatocytes and hepatic nonparenchymal cells. *Hepatology*. **29**, 111-125.
- Mitalipov, S. & Wolf, D., 2009. Totipotency, Pluripotency and Nuclear Reprogramming. In Martin, U., ed, Springer Berlin Heidelberg. 185-199.
- Mitchell, K.E., Weiss, M.L., Mitchell, B.M., Martin, P., Davis, D., Morales, L., Helwig, B., Beerenstrauch, M., Abou-Easa, K., Hildreth, T., Troyer, D., 2003. Matrix cells from Wharton's jelly form neurons and glia. *Stem Cells*. **21**, 50-60.
- Mizoguchi, M., Suga, Y., Sanmano, B., Ikeda, S., Ogawa, H., 2004. Organotypic culture and surface plantation using umbilical cord epithelial cells: morphogenesis and expression of differentiation markers mimicking cutaneous epidermis. *Journal of Dermatological Science*. **35**, 199-206.
- Molloy, S.S., Bresnahan, P.A., Leppla, S.H., Klimpel, K.R., Thomas, G., 1992. Human furin is a calcium-dependent serine endoprotease that recognizes the sequence Arg-X-X-Arg and efficiently cleaves anthrax toxin protective antigen. *Journal of Biological Chemistry*. **267**, 16396-16402.
- Momin, E.N., Vela, G., Zaidi, H.A., Quinones-Hinojosa, A., 2010. The Oncogenic Potential of Mesenchymal Stem Cells in the Treatment of Cancer: Directions for Future Research. *Current Immunology Reviews*. **6**, 137-148.
- Moran, N., 2013. Banking iPS cells. *Nature Biotechnology*. **31**, 11-11.
- Moscoso, I., Centeno, A., Lopez, E., Rodriguez-Barbosa, J.I., Santamarina, I., Filgueira, P., Sanchez, M.J., Dominguez-Perles, R., Penuelas-Rivas, G.P., Domenech, N., 2005. Differentiation "in vitro" of primary and immortalized porcine mesenchymal stem cells into cardiomyocytes for cell transplantation. *Transplantation Proceedings*. **37**, 481-482.
- Murabito, J.M., Pencina, M.J., Nam, B.H., D'Agostino, R.B., Wang, T.J., Lloyd-Jones, D., Wilson, P.W.F., O'Donnell, C.J., 2005. Sibling cardiovascular disease as a risk

factor for cardiovascular disease in middle-aged adults. *Jama-Journal of the American Medical Association*. **294**, 3117-3123.

Muraglia, A., Cancedda, R., Quarto, R., 2000. Clonal mesenchymal progenitors from human bone marrow differentiate in vitro according to a hierarchical model. *Journal of Cell Science*. **113**, 1161-1166.

Must, A., Spadano, J., Coakley, E.H., Field, A.E., Colditz, G., Dietz, W.H., 1999. The disease burden associated with overweight and obesity. *Jama*. **282**, 1523-1529.

Musunuru, K., Strong, A., Frank-Kamenetsky, M., Lee, N.E., Ahfeldt, T., Sachs, K.V., Li, X., Li, H., Kuperwasser, N., Ruda, V.M., Pirruccello, J.P., Muchmore, B., Prokunina-Olsson, L., Hall, J.L., Schadt, E.E., Morales, C.R., Lund-Katz, S., Phillips, M.C., Wong, J., Cantley, W., Racie, T., Ejebe, K.G., Orho-Melander, M., Melander, O., Koteliensky, V., Fitzgerald, K., Krauss, R.M., Cowan, C.A., Kathiresan, S., Rader, D.J., 2010. From noncoding variant to phenotype via SORT1 at the 1p13 cholesterol locus. *Nature*. **466**, 714-U2.

Nanaev, A.K., Kohnen, G., Milovanov, A.P., Domogatsky, S.P., Kaufman, P., 1997. Stromal differentiation and architecture of the human umbilical cord. *Placenta*. **18**, 53-64.

Narita, Y., Yamawaki, A., Kagami, H., Ueda, M., Ueda, Y., 2008. Effects of transforming growth factor-beta 1 and ascorbic acid on differentiation of human bone-marrow-derived mesenchymal stem cells into smooth muscle cell lineage. *Cell and Tissue Research*. **333**, 449-459.

Nasir, K., Michos, E.D., Rumberger, J.A., Braunstein, J.B., Post, W.S., Budoff, M.J., Blumenthal, R.S., 2004. Coronary artery calcification and family history of premature coronary heart disease - Sibling history is more strongly associated than parental history. *Circulation*. **110**, 2150-2156.

Nasir, K., Budoff, M.J., Wong, N.D., Scheuner, M., Herrington, D., Arnett, D.K., Szklo, M., Greenland, P., Blumenthal, R.S., 2007. Family history of premature coronary heart disease and coronary artery calcification - Multi-Ethnic Study of Atherosclerosis (MESA). *Circulation*. **116**, 619-626.

Neubauer, M., Fischbach, C., Bauer-Kreisel, P., Lieb, E., Hacker, M., Tessmar, J., Schulz, M.B., Goepferich, A., Blunk, T., 2004. Basic fibroblast growth factor enhances PPAR $\gamma$  ligand-induced adipogenesis of mesenchymal stem cells. *FEBS Letters*. **577**, 277-283.

Newman, B., Selby, J.V., King, M.C., Slemenda, C., Fabsitz, R., Friedman, G.D., 1987. Concordance for type 2 (non-insulin-dependent) diabetes mellitus in male twins. *Diabetologia*. **30**, 763-768.

- Newton, G., Weremowicz, S., Morton, C.C., Copeland, N.G., Gilbert, D.J., Jenkins, N.A., Lawler, J., 1994. Characterization of Human and Mouse Cartilage Oligomeric Matrix Protein. *Genomics*. **24**, 435-439.
- Nishikawa, Y., Doi, Y., Watanabe, H., Tokairin, T., Omori, Y., Su, M., Yoshioka, T., Enomoto, K., 2005. Transdifferentiation of Mature Rat Hepatocytes into Bile Duct-Like Cells in Vitro. *The American Journal of Pathology*. **166**, 1077-1088.
- Noer, A., Boquest, A.C., Collas, P., 2007. Dynamics of adipogenic promoter DNA methylation during clonal culture of human adipose stem cells to senescence. *BMC Cell Biology*. **8**, 18.
- Nolte, R.T., Wisely, G.B., Westin, S., Cobb, J.E., Lambert, M.H., Kurokawa, R., Rosenfeld, M.G., Willson, T.M., Glass, C.K., Milburn, M.V., 1998. Ligand binding and co-activator assembly of the peroxisome proliferator-activated receptor-gamma]. *Nature*. **395**, 137-143.
- Novak, A., Barad, L., Zeevi-Levin, N., Shick, R., Shtrichman, R., Lorber, A., Itskovitz-Eldor, J., Binah, O., 2012. Cardiomyocytes generated from CPVTD307H patients are arrhythmogenic in response to beta-adrenergic stimulation. *Journal of Cellular and Molecular Medicine*. **16**, 468-482.
- Okada, Y., Kubo, M., Ohmiya, H., Takahashi, A., Kumasaka, N., Hosono, N., Maeda, S., Wen, W., Dorajoo, R., Go, M.J., Zheng, W., Kato, N., Wu, J., Lu, Q., Tsunoda, T., Yamamoto, K., Nakamura, Y., Kamatani, N., Tanaka, T., 2012. Common variants at CDKAL1 and KLF9 are associated with body mass index in east Asian populations. *Nature Genetics*. **44**, 302-306.
- Olsavsky Goyak, K.M., Laurenzana, E.M., Omiecinski, C.J., 2010. Hepatocyte differentiation. *Methods in Molecular Biology (Clifton, N.J.)*. **640**, 115-138.
- Orlandi, A., Ropraz, P., Gabbiani, G., 1994. Proliferative Activity and  $\alpha$ -Smooth Muscle Actin Expression in Cultured Rat Aortic Smooth Muscle Cells Are Differently Modulated by Transforming Growth Factor- $\beta$ 1 and Heparin. *Experimental Cell Research*. **214**, 528-536.
- Oswald, J., Boxberger, S., Jorgensen, B., Feldmann, S., Ehninger, G., Bornhauser, M., Werner, C., 2004. Mesenchymal stem cells can be differentiated into endothelial cells in vitro. *Stem Cells*. **22**, 377-384.
- Owens, G.K., 1995. Regulation of differentiation of vascular smooth muscle cells. *Physiological Reviews*. **75**, 487-517.
- Owens, G.K., 1998. Molecular control of vascular smooth muscle cell differentiation. *Acta Physiologica Scandinavica*. **164**, 623-635.

- Owens, G.K., Kumar, M.S., Wamhoff, B.R., 2004. Molecular Regulation of Vascular Smooth Muscle Cell Differentiation in Development and Disease. *Physiological Reviews*. **84**, 767-801.
- Ozaki, K., Ohnishi, Y., Iida, A., Sekine, A., Yamada, R., Tsunoda, T., Sato, H., Sato, H., Hori, M., Nakamura, Y., Tanaka, T., 2002. Functional SNPs in the lymphotoxin-alpha gene that are associated with susceptibility to myocardial infarction. *Nature Genetics*. **32**, 650-654.
- Pacini, S., 2014. Deterministic and Stochastic Approaches in the Clinical Application of Mesenchymal Stromal Cells (MSCs). *Frontiers in Cell and Developmental Biology*. **2**, 50.
- Pappa, K.I. & Anagnou, N.P., 2009. Novel sources of fetal stem cells: where do they fit on the developmental continuum? *Regenerative Medicine*. **4**, 423-433.
- Patel, R. & Ye, S., 2011. Genetic determinants of coronary heart disease: new discoveries and insights from genome-wide association studies. *Heart*. **97**, 1463-1473.
- Penolazzi, L., Vecchiatini, R., Bignardi, S., Lambertini, E., Torreggiani, E., Canella, A., Franceschetti, T., Calura, G., Vesce, F., Piva, R., 2009. Influence of obstetric factors on osteogenic potential of umbilical cord-derived mesenchymal stem cells. *Reproductive Biology and Endocrinology*. **7**, 106.
- Petretto, E., Liu, E.T., Aitman, T.J., 2007. A gene harvest revealing the archeology and complexity of human disease. *Nature Genetics*. **39**, 1299-301.
- Pevsner-Fischer, M., Levin, S., Zipori, D., 2011. The Origins of Mesenchymal Stromal Cell Heterogeneity. *Stem Cell Reviews and Reports*. **7**, 560-568.
- Phinney, D.G., Kopen, G., Righter, W., Webster, S., Tremain, N., Prockop, D.J., 1999. Donor variation in the growth properties and osteogenic potential of human marrow stromal cells. *Journal of Cellular Biochemistry*. **75**, 424-436.
- Phinney, D.G., 2012. Functional heterogeneity of mesenchymal stem cells: Implications for cell therapy. *Journal of Cellular Biochemistry*. **113**, 2806-2812.
- Pierdomenico, L., Lanuti P., Lachmann R., Grifone G., Cianci E., Gialò L., Pacella, S., Romano, M., Vitacolonna, E., Miscia, S., 2011. Diabetes mellitus during pregnancy interferes with the biological characteristics of wharton's jelly mesenchymal stem cells. *The Open Tissue Engineering and Regenerative Medicine Journal*. **4**, 103–111.
- Pittenger, M.F., Mackay, A.M., Beck, S.C., Jaiswal, R.K., Douglas, R., Mosca, J.D., Moorman, M.A., Simonetti, D.W., Craig, S., Marshak, D.R., 1999. Multilineage potential of adult human mesenchymal stem cells. *Science*. **284**, 143-147.

Platt, I.D. & El-Sohemy, A., 2009. Regulation of osteoblast and adipocyte differentiation from human mesenchymal stem cells by conjugated linoleic acid. *The Journal of Nutritional Biochemistry*. **20**, 956-964.

Pless, G., Steffen, I., Zeilinger, K., Sauer, I.M., Katenz, E., Kehr, D.C., Roth, S., Mieder, T., Schwartlander, R., Müller, C., Wegner, B., Hout, M.S., Gerlach, J.C., 2006. Evaluation of Primary Human Liver Cells in Bioreactor Cultures for Extracorporeal Liver Support on the Basis of Urea Production. *Artificial Organs*. **30**, 686-694.

Polder, H., Weskamp, M., Linz, K. and Meyer, R., 2005. Voltage-Clamp and Patch-Clamp Techniques. In Dhein, S., Mohr, F. and Delmar, M., eds, Springer Berlin Heidelberg. 272-323.

Prasajak, P. & Leeanansaksiri, W., 2013. Developing a New Two-Step Protocol to Generate Functional Hepatocytes from Wharton's Jelly-Derived Mesenchymal Stem Cells under Hypoxic Condition. *Stem Cells International*. **2013**, 762196.

Pritchard, J.K., 2001. Are Rare Variants Responsible for Susceptibility to Complex Diseases? *The American Journal of Human Genetics*. **69**, 124-137.

Prockop, D.J., 1997. Marrow stromal cells as stem cells for nonhematopoietic tissues. *Science (Washington D C)*. **276**, 71-74.

Pu, X., Xiao, Q., Kiechl, S., Chan, K., Ng, F., Gor, S., Poston, R., Fang, C., Patel, A., Senver, E., Shaw-Hawkins, S., Willeit, J., Liu, C., Zhu, J., Tucker, A., Xu, Q., Caulfield, M., Ye, S., 2013. ADAMTS7 Cleavage and Vascular Smooth Muscle Cell Migration Is Affected by a Coronary-Artery-Disease-Associated Variant. *The American Journal of Human Genetics*. **92**, 366-374.

Qian, S., Li, X., Zhang, Y., Huang, H., Liu, Y., Sun, X., Tang, Q., 2010. Characterization of adipocyte differentiation from human mesenchymal stem cells in bone marrow. *BMC Developmental Biology*. **10**, 47.

Qiao, C., Xu, W., Zhu, W., Hu, J., Qian, H., Yin, Q., Jiang, R., Yan, Y., Mao, F., Yang, H., Wang, X., Chen, Y., 2008. Human mesenchymal stem cells isolated from the umbilical cord. *Cell Biology International*. **32**, 8-15.

Raimondo, S., Penna, C., Pagliaro, P., Geuna, S., 2006. Morphological characterization of GFP stably transfected adult mesenchymal bone marrow stem cells. *Journal of Anatomy*. **208**, 3-12.

Raio, L., Ghezzi, F., Di Naro, E., Gomez, R., Franchi, M., Mazor, M., Bruhwiler, H., 1999. Sonographic measurement of the umbilical cord and fetal anthropometric parameters. *European Journal of Obstetrics Gynecology and Reproductive Biology*. **83**, 131-135.

Rashid, S.T., Corbineau, S., Hannan, N., Marciniak, S.J., Miranda, E., Alexander, G., Huang-Doran, I., Griffin, J., Ahrlund-Richter, L., Skepper, J., Semple, R., Weber, A.,

- Lomas, D.A., Vallier, L., 2010. Modeling inherited metabolic disorders of the liver using human induced pluripotent stem cells. *The Journal of Clinical Investigation*. **120**, 3127-3136.
- Reich, D.E. & Lander, E.S., 2001. On the allelic spectrum of human disease. *Trends in Genetics*. **17**, 502-510.
- Reilly, M.P., Li, M., He, J., Ferguson, J.F., Stylianou, I.M., Mehta, N.N., Burnett, M.S., Devaney, J.M., et al. 2011. Identification of ADAMTS7 as a novel locus for coronary atherosclerosis and association of ABO with myocardial infarction in the presence of coronary atherosclerosis: two genome-wide association studies. *Lancet*. **377**, 383-392.
- Riessen, R., Fenchel, M., Chen, H., Axel, D.I., Karsch, K.R., Lawler, J., 2001. Cartilage Oligomeric Matrix Protein (Thrombospondin-5) Is Expressed by Human Vascular Smooth Muscle Cells. *Arteriosclerosis, Thrombosis, and Vascular Biology*. **21**, 47-54.
- Roberts, R. & Stewart, A.F.R., 2012. 9p21 and the Genetic Revolution for Coronary Artery Disease. *Clinical Chemistry*. **58**, 104-112.
- Roberts, R., 2014. Genetics of Coronary Artery Disease. *Circulation Research*. **114**, 1890-1903.
- Rogiers, V. & Vercruyse, A., 1993. Rat hepatocyte cultures and co-cultures in biotransformation studies of xenobiotics. *Toxicology*. **82**, 193-208.
- Runge, D., Runge, D.M., Jäger, D., Lubecki, K.A., Beer Stolz, D., Karathanasis, S., Kietzmann, T., Strom, S.C., Jungermann, K., Fleig, W.E., Michalopoulos, G.K., 2000. Serum-Free, Long-Term Cultures of Human Hepatocytes: Maintenance of Cell Morphology, Transcription Factors, and Liver-Specific Functions. *Biochemical and Biophysical Research Communications*. **269**, 46-53.
- Russell, K.C., Phinney, D.G., Lacey, M.R., Barrilleaux, B.L., Meyertholen, K.E., O'Connor, K.C., 2010. In Vitro High-Capacity Assay to Quantify the Clonal Heterogeneity in Trilineage Potential of Mesenchymal Stem Cells Reveals a Complex Hierarchy of Lineage Commitment. *Stem Cells*. **28**, 788-798.
- Rust, S., Rosier, M., Funke, H., Real, J., Amoura, Z., Piette, J., Deleuze, J., Brewer, H.B., Duverger, N., Deneffe, P., Assmann, G., 1999. Tangier disease is caused by mutations in the gene encoding ATP-binding cassette transporter 1. *Nature Genetics*. **22**, 352-355.
- Ruzicka, D.L. & Schwartz, R.J., 1988. Sequential activation of alpha-actin genes during avian cardiogenesis: vascular smooth muscle alpha-actin gene transcripts mark the onset of cardiomyocyte differentiation. *The Journal of Cell Biology*. **107**, 2575-2586.
- Sakaguchi, Y., Sekiya, I., Yagishita, K., Muneta, T., 2005. Comparison of human stem cells derived from various mesenchymal tissues: Superiority of synovium as a cell source. *Arthritis & Rheumatism*. **52**, 2521-2529.

- Sakai, Y., Jiang, J., Kojima, N., Kinoshita, T., Miyajima, A., 2002. Enhanced in vitro maturation of fetal mouse liver cells with oncostatin M, nicotinamide, and dimethyl sulfoxide. *Cell Transplantation*. **11**, 435-441.
- Samani, N.J., Erdmann, J., Hall, A.S., Hengstenberg, C., Mangino, M., Mayer, B., Dixon, R.J., Meitinger, T., Braund, P., et al. 2007. Genome-wide association analysis of coronary artery disease. *New England Journal of Medicine*. **357**, 443-453.
- Sanna, S., Li, B., Mulas, A., Sidore, C., Kang, H.M., Jackson, A.U., Piras, M.G., Usala, G., Maninchedda, G., Sassu, A., Serra, F., Palmas, M.A., Wood, William H., I., II, Njølstad, I., Laakso, M., Hveem, K., Tuomilehto, J., Lakka, T.A., Rauramaa, R., Boehnke, M., Cucca, F., Uda, M., Schlessinger, D., Nagaraja, R., Abecasis, G.R., 2011. Fine Mapping of Five Loci Associated with Low-Density Lipoprotein Cholesterol Detects Variants That Double the Explained Heritability. *PLoS Genet*. **7**, e1002198.
- Santa Maria, L., Rojas, C.V., Minguell, J.J., 2004. Signals from damaged but not undamaged skeletal muscle induce myogenic differentiation of rat bone-marrow-derived mesenchymal stem cells. *Experimental Cell Research*. **300**, 418-426.
- Sawtell, N.M. & Lessard, J.L., 1989. Cellular distribution of smooth muscle actins during mammalian embryogenesis: expression of the alpha-vascular but not the gamma-enteric isoform in differentiating striated myocytes. *The Journal of Cell Biology*. **109**, 2929-2937.
- Scarborough, P., Bhatnagar, P., Wickramasinghe, K., Smolina, K., Mitchell, C., Rayner, M., 2010. Coronary Heart Disease Statistics 2010 Edition. British Heart Foundation Health Promotion Research Group. Available: [https://www.bhf.org.uk/~media/files/research/heart-statistics/hs2010\\_coronary\\_heart\\_disease\\_statistics.pdf](https://www.bhf.org.uk/~media/files/research/heart-statistics/hs2010_coronary_heart_disease_statistics.pdf)
- Schönbeck, U., Mach, F., Sukhova, G.K., Herman, M., Graber, P., Kehry, M.R., Libby, P., 1999. CD40 Ligation Induces Tissue Factor Expression in Human Vascular Smooth Muscle Cells. *The American Journal of Pathology*. **156**, 7-14.
- Schaedlich, K., Knelangen, J.M., Navarrete Santos, A., Fischer, B., Navarrete Santos, A., 2010. A simple method to sort ESC-derived adipocytes. *Cytometry Part A*. **77A**, 990-995.
- Schildkraut, J.M., Myers, R.H., Cupples, L.A., Kiely, D.K., Kannel, W.B., 1989. Coronary risk associated with age and sex of parental heart disease in the Framingham Study. *The American Journal of Cardiology*. **64**, 555-559.
- Schmidt, C., Bladt, F., Goedecke, S., Brinkmann, V., Zschiesche, W., Sharpe, M., Gherardi, E., Birchmeier, C., 1995. Scatter factor/hepatocyte growth factor is essential for liver development. *Nature*. **373**, 699-702.
- Schunkert, H., König, I.R., Kathiresan, S., Reilly, M.P., Assimes, T.L., Holm, H., Preuss, M., Stewart, A.F.R., et al. 2011. Large-scale association analysis identifies 13 new susceptibility loci for coronary artery disease. *Nature Genetics*. **43**, 333-338.

- Schwartz, S.M., 1997. Perspectives series: cell adhesion in vascular biology. Smooth muscle migration in atherosclerosis and restenosis. *The Journal of Clinical Investigation*. **99**, 2814–2816.
- Schwartz, R.E., Reyes, M., Koodie, L., Jiang, Y., Blackstad, M., Lund, T., Lenvik, T., Johnson, S., Hu, W., Verfaillie, C.M., 2002. Multipotent adult progenitor cells from bone marrow differentiate into functional hepatocyte-like cells. *The Journal of Clinical Investigation*. **109**, 1291-1302.
- Scuteri, A., Sanna, S., Chen, W., Uda, M., Albai, G., Strait, J., Najjar, S., Nagaraja, R., OrrÃº, M., Usala, G., Dei, M., Lai, S., Maschio, A., Busonero, F., Mulas, A., Ehret, G.B., Fink, A.A., Weder, A.B., Cooper, R.S., Galan, P., Chakravarti, A., Schlessinger, D., Cao, A., Lakatta, E., Abecasis, G.R., 2007. Genome-Wide Association Scan Shows Genetic Variants in the FTO Gene Are Associated with Obesity-Related Traits. *PLoS Genetics*. **3**, e115.
- Seidah, N.G., Benjannet, S., Wickham, L., Marcinkiewicz, J., Jasmin, S.B., Stifani, S., Basak, A., Prat, A., Chrétien, M., 2003. The secretory proprotein convertase neural apoptosis-regulated convertase 1 (NARC-1): Liver regeneration and neuronal differentiation. *Proceedings of the National Academy of Sciences*. **100**, 928-933.
- Sekiya, I., Larson, B.L., Vuoristo, J.T., Cui, J., Prockop, D.J., 2004. Adipogenic Differentiation of Human Adult Stem Cells From Bone Marrow Stroma (MSCs). *Journal of Bone and Mineral Research*. **19**, 256-264.
- Sexton, T., Bantignies, F., Cavalli, G., 2009. Genomic interactions: Chromatin loops and gene meeting points in transcriptional regulation. *Seminars in Cell & Developmental Biology*. **20**, 849-855.
- Shapland, C., Hsuan, J.J., Totty, N.F., Lawson, D., 1993. Purification and properties of transgelin: a transformation and shape change sensitive actin-gelling protein. *The Journal of Cell Biology*. **121**, 1065-1073.
- Shaw, S.Y. & Brettman, A.D., 2011. Phenotyping Patient-Derived Cells for Translational Studies in Cardiovascular Disease. *Circulation*. **124**, 2444-2455.
- Shi, Y. & Massagué, J., 2003. Mechanisms of TGF- $\beta$  Signaling from Cell Membrane to the Nucleus. *Cell*. **113**, 685-700.
- Silva, G.V., Litovsky, S., Assad, J.A.R., Sousa, A.L.S., Martin, B.J., Vela, D., Coulter, S.C., Lin, J., Ober, J., Vaughn, W.K., Branco, R.V.C., Oliveira, E.M., He, R.M., Geng, Y.J., Willerson, J.T., Perin, E.C., 2005. Mesenchymal stem cells differentiate into an endothelial phenotype, enhance vascular density, and improve heart function in a canine chronic ischemia model. *Circulation*. **111**, 150-156.
- Singh, V.K., 2015. Induced Pluripotent Stem Cells: Applications in regenerative medicine, disease modelling and drug discovery. *Frontiers in Cell and Developmental Biology*. **3**, 2.

- Sobolewski, K., Bankowski, E., Chyczewski, L., Jaworski, S., 1997. Collagen and glycosaminoglycans of Wharton's jelly. *Biology of the Neonate*. **71**, 11-21.
- Somerville, R.P.T., Longpre, J., Apel, E.D., Lewis, R.M., Wang, L.W., Leduc, R., Apte, S.S., 2004. ADAMTS7B, the full-length product of the ADAMTS7 gene, is a chondroitin sulphate-proteoglycan containing a mucin domain. *Journal of Biological Chemistry*.
- Somerville, R.P.T., Longpre, J., Jungers, K.A., Engle, J.M., Ross, M., Evanko, S., Wight, T.N., Leduc, R., Apte, S.S., 2003. Characterization of ADAMTS-9 and ADAMTS-20 as a Distinct ADAMTS Subfamily Related to Caenorhabditis elegans GON-1. *Journal of Biological Chemistry*. **278**, 9503-9513.
- Sörby, M. & östman, A., 1996. Protein-tyrosine Phosphatase-mediated Decrease of Epidermal Growth Factor and Platelet-derived Growth Factor Receptor Tyrosine Phosphorylation in High Cell Density Cultures. *Journal of Biological Chemistry*. **271**, 10963-10966.
- Sordi, V., Malosio, M.L., Marchesi, F., Mercalli, A., Melzi, R., Giordano, T., Belmonte, N., Ferrari, G., Leone, B.E., Bertuzzi, F., Zerbini, G., Allavena, P., Bonifacio, E., Piemonti, L., 2005. Bone marrow mesenchymal stem cells express a restricted set of functionally active chemokine receptors capable of promoting migration to pancreatic islets. *Blood*. **106**, 419-427.
- Sorensen, T.I.A., Nielsen, G.G., Andersen, P.K., Teasdale, T.W., 1988. Genetic and Environmental-Influences on Premature Death in Adult Adoptees. *New England Journal of Medicine*. **318**, 727-732.
- Speliotes, E.K., Willer, C.J., Berndt, S.I., Monda, K.L., Thorleifsson, G., Jackson, A.U., Allen, H.L., Lindgren, C.M., et al. 2010. Association analyses of 249,796 individuals reveal 18 new loci associated with body mass index. *Nature Genetics*. **42**, 937-948.
- Stein, E.A., Mellis, S., Yancopoulos, G.D., Stahl, N., Logan, D., Smith, W.B., Lisbon, E., Gutierrez, M., Webb, C., Wu, R., Du, Y., Kranz, T., Gasparino, E., Swergold, G.D., 2012. Effect of a Monoclonal Antibody to PCSK9 on LDL Cholesterol. *N Engl J Med*. **366**, 1108-1118.
- Sterneckert, J.L., Reinhardt, P., Scholer, H.R., 2014. Investigating human disease using stem cell models. *Nature Reviews. Genetics*. **15**, 625-639.
- Stock, P., Bruckner, S., Ebensing, S., Hempel, M., Dollinger, M.M., Christ, B., 2010. The generation of hepatocytes from mesenchymal stem cells and engraftment into murine liver. *Nature Protocols*. **5**, 617-627.
- Stossel, T.P., 2008. The Discovery of Statins. *Cell*. **134**, 903-905.
- Suto, J., Matsuura, S., Imamura, K., Yamanaka, H., Sekikawa, K., 1998. Genetics of obesity in KK mouse and effects of A(y) allele on quantitative regulation. *Mammalian Genome : Official Journal of the International Mammalian Genome Society*. **9**, 506-510.

- Suto, J. & Sekikawa, K., 2004. Confirmation and Characterization of Murine Body Weight QTLs, *Bwq1* and *Bwq2*, Identified in C57BL/6J  $\times$  KK-*A<sup>y</sup>/a* F<sub>2</sub>-*A<sup>y</sup>/a* Mice. *Journal of Veterinary Medical Science*. **66**, 1039-1045.
- Tabas, I., 2010. Macrophage death and defective inflammation resolution in atherosclerosis. *Nature Reviews Immunology*. **10**, 36-46.
- Takagi, M., Kojima, N., Yoshida, T., 2000. Analysis of the ammonia metabolism of rat primary hepatocytes and a human hepatocyte cell line Huh 7. *Cytotechnology*. **32**, 9-15.
- Takahashi, K., Tanabe, K., Ohnuki, M., Narita, M., Ichisaka, T., Tomoda, K., Yamanaka, S., 2007. Induction of Pluripotent Stem Cells from Adult Human Fibroblasts by Defined Factors. *Cell*. **131**, 861-872.
- Takahashi, K. & Yamanaka, S., 2006a. Induction of Pluripotent Stem Cells from Mouse Embryonic and Adult Fibroblast Cultures by Defined Factors. *Cell*. **126**, 663-676.
- The IBC 50K, C.C., 2011. Large-Scale Gene-Centric Analysis Identifies Novel Variants for Coronary Artery Disease. *PLoS Genet*. **7**, e1002260.
- The International HapMap Consortium., 2005. A haplotype map of the human genome. *Nature*. **437**, 1299-1320.
- The Wellcome Trust Case Control Consortium, 2007. Genome-wide association study of 14,000 cases of seven common diseases and 3,000 shared controls. *Nature*. **447**, 661-678.
- Thomas, G., 2002. Furin at the cutting edge: From protein traffic to embryogenesis and disease. *Nature Reviews. Molecular Cell Biology*. **3**, 753-766.
- Thomson, J.A., Itskovitz-Eldor, J., Shapiro, S.S., Waknitz, M.A., Swiergiel, J.J., Marshall, V.S., Jones, J.M., 1998. Embryonic Stem Cell Lines Derived from Human Blastocysts. *Science*. **282**, 1145-1147.
- Thorleifsson, G., Walters, G.B., Gudbjartsson, D.F., Steinthorsdottir, V., Sulem, P., Helgadóttir, A., Styrkarsdóttir, U., Gretarsdóttir, S., et al. 2009. Genome-wide association yields new sequence variants at seven loci that associate with measures of obesity. *Nature Genetics*. **41**, 18-24.
- Thyberg, J. & Hultgårdh-Nilsson, A., 1994. Fibronectin and the basement membrane components laminin and collagen type IV influence the phenotypic properties of subcultured rat aortic smooth muscle cells differently. *Cell and Tissue Research*. **276**, 263-271.
- Toda, S., Uchihashi, K., Aoki, S., Sonoda, E., Yamasaki, F., Piao, M., Ootani, A., Yonemitsu, N., Sugihara, H., 2009. Adipose tissue-organotypic culture system as a

promising model for studying adipose tissue biology and regeneration. *Organogenesis*. **5**, 50-56.

Tontonoz, P., Hu, E., Devine, J., Beale, E.G., Spiegelman, B.M., 1995. PPAR gamma 2 regulates adipose expression of the phosphoenolpyruvate carboxykinase gene. *Molecular and Cellular Biology*. **15**, 351-357.

Tremain, N., Korkko, J., Ibberson, D., Kopen, G.C., DiGirolamo, C., Phinney, D.G., 2001. MicroSAGE Analysis of 2,353 Expressed Genes in a Single Cell-Derived Colony of Undifferentiated Human Mesenchymal Stem Cells Reveals mRNAs of Multiple Cell Lineages. *Stem Cells*. **19**, 408-418.

Troyer, D.L. & Weiss, M.L., 2008. Concise review: Wharton's jelly-derived cells are a primitive stromal cell population. *Stem Cells*. **26**, 591-599.

Tsagias, N., Koliakos, I., Karagiannis, V., Eleftheriadou, M., Koliakos, G.G., 2011. Isolation of mesenchymal stem cells using the total length of umbilical cord for transplantation purposes. *Transfusion Medicine*. **21**, 253-261.

Turner, P.A., Harris, L.M., Purser, C.A., Baker, R.C., Janorkar, A.V., 2014. A surface-tethered spheroid model for functional evaluation of 3T3-L1 adipocytes. *Biotechnology and Bioengineering*. **111**, 174-183.

Uchida, K., Sasahara, M., Morigami, N., Hazama, F., Kinoshita, M., 1996. Expression of platelet-derived growth factor B-chain in neointimal smooth muscle cells of balloon injured rabbit femoral arteries. *Atherosclerosis*. **124**, 9-23.

Udler, M.S., Meyer, K.B., Pooley, K.A., Karlins, E., Struewing, J.P., Zhang, J., Doody, D.R., et al. 2009. FGFR2 variants and breast cancer risk: fine-scale mapping using African American studies and analysis of chromatin conformation. *Human Molecular Genetics*. **18**, 1692-1703.

Ussar, S., Lee, K.Y., Dankel, S.N., Boucher, J., Haering, M., Kleinridders, A., Thomou, T., Xue, R., Macotela, Y., Cypess, A.M., Tseng, Y., Mellgren, G., Kahn, C.R., 2014. Asc-1, PAT2 and P2RX5 are novel cell surface markers for white, beige and brown adipocytes. *Science Translational Medicine*. **6**, 247ra103.

van der Loop, F.T., Schaart, G., Timmer, E.D., Ramaekers, F.C., van Eys, G.J., 1996. Smoothelin, a novel cytoskeletal protein specific for smooth muscle cells. *The Journal of Cell Biology*. **134**, 401-411.

van Eys, G.J., Niessen, P.M., Rensen, S.S., 2007. Smoothelin in Vascular Smooth Muscle Cells. *Trends in Cardiovascular Medicine*. **17**, 26-30.

Villéger, L., Abifadel, M., Allard, D., Rabès, J., Thiart, R., Kotze, M.J., Bérout, C., Junien, C., Boileau, C., Varret, M., 2002. The UMD-LDLR database: additions to the software and 490 new entries to the database. *Human Mutation*. **20**, 81-87.

Visel, A., Zhu, Y., May, D., Afzal, V., Gong, E., Attanasio, C., Blow, M.J., Cohen, J.C., Rubin, E.M., Pennacchio, L.A., 2010. Targeted deletion of the 9p21 non-coding coronary artery disease risk interval in mice. *Nature*. **464**, 409-412.

Wagers, A.J. & Weissman, I.L., 2004. Plasticity of Adult Stem Cells. *Cell*. **116**, 639-648.

Wagner, W., Ho, A.D., Zenke, M., 2010. Different facets of aging in human mesenchymal stem cells. *Tissue Engineering.Part B, Reviews*. **16**, 445-453.

Wagner, W., Horn, P., Castoldi, M., Diehlmann, A., Bork, S., Saffrich, R., Benes, V., Blake, J., Pfister, S., Eckstein, V., Ho, A.D., 2008. Replicative Senescence of Mesenchymal Stem Cells: A Continuous and Organized Process. *PLoS ONE*. **3**, 5 e2213.

Wang, L.J., Fan, C., Topol, S.E., Topol, E.J., Wang, Q., 2003. Mutation of MEF2A in an inherited disorder with features of coronary artery disease. *Science*. **302**, 1578-1581.

Wang, L., Zheng, J., Bai, X., Liu, B., Liu, C., Xu, Q., Zhu, Y., Wang, N., Kong, W., Wang, X., 2009. ADAMTS-7 Mediates Vascular Smooth Muscle Cell Migration and Neointima Formation in Balloon-Injured Rat Arteries. *Circulation Research*. **104**, 688-698.

Wang, L., Zheng, J., Du, Y., Huang, Y., Li, J., Liu, B., Liu, C., Zhu, Y., Gao, Y., Xu, Q., Kong, W., Wang, X., 2010. Cartilage Oligomeric Matrix Protein Maintains the Contractile Phenotype of Vascular Smooth Muscle Cells by Interacting With  $\alpha 7\beta 1$  Integrin. *Circulation Research*. **106**, 514-525.

Wang, T.J., Nam, B.H., D'Agostino, R.B., Wolf, P.A., Lloyd-Jones, D.M., MacRae, C.A., Wilson, P.W., Polak, J.F., O'Donnell, C.J., 2003. Carotid intima-media thickness is associated with premature parental coronary heart disease - The Framingham Heart Study. *Circulation*. **108**, 572-576.

Wang, X., Lan, Y., He, W., Zhang, L., Yao, H., Hou, C., Tong, Y., Liu, Y., Yang, G., Liu, X., Yang, X., Liu, B., Mao, N., 2008. Identification of mesenchymal stem cells in aorta-gonad-mesonephros and yolk sac of human embryos. *Blood*. **111**, 2436-2443.

Wanjare, M., Kuo, F., Gerecht, S., 2012. Derivation and maturation of synthetic and contractile vascular smooth muscle cells from human pluripotent stem cells. *Cardiovascular Research*. **97**, 321-330.

Warren, L., Manos, P.D., Ahfeldt, T., Loh, Y.H., Li, H., Lau, F., Ebina, W., Mandal, P.K., Smith, Z.D., Meissner, A., et al., 2010. Highly efficient reprogramming to pluripotency and directed differentiation of human cells with synthetic modified mRNA. *Cell Stem Cell*. **7**, 618-630.

Watkins, H. & Farrall, M., 2006. Genetic susceptibility to coronary artery disease: from promise to progress. *Nature Reviews Genetics*. **7**, 163-173.

Watson, K.E., Boström, K., Ravindranath, R., Lam, T., Norton, B., Demer, L.L., 1994. TGF-beta 1 and 25-hydroxycholesterol stimulate osteoblast-like vascular cells to calcify. *Journal of Clinical Investigation*. **93**, 2106-2113.

Webb, R.C., 2003. *Advances in Physiology Education*. **27**, 201-206.

Wei, X., Wang, C.Y., Liu, Q.P., Li, J., Li, D., Zhao, F.T., Lian, J.Q., Xie, Y.M., Wang, P.Z., Bai, X.F., Jia, Z.S., 2008. In vitro hepatic differentiation of mesenchymal stem cells from human fetal bone marrow. *Journal of International Medical Research*. **36**, 721-727.

Weiss, M.L., Medicetty, S., Bledsoe, A.R., Rachakatla, R.S., Choi, M., Merchav, S., Luo, Y., Rao, M.S., Velagaleti, G., Troyer, D., 2006. Human umbilical cord matrix stem cells: Preliminary characterization and effect of transplantation in a rodent model of Parkinson's disease. *Stem Cells*. **24**, 781-792.

Wen, W., Cho, Y., Zheng, W., Dorajoo, R., Kato, N., Qi, L., Chen, C., Delahanty, R.J., et al. 2012. Meta-analysis identifies common variants associated with body mass index in east Asians. *Nature Genetics*. **44**, 307-311.

Williams, R.R., Hunt, S.C., Heiss, G., Province, M.A., Bensen, J.T., Higgins, M., Chamberlain, R.M., Ware, J., Hopkins, P.N., 2001. Usefulness of cardiovascular family history data for population-based preventive medicine and medical research (The Health Family Tree Study and the NHLBI Family Heart Study). *American Journal of Cardiology*. **87**, 129-135.

Wilson, P.W.F., D'Agostino, R.B., Levy, D., Belanger, A.M., Silbershatz, H., Kannel, W.B., 1998. Prediction of Coronary Heart Disease Using Risk Factor Categories. *Circulation*. **97**, 1837-1847.

Wong, N., Lai, P., Pang, E., Wai-Tong Leung, T., Wan-Yee Lau, J., James Johnson, P., 2000. A comprehensive karyotypic study on human hepatocellular carcinoma by spectral karyotyping. *Hepatology*. **32**, 1060-1068.

Wong, R.S.Y., 2011. Mesenchymal Stem Cells: Angels or Demons? *Journal of Biomedicine and Biotechnology*. 459510.

Woodbury, D., Reynolds, K., Black, I.B., 2002. Adult bone marrow stromal stem cells express germline, ectodermal, endodermal, and mesodermal genes prior to neurogenesis. *Journal of Neuroscience Research*. **69**, 908-917.

World Health Organisation, 2015. January 2015-Fact sheet no.311. Obesity and Overweight. Available: <http://www.who.int/mediacentre/factsheets/fs311/en/>

World Health Organisation, 2015. January 2015-Fact sheet no.317. Cardiovascular diseases (CVDs). Available: <http://www.who.int/mediacentre/factsheets/fs317/en/>

- Wright, A.F. & Hastie, N.D., 2001. Complex genetic diseases: controversy over the Croesus code. *Genome Biology*. **2**, 8.
- Wu, S.C. & Zhang, Y., 2010. Active DNA demethylation: many roads lead to Rome. *Nature Reviews.Molecular Cell Biology*. **11**, 607-620.
- Wynne, B.M., Chiao, C., Webb, R.C., 2009. Vascular Smooth Muscle Cell Signaling Mechanisms for Contraction to Angiotensin II and Endothelin-1. *Journal of the American Society of Hypertension : JASH*. **3**, 84-95.
- Xie, C., Huang, H., Wei, S., Song, L., Zhang, J., Ritchie, R.P., Chen, L., Zhang, M., Chen, Y.E., 2008. A Comparison of Murine Smooth Muscle Cells Generated from Embryonic versus Induced Pluripotent Stem Cells. *Stem Cells and Development*. **18**, 741-748.
- Yamanaka, S., 2012. Induced pluripotent stem cells: past, present and future. *Cell Stem Cell*.**10**, 678-684.
- Yap, K.L., Li, S., Munoz-Cabello, A.M., Raguz, S., Zeng, L., Mujtaba, S., Gil, J., Walsh, M.J., Zhou, M., 2010. Molecular Interplay of the Noncoding RNA ANRIL and Methylated Histone H3 Lysine 27 by Polycomb CBX7 in Transcriptional Silencing of INK4a. *Molecular Cell*. **38**, 662-674.
- Yatabe, Y., Tavaré, S., Shibata, D., 2001. Investigating stem cells in human colon by using methylation patterns. *Proceedings of the National Academy of Sciences*. **98**, 10839-10844.
- Yoshida, T. & Owens, G.K., 2005. Molecular Determinants of Vascular Smooth Muscle Cell Diversity. *Circulation Research*. **96**, 280-291.
- Yusuf, S., Hawken, S., Ounpuu, S., 2004. Effect of potentially modifiable risk factors associated with myocardial infarction in 52 countries (the INTERHEART study): case-control study. *Lancet*. **364**, 2020-2020.
- Zaim, M., Karaman, S., Cetin, G., Isik, S., 2012. Donor age and long-term culture affect differentiation and proliferation of human bone marrow mesenchymal stem cells. *Annals of Hematology*. **91**, 1175-1186.
- Zaitlen, N., Kraft, P., Patterson, N., Pasaniuc, B., Bhatia, G., Pollack, S., Price, A.L., 2013. Using Extended Genealogy to Estimate Components of Heritability for 23 Quantitative and Dichotomous Traits. *PLoS Genetics*. **9**, e1003520.
- Zaret, K.S., 2002. Regulatory phases of early liver development: paradigms of organogenesis. *Nature Reviews. Genetics*. **3**, 499-512.
- Zhang, H.H., Kumar, S., Barnett, A.H., Eggo, M.C., 2000. Ceiling culture of mature human adipocytes: use in studies of adipocyte functions. *The Journal of Endocrinology*. **164**, 119-128.

Zhang, Y., Li, C.D., Jiang, X.X., Li, H.L., Tang, P.H., Mao, N., 2004. Comparison of mesenchymal stem cells from human placenta and bone marrow. *Chinese Medical Journal*. **117**, 882-887.

Zhou, A., Webb, G., Zhu, X., Steiner, D.F., 1999. Proteolytic Processing in the Secretory Pathway. *Journal of Biological Chemistry*. **274**, 20745-20748.

Zipori, D., 2009. *Biology of stem cells and the molecular basis of the stem state*. [e-book]. Dordrecht; London: Springer.

Zvaifler, N.J., Marinova-Mutafchieva, L., Adams, G., Edwards, C.J., Moss, J., Burger, J.A., Maini, R.N., 2000. Mesenchymal precursor cells in the blood of normal individuals. *Arthritis Research*. **2**, 477-488.